

Behind the Scents!

A multidisciplinary approach for unveiling the protein-flavor binding mechanism



Cristina Barallat Pérez

Propositions

1. Protein-flavor binding depends on the flavor's structural and physicochemical properties.
(this thesis)
2. Assessing aroma perception through a single intake oversimplifies the complexity of aroma release.
(this thesis)
3. The focus on sustainable alternative proteins diverts attention from addressing unsustainable food production processes and consumption behavior.
4. Pursuing a Ph.D. prioritizes external recognition over internal personal growth and autonomy.
5. Gender quotas for leadership positions are more effective in closing the gender representation gap than merely encouraging women to pursue top-level roles.
6. Prioritizing emotional intelligence for achieving professional success helps shift traditional notions of intelligence.

Propositions belonging to the thesis, entitled

Behind the Scents! A multidisciplinary approach for unveiling the protein-flavor binding mechanism

Cristina Barallat Pérez
Wageningen, 13 December 2024

Behind the Scents!

A multidisciplinary approach for
unveiling the protein-flavor binding
mechanism

Cristina Barallat Pérez

Thesis committee

Promotor

Prof. Dr Vincenzo Fogliano

Personal chair, Food Quality and Design

Wageningen University & Research

Co-promotors

Dr Teresa Oliviero

Researcher and Education Coordinator, Food Quality and Design

Wageningen University & Research

Dr Sara I.F.S. Martins

Global Director Science & Technology

AFB International, Oss

Other members

Prof. Dr J.P. Vincken, Wageningen University & Research, the Netherlands

Prof. Dr V. Somoza, Technical University of Munich, Germany

Dr K. Reichelt, Symrise AG, Hannover, Germany

Dr S. Boesveldt, Wageningen University & Research, the Netherlands

This research was conducted under the auspices of VLAG Graduate School (Biobased, Biomolecular, Chemical, Food and Nutrition Sciences).

Behind the Scents!

A multidisciplinary approach for
unveiling the protein-flavor binding
mechanism

Cristina Barallat Pérez

Thesis

submitted in fulfillment of the requirements for the degree of doctor
at Wageningen University

by the authority of the Rector Magnificus,

Prof. Dr. C. Kroeze,

in the presence of the

Thesis Committee appointed by the Academic Board

to be defended in public

on Friday 13 December 2024

at 10.30 a.m. in the Omnia Auditorium.

Cristina Barallat Pérez

Behind the Scents! A multidisciplinary approach for unveiling the protein-flavor binding mechanism.

241 pages

Ph.D. thesis, Wageningen University, Wageningen, the Netherlands (**2024**).

With references and summaries in English and Spanish.

DOI: [10.18174/676211](https://doi.org/10.18174/676211)

Always keep your drive to move forward

Table of Contents

Chapter 1: General Introduction	10-19
Chapter 2: Flavor them up! Exploring the challenges of flavored plant-based foods	22-39
Chapter 3: Unraveling the role of flavor structure and physicochemical properties in the binding phenomena with commercial food protein isolates	42-70
Chapter 4: Development of a QSAR model to predict protein-flavor binding in protein-rich food systems	74-108
Chapter 5: The role of mucin in the protein-flavor binding mechanism: an <i>in vitro</i> approach	112-129
Chapter 6: Drivers of the in-mouth interaction between lupin protein isolate and selected aroma compounds: a PTR-MS and Dynamic Time Intensity analysis	132-159
Chapter 7: General Discussion	162-186
References	190-210
Summary	214-216
Appendices	226-240



General Introduction

In recent years, plant-based foods have made significant inroads into the meat and dairy markets as more consumers shift towards plant-based diets. Pulses, particularly, are gaining traction in innovative products such as vegan and vegetarian options due to their high protein content. However, the presence of off-flavors can negatively impact consumer acceptance. To address this, flavor compounds are often added, but they can bind to plant proteins—either reversibly or irreversibly—affecting their release and the overall flavor profile. This thesis aims to examine how flavor compounds' structural and physicochemical properties and plant protein types influence the binding mechanism and sensory perception in flavored protein-based aqueous model systems (FPBAS). We did so by using Gas Chromatography-Mass Spectrometry (GC-MS) and Proton Transfer Reaction Mass Spectrometer (PTR-MS), along with Time Intensity (TI) for sensory analysis.

1.1. Plant proteins in food systems: an overview

The United Nations and FAO expect the global population to rise from 7.6 billion to 8.6 billion by 2030 and 9.8 billion by 2050, increasing the global demand for food by at least 60% (Hayes, 2023). To meet global protein demands and feed the growing population, food scientists are insatiable in their search for alternative protein sources besides meat and dairy. In the last decade, hemp, quinoa, algae, edible insects, cultured meat, and fermentation-derived sources have gained significant attention (Boukid et al., 2024; Fatima et al., 2023; Lingiardi et al., 2022). Even though it is still far from the complete application of the most cutting-edge alternative proteins available, the niche of plant proteins has kept growing progressively, expanding their offer. Some examples of commonly consumed pulses worldwide include soybeans (*Glycine max*), peas (*Pisum sativum* L.), lentils (*Lens culinaris* L.), lupins (*Lupinus spp.*), chickpeas (*Cicer arietinum* L.), cowpeas (*Vigna unguiculata* L.), faba beans (*Vicia faba* L.), and common beans such as kidney, black, navy, and pinto beans (*Phaseolus vulgaris* L.). Pulses are commonly known for their rich nutritional profile, mainly due to their high content of proteins (~21-25%) and minor levels of vitamins, minerals, and other compounds such as saponins, flavonoids, and phenolic

compounds (Ismail et al., 2020; Lam et al., 2018; Singh, 2017). From a molecular point of view, plant-based proteins primarily consist of salt-soluble globulin proteins, followed by water-soluble albumin proteins as the second-largest group (Sha & Xiong, 2022; Yang et al., 2022).

With the rapid increase of emerging food technology, the food industry has largely made efforts to increase the production of isolates (80-90% protein content) and concentrates (40-70%) due to their optimal techno-functional and nutritional properties (Bou et al., 2022). Dry fractionation and wet extraction are the most commonly used methods for this goal. The protein separation process involves acid-base extraction (pH adjustment), mechanical separation (grinding and sieving), enzymatic hydrolysis (breakage into smaller fragments), and centrifugation steps (Sandberg, 2011). The extraction methods yield varying protein purities, with isolates displaying higher purity levels than concentrates.

Off-notes in pulses

Despite the potential benefits of using pulses, off-flavors are often present, implying a challenge to the sensory acceptability of the product (Xiang et al., 2023), where beany, earthy, grassy, bitter, and astringent are commonly addressed (Wang et al., 2021). Many of these off-flavors can be caused by reactions, such as oxidation, Maillard reaction, Strecker degradation, and ethanol fermentation, that occur during the manufacturing processes (*i.e.*, harvesting, post-harvesting, and storage), or they may be naturally present in the plant material itself (Bi et al., 2020; Roland et al., 2017). Off-flavors in pulses may account for a wide diversity of different compounds ranging from 50 to 250. However, only odor-active compounds with low thresholds and commonly found in deficient concentrations (parts per million, ppm or parts per billion, ppb) play a significant role in causing the perceived odor (Saffarionpour, 2024). Off-flavors in pulses involve aldehydes, ketones, alcohols, pyrazines, furans, acids, and sulfur compounds (Saffarionpour, 2024) (**Figure 1.1**), as well as non-volatile compounds such as saponins, isoflavones, phenolic compounds, *etc.*

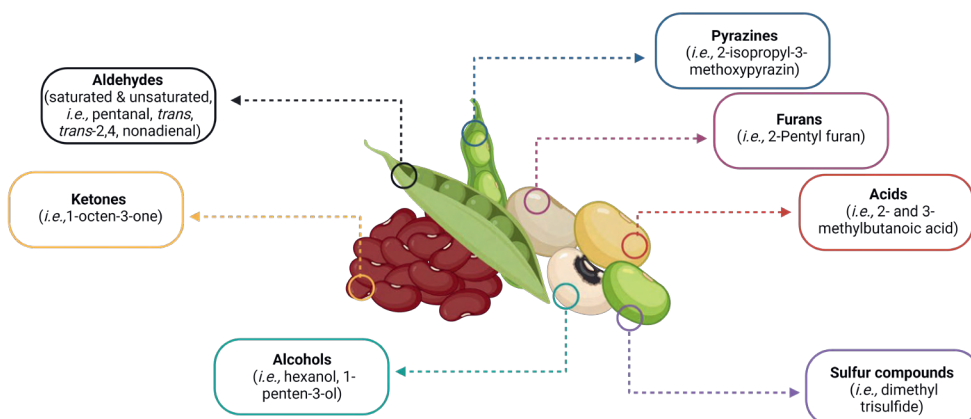


Figure 1.1. Commonly volatile compounds found in pulses. Examples in the illustration: soybeans, pinto beans, peas, and cow beans (Biorender software).

Consumers demand that these unpleasant off-notes be removed. Currently, some technologies and methods use biotechnology, such as genetic modification, enzymatic treatment, fermentation, and germination; physical technology, such as high-frequency electromagnetic fields and radiation; and chemical methods, including solvent extraction (Lippolis et al., 2023; Wang et al., 2021). Flavoring addition has been considered an effective strategy for hindering or masking the off-flavors in pulses and enhancing the flavor profile of plant-based foods.

1.2. Flavor compounds and terminology

The European Commission provided the main definitions and categories on flavorings and certain food ingredients with flavoring properties for use in and on food Regulation (EC) 1334/2008 of the European Parliament and of the Council of 16th December 2008 (**Figure 1.2**) to ensure transparent, safe and high-quality flavored food products.

Definitions of Flavorings and Certain Food Ingredients with Flavoring Properties for Use in and on Foods	Flavoring substances	Chemical substances with flavoring properties.
	Natural flavoring substance	Obtained through physical, enzymatic, or microbiological processes from plant, animal, or microbiological materials, either raw or processed for consumption.
	Flavoring preparation	A product, other than a flavoring substance, derived from food or non-food plant, animal, or microbiological materials via appropriate physical, enzymatic, or microbiological processes.
	Thermal process flavoring	Created by heating a mixture of ingredients, including at least one nitrogen-containing component (amino) and one reducing sugar, from food or non-food sources.
	Smoke flavoring	Obtained by fractionation and purification of condensed smoke, producing primary smoke condensates, primary tar fractions, and/or derived smoke flavorings.
	Flavor precursor	Added to food to produce flavor by reacting with other components during processing; can be derived from food or non-food sources.
	Food ingredient with flavoring properties	An ingredient added to food primarily to enhance or modify flavor, contributing to certain undesirable substances.
	Source material	Plant, animal, microbiological, or mineral origin material used to produce flavorings or food ingredients with flavoring properties.
	Other flavoring	A flavoring added to food to impart odor and/or taste, not covered by previous definitions.

Figure 1.2. Definition of the nine flavor categories described in the Article 3 of the Regulation 1334/2008: flavoring substances, natural flavoring substances, flavoring preparation, thermal process flavorings, smoke flavorings, flavor precursors, food ingredients with flavoring properties, source materials, and others.

In this Ph.D, pure, synthetic flavor compounds were used. However, the scientific literature does not consistently agree on terms such as "flavor," "smell," "taste," "scents," "odor," "volatile compounds," and "aroma," which are often used interchangeably. This lack of consistency stems from their overlapping definitions and subjective interpretations within the scientific community. **Flavor** refers to the combination of *aroma* (commonly addressed as pleasant volatile compounds) and *taste* (soluble substances perceived by the gustatory system) (Chen et al., 2023). *Odor* can be understood as the sensation of volatile compounds sensed by the olfactory system (Aprea, 2020), *smell* refers to the volatile compounds detected by the olfactory system, and *scents* involve a distinctive smell. Whether one term is used, or not, will depend on the subcluster within the flavor field. For instance, while a flavor chemist might define "volatile organic compounds (VOC)" or "flavor compounds" based on their molecular structure and physical properties, a sensory scientist might use "aroma compounds", "scents", and "odor." Therefore, the term "flavor compounds" will be consistently used to ensure clarity in this thesis. "Aroma" will only be used in this Ph.D thesis when referring to *in vivo* measurements.

Generally, food flavors are small molecules (<250 Da) (Cayot, 2014) which are added in low concentrations, constituting 0.01-0.8(w/w)% of the final food composition (Fan et al., 2024). For instance, *trans*-6-octenal, known for its leafy, melon-like aroma, is found in levels between 0.03 ppm in breakfast cereals and 1 ppm in sweet sauces, whereas 4-(4-Methyl-3-penten1-yl)-2(5H)-furanone (woody odor) is commonly found in $1 \cdot 10^5$ ppm in fruit juices and up to $1 \cdot 10^2$ ppm in gravies (Cohen et al., 2017).

These molecules can be classified into numerous chemical families, such as carbonyl compounds (aldehydes and ketones), alcohols, esters, sulfur compounds, furans, pyrazines, and hydrocarbons (Reineccius, 2022), varying in physicochemical properties (*e.g.*, hydrophobicity, volatility, solubility), spatial configuration (*e.g.*, functional group, unsaturation, chain length), and their characteristic odor threshold.

1.3. Protein-flavor binding mechanism

Over the last century, researchers have extensively studied flavor-food matrix interactions such as lipids, complex carbohydrates, sugar, salt, and proteins have been largely studied (Gremli, 1974; Jasinski & Kilara, 1985; Mills & Solms, 1984; O'Neill & Kinsella, 1987). The high complexity of the underlying mechanism prompted special attention to protein-flavor interactions. Generally, protein-flavor interaction can be classified into two categories: (1) physical trapping through adsorption onto the protein surface and (2) molecular interactions, which can be reversible or irreversible) (Wang & Arntfield, 2017). **Chapter 2** provides further clarification on the binding categories.

1.3.1. Driving forces for flavor binding and aroma release

Whether flavor binding to proteins has an undesirable effect on food product development, remains subjective and depends on the final food application. Finding the delicate equilibrium between masking unpleasant off-notes with intentionally added pleasant flavor compounds without overdosing on the food product remains key to food sensory acceptability.

Due to the multifaceted nature of the flavor binding mechanism, it remains challenging to address this phenomenon. However, efforts to build understanding have focused on the molecular structure of proteins and flavor compounds (Chen et al., 2023). Experts speculate that the protein's amino acid sequence and composition, including functional groups like -SH and NH₂, and different spatial arrangements like disulfide bridges, hydrogen bonds, and 3D structure, partially contribute to the flavor binding mechanism. Nevertheless, to what extent remains unclear. Studies have demonstrated a correlation between flavor binding affinity and structural features such as chain length, unsaturation, type, and location of the functional groups, as well as the physicochemical parameters, like hydrophobicity, solubility, and volatility (Bi et al., 2022; Chen et al., 2023; Li et al., 2024; Perez-Jiménez et al., 2020; Wei et al., 2024). Further clarification is described throughout the thesis (**Chapters 2-6**). Besides, the composition of the food matrix, like the presence or absence of other food nutrients, along with external factors such as temperature and pH, influence the affinity of flavor binding too (Ammari & Schroen, 2018; De Roos, 2003).

Analytical measurements such as distillation/high vacuum/extraction/purging (Gremli, 1974), Equilibrium Dialysis (Gianelli et al., 2003), Static Headspace Gas Chromatography-Mass Spectrometry (GC-MS) (Wang & Arntfield, 2015), High-performance Liquid Chromatography (Zhou & Cadwallader, 2006), Solid Phase Microextraction (Gkionakis et al., 2007), radioisotopes (Anantharamkrishnan et al., 2020), and Atmospheric Pressure Chemical Ionisation-Mass Spectrometry (APCI-MS) (Snel et al., 2023) have been used to quantify flavor binding. While no single approach can provide a comprehensive, quantitative understanding of the flavor-binding phenomena, GC-MS is the most widely employed technique for studying protein-flavor binding (Reineccius, 2010).

1.3.2. Equilibrium phenomena

To measure flavor release and, thus, protein-flavor interactions, the system may reach an equilibrium state between the liquid and the air phases (**Figure 1.3**).

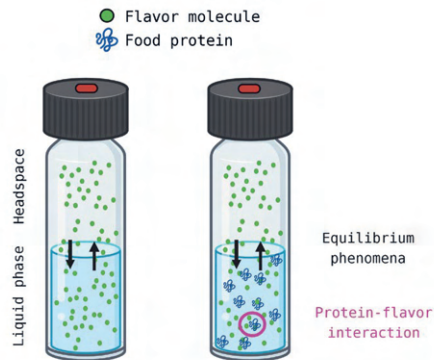


Figure 1.3. Equilibrium phenomena between sample and headspace. (Biorender software).

As earlier described by Ammari & Schroen, 2018; De Roos, 2003, thermodynamic (volatility), and kinetic factors (barrier to mass transfer across phases) represent the main drivers of flavor release, controlling its rate. In general, the equilibrium state obeys the following relationship [1]:

$$P_{ap} = \frac{C_a}{C_p} \quad [1]$$

where P_{ap} is the air-product partition coefficient, C_a is the flavor concentration in the air phase, and C_p is the flavor concentration in the product, expressed as g/L (De Roos, 2003).

Nevertheless, due to differences in flavor volatility, allowing sufficient time for all flavor compounds to reach equilibrium when designing a food product is crucial.

1.3.3. Effect of the protein-flavor binding phenomena on aroma release

During oral processing, flavor compounds are not released simultaneously, following a dynamic mass transport and lack of equilibrium (Mao et al., 2017; Weterings et al., 2020). Advanced high-throughput methods have been developed to better understand in vivo aroma release and analyze volatile compounds in real-time, including Proton Transfer Reaction-Time Of Flight-Mass Spectrometry (PTR-ToF-MS). PTR-ToF-MS relies on ionizing VOCs using protonated water, specifically hydronium ions (H_3O^+). The transfer of protons

from hydronium ions becomes exothermic if the proton affinities of the VOC targeted are higher than those of water (Pedrotti et al., 2019).

Under *in vivo* conditions, odorant molecules can be perceived via two routes: (1) orthonasal and (2) retronasal (**Figure 1.4**) (Blankenship et al., 2019; Hannum et al., 2018). The first route involves volatile compounds being smelled directly through the nose (**Figure 1.4 A**). In contrast, retronasally, volatile compounds are detected by the nose via the throat during food consumption (**Figure 1.4 B**).

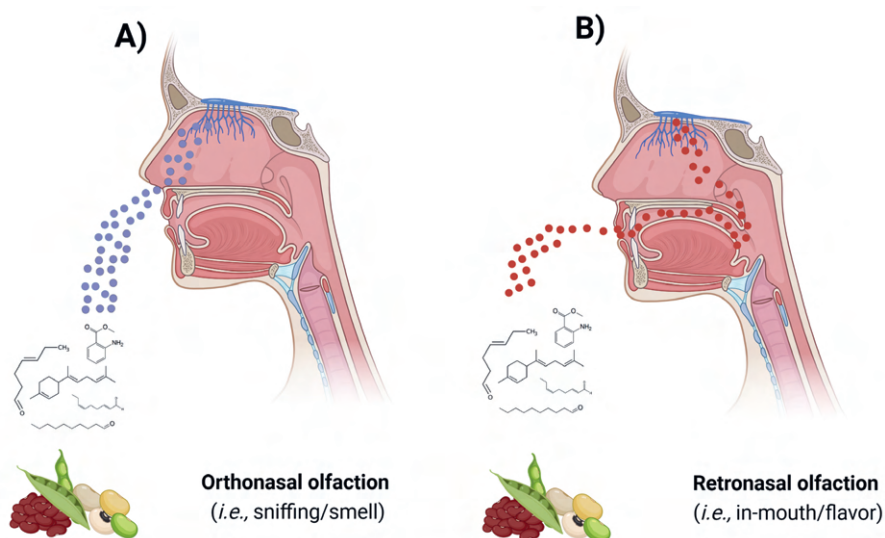


Figure 1.4. Schematic representation of olfaction pathways. (Biorender software).

Integrating sensory evaluation with real-time PTR-ToF-MS measurements provides insights into aroma release and perception (**Chapters 2 and 6**). However, the human nose can detect odors at concentrations as low as 10^{-19} moles, which exceeds the sensitivity of current analytical techniques (Pedrotti et al., 2019; Reineccius & Heath, 2006). As a result, discrepancies between sensory and analytical techniques are often encountered in flavor studies (Le Quéré & Schoumacker, 2023).

It is still unclear whether the observed *in vitro* protein-flavor binding interaction remains under *in vivo* conditions. However, it is a significant factor in determining the success of a food product. Unveiling the main drivers, nature, and strength of protein-flavor interactions, with a particular emphasis on protein isolates, will open up ways for formulating novel high-protein-based foods with a balanced flavor profile.

1.4. Aim and outline of the Ph.D. thesis

The main aim of this Ph.D. project was to investigate the binding phenomena between commercial food protein isolates and flavors to uncover the key factors driving its mechanism. Our ultimate goal was to understand its impact on food aroma release and perception. To achieve this objective, both *in vitro* GC-MS and real-time *in vivo* assessments of aroma release were conducted using PTR-ToF-MS. The latter was paired with sensory profiling. **Chapter 1** includes a general introduction to the field of study, delving into the leading players of this Ph.D.: plant proteins and flavor compounds. **Chapter 2** provides an overview of the current knowledge on flavor binding, aiding food scientists in identifying the main binding factors for successful product development. **Chapter 3** focused on utilizing *in vitro* GC-MS measurements to monitor protein-flavor interactions and understand the key factors involved in the binding process. This was achieved by considering proteins and flavor compounds' molecular structure and physicochemical properties. **Chapter 4** delves into the development and validation of a QSAR prediction model. The model aims to uncover the relationship between structural and physicochemical properties of flavor compounds and their binding affinity to commercial food protein isolates and concentrates. **Chapter 5** explores the effect of salivary proteins (*e.g.*, mucin) on the food protein-flavor binding mechanism through *in vitro* GC-MS measurements. **Chapter 6** examines the drivers underlying the food protein-flavor binding phenomena between commercial food protein isolates and carbonyl flavor compounds in aqueous systems under dynamic *in vivo* measurements: PTR-ToF-MS coupled with Time Intensity. Lastly, **Chapter 7** presents a general discussion, methodological

considerations, suggestions for future research, and principal conclusions of the thesis. **Figure 1.5** illustrates a schematic overview of the framework of this thesis.

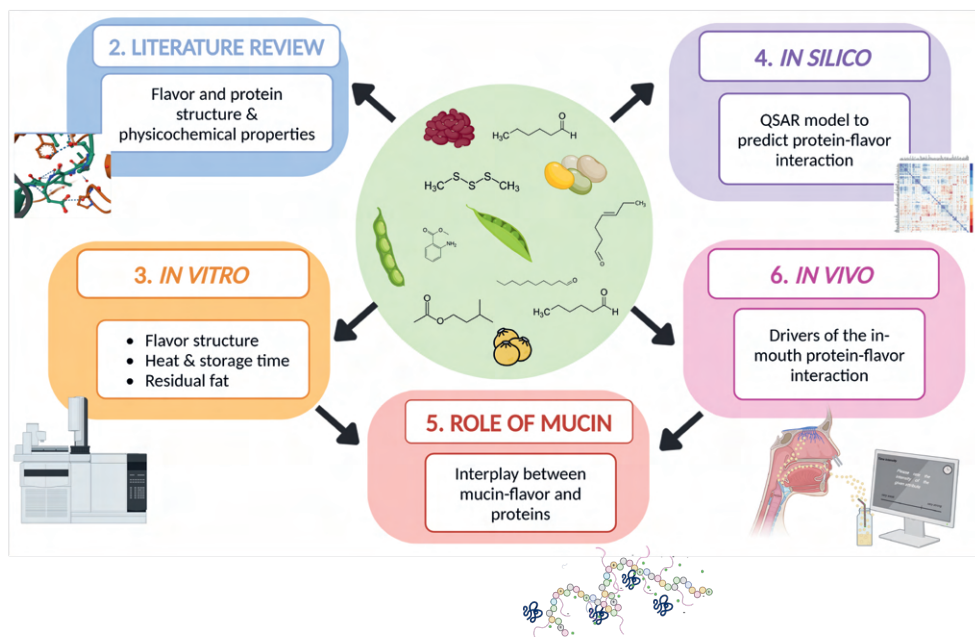


Figure 1.5. Schematic overview of the framework of this thesis, starting with Literature review (2), *in vitro* studies (3) and *in silico* studies (4), into the role of mucin (5), and *in vivo* studies (6). General Introduction (1) and General Discussion (7) are not included in the scheme. (Biorender software).



Flavor them up!

Exploring the challenges of flavored plant-based foods

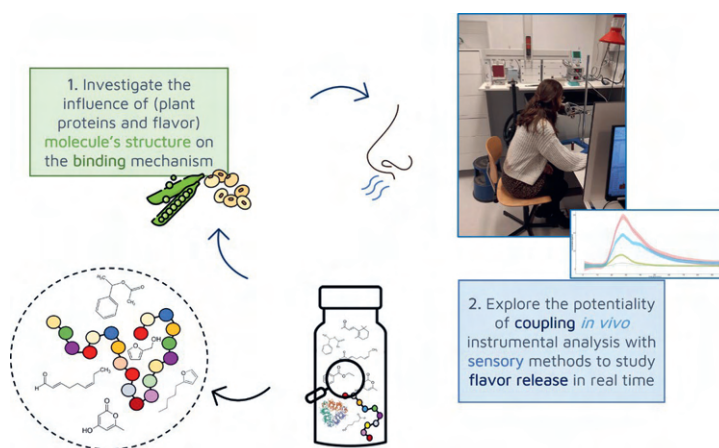
Published as:

Pérez, C. B., Oliviero, T., Fogliano, V., Janssen, H. G., Martins, S. I. F. S. Flavor them up! Exploring the challenges of flavored plant-based foods. *Flavor Fragr. J.* 2023, *38*(3), 125-134. DOI: 10.1002/ffj.3734

Abstract

Food flavorings are often added to enhance the overall flavor experience during food consumption, and their use in plant-based food analogs is crucial. The flavor sensory perception is strongly mediated by flavor-food matrix interactions. Aroma molecules establish chemical and physical bonds with lipids and carbohydrates, but proteins play a pivotal role in strong flavor-binding, minimizing aroma release, and quenching flavor perception. Consequently, final food quality is reduced, and so is consumer acceptance. Depending on the chemical structure of the flavor and the type of protein involved, the strength of the protein-flavor binding can vary. It is important to understand if this interaction remains under dynamic conditions such as oral processing during food consumption. This review aims to gain insights into the influence of both proteins and flavors' chemical structure and physicochemical features on the binding mechanism. Moreover, the potentiality of coupling *in vivo* instrumental analysis with sensory methods to study flavor release in real-time is explored. Elucidating the drivers of flavor interaction with and release from the food matrix is essential to developing flavor solutions for the new generation of plant-based food products.

Keywords: plant-based; proteins; flavor; interaction; release.



TOC Graphic 2. Flavor them up! Exploring the challenges of flavored plant-based foods.

2.1. Introduction

In recent years, plant-based foods are slowly replacing animal-derived food products as consumers are progressively switching to a more vegetable-based diet (Harwatt et al., 2017; Reipurth et al., 2019). Pulses are gaining importance and are increasingly employed in innovative food products, *e.g.*, vegan and vegetarian alternatives, thanks to their rich nutritional profile and suitable techno-functional properties. However, their sensorial appreciation remains a major challenge due to the presence of off-notes (Utz et al., 2022). Flavor science has long been an enigma, where flavor researchers have investigated multiple pathways to reduce, improve, and mask these off-notes by adding desirable aroma compounds. Aroma compounds are known to interact with the constituents of the food matrix, such as the carbohydrates, lipids, and proteins, either through non-specifically partitioning into one of the phases or via specific molecular interactions (Guichard, 2006; Reineccius & Heath, 2006; Weerawatanakorn et al., 2015). Evidence-based understanding of the binding phenomena underlines the key role of food proteins and flavor compounds. In the presence of proteins, flavor molecules are retained in or on the available binding sites of the protein, and consequently, flavor release is suppressed. Consequently, the final food flavor perception is affected, as is consumer acceptance (Overbosch et al., 1991; Suppavorasatit & Cadwallader, 2010).

Flavor binding has been the topic of numerous investigations. Static analytical methods have been primarily employed to assess protein-flavor interactions. Over the last few years, dynamic high-throughput tools have been developed to capture volatile compounds using real-time mass spectrometry, such as Atmospheric Pressure Chemical Ionisation-Mass Spectrometry (APCI-MS) (Su et al., 2021; Yang et al., 2021) and Proton Transfer Reaction-Time of Flight-Mass Spectrometer (PTR-ToF-MS). Progressively, nose space *in vivo* analytical analysis has become more frequently employed to study aroma release from food systems in real-time (Heenan et al., 2012).

Sensory analysis has been interesting in studying sensory responses due to sensory stimuli during food consumption. The Time Intensity (TI), the Temporal Dominance of Sensations (TDS), and the Temporal Check-all-That-Apply (TCATA) have been proven to elucidate relevant information in food flavor release and sensation (Gonzalez-Estanol et al., 2023; Le Calvé et al., 2019; Pionnier et al., 2004).

Although both analytical and sensory methodologies are currently being used to unearth some components of this complex puzzle, there is still a lack of knowledge on the flavor binding domain when combining sensory evaluation and dynamic analytical real-time measurements. Coupling TI or TDS and PTR-ToF-MS offers a peek into aroma release and perception in different food systems, *e.g.*, coffee, chewing gum, mayonnaises, and wine (Charles et al., 2015; Pedrotti et al., 2019; Pittari et al., 2022; Van Eck et al., 2021) and facilitates querying on flavor release and its correlation to flavor perception (Biasioli et al., 2006).

Additionally, despite the rather large number of studies on the binding of flavors to proteins, little is known about the role of both protein and flavor molecular structures and their repercussion on the retention phenomena. Protein-flavor interaction relies strongly on the protein's conformational state and the chemical nature of the aroma molecules. Only a few studies focussed on plant-based proteins, covering mainly soybean (*Glycine max*), pea (*Pisum sativum* L.), and faba (*Vicia faba* L.) proteins (Damodaran & Kinsella, 1981; Heng et al., 2004; Ng et al., 1989) albeit that in the last five years, there has been some interest in studying canola and potato proteins (Lopez et al., 2018; Wang & Arntfield, 2017).

The present paper reviews the scientific approaches to describing flavor and protein (chemical) structures and physicochemical features and uses these to explain their impact on flavor retention and release. Although plant-based proteins are mainly described, animal-derived proteins are also considered for comparison purposes to discuss the flavor binding paradigm.

2.2. Chemical and physical features of both proteins and flavors influencing the interaction mechanism

Hydrophobic interactions, hydrogen bonds, van der Waals, ionic/electrostatic forces, and covalent bonds are the primary protein-flavor interactions (**Figure 2.1**) (Andriot et al., 1999; Chobpattana et al., 2002). These interactions can be reversible if resulting from physical adsorption via non-covalent bonds or irreversible if caused by chemical reactions and the formation of covalent bonds (Gremlı, 1974; Van Ruth et al., 2001). The nature of the interaction depends on the type and spatial configuration of the protein, the aroma molecules involved, and the experimental conditions (pH, ionic strength, temperature, *etc.*).

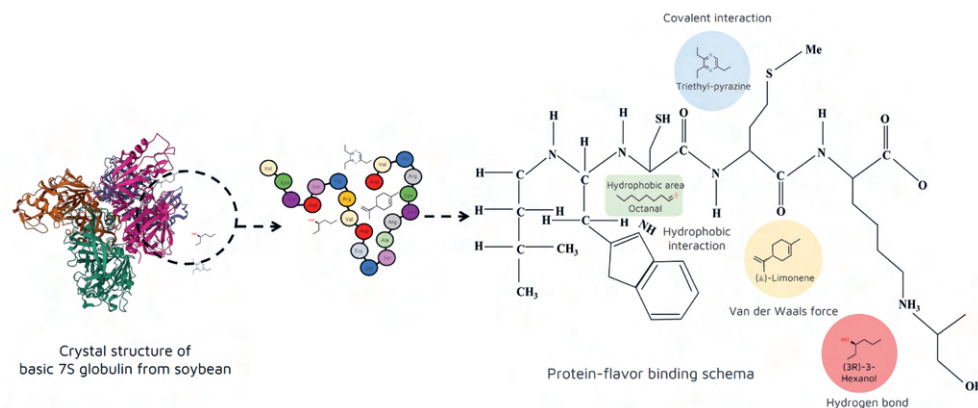


Figure 2.1. Overview of the different protein-flavor interactions depending on the flavor molecule. Hydrogen bonds, hydrophobic interaction, van der Waals force, and covalent binding are reflected in various colors. Adapted from Reineccius & Heath, 2006; Yoshizawa et al., 2011.

2.2.1. Plant protein's physicochemical features

Protein chains are folded in a particular manner, giving a well-defined three-dimensional structure that is held together by disulfide bridges and hydrogen bonds, influencing the protein-binding affinity (Plug & Haring, 1993). A protein's surface contains "*hollow cavities*", or "*hydrophobic sites*", where small ligands can bind (Sotriffer & Klebe, 2002). Not all these cavities are ligand-binding

sites for all flavor species (Rossi et al., 2006). Binding sites can be specific to certain flavor molecules where only certain molecules fit. Additionally, the number of these specific sites is limited, and consequently, these sites can be readily saturated when flavor substances bind (Kühn et al., 2006). Proteins that have structurally comparable binding sites are more predisposed to bind to similar incoming ligands (Tachibana et al., 2021). The multiple functional areas of the proteins offer numerous available binding sites for a diverse range of molecular interactions differing in nature and strength (**Table 2.1**). As plant-based proteins such as soybeans and peas have gradually gained interest in being used as meat protein replacers in new food applications (Kim et al., 2020; Wang & Arntfield, 2017), their structural differences and impact on flavor binding will be evaluated (**Table 2.1**).

Table 2.1. Soybean and pea protein's structure features and their possible implications in the protein-flavor interaction.

Proteins	Secondary structure	Amino acid composition	Role on binding	References
Soybean (<i>Glycine max</i>)	<p>80% of salt-extractable globulins: glycinin (11S) and β-conglycinin (7S) protein fractions:</p> <ul style="list-style-type: none"> 11S is a hexamer with five subunits. It consists of α and β polypeptides linked by disulfide bonds and held together by electrostatic and/or hydrogen forces. Hydrophobic interactions stabilize the entire structure. 7S is a glycoprotein formed by α, α', and β subunits clustered together by non-covalent interactions. 	<ul style="list-style-type: none"> 11S is rich in sulfur-containing amino acids, which promote flavor binding. 7S is low in sulfur-containing amino acids. β subunits lack methionine, cysteine, and tryptophan residues. The extension regions at the N-terminal side display large quantities of glutamic and aspartic acid. 	<p>The protein's structure is stabilized by hydrophobic interactions essential for flavor binding.</p>	<p>O'Keefe, 1988; Damodaran & Kinsella, 1981; Hsiao et al., 2015; Kim et al., 2020; Wang & Arntfield, 2017</p>
Pea (<i>Pisum sativum</i> L.)	<p>70-80% of globulins and 30% of water-soluble albumins. Globulins consist of legumin (11S), vicilin (7S), and convicilin protein fractions:</p> <ul style="list-style-type: none"> 11S comprises an acidic (α) and a basic (β) subunit covalently linked by a disulfide bridge. Acid subunits are located at the N-terminal side, on the surface, while basic units are found at the hydrophobic core. 7S is a trimer maintained by hydrophobic interactions. Convicilin is linked by non-covalent bonds 	<ul style="list-style-type: none"> 11S is known for its sulfur amino acids. 7S contains high levels of aspartic and glutamic acids, arginine, and lysine but has low levels of sulfur-containing amino acids and tryptophan. Convicilin possesses acidic and hydrophobic residues. It contains sulfur amino acids with highly charged N-terminal regions but lacks polar regions. 	<p>β-sheet is the major secondary structure located in the interior of the folded hydrophobic protein patches. Pea proteins are depicted by the absence of a disulfide structure, which could contribute to their low affinity for binding aldehydes.</p>	<p>Heng et al., 2004; Lam et al., 2018; O'Kane, 2004; Tulbek et al., 2017; Wang & Arntfield, 2014</p>

Proteins are susceptible to structural modifications due to the adsorption of a flavor molecule; however, the extent of these alterations is dependent on the concentration and chemistry of the flavor compounds (Dinu et al., 2022). Guo et al., 2019 proved the presence of two classes of binding sites for hexyl acetate (HxAc) and heptyl acetate (HpAc) in SPI systems. In contrast, linalyl formate (LiFo) and linalyl acetate (LiAc) displayed a distinctly binding pattern. The studied ester molecules showed non-specific binding to the hydrophobic surface of the SPI rather than specific adsorption in one of the protein's hydrophobic pockets as a result of the presence of a flexible acyl chain in their structure (Adachi et al., 2003) (**Figure 2.2**). The authors suggested that flavor compounds with low binding constants and a non-flexible structure will not fit properly in the protein's cavity and will not bind correctly on its surface.

Until now, due to the protein's molecular heterogeneity, it has been challenging to precisely assess by X-ray crystallography the SPI's conformation and, consequently, the binding sites (Adachi et al., 2003; Guo et al., 2019). However, five major 11S globulin subunits have been identified in soybeans. **Figure 2.2** shows a schematic illustration of the A3B4 homohexamer subunit and its possible interaction with flavor molecules. Adachi et al., 2003 described twenty-five hydrophobic residues in the binding regions of the A3B4 homohexamer. Exclusively and arbitrarily, Val-322, Pro-346, and Leu-357 have been selected to illustrate the interaction with the ester molecules. Developing a more detailed understanding of specific binding regions and binding mechanisms could aid in understanding the flavor of plant proteins.

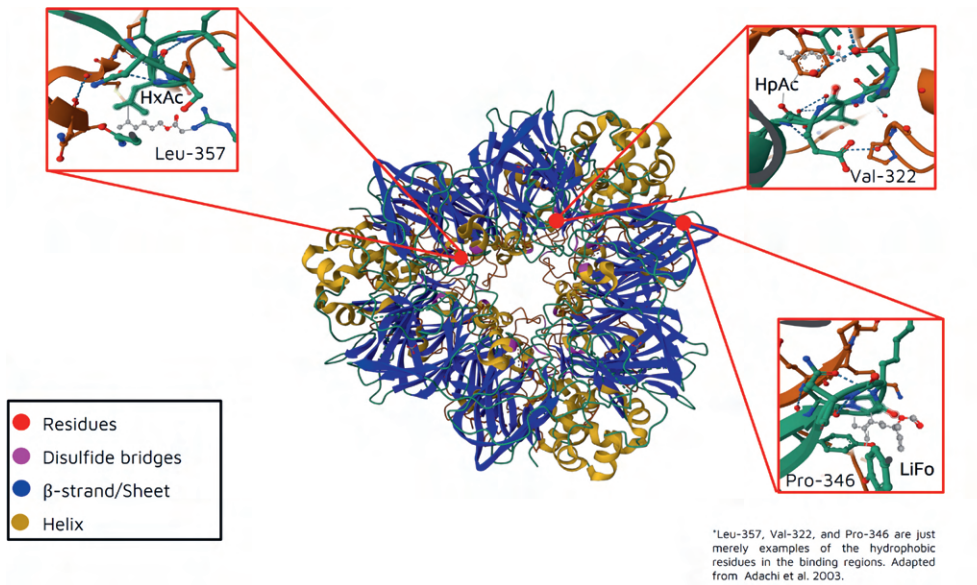


Figure 2.2. Crystal structure of soybean 11S globulin: Glycinin A3B4 homohexamer (RCSB, 1OD5). Adapted from Adachi et al., 2003.

Generally, the number of binding sites depends on the type of flavor, protein source, and the experimental conditions applied (**Table 2.2** and **Table 2.3**). Binding parameters are computed from the Scatchard plots (Scatchard, 1949) and/or Klotz plots following the formula [2]:

$$\frac{1}{v} = \frac{1}{n} + \frac{1}{nK[L]} \quad [2]$$

where v is the number of moles of the flavor compound bound per mole of protein, n is the number of binding sites on the protein, K is the binding constant, and L is the concentration of the incoming ligand.

Table 2.2. Soybean protein's binding sites based on the interaction with different aroma compounds.

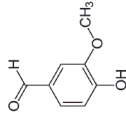
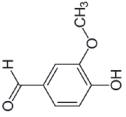
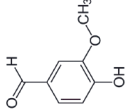
Proteins	Compounds	Chemical structure	Flavor molecular weight (g/mol)	Binding sites	Techniques/conditions	References
Soy Protein Isolate (SPI)	2-nonanone		142.24	4	Equilibrium dialysis (30 mM Tris-HCl buffer, pH 8.0), 10 mM 2-mercapto-ethanol, 0.02% sodium azide, 1(w/v)% protein solution.	Damodaran & Kinsella, 1981
	2-nonanone		142.24	10	Equilibrium dialysis (30 mM Tris-HCl buffer, pH 8.0), 10 mM 2-mercapto-ethanol 0.2% sodium azide, 1(w/v)% protein solution.	O'Neill & Kinsella, 1987
Glycinin/β-Conglycinin	Methyl pyrazine		94.11	3.3/3.6	Microreactor with volatile trapping in a low moisture model system.	Einig, 1983; Wang & Arntfield, 2014
	Vanillin		152.15	10.92/ 3.8	Micropartition system (MPS) and high-performance liquid chromatography (HPLC), 2(w/v)% protein solution, 50 mg/kg vanillin at 4 or 12 °C.	Li et al., 2000
Soy Protein Isolate (SPI)	Vanillin		152.15	13.6/ 2.31/ 0.48	Gas Chromatography-Mass Spectrometry (GC-MS), (50 mM phosphate buffer, pH 7.0), 3(w/v)% protein solution, 9.96 mg/kg vanillin at 5, 15, 21 °C.	Suppavorasatit & Cadwallader, 2010

Table 2.3. Pea and *Vicia faba* protein's binding sites based on the interaction with different aroma compounds.

Proteins	Compounds	Chemical structure	Flavor molecular weight (g/mol)	Binding sites	Techniques/conditions	References
Pea Protein Isolate (PPI)	Diacetyl		86.09	18	Gas Chromatography (GC), (distilled water, pH 7.0), 4(w/v)% protein concentration, 0.1 mg/kg diacetyl.	Dumont and Land, 1986
Pea Protein Concentrate (PPC)	Vanillin		152.15	1.79	Fluorescence spectroscopy (10 mM citrate buffer, pH 6.0), 2(w/v)% protein concentration, vanillin concentrations from 3.29 to 32.86 mM.	Houde et al., 2018
<i>Vicia faba</i> 11S Globulin	Hexyl acetate		144.2	13	Gas-liquid chromatographer (50 mM phosphate buffer, pH 7.2), 1(w/v)% protein concentration, 0.5 mM hexyl acetate.	Semenova et al., 2002

Binding sites could be structurally more suitable and specific to one or another flavor molecule. For instance, the interior of the legumin is only available for aroma molecules with short chains, *e.g.*, butyl acetate (BuAc) and amyl acetate (AmAc) (**Figure 2.3**) (Semenova et al., 2002).

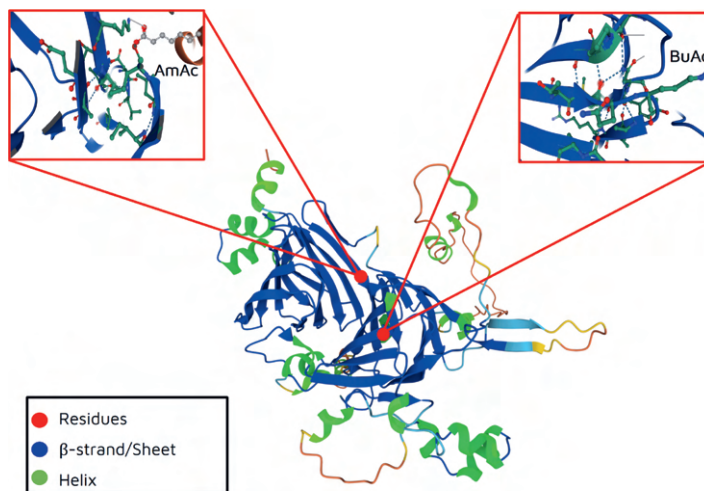


Figure 2.3. Schematic representation of both butyl acetate (BuAc) and amyl acetate (AmAc) binding behavior to legumin A CAA38758.1 of *Vicia faba* L. Adapted from Semenova et al., 2002 and UniProtKB/Swiss-Prot.

Protein-flavor binding mechanisms rely on possible phenomena that influence the final state of both protein and flavor. Flavor-binding to proteins can cause protein structural modifications (Wang & Arntfield, 2015; Zhang et al., 2023), where the protein can partly unfold and expose alternative binding sites (Damodaran & Kinsella, 1981; Kim et al., 2020), or even open new ones (Jouenne & Crouzet, 2000; Landy et al., 1995). Physical changes in the secondary structure of the protein after flavor binding promote the interaction between the flavor's hydrophobic groups and those exposed on the protein's surface; thereby, the protein's surface hydrophobicity is decreased (Landy et al., 1995). As a consequence of the binding, if aldehyde flavor compounds are present, covalent bonds can be formed between the aldehyde group and the lysine amino residue, and, accordingly, the available free lysine residues are reduced. Hence, not only

physical but chemical changes also occur. Protein sulfhydryl groups may interact with sulfur flavor compounds through interchange reactions (Adams et al., 2001), which eventually will result in the loss of disulfides and the formation of free thiols.

So, not only does the protein's configuration and state influence the accessibility of flavor molecules to its binding sites, but binding can also influence the protein's configuration.

Next to routine analytical methods, molecular modeling approaches are currently being applied to predict interactions between small molecules and proteins. Software tools for protein-ligand binding affinity prediction, such as molecular docking, could provide further information to identify the protein cavities that play a major role in flavor binding (Zhao et al., 2020). Additionally, such software programs can also be used to understand how flavor binding affects the structure and conformation of proteins (Dinu et al., 2022). Analyzing the surface of the protein and calculating energetically favorable locations for flavor molecules to bind might yield an alternative technique for quantitative assessment of flavor binding to proteins. Recently, protein's binding affinity has been characterized by implementing both spectroscopic analyses and docking studies under physiological conditions (Cheng et al., 2017). The interaction between β -Lactoglobulin (BLG) and cyanidin-3-O-glucoside was successfully defined and monitored, providing solid knowledge of the binding forces involved and on protein's structural changes resulting from the binding. Authors observed that the binding between BLG and cyanidin-3-O-glucoside displayed modifications on the protein's secondary and tertiary conformation, which were shown as an increase in the structure of β -sheet and a decrease in the structure of α -helix (Cheng et al., 2017). The use of molecular docking and spectroscopy techniques was recently investigated in plant-based proteins (Bi et al., 2022). Bi et al., 2022 confirmed that hydrogen bonding and hydrophobic interactions occurred between the flavor molecules and pea protein.

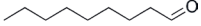
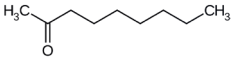
2.2.2. Flavor's physicochemical features

Flavor is one of the most relevant and critical attributes determining the consumer's food choice (Guichard, 2006). There are an extensive number of flavor species representing an array of different chemical functionalities and structures. Variation in the flavor molecule's structure leads not only to a variety of aroma and taste profiles (sweet, bitter, fresh, rancid, *etc.*) but also to different binding affinities to proteins and, as a result, to the protein-flavor interaction. Flavor-related factors such as chemical class, location of the functional group, spatial configuration, chain length, and unsaturation all contribute to the retention phenomena and the final product sensory profile (Weerawatanakorn et al., 2015; Zhou & Cadwallader, 2006).

Influence of different chemical classes and location of the functional group of flavor molecules on the interaction mechanism

Flavor's architecture affects protein-flavor interaction and binding capability. The location of the flavor's functional group dictates flavor affinity toward protein binding and is fundamental in defining the flavor retention degree. Molecules structurally similar can show different binding capacities to proteins. As an example, linear chain carbonyl compounds nonanal and 2-nonanone were studied in buffered 1% SPI (Damodaran & Kinsella, 1981) and 0.5% whey protein isolate (WPI) systems (Kühn et al., 2008). Samples were analyzed by measuring the volatiles in the headspace (HS). The position of the keto group at the end of the structure (nonanal) led to a greater retention as compared to when the functional group was positioned closer to the core of the structure (2-nonanone) (**Table 2.4**). If the functional group is located in the second position, hydrophobic interactions are limited (Kühn et al., 2008) and binding affinity is reduced. On the contrary, if the polar group is positioned at the very end of the structure, it allows full contact between the entire chain of the aldehyde and the protein (Damodaran & Kinsella, 1981). Structural differences influence the ability of the molecules for hydrogen bonding interaction (Ayed et al., 2014).

Table 2.4. Binding of selected nine carbon atom flavor compounds (1 mg/kg) to whey protein isolate (WPI) (0.5%) (Kühn et al., 2008).

Compounds	Chemical structure	LogP	Flavor molecular weight (g/mol)	Binding (%)
Nonanal		3.27	142.24	68.3
2-nonanone		2.9	142.24	39.2

In vivo approaches have been additionally and simultaneously conducted to static measurements to further understand how the flavor's structure affects the protein binding. Buettner & Schieberle, 2000 applied the spit-off odorant methodology to determine the effect of the flavor's chemical class on their release in the mouth. In aqueous flavored model solutions (100 µg/L), the presence of the hydroxyl group on the flavor's structure led to higher retention in the mouth than in the absence of it.

Influence of the molecular spatial configuration of flavor molecules on the interaction mechanism

Flavor dimensions are likewise relevant in the binding process. Selectivity in cyclodextrin chemistry was investigated by Kano, 1993, where the crystal structures of α , β , γ - cyclodextrins were determined by X-ray analyses. The author reported that the increase in bulkiness of the molecule contributed to van der Waals interactions. Van der Waals forces will dominate if the size of the cyclodextrin's cavity resembles the guest molecule's dimensions and *vice versa*, while hydrophobic interactions will be dominant if the size of the host molecule is smaller in comparison to the cyclodextrin (Seuvre & Voilley, 2017; Kano, 1993). Kano, 1993 concluded that the binding force will depend on the host molecule's size or spatial configuration, which will consequently influence the contact between the aroma compounds and the protein's binding sites (Seuvre & Voilley, 2017).

The effect of a flavor compound's chemical structure (*e.g.*, *cis*-3-hexen-1-ol and 1-hexanol) on the binding to SPI was investigated by inverse gas chromatography (Zhou & Cadwallader, 2006). *Cis*-3-hexen-1-ol was retained to SPI to a lesser degree due to its greater molecular width. Molecules with a spherical structure are more likely to experience steric hindrance and, hence, are restricted from accessing the protein's hydrophobic pockets (Zhou & Cadwallader, 2006) which in turn prevents their binding.

The prevalence of binding of a protein and a ligand might follow the principle of complementarity of shape (Crowe & Bradshaw, 2014), where there is a recognition effect. Note that strong binding in a cavity is not just about a size match but also about specific interactions of the molecule caught in the three-dimensional cavity with the amino acids that form it.

Not only static but also dynamic approaches were implemented to study flavor release in animal-based foams by Tyapkova et al. 2016 through nose space-PTR-MS analysis. For that, ethyl butanoate and *cis*-3-hexen-1-ol were compared in each egg foam formulation. The authors demonstrated that the ester flavor molecule was released less than the alcohol flavor molecule. Based on the rule of hydrophobicity, it is generally recognized that the more hydrophobic a flavor molecule is, the more it will be retained. Contrary to this universal statement, *cis*-3-hexen-1-ol (LogP=1.61) interacts more strongly with the egg albumen foam matrix than its counterpart ethyl butanoate (LogP=1.77). This confirms that, indeed, not only the hydrophobicity but also a flavor's spatial configuration impacts the protein binding phenomena.

Next, exhaled air from human breath was analyzed and monitored in real-time to determine flavor transfer from the food system to the olfactory epithelial tissue as a function of flavor's molecule spatial configuration (Beauchamp et al., 2010; Buettner & Beauchamp, 2010; Buettner & Welle, 2004). For that, Buettner & Welle, 2004 employed an olfactometer device connected to a PTR-MS. The authors addressed differences in volatile persistence and adsorptive potencies due to **(1)** possible panelist's adaptation, which may reduce sensory acuity, **(2)**

flavor compounds were no longer available in the oral cavity and **(3)** flavor structure.

Influence of the chain length of flavor molecules on the interaction mechanism

It is agreed that increasing a molecule's carbon chain length leads to a higher adsorption ability, irrespective of the flavor's chemical class or type of protein involved (Guichard, 2006; Pelletier et al., 1998; Wang & Arntfield, 2014). Studies of the effect of a flavor's chain length on protein binding are universally of interest and, thus, have been performed with carbonyl compounds, alcohols, pyrazines, and esters when binding to whey, soybean, and pea protein solutions. Affinity chromatography, exclusion size chromatography, GC-MS, and APCI-MS were commonly used in binding studies to identify and quantify the chain length impact. The binding affinity between ligand and substrate can be experimentally measured by calculating the binding constant at equilibrium. Andriot et al., 2000 determined the binding constants between ketones and BLG. 2-Heptanone (C₇) revealed a binding constant of 330 M⁻¹, whereas 2-octanone (C₈) and 2-nonanone (C₉) showed values of 950 M⁻¹ and 2440 M⁻¹, respectively. According to Andriot et al., 2000 the stronger tendency of the longer carbon chain structures to bind proteins is linked to hydrophobic interactions.

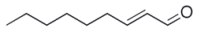
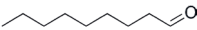
Correspondingly, a sensory approach based on the imitation of retronasal conditions was applied to determine the effect of flavor chain length and hydrophobicity on flavor release from wine matrices (Piombino et al., 2019). Thus, an experimental retronasal aroma simulator device was equipped with a solid phase microextraction (SPME). The obtained results Piombino et al., 2019 showed that under retronasal conditions, the most hydrophilic flavor compounds (LogP≤0) were released to a greater extent from wine matrices than flavor compounds with a LogP between 0 and 2, which were most affected by the wine matrix formulation instead.

Influence of double bonds of flavor molecules on the interaction mechanism

Unsaturation or the presence of double bonds in the flavor's structure may influence protein retention (Ayed et al., 2014). First, double bonds provide structural rigidity, as they lack the flexibility to turn (Atkins, 2003). Second, the presence of π electrons in the double bond enhances the flavor's negatively charged surface area (Zhou & Cadwallader, 2006).

Kühn et al., 2008 studied protein-flavor binding by HS-SPME and GC, where *trans*-2-nonenal and nonanal were used at a flavor concentration of 1 mg/kg. *Trans*-2-nonenal (characterized by one double bond) displayed a higher affinity for 0.5% buffered WPI solutions than nonanal (absence of double bonds). Despite *trans*-2-nonenal being less hydrophobic than nonanal (see **Table 2.5**), it bound to a greater extent. The authors attributed this to the reaction that occurred between the alkenal double bond and lysine and histidine residues, named Michael addition (Kühn et al., 2008). To validate the hypothesis, the amino acid profile of WPI (0.025%) was analyzed in the absence and presence of *trans*-2-nonenal (25 mg/kg). Histidine, lysine, cysteine, and methionine reacted with *trans*-2-nonenal, suggesting that the interaction between WPI and *trans*-2-nonenal tended to be irreversible.

Table 2.5. Physicochemical properties of some specific nine-carbon atom flavor compounds (Kühn et al., 2008).

Compounds	Chemical structure	LogP	Flavor molecular weight (g/mol)	Binding (%)
<i>trans</i> -2-nonenal		3.06	140.23	72.3
Nonanal		3.27	142.24	68.3

Under static conditions, the significance of a molecule's architecture on protein-flavor interaction is evident. However, integrating dynamic analysis with sensory methods to assess aroma release and perception in plant-based food systems has rarely been explored. To date, no studies have reported pairing sensory evaluation with *in vivo* PTR-ToF-MS to evaluate the relevance of flavor and protein structure on the kinetics of flavor release during the consumption of flavored plant-based protein solutions.

2.3. Conclusions

Understanding the fundamentals of flavor chemistry opens the door to new insights in the field. Flavor plays a crucial role in food acceptance, yet protein-flavor binding can impede aroma release. Uncovering the drivers behind the protein-flavor phenomena is essential to address this concern. The molecular dynamics of protein-flavor interaction constitute a multifaceted mechanism. The structure of proteins plays a significant role in determining how they bind with flavor compounds. Specific regions of the protein molecule exhibit a preference for certain flavors dictated by its three-dimensional structure. Additionally, the geometry of flavors is a key factor in protein retention, as it can induce steric hindrance or even lead to chemical reactions resulting in covalent binding.

As human oral processing is a dynamic event where flavors are not continuously released from the food system into the oral phase, these interactions should be measured over time. Combining dynamic *in vivo* techniques and sensory methodologies could provide a more comprehensive understanding of the flavor molecules involved in the binding mechanism when proteins are present, shedding light on the protein-flavor interaction domain.

Clarifying the underlying protein-flavor mechanism will undoubtedly be a significant step in strategically modulating the protein-flavor interaction and balancing aroma composition in a food system, ultimately enhancing the overall flavor profile.



Unraveling the role of flavor structure and physicochemical properties in the binding phenomena with commercial food protein isolates

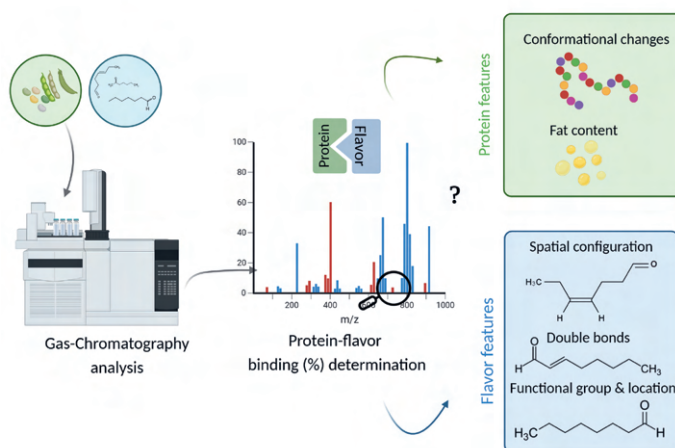
Published as:

Barallat-Pérez, C. B., Janssen, H. G., Martins, S., Fogliano, V., Oliviero, T. Unraveling the role of flavor structure and physicochemical properties in the binding phenomena with commercial food protein isolates. *J. Agric. Food Chem.* 2023, *71*, 50, 20274-20284. DOI: 10.1021/acs.jafc.3c05991

Abstract

Food protein-flavor binding influences flavor release and perception, with the complexity of the binding phenomena rooted in the properties of both the flavor and the protein. To explore this complexity, molecular interactions between commercial whey- or plant-based protein isolates (PI) such as pea, soy, and lupin and carbonyl and alcohol flavor compounds were assessed using static headspace (HS) GC-MS. The HS results revealed that not only did the displacement of the carbonyl group from the inner part of the flavor structure towards the edge promote binding up to $52.76\% \pm 5$, but also the flavor's degree of unsaturation played a role. Similarly, thermal treatment led to a slight increase in hexanal-protein binding, likely due to protein conformational changes. Protein's residual fat (<1%) appeared insufficient to significantly enhance flavor binding to PI. Despite the complexity of commercial food protein isolates, the results suggest that binding is primarily influenced by the flavor's structure and physicochemical properties, with the protein source and residual fat playing a secondary role

Keywords: flavor structure; protein-flavor binding; plant-based proteins; commercial food protein isolates; molecular interactions.



TOC Graphic 3. Unraveling the role of flavor structure and physicochemical properties in the binding phenomena with commercial food protein isolates. (Biorender software).

3.1. Introduction

Over the last decades, consumers' food-related preferences have shifted towards the exploration and consumption of more plant-based foods (Cordelle et al., 2022). Plant-based protein isolates (PI), such as proteins isolated from peas (*Pisum sativum* L.) (PPI) and soybeans (*Glycine max*) (SPI), have emerged as substitutes for animal proteins in the development of novel plant-based protein foods, including plant-based beverages. This is due to their high protein levels, low-fat content, and favorable techno-functional properties (Manski et al., 2007). Currently, lupin (*Lupinus angustifolius* L.) protein isolate (LPI) has garnered significant interest for use in high-protein-based beverage applications, attributed to its low gelling and viscosity properties (Berghout, 2015).

From a molecular perspective, plant-based proteins exhibit structural differences compared to animal-derived proteins. Plant-based proteins are usually seed proteins characterized by more complex tertiary and quaternary structures, higher hydrophobicities, and greater molecular weight. This is often accompanied by a higher abundance of non-polar amino acids in the protein sequence (Anantharamkrishnan et al., 2020). Structural disparities not only exist between animal- and plant-derived proteins but also among various plant-based protein sources. Despite their seemingly similar structures, plant-derived proteins vary due to the presence of intra- and inter-disulfide bridges, α -helices, or β -sheets, resulting in unique molecular interactions with other food components (such as carbohydrates, fats, sugars, flavor compounds, etc.) in the food system. Consumer studies often rate plant-based protein foods, including beverages, as lower in taste, texture, and appearance compared to their animal counterparts (Cordelle et al., 2022). To address this issue and optimize the final food flavor profile, food developers frequently incorporate flavor compounds as additives to enhance the organoleptic characteristics of plant-based foods. It is worth noting that the literature does not consistently use the terms "flavor compounds", "aroma compounds", and "volatile organic compounds". This study will use the term "flavor compounds" to maintain consistency.

The added flavor compounds are known to extensively interact with plant-based proteins through physical or chemical molecular interactions (Reineccius, 2006). These interactions may result in reversible and weak bonds (such as hydrophobic interactions, hydrogen bonds, van der Waals forces, and ionic/electrostatic forces) or non-reversible and stronger bonds (covalent linkages) (Anantharamkrishnan et al., 2020; Andriot et al., 1999). Hydrophobic interactions typically involve the intricate interplay between the non-polar hydrophobic interior of the protein and the non-polar (aliphatic) segment within the flavor compounds (*e.g.*, aldehydes and ketones). Similarly, aldehydes can form chemical bonds via covalent linkages with proteins by reacting with the ϵ -amino group of lysine, resulting in amide linkages (Anantharamkrishnan et al., 2020). Conversely, hydrogen bonds tend to play a predominant role in the presence of aliphatic alcohols. Thus, it is reasonable to assume that the complexity of protein-flavor binding largely depends on the flavor's molecular structure and physicochemical properties, significantly impacting flavor perception. Nevertheless, the protein structure should not be overlooked when using commercial food protein isolates.

Since the early 1950s, two-step extraction/isolation procedures have been used industrially to produce pea, soy, and lupin protein concentrates/isolates (Gueguen, 1983). Protein purity in isolates and concentrates depends on the separation method and starting substrate, resulting in different purity levels in carbohydrates, fat, and sugars. However, most protein-flavor investigations use extracted, defatted, and highly purified proteins and/or protein fractions (such as β -conglycinin, glycinin, β -lactoglobulin, and α -lactoglobulin, *etc.*) (Bi et al., 2022; Heng et al., 2004; Wang & Arntfield, 2014), which are generally not used in food processing. Commercial and laboratory-purified proteins widely differ in structural, physicochemical, and techno-functional properties (such as rheological behavior, viscosity, gelling properties, water solubility, *etc.*) (Añón et al., 2001; Ma et al., 2022). From a molecular perspective, an in-depth structural investigation of a single protein structure is necessary to fully understand the protein's role in the flavor binding phenomena. However, it may not have practical and realistic food applications. Currently, it seems unfeasible to achieve the

requested requirements of food texture and appearance solely with individual isolated protein fractions. The meat and dairy analogs industry relies on using a mixture of non-refined protein isolates to successfully meet the desired food standards. Despite their high protein content, fat residues may still be present, which is a factor of concern. Fat promotes the binding of flavor as these are mostly hydrophobic (Roberts et al., 2003). From an industrial-applied perspective, the fat-flavor binding mechanism is generally considered a barrier during food formulation. The food's flavor profile may be imbalanced, resulting in challenges in releasing and perceiving the flavor during consumption. Thus, the relative contribution of protein's residual fat to the protein-flavor binding mechanism should not be neglected.

Throughout food industrial processes, protein-based foods are held uninterrupted for extended periods under different temperature conditions to prevent bacterial growth and assure food product freshness and safety. The storage period between food manufacturing and food consumption may be lengthy, resulting in both changes in food texture and color and many cases, deterioration of food flavor, leading to a loss of food flavor quality (Reineccius, 2010). When thermal treatment is applied to further process the food product, protein structural modifications can occur (Wang & Arntfield, 2015), as proteins may (partly) unfold and aggregate. Bread (Schieberle & Grosh, 1992), coffee (Müller & Hofmann, 2007), and peanuts (Williams et al., 2006) are some examples that have been studied to determine flavor binding under time-temperature conditions. To the best of our knowledge, there is hardly any information on the impact of both time and processing temperatures on the flavor binding behavior of animal-based proteins, such as WPI and PI.

We hypothesize that the protein-flavor binding mechanism is mainly governed by the flavor's molecular structure and configuration. Thus, the present study aims to uncover the key role of flavor structure underlying the protein-flavor binding phenomena with a special focus on commercial food protein isolates (*e.g.*, animal and plant-derived proteins). As flavor binding to proteins is a multifactorial rather than one-directional mechanism, the role of the flavor's physicochemical

properties may need to be considered. For this purpose, three PI (PPI, SPI, and LPI) and one animal-based protein (whey protein isolate, WPI), non-purified and commercially available, were characterized utilizing spectrofluorimetric and NMR technology. Five aldehydes, four ketones, and one alcohol flavor compound were specifically selected to determine the influence of the unsaturation, spatial configuration, alkyl chain type, position of the carbonyl group, and chain length on the degree of binding and the binding mechanism. Flavor-matrix interactions were assessed by static headspace (HS) GC-MS.

The ultimate goal is to guide food manufacturers in flavor creation, and in efficiently designing novel plant-based food products based on consumer-desired flavor profiles while minimizing flavor dosing.

3.2. Materials and Methods

3.2.1. Flavor compounds

The flavor compounds investigated were chosen based on their conformational and intrinsic physicochemical characteristics, such as the unsaturation, spatial configuration, alkyl chain type, location of the carbonyl group, and chain length (**Table S3.1**) (PubChem). Hexanal, heptanal, *trans*-2-heptenal, *cis*-4-heptenal, octanal, 2-octanol, 2-heptanone, 2-octanone, 2-nonanone and 2-decanone were purchased from Sigma-Aldrich (St. Louis, Missouri, USA) and all had a purity of $\geq 95\%$.

3.2.2. Protein sources

Plant-based protein isolates (PI) were acquired from different suppliers; soy protein isolate (SPI) Supro[®] XT219D IP was kindly supplied by Solae (St. Louis, Missouri, USA). Pea protein isolate (PPI) FYPP-85-C-EU was obtained from AGT (Waalwijk, The Netherlands), and lupin protein isolate (LPI) 10600 was purchased from ProLupin (Grimmen, Germany). The animal-based protein used in this study, whey protein isolate (WPI) BiPro[®], was provided by Davisco International (Le Sueur, Minnesota, USA). Manufacturer-specified specifications are shown in **Table**

S3.2 and **Table S3.4**. Nitrogen-to-protein conversion applied was $N \times 6.25$. Proteins were selected based on their chemical structure, composition, and frequency of use in plant-based food alternatives (*i.e.*, beverages). To decrease variability in the results, protein batches were kept away from light and oxygen, and they were adequately sealed and stored in a cool (10-15 °C) and dry place.

3.2.3. Other chemicals or materials

$\text{Na}_2\text{HPO}_4 \cdot 7\text{H}_2\text{O}$, $\text{NaH}_2\text{PO}_4 \cdot 2\text{H}_2\text{O}$, Na_2HPO_4 , 8-anilino-1-naphthalenesulfonate, chloroform (99.8%), and methanol were analytical grade and purchased from Sigma-Aldrich. Pierce™ BCA ($\text{HO}_2\text{CC}_9\text{H}_5\text{N}_2$) assay kits were acquired from Thermo Fisher Scientific Inc., (Waltham, Massachusetts, USA) and contained albumin standard ampules (2 mg/mL, 10 x 1 mL containing bovine serum albumin (BSA) at a concentration of 2 mg/mL in 0.9% saline and 0.05% sodium azide), and two BCA™ (bicinchoninic acid) reagents: A) Na_2CO_3 , NaHCO_3 , $(\text{HO}_2\text{CC}_9\text{H}_5\text{N})_2$ and $\text{C}_4\text{H}_4\text{N}_2\text{O}_6$ in 0.1 M NaOH; B) 4% $\text{CuSO}_4 \cdot 5\text{H}_2\text{O}$ (25 mL). Ellman's reagent (5',5'-dithio-bis (2-nitrobenzoic acid) (DTNB)) from Thermo Fisher Scientific Inc., was used to estimate the protein sulfhydryl content (-SH). Tris-glycine buffer and ethylenediaminetetraacetic acid (EDTA) were obtained from Sigma-Aldrich.

3.2.4. Preparation of food flavor stock solutions

Each of the selected flavors was separately prepared in a 100 mL amber bottle (Pyrex®, Thermo Fisher Scientific Inc.) and closed with a screw cap. Flavor stock solutions were made with sodium phosphate buffer (pH 7.0, 50 mM) at an initial concentration of 10 mg/L according to Wang & Arntfield, 2015. Flavor stock solutions were placed in an ultrasonic water bath (Elma Schmidbauer GmbH, Singen, Germany) for 1 hour at 20 °C to ensure a satisfactory dissolution of the flavor.

3.2.5. Preparation of food protein solutions

Likewise, both animal and plant-derived protein solutions were created following an adapted version of the protocol by Wang & Arntfield, 2015. Specifically, each of the selected proteins (PPI, SPI, LPI, and WPI) was dissolved in sodium phosphate buffer (pH 7.0, 50 mM) at an initial concentration of 2(w/v)%. The choice of a 2(w/v)% protein content was based on high-protein-based beverages available in the market. Subsequently, samples were vortexed for 10-20 seconds at 3200 rpm using a Genie II vortex mixer (Genie™, Sigma-Aldrich, USA) and then placed into an ultrasonic water bath for 20 minutes at 20 °C to ensure thorough mixing of the solutions. Following this, the protein solutions were vortexed again for an additional 10-20 seconds to guarantee homogeneous dispersion of the mixture.

To assess the effect of residual fat on flavor binding to PI (PPI, SPI, and LPI), the proteins were defatted (DPPI, DSPI, and DLPI) using an adapted version of the Bligh & Dyer, 1959 protocol. A solvent mixture of chloroform and methanol in a 1:2(v/v) ratio was utilized, with a product-to-solvent ratio of 1:9(v/v). Samples were vortexed for 5 minutes to facilitate proper contact between the phases, then centrifuged at 4700 x g for 10 minutes using a Multifuge X3R centrifuge (Thermo Fisher Scientific Inc.). After removing all solvents, the samples were air-dried and stored overnight in a fume hood at room temperature (20-22 °C). The remaining fat content was measured using an NMR fat content analyzer (Oracle, CEM Corporation, Abcoude, The Netherlands).

3.2.6. Preparation of the Gas Chromatography-Mass Spectrometry samples (GC-MS)

From a 2(w/v)% protein solution, 1 mL of each protein type was added into a 20 mL GC-MS vial, followed by adding 1 mL of flavor stock solution. This resulted in a final protein concentration of 1(w/v)% and a final flavor concentration of 5 mg/L. The reference sample consisted of a buffered protein solution with no added flavors. The vials were then sealed with metallic screw caps and placed in a water bath (SW22, Julabo GmbH, Seelbach, Germany) at

temperatures of 30 °C, 70 °C, or 90 °C, respectively, with agitation at 125 rpm for 3 hours before headspace analysis. Samples were prepared in triplicate, and after their preparation, they were stored at 5 °C and analyzed weekly.

3.2.7. Binding measurement and calculation

Protein-flavor binding was assessed by HS through GC-MS (Agilent-7890A GC coupled to an Agilent 5975C triple-axis detector MS, Agilent, Amstelveen, the Netherlands). The GC operated in split mode 1:10 at 8 mL/min split flow. Samples were incubated and shaken for 14 minutes at 40 °C, following a modified version of the protocol by Wang & Arntfield, 2015. Subsequently, 1 mL of sample headspace was injected. A DB-WAX 121-7023 column (20 m × 180 μm × 0.3 μm) run at a constant flow of 0.8 mL/min was used. The column temperature was programmed to increase at 40 °C/min to reach 240 °C. The mass spectrometer (MS) operating conditions included 70 eV EI with a mass range of 35-200 Da. MassHunter Quantitative Analysis (MSD ChemStation F.01.03.2357) software was utilized for flavor quantitation. The NIST Mass Spectrometry Library (InChI Library v.105) provided chemical and physical information about the selected flavors. Flavors were analyzed individually to avoid mutual competition for the protein binding sites. Flavor binding to proteins was calculated and expressed as a percentage in the absence and presence of protein using the following equation (Wang & Arntfield, 2015) [3.1]:

$$Binding (\%) = \left(1 - \frac{HS_1 - HS_2}{HS_3}\right) \times 100 \quad [3.1]$$

where HS_1 (protein solution + flavor) is the abundance in the headspace of the flavored protein-based aqueous solution. HS_2 and HS_3 are the abundances in the headspace in the absence of flavor (HS_2) or protein (HS_3).

3.2.8. Protein surface hydrophobicity

The surface hydrophobicity (H_0) of PI and WPI was measured using an adapted version of the protocol described by Li-Chan, Nakai, and Wood (1984). The H_0 was determined using a spectrofluorometer (Perkin Elmer LS50B, Thermo

Fisher Scientific Inc.). This measurement relies on the interaction between 8-anilino-1-naphthalenesulfonate (8-ANS) and the hydrophobic patches on the protein's surface. Protein stock solutions were prepared in duplicate by mixing (Heidolph multi-Reax speed setting 9, Sigma-Aldrich, St. Louis, Missouri) for 4 hours in 3.5 mg/mL sodium phosphate buffer (pH 7.0, 10 mM). After 4 hours, the stock solution is centrifuged (Multifuge X3R, Thermo Fisher Scientific Inc.) at 4700 rpm for 20 minutes. The protein concentration of the remaining solution was determined using a Pierce™ BCA protein assay kit according to the manufacturer's instructions (Pierce, Thermo Fisher). After the soluble protein concentration was determined, a serial dilution was prepared in the 0.4-0.025 mg/mL protein range. 25 µL of 8-ANS was added to 3 mL of each protein solution. The samples were left in the dark for 1 hour to equilibrate. The samples' fluorescence intensity (FI) was measured at an emission wavelength of 470 nm using an excitation wavelength of 390 nm (Chang et al., 2019). The H_0 index was calculated as the slope of the plotted FI measurements vs. concentration. The H_0 was calculated from linear regression at a 95% confidence interval.

3.2.9. Protein sulfhydryl groups

Sulfhydryl groups (-SH) of PI and WPI were determined according to the adapted method of Ellman (1959). Ellman's reagent was prepared by dissolving 4 mg of DTNB reagent in 1 mL of tris-glycine buffer (0.086 M Tris, 0.09 M glycine, 4 mM EDTA, pH 8.0). Total and exposed -SH protein contents were obtained by suspending 3 mL of protein samples in 5 mL of reaction buffer and tris-glycine buffer with (total -SH) or without 8 M urea (exposed -SH), respectively. Then, 50 µL of Ellman's reagent was added. The mixtures were incubated for 1 hour at 95 °C in the water bath (SW22, Julabo GmbH, Seelbach, Germany) shaking at 125 rpm and then centrifuged (Multifuge X3R, Thermo Fisher Scientific Inc.,) at 12000 x g for 10 minutes. The absorbance of the supernatant was determined at 412 nm with reagent buffer as the blank. The exposed -SH contents (µmol -SH/g) were calculated by the following equation [3.2]:

$$SH = 73.53 \times A_{412} \times \frac{D}{C} \quad [3.2]$$

where A₄₁₂ is the absorbance at 412 nm, C is the protein concentration (mg/mL), and D is the dilution factor (considered 1 in the current study). The factor 73.53 is derived from the molar extinction coefficient. Total -SH was calculated by adding up the results obtained with and without urea.

3.2.10. Statistical analysis

Data were computed and analyzed with Microsoft Excel and RStudio 4.2.1 (Boston, Massachusetts, USA). Tukey's test, following the analysis of variance, was implemented to determine significant differences with a level of $p < 0.05$. Letters in captions denote significant differences in protein-flavor binding. Treatments with the same letter are not significantly different.

3.3. Results and Discussion

3.3.1. Flavor-related factors influencing the binding phenomena with commercial food protein isolates

Influence of the flavor's degree of unsaturation and spatial configuration: the case of 7-carbon chain length flavors

To investigate the relationship between the flavor's degree of unsaturation and the extent of the binding with PI and WPI, *trans*-2-heptenal and heptanal were compared (**Figure 3.1**). **Figure 3.1** shows that flavor binding to proteins increased with the unsaturation of the flavors. The addition of double bonds to the flavor chain, from heptanal to *trans*-2-heptenal, resulted in a significant binding increase from 13.73% to 54.60%±4 for PPI, SPI, and LPI. However, no significant differences were found for WPI. Note that, occasionally, a slight variability of data across repeated measurements of the same sample in independent measurements might be observed. As sample composition remains consistent across the replicates, the minor variation in the data might be because of small irregularities (*e.g.*, sample carry-over contamination) from the analytical

instrumentation. However, possible inhomogeneity within the protein + flavor mixture should not be ignored.

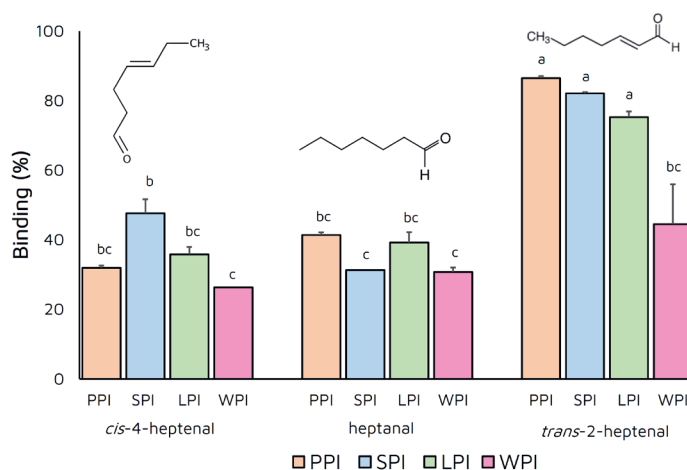


Figure 3.1. Influence of the flavor's degree of unsaturation and spatial configuration on the binding phenomena with commercial food protein isolates: *cis*-4-heptenal, heptanal, and *trans*-2-heptenal at 5 mg/L and protein isolates at 1(w/v)%: pea (PPI), soy (SPI), lupin (LPI), and whey (WPI). Results are expressed as mean \pm standard deviation. Letters denote significant differences ($p < 0.05$). Treatments with the same letter are not significantly different. Binding was calculated using the equation [3.1].

The presence of a double bond in the flavor structure increases the molecular rigidity and electron density of the carbonyl group, thus enhancing protein binding (Zhou & Cadwallader, 2006). Unsaturation is majorly responsible for the compound's structural stiffness (Atkins, 2003) and lack of flexibility to turn. Molecular rigidity promotes the exposure of the given functional group and, therefore, its propensity for interaction with the surrounding proteins (Zhou & Cadwallader, 2006).

Additionally, *trans*-2-heptenal is two times less volatile than heptanal (Table S3.1), which may explain its stronger protein binding (Figure 3.1). These findings are consistent with those of Zhou & Cadwallader, 2006 and Kühn et al., 2008, who evaluated the impact of the presence/absence of double bonds on the flavor structure and its binding effect on commercial food SPI and WPI, respectively.

Similarly, the authors showed that *trans*-2-hexen-1-ol and *trans*-2-nonenal interacted more strongly with SPI and WPI than hexanal and nonanal. The closer proximity of the double bond and hydroxyl group (*trans*-2-hexen-1-ol) resulted in increased rigidity of the hydroxyl end of the molecule, facilitating the formation of hydrogen bonds with soy protein (Zhou & Cadwallader, 2006). Likewise, the occurring Michael addition or Schiff base reactions may imply strong covalent binding (Anantharamkrishnan et al., 2020; Kühn et al., 2008), where the available double bonds react with lysine and histidine amino acids of the given protein.

The results obtained in the present section with commercial food protein isolates corroborate that the presence of double bonds plays a significant role in the binding phenomena and seems to control the mechanism independently from the plant-based protein used. Interestingly, the comparison between plant- and animal-based proteins suggests that differences in protein architecture (**Figure S3.1** and **Table S3.3**) (Czubinski et al., 2015; Kurpiewska et al., 2018; Lam et al., 2018; Maruyama et al., 2007; RCSB; Robinson et al., 2022) maybe a reason for the different flavor binding affinity to *trans*-2-heptenal.

Based on the resulting binding similarity across plant-based protein isolates, this information may help food developers expand the use of alternative commercial plant-based protein isolates in flavored protein-based foods (*e.g.*, meat and dairy alternatives). They can achieve this by tailoring flavor compositions based on the acquired knowledge regarding the importance of unsaturation in flavor structure.

Nevertheless, the flavor's spatial configuration and resulting binding effect on PI and WPI are also considered and shown in **Figure 3.1**. The change in flavor's spatial configuration from spherical (*cis*-4-heptenal) to linear-shaped (*trans*-2-heptenal) significantly increased the protein binding from 18.19% to 54.60%±3 (**Figure 3.1**), regardless of the commercial food protein isolates used. Overall, across the studied proteins and under the specific experimental conditions applied, binding increased from *cis*-4-heptenal to *trans*-2-heptenal regardless of the proteins used.

Presumably, spherical-shaped flavors lead to weaker binding to proteins than linear ones. The protein surface is characterized by "*hydrophobic cavities*" where small ligands can bind (Sotriffer & Klebe, 2002). Protein-flavor binding is partly governed by the specificity of the protein binding sites and the flavor's stereostructure, where similar geometric shapes might fit precisely together (Crowe & Bradshaw, 2014). Therefore, as observed in **Figure 3.1**, the flavor's spherical shape may potentially cause steric hindrance, blocking its access to the protein's hydrophobic binding sites.

The relevance of flavor spatial configuration on the protein binding phenomena has already been pointed out, and our results are in line with those of Zhou & Cadwallader, 2006, who noted that *cis*-3-hexen-1-ol (spherical-shaped) was retained to a smaller extent than 1-hexanol (linear-shaped) when studying commercial dehydrated SPI. The authors revealed that steric hindrance effects may lead to a decrease in accessibility to the hydrophobic binding sites on the protein, resulting in a reduction in binding.

The binding of flavors to proteins is a multifactorial mechanism rather than a one-directional phenomenon where the hydrophobicity and volatility of the flavor should not be overlooked. *Cis*-4-heptenal is considered more hydrophilic and volatile and hence, a more polar compound than *trans*-2-heptenal, as indicated by a $\text{LogP} < 2$ (**Table S3.1**). The lower hydrophobicity and volatility of *cis*-4-heptenal explain its low binding ability, as seen in **Figure 3.1**.

The results obtained with industrial protein isolates repeatedly confirm that flavor structure (*i.e.*, unsaturation and spatial configuration) and physicochemical properties (*i.e.*, hydrophobicity) appear to influence binding more than the source of protein. However, it is advisable to consider that the degree of flavor retention may be affected by the experimental conditions (Pérez et al., 2023).

Influence of alkyl chain type and location of the carbonyl group: the case of 8-carbon chain length flavors

The alkyl chain type is hypothesized to have a substantial impact on the binding of flavors to proteins. Therefore, to confirm this assumption, two flavors with the same carbon chain length (C₈) and the same position of the radical group but different chemical functionalities and functional groups, such as 2-octanol (alcohol) and 2-octanone (ketone), were selected. The binding behavior across PI and WPI is summarized in **Figure 3.2**. As seen in **Figure 3.2**, flavor binding to commercial food protein isolates was found to be in the range of 28.85% to 57.7%±6 for 2-octanol and 17.53% to 23.30%±3 for 2-octanone, with significant differences found for PI.

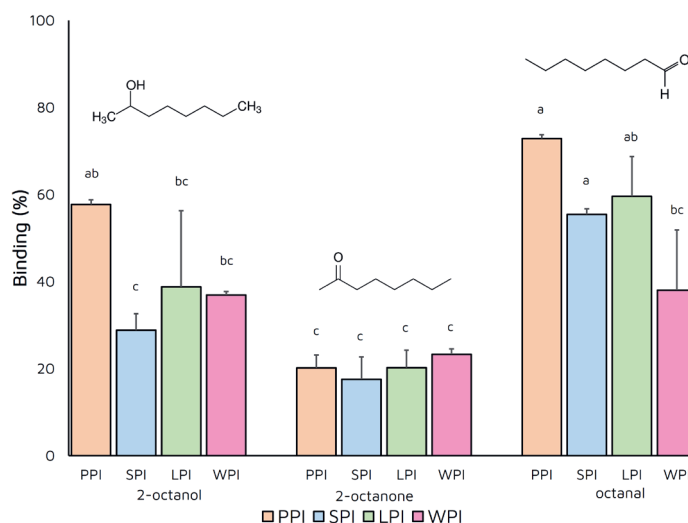


Figure 3.2. Influence of alkyl chain type and location of the carbonyl group on the binding phenomena with commercial food protein isolates: 2-octanone 2-octanol and octanal at 5 mg/L and protein isolates at 1(w/v)%: pea (PPI), soy (SPI), lupin (LPI), and whey (WPI). Results are expressed as mean ± standard deviation. Letters denote significant differences ($p < 0.05$). Treatments with the same letter are not significantly different. Binding was calculated using the equation [3.1].

Most alcohols are relatively hydrophilic; hence, they tend to show a weaker affinity to bind to proteins (Bi et al., 2022; Tan & Siebert, 2008). Conversely, the

interaction between ketones and proteins is likely to be hydrophobic, thus demonstrating stronger and higher binding affinity in an aqueous system. Despite the existing role of flavor alkyl chain type in retention with proteins, the hydrophobicity reflected by LogP possibly suffices to explain the slight variations in binding affinity. A linear correlation is generally found between the hydrophobicity of the flavor and its binding affinity, with binding increasing as the flavor's hydrophobicity increases (Damodaran & Kinsella, 1981). Presumably, 2-octanol is faintly more hydrophobic than 2-octanone (**Table S3.1**), which may explain the tendency for stronger retention across PI and WPI. Additionally, the higher boiling and melting point values of 2-octanol (**Table S3.1**) may provide comprehension of the resulting counterintuitive differences attributed to the strength of the hydrogen bonds. Hydrogen bonding facilitates intermolecular attraction, resulting in increased molecular adhesion. Consequently, a greater amount of thermal energy is needed to disengage these molecules, which is reflected in high melting and boiling points.

Not only does the alkyl chain type play a role in the flavor-binding mechanism, but also the location of the carbonyl group may have significance. As observed in **Figure 3.2**, the studied ketone (2-octanone) is bound with a much lower affinity than the aldehyde (octanal). The carbonyl group located at one end of the octanal molecule resulted in larger binding than the carbonyl group located in the middle of 2-octanone, regardless of the protein source. Generally, the displacement of the carbonyl group from the inner part of the molecule towards the edge leads to a significant increase in binding from 14.73% to 52.76%±5 for the studies with plant protein isolates (PPI, SPI, and LPI). However, no significant differences were found for WPI. Overall, among the studied proteins and under the specific laboratory conditions applied in this investigation, binding increased from 2-octanone to octanal regardless of the protein used.

A polar keto group located at the end of the flavor structure is more easily accessible to establish interaction with the surroundings (Damodaran & Kinsella, 1981), including the hydrophobic pockets of proteins. If the keto group is found at the second position in the ketone structure, it may hinder hydrophobic flavors

from binding to the proteins, thereby reducing hydrophobic interactions and decreasing binding attraction. These results are aligned with those of Heng et al., 2004, who studied the interactions of PPI fractions (legumin and vicilin) with aldehydes and ketones. Compared to aldehydes, ketones bind much less to vicilin, whereas no binding was observed between legumin and ketones. Damodaran & Kinsella, 1981 reported that the free energy of association increases by 105 cal/mol for every move of the keto group from the terminal position to the middle of the chain.

Protein-flavor interaction is primarily hydrophobic, but chemical bonding via non-reversible covalent interactions may be present depending on the flavor's chemical class. Aldehydes, such as octanal, are known to react in Schiff base formation to establish covalent bonds with the ϵ -amino group of lysine residues (Anantharamkrishnan et al., 2020), resulting in amide linkages. This interaction may lead to the observed lack of release, potentially disrupting perception.

As seen previously, the role of hydrophobicity seems crucial in unveiling the binding mechanism on protein matrices with flavors. Based on the hydrophobicity rule, octanal is slightly more hydrophobic than 2-octanone (**Table S3.1**), which may cause stronger retention across the studied proteins.

It is worth noting that examination of plant- and animal-based proteins has occasionally indicated that disparities in protein structure (*i.e.*, differences in quaternary structure or sulfur-containing amino acids) (**Figure S3.1**, **Table S3.3**, and **Table S3.4**) could potentially account for variations in their ability to bind with octanal.

3.3.2. Commercial food protein isolates: Factors influencing the binding phenomena with food flavors

Influence of protein residual fat on the protein-to-flavors binding capacity: the case of ketones

The effect of protein residual fat content on flavor binding was studied using a homologous series of ketones with increasing chain lengths. Ketones with seven to ten carbon atoms were selected due to their simple molecular structure, which may also simplify the interpretation of results. For this purpose, PI (PPI, SPI, and LPI) were defatted (DPPI, DSPI, and DLPI). WPI was not considered for the binding assessment, as its non-defatted version already contained a negligible amount of fat (< 0.05 wt%). Manufacturer-specified (**Table S3.2**) and measured values of fat content before (non-defatted) and after (defatted) defatting for PPI, SPI, and LPI are as follows: For PPI: 8.3 wt% and DPPI: 2.46 wt%, for SPI: 3.1 wt% and DSPI: 1.10 wt%, for LPI: 3 wt% and DLPI: 0.11 wt%. Fat removal followed the chloroform/methanol extraction protocol (see Materials and Methods section).

Figure 3.3 shows that all studied PI bind the selected volatile flavors. The extent of flavor binding increases with increasing flavor chain length and hydrophobicity. As observed in **Figure 3.3**, a slight increase in flavor binding affinity to PI can be noticed when increasing the fat content of PI. However, these differences were not statistically significant, as treatments with the same letter are not significantly different. Specifically, PPI showed $15.38\% \pm 3$, $8.9\% \pm 4$, and $6.07\% \pm 2$ more significant binding to 2-octanone, 2-nonanone, and 2-decanone, respectively, than defatted PPI (DPPI). Similarly, the binding values for SPI to 2-heptanone and LPI to 2-decanone were $10.29\% \pm 8$ and 8.34 ± 10 higher, respectively, compared to their defatted versions, DSPI and DLPI (**Figure 3.3**). Unexpectedly, in DSPI and DLPI systems, 2-heptanone seemed to bind to a greater extent than in non-defatted systems.

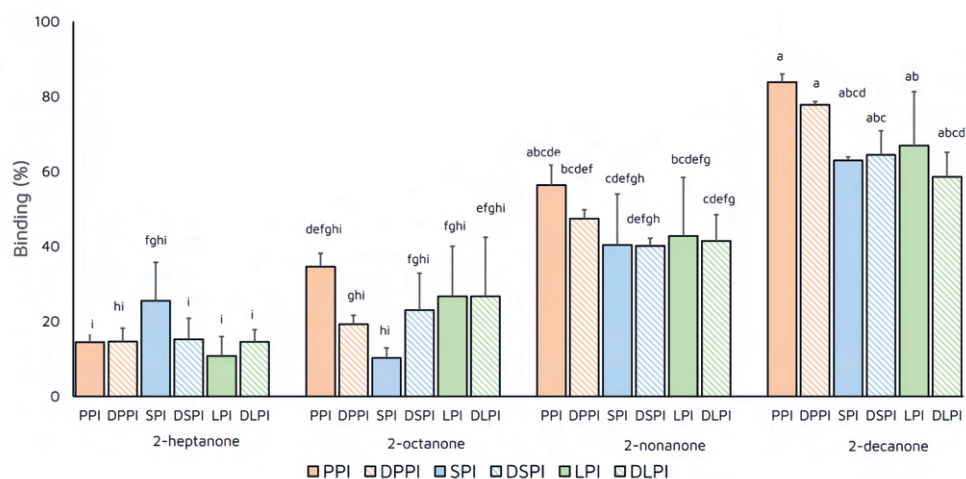


Figure 3.3. Influence of protein residual fat on the binding phenomena with food flavors: 2-heptanone, 2-octanone 2-nonanone, and 2-decanone at 5 mg/L and protein isolates at 1(w/v)%: pea (PPI), soy (SPI), and lupin (LPI). Non-defatted samples (PPI, SPI, and LPI) are the filled-colored columns, whereas the defatted samples (DPPI, DDSPI, and DLPI) are the stripped-colored columns. Results are expressed as mean \pm standard deviation. Letters denote significant differences ($p < 0.05$). Treatments with the same letter are not significantly different. Binding was calculated using the equation [3.1].

On the one hand, the increase in ketone-PI binding observed with increased chain length (**Figure 3.3**) suggests hydrophobic interaction, consistent with findings by Damodaran and Kinsella (1981). These authors noted that with each increment in flavor chain length, binding increased accordingly, with a corresponding change in free energy of about -600 cal/CH_2 residue (Damodaran & Kinsella, 1981).

On the other hand, while not statistically significantly different, flavor binding to PI is slightly more noticeable in non-defatted samples due to the lipophilic nature of the flavors (**Figure 3.3**). This effect becomes more pronounced with increasing lipophilicity of the flavors, in agreement with findings by Repoux et al., 2012. Their study on processed casein model cheeses showed higher binding for 2-nonanone in high-fat cheeses (50% fat content per dry matter) compared to low-fat cheeses (25%) due to the strong hydrophobicity of the compound (Repoux et al., 2012).

PI primarily consist of protein ($> 83\%$, **Table S3.2**). PPI had the highest fat level (8.3 wt%) compared to SPI and LPI (3.1 wt% and 3 wt%, respectively), showing

the highest overall binding effect. However, even though relatively higher binding was observed for PPI compared to DPPI, the residual fat available (< 1%) appeared insufficient to promote significant flavor binding to PPI (**Figure 3.3**). The direct effect of fat has been observed between commercial WPI (0.017 wt%) and aldehydes (Weel, 2004). Weel, 2004 added fat to the flavor solutions to match the fat levels present in WPI, concluding that residual fat available in WPI played only a secondary role in aldehyde retention.

Flavor affinity to fat appears to depend more on flavor hydrophobicity than on the protein's residual fat content or source. Roberts et al., 2003 studied the effect of fat content on flavor release from milk-based emulsions, noting differences in flavor affinity to fat. The study showed that a compound's lipophilicity is inversely proportional to the amount of fat required to decrease its headspace concentration (Roberts et al., 2003).

Despite the complexity of commercial food PI, the results suggest that protein source and residual fat (< 1%) have little to no significant binding effect. Flavor-to-fat affinity seems to depend on flavor hydrophobicity rather than the protein's residual fat level and/or PI source. These findings highlight the critical role of fat availability and content (when > 1%) in flavored plant-based food production for successful flavor release and perception.

Considering that PPI, SPI, and WPI are widely used in food production as whole food ingredients rather than isolated highly purified protein fractions, understanding the impact of whole (non-purified) protein isolate on protein-flavor binding mechanisms is of practical significance in food formulations.

Influence of processing temperatures and storage time on the protein-to-flavor binding capacity: the case of hexanal

Headspace concentration in different protein samples was examined to determine the effect of time and temperature conditions on protein-flavor binding. Hexanal was chosen due to its simple and straight-chain molecular structure. Flavored protein solutions were stored at 5 °C, 70 °C, and 90 °C for

several weeks to simulate refrigerated and elevated temperature storage conditions typically encountered in industrial food processing. Results are presented in **Figure 3.4**. All measurements were performed in triplicate, with hexanal in the absence of protein as a control.

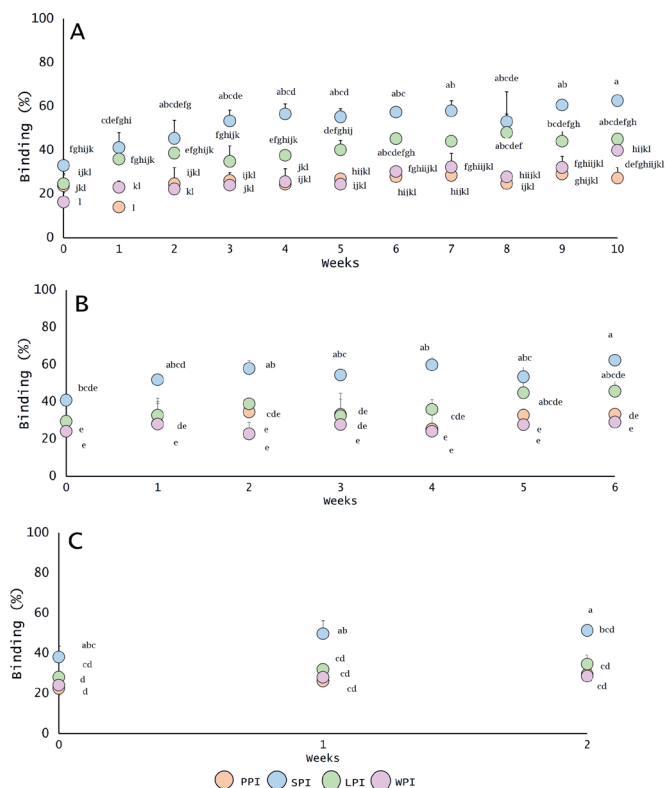


Figure 3.4. Influence of processing temperatures and storage time on the hexanal binding phenomena with commercial food protein isolates: hexanal at 5 mg/L and protein isolates at 1(w/v)%: pea (PPI), soy (SPI), lupin (LPI), and whey (WPI) during storage at 5 °C (A), 70 °C (B) and 90 °C (C). Results are expressed as mean ± standard deviation. Letters denote significant differences ($p < 0.05$). Treatments with the same letter are not significantly different. Binding was calculated following equation [3.1].

During the first three weeks of storage, a slight but gradual increase in hexanal binding was observed for SPI, LPI, and WPI, regardless of the temperature treatment applied (5 °C and 70 °C). After the third week, hexanal binding reached a plateau, with little or no further change in behavior observed. SPI exhibited the highest binding affinity for hexanal, followed by LPI, independently of the

temperature applied. In contrast, PPI and WPI showed the lowest binding affinity for hexanal, although these differences were often not statistically significant. Minor differences in flavor binding may be attributed to variances in protein configuration.

In addition to time, increasing the temperature led to a slight increase in hexanal binding. This observation suggests that proteins may have undergone structural changes, as proteins are known to denature and unfold at temperatures above approximately 70 °C (72 - 84.5 °C) (Mession et al., 2015). Structural changes can promote the exposure of buried internal hydrophobic regions, increasing their availability for flavor binding (Wang & Arntfield, 2015). These results are consistent with previous findings by Hansen & Booker, 1996 and Wang & Arntfield, 2015 who observed increased flavor binding with increasing temperature.

To confirm the structural modifications of proteins due to temperature treatment, surface hydrophobicity (H_0) was measured. Surface hydrophobicity reflects the number of hydrophobic groups on the surface of a protein molecule and is an excellent indicator of protein properties and conformational changes. The H_0 values of the studied proteins are reported in **Table 3.1**. After heat treatment at 70 °C, H_0 decreased by 21.82%, 6.62%, and 4.70% for PPI, WPI, and SPI, respectively. At 90 °C, H_0 decreased further, reaching 56%, 27.67%, and 24.26% for LPI, SPI, and PPI, respectively.

Table 3.1. Experimental values of the surface hydrophobicity (H_0) of pea (PPI), soy (SPI), lupin (LPI), and whey (WPI) protein isolates at a 95% confidence interval.

	H_0 5 °C	H_0 70 °C	H_0 90 °C
PPI	953 [649, 1257]	745 [505, 985]	564 [463, 666]
SPI	2010 [1605, 2415]	1916 [1541, 2291]	1385 [1188, 1582]
LPI	834 [752, 916]	1291 [1056, 1526]	566 [368, 765]
WPI	1692 [1585, 1797]	1579 [1245, 1914]	2374 [2303, 2446]

Protein oligomers can dissociate and reorganize themselves via hydrophobic forces to form high-molecular-weight aggregates when subjected to heat treatment (Mession et al., 2015). The slight decrease in H_0 observed upon coagulation may suggest a partial implication of hydrophobic residues in the aggregation process. Similarly, Li-Chan et al., 1984 studied beef protein under thermal treatment. The authors reported a dramatic decrease in H_0 at 70 °C, coinciding with the visibility of coagulated meat particles. This substantial reduction was attributed to the role of hydrophobic interactions in the aggregation and coagulation process, indicating protein structural changes. Heating at 90 °C led to an increase in H_0 for WPI, indicating the exposure of hydrophobic regions initially concealed inside the protein core (Wang & Ismail, 2012).

To further verify these conformational changes in proteins after heat treatment, changes in the exposed and total sulfhydryl content (-SH) of the proteins were measured (**Table 3.2**). The number of sulfhydryl groups in proteins is determined by the amount of sulfur-containing amino acids, *i.e.*, methionine and cysteine. Specifically, comparisons were made between non-heated and heated (>90 °C) conditions. The data for exposed and total -SH content are presented in **Table 3.2**. Both exposed and total sulfhydryl content decreased after heat treatment for all studied proteins. Among them, SPI exhibited the highest -SH content.

Table 3.2. Experimental values of sulfhydryl content (-SH ($\mu\text{mol/g}$)) of pea (PPI), soy (SPI), lupin (LPI), and whey (WPI) protein isolates non-heated (NH) and heated (H).

	Exposed -SH	Total -SH
PPL_NH	3.98 \pm 0.03	9.14 \pm 0.24
PPL_H	2.88 \pm 0.04	5.34 \pm 0.08
SPL_NH	9.16 \pm 0.19	15.62 \pm 0.25
SPL_H	5.92 \pm 0.15	11.54 \pm 0.36
LPL_NH	7.13 \pm 0.63	11.42 \pm 0.64
LPL_H	4.19 \pm 0.18	10.26 \pm 0.24
WPL_NH	4.53 \pm 0.02	8.78 \pm 0.04
WPL_H	2.86 \pm 0.08	6.39 \pm 0.02

The total and exposed -SH content decrease is attributed to protein structure alterations. Protein denaturation and unfolding lead to intra- or intermolecular thiol/disulfide (-SH/S-S) interchange or thiol/thiol (-SH/-SH) oxidation reactions (Monahan et al., 1995). This chemical reaction reduces the overall -SH content, confirming the proteins' structural changes. This observation is consistent with previous reports by Berghout, 2015 and Jiang et al., 2018. These authors observed that heat treatment promoted a decrease in the amount of free sulfhydryl groups present in LPI and WPI, respectively, due to oxidation and/or conversion of sulfhydryl groups into disulfide bonds. The results demonstrate that thermal treatment induces structural modifications of the protein, such as the reduction of H_0 and -SH content, which consequently leads to increased hexanal binding.

The exposed and total -SH content quantified for SPI is higher than for the other commercial protein isolates, as expected from SPI's relatively high amount of sulfur-containing amino acids (**Table S3.4**).

Influence of commercial food protein isolate type on the protein-to-flavor binding capacity

Certainly, not all flavors are bound to the same degree to a given protein, and certain proteins may have a greater binding capacity for some flavors than others. Among the PI, SPI generally showed the highest binding capacity to aldehydes (hexanal, heptanal, and *cis*-4-heptenal). In contrast, WPI binds to aldehydes to a lesser degree (**Figure 3.1** and **Figure 3.4**). PPI has the highest binding for ketones (2-heptanone to 2-decanone), followed by SPI and LPI (**Figure 3.3**). The differences in quaternary structure between plant- and animal-based protein isolates may explain this study's occasional variable flavor binding patterns. From a structural perspective, differences in a protein's disulfide bond content might play a role in the binding mechanism (see **Figure S3.1** and **Table S3.3**). WPI consists principally of globular proteins with a tertiary structure stabilized by intramolecular disulfide bonds between cysteine residues (**Figure S3.1** and **Table S3.3**) (Gulzar, 2011; Hendrix et al., 1996). In contrast, PPI contains fewer disulfide bridges (Wang & Arntfield, 2014), allowing flavors to readily interact with the hydrophobic sites of the protein, enhancing binding. Additionally, the higher amount of disulfide bonds in WPI (**Figure S3.1** and **Table S3.3**) may contribute to its lower flavor-binding affinity (**Figures 3.1, 3.2, and 3.4**). Inter- and intra-disulfide bridges stabilize the protein structure, leading to a more compact protein structure (Hernandez-Munoz et al., 2004) and promoting steric hindrance, which blocks the access of small ligands such as flavors, thus reducing flavor binding.

Based on the results, flavor structure and intrinsic physicochemical properties principally contributed to protein binding. Double bonds enhanced flavor binding to PI and WPI more than in their absence. The degree of unsaturation of the flavor appeared to govern flavor binding rather than the type of protein. Similarly, the displacement of the carbonyl group from the inner part of the flavor structure towards the edge led to a significant increase in binding. Contrarily, spherical-shaped flavors resulted in a lower degree of binding than linear-shaped ones.

Flavor affinity to fat appeared to strongly depend on the lipophilicity of the flavor rather than on the residual fat content present in the protein used. Therefore, defatting may not be strictly required when assessing the protein-flavor binding mechanism using PI (> 83% protein).

3.4. Conclusions

In the context of industrial food processing, it is imperative to consider the continuous exposure of protein-based food products to varying temperature conditions for prolonged durations. The results showed that an increase in temperature led to a slight overall increase in hexanal binding to the commercial food protein isolates. This observation possibly indicates that proteins might have undergone structural changes. Surface hydrophobicity and sulfhydryl content confirmed the idea of protein conformational changes, resulting in stronger flavor binding. Despite the complexity of flavored-protein-based systems with commercial food protein isolates, the differences in flavor structure explained the varied flavor binding patterns. The acquired outcomes suggested that there is hardly any influence of the protein source and residual fat levels on the protein-flavor binding mechanism.

The above results may shed light on the fundamental mechanism of protein-flavor binding. Additional research may be necessary to explore a broader range of flavor chemical structures and intrinsic physicochemical properties, as flavor structure has significantly impacted the binding phenomena. When studying protein-flavor binding mechanisms, most authors have investigated defatted, purified, and isolated protein fractions, which are not realistic for use in food processing. Instead, commercially available food protein isolates have more practical applicability. Accordingly, rising awareness of the impact of industrial processing on protein structure by isolation techniques can provide valuable insights into the degree of denaturation of the starting protein isolate. This knowledge will assist food developers in enhancing the quality of flavored plant-based foods that incorporate industrially processed protein isolates.

3.5. Supplementary Material

Figure S3.1. Crystal structure of **A)** 7S δ -conglutin (4PPH) from *Lupinus angustifolius* L., **B)** 7S Vicilin (7U1) from *Pisum sativum* L., **C)** 7S β -conglycinin (1IPK) from *Glycine Max*, **D)** β -Lactoglobulin (5IO5). Adapted from Czubinski et al., 2015; Kurpiewska et al., 2018; Lam et al., 2018; Maruyama et al., 2007; RCSB; Robinson et al., 2022.

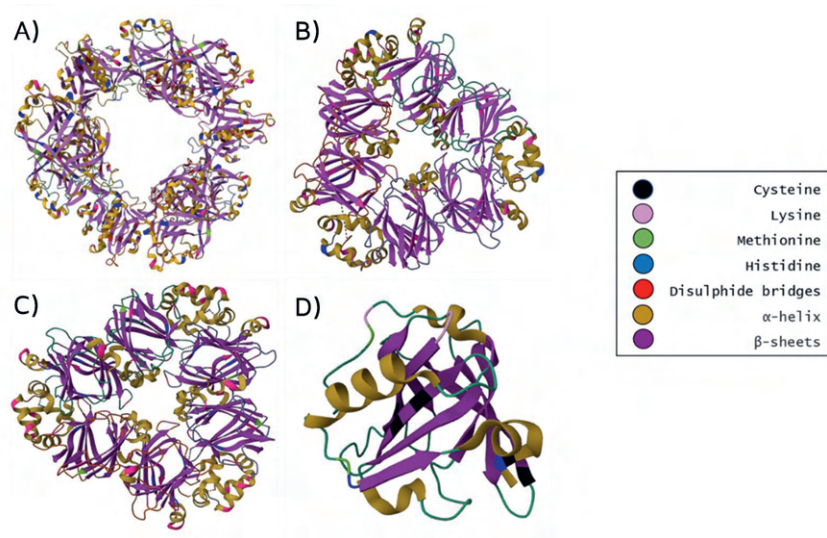
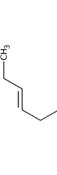
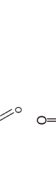
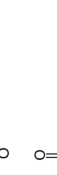


Table S3.1. Physicochemical and structural features of the selected flavor compounds.

Compounds	CAS	Chemical structure ¹	LogP ²	Flavor molecular weight (g/mol) ³	Vapor pressure (mmHg) at 25°C ⁴	Melting point (°C) ⁵	Boiling point (°C) at 760 mmHg ⁶
Hexanal (C ₆ H ₁₂ O)	66-25-1		1.8	100.16	11.3	-58.2	130.0
Heptanal (C ₇ H ₁₄ O)	111-71-7		2.3	114.19	3.52	-43.3	152.0
<i>Trans</i> -2-heptenal (C ₇ H ₁₂ O)	18829-55-5		2.1	112.17	1.82	-53.35	166.6
<i>Cis</i> -4-heptenal (C ₇ H ₁₂ O)	6728-31-0		1.4	112.17	3.64	-53.35	151.6-160.0
2-heptanone (C ₇ H ₁₄ O)	110-43-0		2	114.19	3.85	-35.5	151.5
Octanal (C ₈ H ₁₆ O)	124-13-0		2.7	128.21	1.18	-23.0	171.0
2-octanol (C ₈ H ₁₈ O)	123-96-6		2.9	130.22	0.24	-31.3	179.0-181.0
2-octanone (C ₈ H ₁₆ O)	111-13-7		2.4	128.21	1.35	-16.0	173.0-175.0
2-nonanone (C ₉ H ₁₈ O)	821-55-6		3.1	142.24	0.62	-150	193.5-198.0
2-decanone (C ₁₀ H ₂₀ O)	693-54-9		3.7	156.26	0.27	14.0	210.0

¹⁻⁶ Properties obtained from PubChem (National Center for Biotechnology Information) and The Good Scents Company Information System

Unraveling the role of flavor structure and physicochemical properties in the binding phenomena with commercial protein isolates

Table S3.2. Manufacturer-specified values of protein and fat content for pea (PPI), soy (SPI), lupin (LPI), and whey (WPI) protein isolates. Nutritional information per 100 g of product.

	Total fat (triglycerides) content	Total protein content
PPI	8.3%	79%
SPI	3.1%	91.2%
LPI	3%	91%
WPI	<0.05%	97.6%



Table S3.3. Molecular characterization of pea (PPI), soy (SPI), lupin (LPI), and whey (WPI) protein isolates (Berghout, 2015; Gulzar, 2011; Hendrix et al., 1996; Lam et al., 2018).

	PPI		SPI		LPI		WPI					
Protein fraction	11S legumin	7S vicilin	2S convicilin	11S glycinin	7S β- conglycinin	11S α- conglutin	7S β- conglutin	7S γ- conglutin	7S δ- conglutin	α- lactoglobulin	β- lactoglobulin	
Molecular weight (kDa)	300-400	150-170	290	300-360	150-200	8-22	330-430	143-260	200	13	14	18.4
Disulfide bridges	6	0	N/A ¹	2	0	0	6	0	2	4	4	2

¹N/A= no available data

Table S3.4. Manufacturer-specified values of amino acid content for pea (PPI), soy (SPI), lupin (LPI), and whey (WPI) protein isolates. Sulfur-containing amino acids per 100 g of product.

	Methionine	Cysteine	Lysine	Histidine
PPI	1.16%	1.23%	6.34%	2.04%
SPI	1.3%	1.3%	6.3%	2.6%
LPI	0.5%	1.2%	3.9%	2.3%
WPI	2.3%	2.8%	10.2%	2.0%



Development of a QSAR model to predict protein- flavor binding in protein-rich food systems

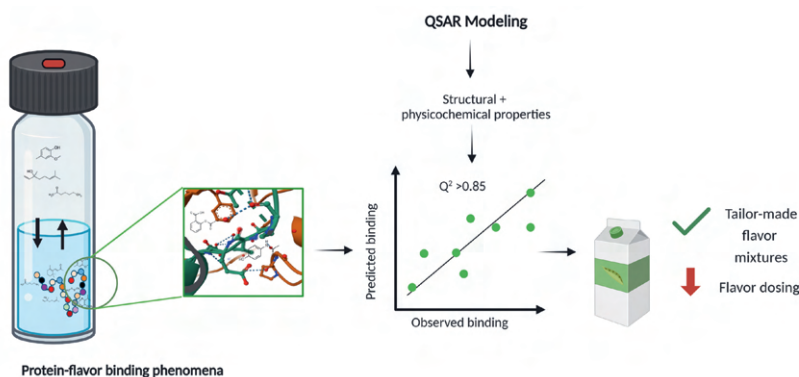
Submitted as:

Barallat-Pérez, C. B., Hollebrands, B., Janssen, H. G., Martins, S., Fogliano, V., Hageman, J., Oliviero, T. Development of a QSAR model to predict protein-flavor binding in protein-rich food systems. *Food Chem.* 2024.

Abstract

Protein-flavor binding is a common challenge in food formulation. Prediction models provide a time-, resource-, and cost-efficient way to investigate how the structural and physicochemical properties of flavor compounds affect this binding mechanism. This study presents a Quantitative Structure-Activity Relationship model derived from five commercial plant-based proteins and thirty-three flavor compounds. The results showed that protein-flavor binding is primarily influenced by the structure and physicochemical properties of the flavor compound, with the protein source having a minor contribution. In addition to hydrophobicity, topological, electronic, and geometrical descriptors significantly contribute to the observed protein-flavor binding. The Random Forest model demonstrated a strong correlation between predicted and experimental values ($Q^2=0.93$) and a high predictive ability for a validation set of flavors and proteins not previously used ($Q^2=0.88$). The prediction model developed holds promise for customizing flavor combinations and streamlining product design, thereby, optimizing efficiency while reducing the risk of flavor overdose.

Keywords: commercial plant-based proteins; flavor compounds; protein-flavor binding; Quantitative Structure-Activity Relationship; prediction; physicochemical properties.



TOC Graphic 4. Development of a QSAR model to predict protein-flavor binding in protein-rich food systems. (Biorender software).

4.1. Introduction

The effort of a balanced global food system led to a shift towards more sustainable protein sources, with a particular emphasis on plant-based alternatives (Schreuders et al., 2019). The most common animal replacements are plant proteins (PP) derived from soybeans (*Glycine max*) and peas (*Pisum sativum* L.) due to their excellent techno-functional properties such as water-holding, gelling, fat-absorbing, and emulsifying capacities (Kyriakopoulou et al., 2019). The need to find alternative protein sources to feed the global population and develop protein-rich protein food products (> 20% protein content) boosted the use of a more diverse offer of pulses, where lupins (*Lupinus angustifolius* L.), faba beans (*Vicia faba* L.), and lentils (*Lens culinaris* L.) have recently gained significant attention (Kyriakopoulou et al., 2019).

Unfortunately, plant-derived proteins present undesirable off-flavors, which can negatively impact consumer acceptance (Wang et al., 2024; Xiang et al., 2023). Actions to improve the food flavor profile include removing, masking, or reducing off-flavors. This is typically done in the food industry by adding flavorings (*i.e.*, flavor compounds). In nature, flavor compounds encompass various chemical classes like aldehydes, ketones, esters, alcohols, and terpenes, each with unique molecular structures and physicochemical properties. When added to protein-based food matrices, flavor compounds interact with- and may bind to proteins, reducing flavor perception. These interactions can be reversible or non-reversible (Anantharamkrishnan et al., 2020; Wongprasert et al., 2024), influenced by structural, thermodynamic, and physicochemical characteristics, including unsaturation, spatial configuration, alkyl chain type, functional group position, chain length, hydrophobicity, and water solubility (Ammari & Schroen, 2018; Guo et al., 2024; Li et al., 2024; Semenova et al., 2002; Wei et al., 2024).

Analytical measurements such as equilibrium dialysis (Damodaran & Kinsella, 1981), static headspace gas chromatography-mass spectrometry (GC-MS) (Wang & Arntfield, 2015), high-performance liquid chromatography (Li et al., 2000), solid phase microextraction (Gkionakis et al., 2007), and atmospheric pressure

chemical ionization-mass spectrometry (Viry et al., 2018) have been used to quantify flavor binding. Although no single method can yield a complete, quantitative picture of the flavor binding phenomenon, GC-MS is the most widely employed technique for studying binding (Reineccius, 2010). Over the past few decades, mathematical methods and prediction models have been implemented as a powerful and complementary approach to GC-MS studies for quantifying binding interactions (Temthawee et al., 2020; Wongprasert et al., 2024). In practice, prediction models result in time-, resource- and cost-efficient methods compared to conventional experimental laboratory work. Some examples are models based on best-fit partial least-squares regression (Tan & Siebert, 2008) and computational tools. Insightful approaches develop models based on Quantitative Structure-Activity Relationships (QSAR) or molecular docking (Bi et al., 2022; Tromelin & Guichard, 2004). Because both the flavor and the protein's structural and physicochemical features are essential in the binding phenomenon, QSAR models seem to be the optimal tool to model flavor partitioning in complex protein solutions (Tromelin & Guichard, 2004).

Up to now, the application of these prediction models has primarily focused on a narrow and specific range of flavor compounds (*e.g.*, aldehydes) (Snel et al., 2023). There is limited understanding regarding a broader and more varied flavor dataset. Similarly, most of these prediction models have investigated a limited selection of food ingredients, and thus, the use of commercial food proteins remains relatively unexplored. For practical reasons, the food industry employs protein isolates and concentrates as meat and dairy replacers. Protein isolates vary in composition and consist of multiple, non-uniform types of protein fractions (Sadeghi et al., 2023). Furthermore, working with protein isolates offers a more practical approach to daily food applications.

In this study, it is hypothesized that a modeling approach could predict flavor binding in commercial plant protein-based model systems for diverse flavor compounds and reveal the fundamental physicochemical and configurational properties of the flavor compounds, determining the binding mechanism. For this purpose, five different PP (soy protein isolate (SPI), pea protein isolate (PPI), lupin

protein isolate (LPI), faba protein isolate (FPI), and lentil protein concentrate (LPC)) were tested with thirty-three flavor compounds belonging to seven chemical classes (*i.e.*, aldehydes, ketones, alcohols, lactones, pyrazines, furans, and sulfur-type compounds). Besides their significant role in flavoring applications, offering a range of sweet, fruity, floral, smoky, citrus, and fresh notes within the food and beverage industry, the selection criteria for these flavor compounds included both their physicochemical properties and structural configurations, highlighting similarities and differences, including the number of double bonds, spatial configuration, type and position of the functional group, chain length, and hydrophobicity. While studying a single protein's structure is key to understanding its flavor-binding role, it may not translate well to practical food applications. Relying solely on isolated protein fractions to meet texture and appearance requirements seems impractical. Therefore, commercial SPI and PPI were chosen due to their widespread acceptance as alternatives to meat and dairy products in the food industry, following the rationale behind previous work from our group (Barallat-Pérez et al., 2023). Additionally, the need to find alternative protein sources addressing the global food demand has driven interest in a broader variety of pulses such as FPI, LPI, and LPC.

Furthermore, an independent set of five flavor compounds (*p*-anisaldehyde, ethyl octanoate, methyl salicylate, 3-methyl-2,4-nonadione, and δ -dodecalactone) was tested in combination with Whey Protein Isolate (WPI), and Bovine Serum Albumin (BSA) as controls to verify the accuracy of the model. The experimental assessment of protein-flavor binding was done by using static headspace (HS) GC-MS. A QSAR model was trained and validated to develop a relationship between protein-flavor binding and the physicochemical- and configuration properties. This model could assist food developers in crafting customized flavor profiles, by leveraging the most important physicochemical and configurational properties, thereby reducing the need for excessive flavoring addition in (plant-based) product formulations. The distinctiveness of this work is based on the utilization of commercial food proteins that are well-suited for real food applications, offering a more realistic approach to predicting protein-flavor binding.

4.2. Materials and Methods

4.2.1. Flavor compounds

A summary of the chosen flavor compounds, their Canonical Simplified Molecular Input Line Entry System (SMILES) codes, and molecular and physicochemical properties (*i.e.*, chemical structure, LogP, molecular weight, vapor pressure, solubility, and boiling point) can be found in **Table S4.1** (Kim et al., 2023; Wishart et al., 2022). Unsaturation, spatial configuration, alkyl chain type, position of the functional group, chain length, and hydrophobicity were the selection criteria for the flavor compounds to be included in the study (Barallat-Pérez et al., 2023; Bi et al., 2022; Guo et al., 2024; Li et al., 2024; Wei et al., 2024).

Hexanal, heptanal, *trans*-2-heptenal, 4-*cis*-heptenal, *trans-trans*-2,4-heptadienal, octanal, *trans*-2-octenal, nonanal, *trans*-2-nonenal, *trans*-2-*cis*-6-nonadienal, *trans-trans*-2,6-nonadienal, 2,4-dimethylbenzaldehyde, *trans*-decenal, 2,3-butadione, 2-hexanone, 2-heptanone, 2-octanone, 6-methylheptan-2,4-dione, 2-nonanone, 1-pentanol, 1-penten-3-ol, 1-heptanol, 2-octanol, 1-octen-3-ol, creosol, 1-nonanol, linalool, dimethyl disulfide, 2,5-dimethylpyrazine, methyl propyl disulfide, β -ionone, α -ionone, and 2-pentylfuran, were purchased from Sigma-Aldrich (Zwijndrecht, the Netherlands) and all had a purity of $\geq 95\%$.

4.2.2. Protein sources

Commercial plant proteins were provided by different suppliers. Soy Protein Isolate (SPI) SUPRO[®] XT219D IP was obtained from Solae (St. Louis, Missouri, USA); Pea Protein Isolate (PPI) S85F was purchased from Roquette (Lestrem, France); Faba Protein Isolate (FPI) 90-C-EU was acquired from AGT (Waalwijk, The Netherlands); Lupin Protein Isolate (LPI) 10600 was purchased from ProLupin (Grimmen, Germany), and Lentil Protein Concentrate (LPC) VITESSENCE[®] Pulse 2550 37403F00 was obtained from Ingredion (Westchester, Illinois, USA). The two commercial proteins used to verify the model were Whey Protein Isolate (WPI) BiPro[®], which was supplied by Davisco International (Le

Sueur, Minnesota, USA), and Bovine Serum Albumin (BSA) Purified Protein was purchased from Sigma-Aldrich (>98%). Typically, commercial proteins undergo multiple processing steps to purify and optimize functional properties. Protein content varied from 51.9%-97.6%.

Table S4.2 shows manufacturer-specified values such as fat, carbohydrate, and protein content for all PP, WPI, and BSA. Proteins were selected based on their nutritional composition, such as low-fat and high-protein content and prevalence in plant-based food substitutes (*e.g.*, high-protein-based beverages). To minimize the potential for variation in the results, the protein batches were kept in the dark, in sealed bags, and stored in a controlled environment with a cool temperature of 10-15 °C and low humidity.

4.2.3. Other chemicals or materials

$\text{Na}_2\text{HPO}_4 \cdot 7\text{H}_2\text{O}$, $\text{NaH}_2\text{PO}_4 \cdot 2\text{H}_2\text{O}$, Na_2HPO_4 , 8-anilino-1-naphthalenesulfonate, chloroform (99.8%), and methanol were analytical grade and purchased from Sigma-Aldrich. Pierce™ BCA ($\text{HO}_2\text{CC}_9\text{H}_5\text{N}_2$) assay kits were acquired from Thermo Fisher Scientific Inc., (Waltham, Massachusetts, USA) and contained albumin standard ampules (2 mg/mL, 10 x 1 mL containing bovine serum albumin at a concentration of 2 mg/mL in 0.9% saline and 0.05% sodium azide), and two BCA™ (bicinchoninic acid) reagents: A) Na_2CO_3 , NaHCO_3 , ($\text{HO}_2\text{CC}_9\text{H}_5\text{N}$)₂ and $\text{C}_4\text{H}_4\text{N}_2\text{O}_6$ in 0.1 M NaOH; B) 4% $\text{CuSO}_4 \cdot 5\text{H}_2\text{O}$ (25 mL).

4.2.4. Preparation of food flavor stock solutions

The chosen flavor compounds were individually prepared as described by Barallat-Pérez et al., 2023. Additional precautions were taken to overcome the practical difficulties of preparing accurate flavor stock solutions and dealing with volatility (evaporation) and solubility challenges. Individual flavor stock solutions were prepared in 100 mL amber bottles (Pyrex®, Thermo Fisher Scientific Inc.) and closed with screw caps using a sodium phosphate buffer solution (pH 7.0, 50 mM) at an initial concentration of 10 mg/L (Sigma-Aldrich). The flavor stock solutions were subjected to an ultrasonic water bath treatment (25 kHz, ultrasonic time 100%) (Elma Schmidbauer GmbH, Germany) for a duration of 1 hour at a

temperature of 20 °C to achieve homogenization of the solution. The stock solutions were repeatedly prepared in triplicate and stored under refrigeration conditions (3-5 °C).

4.2.5. Preparation of food protein solutions

Food protein solutions were prepared following the protocol proposed by Wang & Arntfield, 2015 and adapted from Barallat-Pérez et al., 2023. Specifically, the selected proteins (SPI, PPI, FPI, LPI, LPC, BSA, and WPI) were individually prepared at an initial concentration of 2(w/v)% in a sodium phosphate buffer (pH 7.0, 50 mM). To address the solubility challenge known in PP, the proteins were gradually added to the solution while stirring, allowing their hydration in water. Subsequently, they were subjected to vortexing for a duration of 10-20 seconds (at 3200 rpm, Genie II, Genie™, Sigma-Aldrich) and subsequently transferred to an ultrasonic water bath (Elma Schmidbauer GmbH, Singen, Germany) for 20 minutes at a temperature of 20 °C, to break down protein clusters and ensure homogenization of the solutions. Mild heating (20 °C) aided in dissolving the proteins. Subsequently, the protein solutions underwent multiple rounds of vortexing (3200 rpm) lasting between 10 to 20 seconds each to guarantee a uniform mixture distribution. Lastly, visual verification ensured that no clumps remained.

4.2.6. Preparation of the Gas Chromatography-Mass Spectrometry samples (GC-MS)

Gas Chromatography-Mass Spectrometry (GC-MS) samples were prepared following the protocol proposed by Wang & Arntfield, 2015 and adapted from Barallat-Pérez et al., 2023. A 20 mL GC-MS vial was utilized to add 1 mL of each protein's 2(w/v)% solution, followed by adding 1 mL of flavor stock solution. Consequently, a protein solution with a final concentration of 1(w/v)% and 5 mg/L flavor concentration was obtained. Subsequently, the vials were closed with screw caps (19 mm silicone PTFE SUPELCO®) and placed in a water bath shaker (SW22, Julabo GmbH, Seelbach, Germany) at 30 °C, 125 rpm for 3 hours before headspace analysis (HS). The samples were prepared and analyzed in triplicate.

4.2.7. Binding measurement and calculation

Protein-flavor binding was measured using headspace GC-MS analysis utilizing an Agilent-7890A GC instrument coupled with an Agilent 5975C triple-axis detector MS (Agilent, Amstelveen, the Netherlands). The GC operated in split mode at a 1:10 ratio with 8 mL/min split flow. The samples underwent incubation and agitation for 14 minutes at a temperature of 40 °C, following a protocol established by Wang & Arntfield, 2015 and accordingly modified by Barallat-Pérez et al., 2023. Subsequently, 1 mL of the sample's HS was introduced into the system. The experiment utilized a DB-WAX column (20 m × 180 μm × 0.3 μm), operated at a constant flow of 0.8 mL/min. Column temperature was programmed at a rate of 40 °C/min to 240 °C. The mass spectrometer operated at 70 eV electron ionization with a mass range from 35 to 200 Da. MassHunter Quantitative Analysis software (MSD ChemStation F.01.03.2357) was used to quantify the flavor. Furthermore, the NIST Mass Spectrometry Library (InChI Library v.105) was employed to provide chemical and physical data on the chosen flavor compounds. Flavor compounds were studied individually to prevent potential flavor-flavor competition for protein binding sites. A quantitative measure for flavor binding to the proteins was obtained utilizing the equation presented by Wang & Arntfield, 2015 [4.1].

$$\text{Binding (\%)} = \left(1 - \frac{HS_1 - HS_2}{HS_3}\right) \times 100 \quad [4.1]$$

HS₁ represents the (relative headspace) abundance, which refers to the peak response of the flavored aqueous protein solution. HS₂ indicates the abundance in the headspace when the flavor is absent, just the protein solution. Meanwhile, HS₃ reflects the abundance in the headspace in the absence of protein, therefore, just the given response from the flavor compound. The main ions and retention times of each flavor were determined using each flavor compound accordingly

4.2.8. QSAR Modeling

A graphical outline of the different steps followed for the QSAR modeling is shown in **Figure 4.1**. The experimental binding values were used as response variables to describe protein-flavor binding, and a set of descriptors was used as explanatory variables in a QSAR model. The descriptors were collected from the literature, experimentally determined, or calculated using the SMILES code of the flavor compounds. A Boruta algorithm was applied to select the important descriptors for the Random Forest (RF) regression model (Kursa, 2010). The effectiveness of the prediction model was evaluated by both a "Leave-One-Out Cross-Validation" (LOOCV) and by assessment of an external validation set.

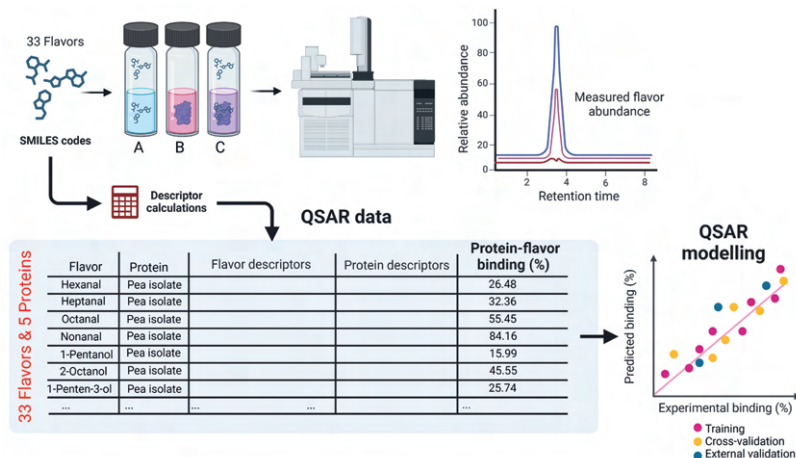


Figure 4.1. Schematic overview of the protein-flavor prediction model. GC-MS measurements experimentally determined the binding between thirty-three flavor compounds and five commercial plant-based proteins, and a set of molecular descriptors was selected, calculated, and measured for QSAR predictive modeling. (Biorender software).

To assess the significance of each descriptor for the RF regression model, the importance value of each descriptor was determined and compared with randomized descriptor values following the Boruta algorithm procedure (Kursa, 2010). The procedure was applied 128 times, and in each iteration, the dataset was randomly divided into training and test sets using a 4:1 ratio. The descriptor importance values for both original- and randomized descriptors were determined using the VarImp function from the R-package Caret (Kuhn, 2008). Then the

descriptors were only considered for the model that exhibited a determined importance value significantly higher than the maximum observed importance value among the randomized descriptors. Response plots (**Figure 4.3 B**) were generated to visualize the relationship between individual descriptors and protein-flavor binding (response). Using 10-fold cross-validation, predictions were made by varying the values of the selected descriptor from its observed minimum to maximum across 100 evenly spaced sampling points, while keeping the values of all other descriptors fixed at their calculated averages.

4.2.9. Molecular descriptors

Molecular descriptors included flavor and protein features. For the selected flavor compounds, SMILES were obtained from the PubChem database (Kim et al., 2023). SMILES is a standardized notation for representing chemical structures in a computer-friendly format. It uses a character string to uniquely denote each structure, allowing for easy exchange and manipulation of chemical information. The list of SMILES codes was submitted to the online chemical database (OCHEM) (Sushko et al., 2011) and the molecular structures were energy-minimized using BALLOON optimization (Vainio & Johnson, 2007). **Table S4.3** provides a full definition of the descriptors according to the OCHEM CDK manual. A set of in total 309 2D and 3D molecular descriptors was calculated using the descriptors calculator tool (The Chemistry Development Kit version 2.8) (Steinbeck et al., 2003). The flavors' LogP, vapor pressure, solubility, and topological polar surface area values were obtained from the PubChem database.

The selection of protein descriptors used in this study was based on experimental laboratory analysis, prior literature and expert knowledge, and open-access availability. The protein descriptors included surface hydrophobicity, protein solubility, particle size, ζ -potential, polydispersity index, isoelectric point (pI), and nutritional information. The surface hydrophobicity of PP was experimentally determined following the approach of Li-Chan et al., 1984. Likewise, the protein solubility was experimentally determined using the BCA assay during the surface hydrophobicity experiments (pH 7.0). The BCA assay was used to determine the

final concentration of soluble protein. The solubility was calculated using the following equation [4.2].

$$\text{Solubility (\%)} = \left(\frac{C_{\text{protein},s}}{C_{\text{product}} * W_{\text{protein}}} \right) \times 100 \quad [4.2]$$

With $C_{\text{protein},s}$ being the final soluble protein concentration determined via the BCA assay, C_{product} the concentration of the protein in the solution before centrifuging, and W_{protein} is the mass fraction of protein in the PP.

Particle size, ζ -potential (surface charge), and polydispersity (heterogeneity) index were measured using a Zetasizer Ultra (Malvern Instruments Ltd, Worcestershire, UK) (Kew et al., 2021) using quartz disposable cuvettes (Hellma, Müllheim, Germany). Protein solutions were first diluted to a concentration of 0.1 wt% and subsequently subjected to filtration through a 0.22 μm syringe filter (PTFE Syringe filters, PerkinElmer, Shelton, Connecticut, USA) for particle size measurement via dynamic light scattering.

The refractive index of the protein solution was set at 1.5 with an absorption of 0.001. The samples were equilibrated for two minutes at 25 °C and analyzed using backscattering technology at a detection angle of 173°. The measurements were performed in triplicate.

The pI values of the PP were obtained from the literature. Values ranged from 4.0 to 5.0 (Lee et al., 2021; Shrestha et al., 2021; Tiong et al., 2024; Verfaillie et al., 2023).

4.2.10. Data preprocessing

Several preprocessing steps were performed before model development. First, 110 non-varying molecular descriptors were removed from the total of 328 descriptors in the dataset. The experimentally determined protein-flavor binding constant was used as the dependent variable. All training data was centered and scaled to unit variance before the training of the models. RF was used for training the models, unless otherwise stated, and was implemented in RStudio (version 2021.09.0 build 351, Boston, Massachusetts, USA) using the `rf` function from the

R-package Caret (version 6.0-94) (Kuhn, 2008). The hyperparameters were optimized by grid search, and the final optimized model had a cost and sigma value of 14 and 0.01, respectively.

4.2.11. Validation of the prediction model

The model was validated through LOOCV, using only the selected descriptors outlined above. To avoid introducing validation bias, all data points related to a single flavor compound in combination with each protein were deliberately excluded during each cross-validation repetition. This approach ensured that each flavor compound was systematically left out during cross-validation. In each cross-validation iteration, the remaining dataset was used for training and, consequently, to predict the excluded values. Subsequently, the values (Q^2) were computed by comparing the predicted values with the observed ones. Q^2 represents a measure of predictive accuracy (Andini et al., 2021; Hageman et al., 2017).

4.2.12. External validation

For external validation, the protein-flavor binding of a new set of flavor compounds (*p*-anisaldehyde, ethyl octanoate, methyl salicylate, 3-methyl-2,4-nonadione, and δ -dodecalactone) and commercial proteins (WPI and BSA), was experimentally determined and predicted using ensemble modeling. The physicochemical properties and spatial configuration of the selected flavor molecules can be found in **Table S4.4**. The flavor and protein descriptors were collected using the previously described procedures to predict the binding values (see section 4.2.9). The protein-flavor binding values of the validation compounds were predicted (**Table S4.5**) using an ensemble of the models employed during LOOCV. The thirty-three models were trained on distinct training sets and used to predict the protein-flavor binding of each validation compound. This approach resulted in thirty-three prediction values for each protein-flavor combination. These predictions were used to calculate average protein-flavor binding values and intervals indicating variability from the validation procedure.

4.3. Results and Discussion

4.3.1. Protein flavor binding mechanism: An overview

The binding mechanism of flavor compounds to commercial plant-based proteins is shown in **Figure 4.2**. **Figure 4.2 A** provides a visual and selective representation of one of these protein-flavor interactions (*e.g.*, lupin + 2-nonanone) to better comprehend the experimentally determined binding mechanism. In flavored protein-containing samples (**Figure 4.2 A**), relative headspace abundance is significantly diminished compared to protein-free samples due to the protein-flavor binding mechanism. **Figure 4.2 B** illustrates a correlation of the protein-flavor binding behavior between the thirty-three flavor compounds combined with the five commercial plant-based proteins. Notably, binding responses widely vary across flavor compounds and, to a certain extent, between protein sources.

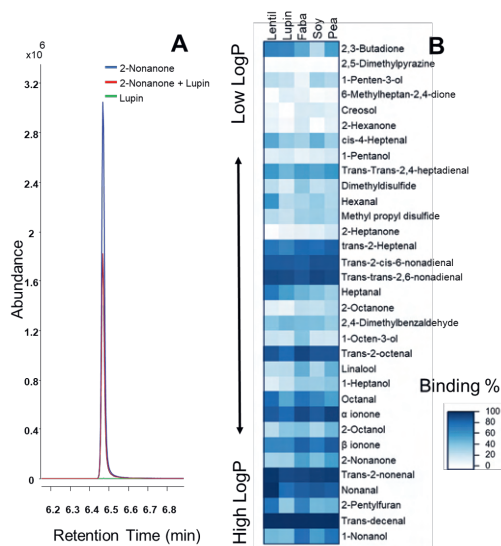


Figure 4.2. The example of a GC-MS chromatogram (**A**) shows the measured abundance of 2-nonanone with and without lupin protein (LPI). The correlation plot (**B**) shows an overview of the experimentally determined protein-flavor binding values of five commercial plant-based proteins (rows) and thirty-three flavor compounds (columns) using equation [4.1]. The flavors are listed in increasing order of their octanol-water partitioning coefficient (LogP). The color intensity scales varied from white to dark blue, indicating the level of protein-flavor binding.

As expected, binding is somewhat influenced by the hydrophobicity of the flavor compound (**Figure 4.2 B**). The dark blue color visualizes flavors with high binding values and is mainly grouped at the bottom of the correlation plot, where the flavors are arranged by their LogP values, which increase with the chain length (Bi et al., 2022; Su et al., 2021). Closer data observation shows low binding <1% for 2,5-dimethylpyrazine (LogP = 0.6) and high variation in the experimental binding of flavors across protein sources for the more hydrophilic flavor compounds (top part of **Figure 4.2 B**). For example, the experimentally determined protein-flavor binding of 2-hexanone (LogP=1.4) ranges from <1% to 15%, where the lowest value is for binding with LPI and the highest value is for binding with FPI. Similarly, binding values for 1-penten-3-ol (LogP = 1.1) vary from 6% to 32% where the lowest value is for binding with FPI, and the highest value is for binding with SPI. On the contrary, low variation in the experimental binding was observed for flavors with higher binding affinity, *e.g.*, *trans*-2-nonenal (LogP=3.1), where values ranged from 90% to 97%. An additional parameter to consider is the accuracy of the experimental data. Determining the protein-flavor binding accurately of hydrophilic flavors is more difficult than that of the more hydrophobic species. Hydrophilic flavors often show low protein-flavor binding affinities and significant experimental errors. Viry et al., 2018, Snel et al., 2023, and Wei et al., 2024 explained hydrophilic flavor compounds' low protein binding values by a "pushing-out (size-exclusion) effect". This phenomenon leads to the expulsion of small and hydrophilic flavor compounds from the solution, pushing them into the headspace (Snel et al., 2023; Viry et al., 2018). Wei et al., 2024 described this effect as a "salting-out effect", where the protein in solution lowers the surface tension of the dispersion, greatly enhancing flavor release to the headspace.

From the modeling perspective, the non-uniform variance of errors, known as heteroskedasticity, is a complication that may impact the reliability of the predicted data obtained from the QSAR models.

4.3.2. Key descriptors involved in the protein-flavor binding mechanism

Reflecting on the first hypothesis, a QSAR study was performed to determine the most important properties that participate in the protein-flavor binding. The RF model was selected to predict flavor binding to proteins because of its high accuracy, robustness, and low likelihood of overfitting data. For selection, only twenty-eight of the initial 328 descriptors consistently performed better than those of repeatedly randomized descriptor data. In essence, only twenty-eight descriptors are here related to protein-flavor binding, which is influenced by flavor structure and physicochemical properties. On the contrary, protein-related descriptors such as particle size, ζ -potential, surface hydrophobicity, pI, and the residual fat content (up to 0.09 (w/v) % in solution)(**Table S4.2**) exhibited minimal influence on the protein-flavor binding mechanism.

Twelve of these twenty-eight candidate descriptors were selected for the prediction model. Their calculated importance scores are plotted in **Figure 4.3 A**. Descriptors significantly impacting protein-flavor binding include constitutional, geometrical, hybrid, electronic, and topological descriptor classes (Toppur & Jaims, 2021a) (**Figure S4.1**). Supplementary Material, **Table S4.3**, provides a complete definition of the descriptors according to the OCHEM CDK manual.

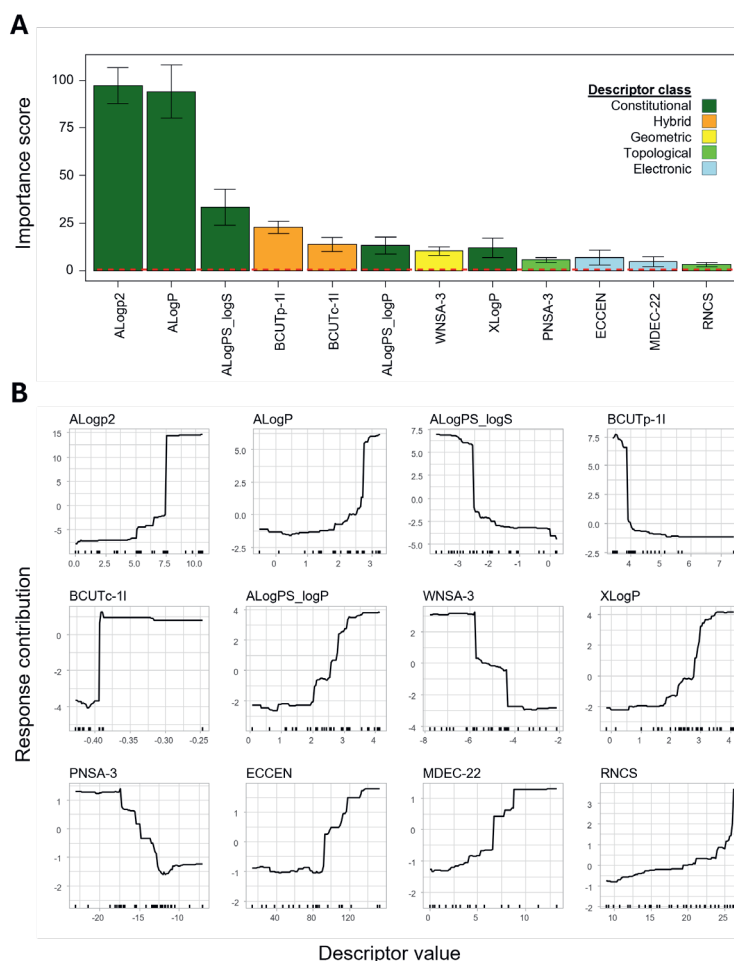


Figure 4.3. Ranking, categorization, and response plots of selected descriptors for the QSAR model predicting protein-flavor binding. **(A)** High importance scores indicate a strong relationship between molecular descriptors (constitutional, hybrid, geometric, topological, and electronic) and protein-flavor binding. Randomization of the descriptor values and replication of the models ($n = 128$) was applied to determine which descriptors perform significantly better than the best result of randomized descriptor data (red line). The error bars indicate the 99% confidence interval. **(B)** The response plots show the contribution to protein-flavor binding (Response contribution) when only the value (Descriptor value) changes of the selected descriptor. The rug marks show how descriptor values were distributed in the used dataset.

As shown also in **Figure 4.2**, protein-flavor binding strongly depends on flavor hydrophobicity (Bi et al., 2022; Su et al., 2021). Hence, it is unsurprising that the constitutional descriptors ALogP2, ALogP, and XLogP, each referring to

hydrophobicity albeit slightly different, demonstrated the most pronounced importance scores within the protein-flavor model, as illustrated in **Figure 4.3 A**.

Besides constitutional, the hybrid and topological descriptors like ECCEN, BCUTc-1l, BCUTp-1l, and MDEC-22 also contribute to the protein-flavor binding model (**Figure 4.3 A**). These descriptors provide information about the proximity of atoms, distances between them, connectivity within a molecule, and overall molecular spatial relationships (Toppur & Jaims, 2021a) and help to describe the flavor compounds' functional groups and the locations within the molecular structures. Results showed that flavor structure (location of the functional group, spatial configuration) and physicochemical properties (LogP) were primary contributors to protein-flavor binding being aligned with previous scientific studies (Damodaran & Kinsella, 1981; Guo et al., 2024; Kühn et al., 2006; Li et al., 2024; Semenova et al., 2002; Wei et al., 2024; Zhou & Cadwallader, 2006). For example, carbonyl group displacement along the molecule enhanced binding significantly in commercial protein isolate-based systems (Damodaran & Kinsella, 1981). The positioning of the keto group within the inner structure of the molecule leads to steric hindrance, causing a reduction in the interaction's free energy.

In addition, the descriptors WNSA-3, PNSA-3, and RNCS define the flavor compounds' surface area and partial charge (**Table S4.3**) (Toppur & Jaims, 2021a) and show significant contributions to protein-flavor binding here as well. For instance, the charge density of a carbonyl flavor compound is comparatively more significant than that of an ester (Ayed et al., 2014). Consequently, carbonyl-type flavor compounds exhibit a higher degree of retention than esters.

Consequently, carbonyl-type flavor compounds exhibit a higher degree of retention than esters.

The response plots (**Figure 4.3 B**) illustrate the contribution to protein-flavor binding (response contribution) when only the input values of the twelve selected descriptors for the model change. Three main patterns were observed: First, an inverse response between polarizability (BCUTp-1l) and partial charge (BCUTc-1l) is observed; Low polarizability or high partial charge seemed to result in higher

binding values. Second, remarkably similar patterns are seen for ECCEN and MDEC-22, providing connectivity information and molecular distance between C, N, and O. Third, a comparable pattern was found between WNSA-3, PNSA-3, and RNCS, which relates to the charge distribution of the flavor compounds (Table S4) (Toppur & Jaims, 2021a).

Confirming the initial hypothesis, the results clearly indicate that the properties of the flavor compound—such as topology, geometry, and hydrophobicity—primarily dictate protein-flavor binding. Aldehydes exhibited the highest affinity, followed by sesquiterpenoids and alcohols, whereas ketones showed the weakest binding.

Under the tested conditions, the protein-related descriptors and protein sources (SPI, PPI, LPI, LPC, and FPI) showed here minimum impact on the model's performance (**Figure 4.3** and **Figure S4.1**). These results are consistent with previously published data by Barallat-Pérez et al., 2023 and Snel et al., 2023 who studied flavor binding to commercial food proteins. Flavor binding proved to be mainly dependent on the flavor molecule and its physicochemical properties, such as spatial configuration, absence/presence of double bonds, and location of the functional group.

In light of the previous information and the additional data presented in **Figure 4.2** and **Figure 4.3 A**, it becomes evident that the interaction between proteins and flavors extends beyond hydrophobicity. Additional factors related to configuration properties and charge distribution also play a crucial role in the observed binding phenomenon, complementing each other in a way that should not be ignored.

4.3.3. Predicting protein-flavor binding

Reflecting on the second hypothesis, the prediction of the protein-flavor binding was conducted employing RF using the 12 selected descriptors. For this purpose, a "Leave-One-Flavor-Out" validation approach was used. Individual data points corresponding to a particular flavor within the dataset were methodically excluded individually, and the model was further trained using the remaining data

points. Subsequently, the model's performance was assessed by making predictions for the excluded data points. This process was repeated for each data point in the dataset. **Figure 4.4** shows the correlation between the predicted and experimentally determined protein-flavor binding values. The $Q^2=0.93$ indicated a strong correlation between predicted and experimental values (**Figure 4.4**). A more detailed overview can be found in Supplementary Material **Figure S4.2**.

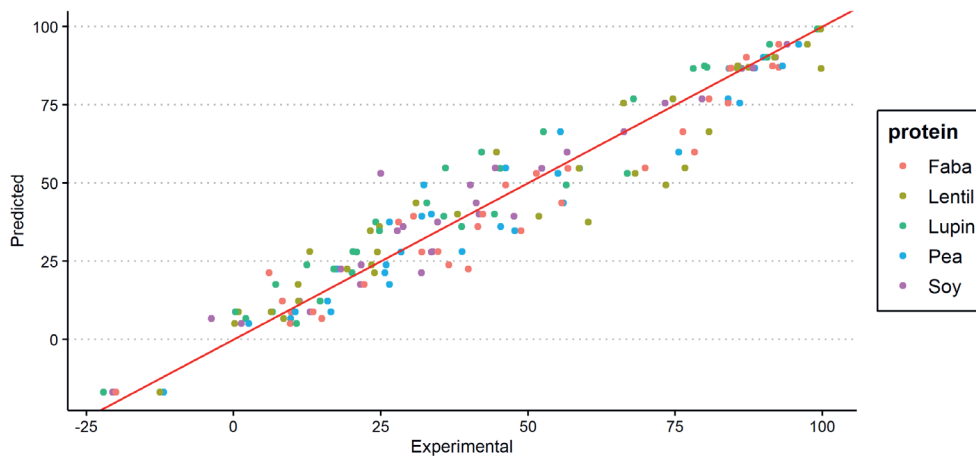


Figure 4.4. Random Forest (RF) model depicting predicted vs. experimental protein-flavor binding values for the studied flavors and commercial protein isolates and concentrates.

From **Figure 4.4**, it is evident that the protein source does not strongly affect flavor binding. None of the protein sources showed significantly larger differences between the predicted and experimental values. These results are in line with the outcome of the descriptor ranking and selection illustrated in **Figure 4.3 A** (showing no significant contribution of protein-related descriptors) and the literature information (Barallat-Pérez et al., 2023; Snel et al., 2023).

4.3.4. Prediction of validation compounds

Training a QSAR model that can predict all possible combinations of proteins and flavors is not feasible. The number of flavor compounds in nature is enormous; thus, model restrictions must be validated and defined for the structural domain and response space. To prove the model's applicability, protein-

flavor binding was predicted and compared to experimentally determined data for compounds not in the training and testing data set (**Table S4.1**). The validation compounds, such as *p*-anisaldehyde, methyl salicylate, and 3-methyl-2,4-nonanedione, shared functional groups with our training set. Ethyl octanoate and δ -dodecalactone, often employed as food flavors, were also added to the data set. Supplementary Material, **Table S4.4**, shows the physicochemical and structural properties of the compounds used in the validation.

The flavor binding values of the validation compounds were predicted by calculation of the twelve descriptor values for each flavor in the validation set. These calculated values were used as input variables for the previously trained model. The ensemble model is comprised of thirty-three different prediction models as a result of the LOOCV and was applied to predict the flavor binding of the validation compounds. For each model, the data of one flavor compound was left out and with the remaining data, the model was trained. **Figure 4.5** shows the predicted and experimental values of the validation compounds.

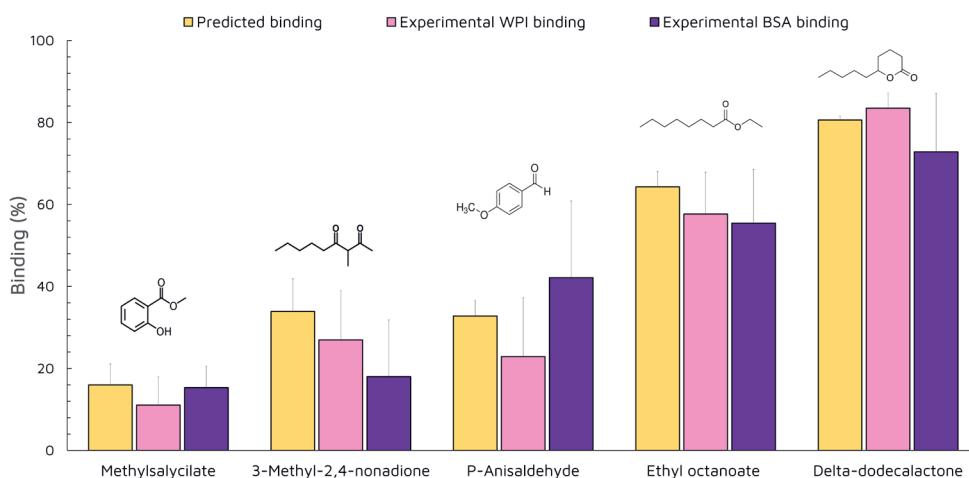


Figure 4.5. Predicted vs. experimental binding data (%) for *p*-anisaldehyde, ethyl octanoate, methyl salicylate, 3-methyl-2,4-nonanedione, and δ -dodecalactone in Whey Protein Isolate (WPI), and Bovine Serum Albumin (BSA) model systems. Results are expressed as mean \pm 2*stdev. Binding was calculated using equation [4.1].

Longer chain-length and linear molecules, such as ethyl octanoate and δ -dodecalactone, consistently displayed a pattern in their response plots (**Figure S4.3**). This consistency indicated that they tend to have higher MDEC values, which provide information about atom connectivity along the molecule and are closely related to higher binding affinity.

Despite the manufacturing and processing history that plant protein isolates and concentrates often go through and the possible remaining traces of fat and carbohydrates present (**Table S4.2**), no large differences in flavor binding affinity were found between the pure protein (BSA) and the isolate (WPI) as seen in **Figure 4.5**. Furthermore, given the current studied system and the selected validation compounds, the proposed prediction model showed high predictive ability ($Q^2=0.88$). Therefore, the obtained knowledge repeatedly confirms the minor role of the protein source on the extent of protein-flavor binding.

Using five verification flavor compounds *p*-anisaldehyde, ethyl octanoate, methyl salicylate, 3-methyl-2,4-nonadione, and δ -dodecalactone may not fully address all flavor chemical classes and physicochemical properties existing in nature. However, it builds an initial understanding of the protein-flavor binding mechanism and strengthens the potential of the current prediction model. Follow-up studies are suggested to expand to more diverse flavor compound datasets and more diverse compositional and experimental conditions to cover broader food applications.

4.4. Conclusions

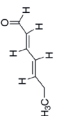
The uniqueness of the present work lies in the use of a blend of different food protein fractions, suited for real food applications and thus, representing a practical approach to predict protein-flavor binding. A modeling approach was hypothesized to predict flavor binding in commercial protein-based model systems for various flavor compounds and to reveal the key physicochemical and configurational properties of the flavor compounds that determine the binding mechanism. The results unequivocally demonstrate a strong correlation between predicted and experimental values, as demonstrated by the Random Forest model

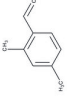
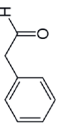
highlighting that protein-flavor binding is primarily dictated by the flavor compound itself under the here researched conditions. Beyond hydrophobicity, topological, electronic, and geometrical descriptors complementarily contribute to the observed protein-flavor binding.

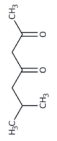
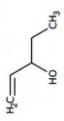
The obtained results have the potential to expand the current understanding of protein-flavor interactions serving as a first step toward developing time-, cost- and resource-efficient methods for predicting flavor binding in protein-rich systems and optimizing flavor formulas (less flavor dosing) based on their structure and physicochemical properties. Although the applied model system in this study may not fully capture the complexity of real-world foods, the prediction model offers valuable preliminary insights. It provides a straightforward method for predicting flavor binding in protein-rich aqueous systems, initially focusing on single-component food systems using commercial protein isolates. Acknowledging the complexity of real food systems, which involve mixtures of flavors, sugar, salt, fat, and extensive processing conditions (heat, pH, ionic strength), further research is needed to explore the broader application of the presented model, reflecting more practical food scenarios.

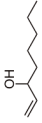
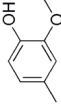
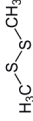
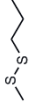
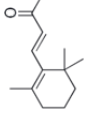
4.5. Supplementary Material

Table S4.1. Physicochemical and structural features of the selected flavor compounds.

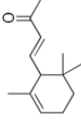
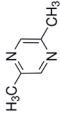
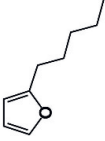
Compounds	CAS	Canonical SMILE	Chemical structure ¹	LogP ²	Flavor molecular weight (g/mol) ³	Vapor pressure (mmHg) 25°C ⁴	Water solubility (mg/L) ⁵	Boiling point (°C) 760 mmHg ⁶
Hexanal (C ₆ H ₁₂ O)	66-25-1	CCCCC=O		1.8	100.16	11.3	5640.0	130.0
Heptanal (C ₇ H ₁₄ O)	111-71-7	CCCCC=O		2.3	114.19	3.52	1250.0	152.0
<i>Trans</i> -2-heptenal (C ₇ H ₁₂ O)	18829-55-5	CCCC/C=C/C=O		2.1	112.17	1.82	1810.0	166.6
<i>Cis</i> -4-heptenal (C ₇ H ₁₂ O)	6728-31-0	CC/C=C\C/C=O		1.4	112.17	3.64	1810.0	151.6-160.0
<i>Trans-trans</i> -2,4-heptadienal (C ₇ H ₁₀ O)	4313-03-5	CC/C=C/C/C=O		1.6	110.15	1.40	2805.0	177.4±9

Octanal (C ₈ H ₁₆ O)	124-13-0	CCCCCCCC=O		2.7	128.21	1.18	560.0	171.0
<i>Trans</i> -2-octenal (C ₈ H ₁₄ O)	2548-87-0	CCCC/C=C/C=O		2.6	126.20	0.59	612.7	190.1
Nonanal (C ₉ H ₁₈ O)	124-19-6	CCCCCCCCC=O		3.3	142.24	0.37	96.0	195.0
<i>Trans</i> -2-nonenal (C ₉ H ₁₆ O)	18829-56-6	CCCCC/C=C/C=O		3.1	140.22	0.25	204.9	188±2
<i>Trans</i> -2- <i>cis</i> -6-nonadienal (C ₉ H ₁₄ O)	557-48-2	CC/C=C\CC/C=C/C=O		2.2	138.21	0.28	318.8	187.0
<i>Trans</i> - <i>trans</i> -2,6-nonadienal (C ₉ H ₁₄ O)	17587-33-6	CC/C=C/CC/C=C/C=O		2.2	138.21	0.28	318.8	203.3
2,4-Dimethylbenzaldehyde (C ₉ H ₁₀ O)	15764-16-6	CC1=CC(=C(C=C1)C=O)C		2.5	134.17	0.30	356.1	215.0
Phenylacetaldehyde (C ₈ H ₈ O)	122-78-1	C1=CC=C(C=C1)CC=O		1.8	120.15	0.39	3026.0	195.0

<i>Trans</i> -2-decenal (C ₁₀ H ₁₈ O)	<chem>CCCCC/C=C/CCC=O</chem>		3.7	154.25	0.06	67.8	229.0
2-hexanone (C ₆ H ₁₂ O)	<chem>CCCCC(=O)C</chem>		1.4	100.60	0.36	17200.0	128.0
2-heptanone (C ₇ H ₁₄ O)	<chem>CCCCC(=O)C</chem>		2	114.19	3.00	4280.0	151.0
2-octanone (C ₈ H ₁₆ O)	<chem>CCCCC(=O)C</chem>		2.4	128.21	1.35	899.0	173.0-175.0
6-methylheptan-2,4-dione (C ₈ H ₁₄ O)	<chem>CC(C)CC(=O)CC(=O)C</chem>		1.1	142.20	N/A	4716.0	183.0
2-nonanone (C ₉ H ₁₈ O)	<chem>CCCCCCC(=O)C</chem>		3.1	142.24	0.62	371.0	193.0-198.0
1-pentanol (C ₅ H ₁₂ O)	<chem>CCCCCO</chem>		1.6	88.15	2.20	22000.0	280.0
1-penten-3-ol (C ₅ H ₁₀ O)	<chem>CCC(C=O)O</chem>		0.9	86.13	9.68	90100.0	114.0
1-heptanol (C ₇ H ₁₆ O)	<chem>CCCCCCCO</chem>		2.7	116.20	0.21	1670.0	175.0

2-octanol (C ₈ H ₁₈ O)	CCCCCCC(C) O		2.9	130.22	0.24	1120.0	179.0-181.0
1-octen-3-ol (C ₈ H ₁₆ O)	CCCCC(C=C) CO		2.6	128.21	0.53	1836.0	175.0
Creosol (C ₇ H ₈ O)	CC1=CC(=C(C=C1)O)OC		1.3	138.16	0.29	2093.0	221.0
1-nonanol (C ₉ H ₂₀ O)	CCCCCCCCC CO		4.3	144.25	0.02	140.0	214.0
Linalool (C ₁₀ H ₁₈ O)	CC(=CCCC(C)(C=C)O)C		2.7	154.25	0.16	1590.0	198.0
Dimethyldisulfid e (C ₂ H ₆ S ₂)	CSSC		1.8	94.20	28.70	22000.0	110.0
Methyl propyl disulfide (C ₄ H ₁₀ S ₂)	CCCCSC		1.8	122.30	4.14	3000.0	94.1±3
β ionone (C ₁₃ H ₂₀ O)	CC1=C(C(C=C1)C)/C=C/C(=O)C		2.9	192.30	0.05	169.0	254.8

Chapter 4

α ionone (C ₁₃ H ₂₀ O)	127-41-3	<chem>CC1=CCCC(C1/C=C/C(=O)C)C</chem>		3.0	192.30	0.02	106.0	257.6
2,5-dimethylpyrazine (C ₆ H ₈ N ₂)	123-32-0	<chem>CC1=CN=C(C=N1)C</chem>		0.6	108.14	1.50	31970.0	154.0
2-pentylfuran (C ₉ H ₁₄ O)	3777-69-3	<chem>CCCCC1=C(C=CO1)</chem>		3.7	138.02	2.02	41.8	169.7
2,3-butanedione (C ₄ H ₆ O ₂)	431-03-8	<chem>CC(=O)C(=O)C</chem>		-1.3	86.09	7.60	200000.0	87.5

¹⁻⁶ Properties obtained from PubChem (National Center for Biotechnology Information) and The Good Scents Company Information System. N/A = Not available data

Table S4.2. Manufacturer-specified values of carbohydrate, protein, and fat content for soy (SPI), pea (PPI), lupin (LPI), faba (FPI), lentil (LPC), whey (WPI), and bovine serum albumin (BSA) protein isolates and/or concentrates. Nutritional information in (%) per 100 g.

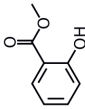
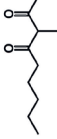
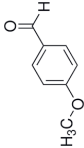
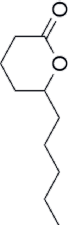
	SPI	PPI	LPI	FPI	LPC	WPI	BSA
Carbohydrate	<1	<1	<1	1.0	31.8	<1	<1
Protein	91.2	79.0	91.0	84.0	51.9	97.6	>99
Fat	3.1	9.0	3.0	5.9	4.2	<0.5	<0.02

Table S4.3. Descriptors definition according to OCHEM CDK manual.

Descriptor	Type	Class	Explanation
ALogP ALogP2	ALOGP	Constitutional Descriptor	Calculates atom additive LogP and molar refractivity values as described by Ghose and Crippen.
ALogPS_ LogS ALogPS_ LogP	ALOGPS	Constitutional Descriptor	Predicted octanol/water partition coefficient (LogP) and solubility in water (LogS). This model was built using EState descriptors (electrotopological EState indices) using the program developed by Dr. Tanchuk.
XLogP	XLogP	Constitutional Descriptor	Prediction of LogP based on the atom-type method called XLogP.
BCUTp_1l, BCUTc_1l	BCUT	Hybrid Descriptor	Eigenvalue based descriptor noted for its utility in chemical diversity described by Pearlman et al.
Kier2	KappaShapeIndices	Topological Descriptor	Descriptor that calculates Kier and Hall kappa molecular shape indices.
MDEC-22	MDE	Topological Descriptor	Evaluate molecular distance edge descriptors for C, N, and O.
ECCEN	EccentricConnectivityIndex	Topological Descriptor	A topological descriptor combining distance and adjacency information.

ATSc5	AutocorrelationCharge	Topological Descriptor	The Moreau-Broto autocorrelation descriptors using partial charges
Weta3.unity	WHIM	Hybrid Descriptor	Holistic descriptors described by Todeschini et al.
WTPT-3	WeightedPath	Topological Descriptor	The weighted path (molecular ID) descriptors described by Randic. They characterize molecular branching.
ATSc3	AutocorrelationCharge	Topological Descriptor	The Moreau-Broto autocorrelation descriptors using partial charges.
Khs.dsCH	KierHallSmarts	Topological Descriptor	Counts the number of occurrences of the E-state fragments.
MOMI-YZ, MOMI-XZ	MomentOfInertia	Geometrical Descriptor	Descriptor that calculates the principal moments of inertia and ratios of the principal moments. Als calculates the radius of gyration.
RNCG, RNCS, FPSA- 1,FNSA-1, FNSA- 3,PNSA-1, PNSA- 2,PNSA-3, WNSA- 1,WNSA-3, TPSA	CPSA	Electronic Descriptor /Geometrical Descriptor	A variety of descriptors combining surface area and partial charge information.

Table S4.4. Physicochemical and structural features of the verification flavor compounds.

Compounds	CAS	Canonical SMILE	Chemical structure ¹	LogP ²	Flavor molecular weight (g/mol) ³	Vapor pressure (mmHg) 25°C ⁴	Water solubility (mg/L) ⁵	Boiling point (°C)/760 mmHg ⁶
Methyl salicylate (C ₈ H ₈ O ₃)	119-36-8	<chem>COC(=O)C1=CC=CC=C1O</chem>		2.3	152.15	0.03	7400.0	222
3-Methyl-2,4-nonadione (C ₁₀ H ₁₈ O ₂)	113486-29-6	<chem>CCCCC(=O)C(C)C(=O)C</chem>		2.3	170.25	0.04	511.4	235
<i>p</i> -Anisaldehyde (C ₈ H ₈ O ₂)	123-11-5	<chem>COC1=CC=C(C=C1)C=O</chem>		1.8	136.15	0.03	4290.0	248
Ethyl octanoate (C ₁₀ H ₂₀ O ₂)	106-32-1	<chem>CCCCCCCC(=O)OCC</chem>		2.5	172.26	0.02	70.1	208
<i>delta</i> -dodecalactone (C ₁₀ H ₁₈ O ₂)	705-86-2	<chem>CCCCC1CCCC(=O)O1</chem>		2.5	170.25	0.008	393.8	267

¹⁻⁶ Properties obtained from PubChem (National Center for Biotechnology Information) and The Good Scents Company Information System.

Table S4.5. Experimentally averaged measured binding data (%) and predicted values between the commercial proteins (whey protein isolate, WPI, and bovine serum albumin, BSA) and the verification flavor compounds.

Compounds	Experimentally averaged measured binding values	Predicted binding values
Methyl salicylate (C ₈ H ₈ O ₃)	13±6	16±5
3-Methyl-2,4-nonadione (C ₁₀ H ₁₈ O ₂)	23±13	34±8
<i>p</i> -Anisaldehyde (C ₈ H ₈ O ₂)	32±16	33±4
Ethyl octanoate (C ₁₀ H ₂₀ O ₂)	57±12	64±4
δ-dodecalactone (C ₁₀ H ₁₈ O ₂)	78±9	81±1

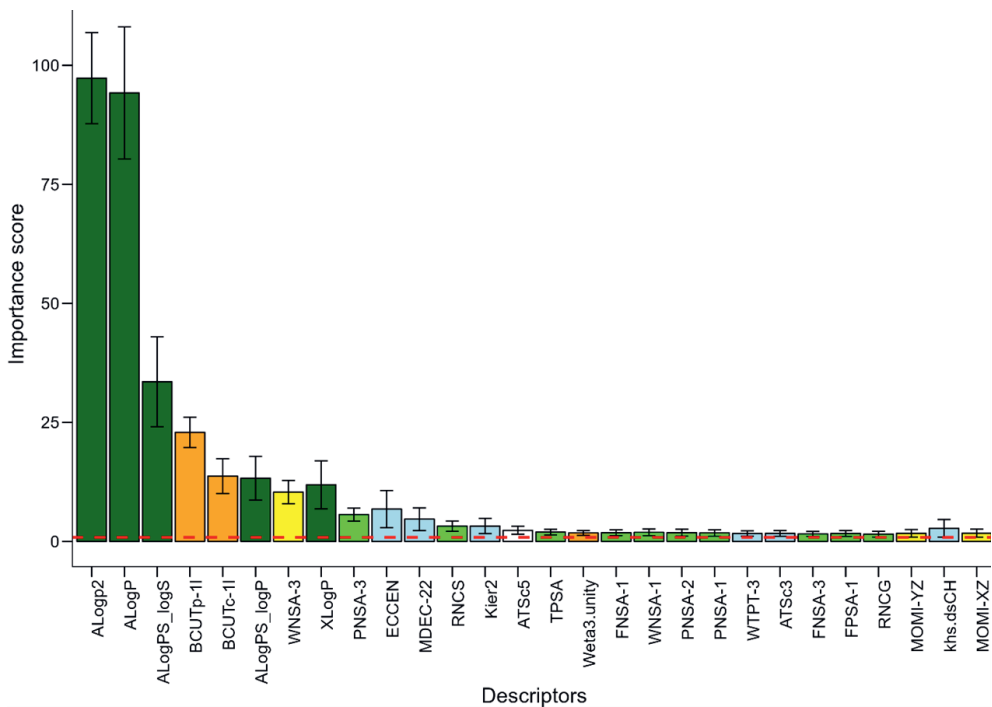
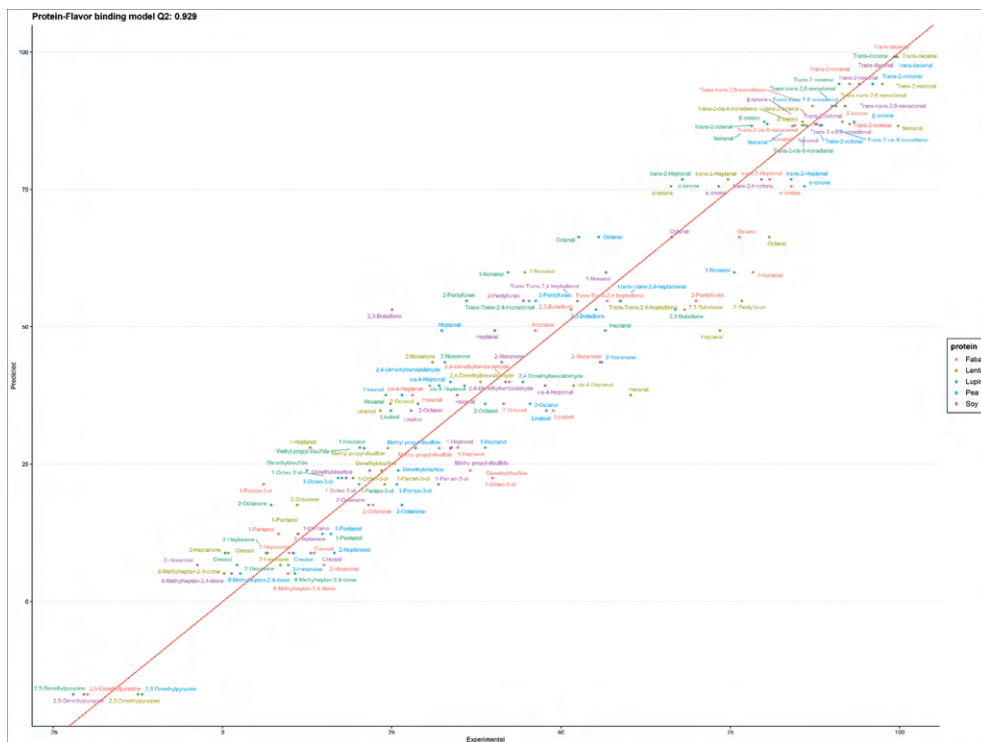


Figure S4.1. Ranking and categorizing the twenty-eight descriptors for the QSAR model predicting protein-flavor binding. High importance scores indicate a strong relationship between molecular descriptor and protein-flavor binding. The descriptors are color-categorized: dark green: constitutional descriptors, orange: hybrid descriptors, yellow: geometric descriptors, light green: topological descriptors, and light blue: electronic descriptors. Randomization of the descriptor values and replication of the models ($n=128$) was applied to determine which descriptors performed significantly better than the best result of randomized descriptor data (red line). The error bars indicate the 99% confidence interval.



4

Figure S4.2. Detailed overview of the correlation between the predicted and experimentally determined protein-flavor binding (%) values.

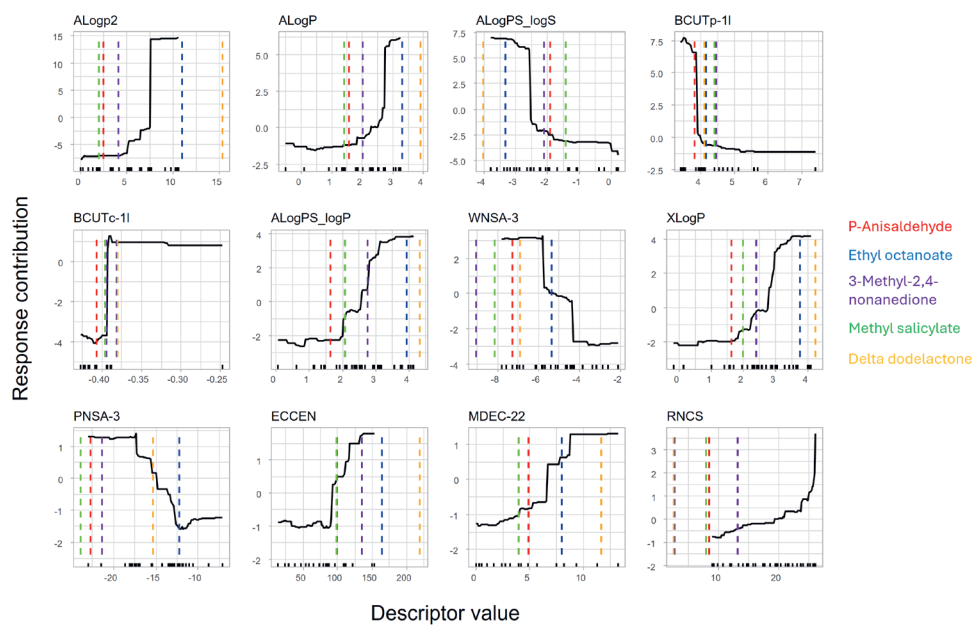


Figure S4.3. Response plots of the selected descriptors used to predict the protein-flavor binding. Each plot shows the effect on the predicted protein-flavor binding (Response) when the specific descriptors change in value. The small black lines on the bottom of each plot show how descriptor values are distributed in our dataset.



The role of mucin in the
protein-flavor binding
mechanism:
an *in vitro* approach

Submitted as:

Barallat-Pérez, C. B., Khazzam, E., Janssen, H. G., Martins, S., Fogliano, V.,
Oliviero, T. The role of mucin in the protein-flavor binding mechanism: an *in vitro*
approach. *npj Sci Food*. 2024.

5.1. Introduction

Flavor represents a key sensory characteristic for food's acceptability (Pagès-Hélary et al., 2014), and food flavorings are often used as an ingredient to improve or enhance the food's flavor profile. Flavor compounds bind to proteins, potentially influencing sensory perception (Weerawatanakorn et al., 2015). Added flavor compounds interact with proteins in several ways. These include weak and reversible bonds like hydrophobic interactions, hydrogen bonds, van der Waals forces, and ionic/electrostatic forces, as well as stronger, non-reversible covalent linkages (Anantharamkrishnan et al., 2020).

Many studies have examined the effects of flavor addition and subsequent binding to animal- or plant-protein-based systems, mainly by using purified and extracted protein fractions (Bi et al., 2022; Li et al., 2024; Wei et al., 2024). For practical reasons, protein isolates (PI) and concentrates are used as meat and dairy replacers in the food industry. PI can vary in composition and may not always consist of a single, uniform type of protein. Instead, they are characterized by different protein fractions (Lam et al., 2018). The most commonly used ingredients are soy protein isolate (SPI) and pea proteins. Lupin protein isolate (LPI) is gradually gaining popularity because of its beneficial emulsification, foam stabilization, and gel formation properties (Kyriakopoulou et al., 2019).

Protein-flavor interactions have been addressed using mathematical models to unravel the binding parameters, nature, and strength of these interactions. For instance, Harrison and Hill's (Harrison et al., 1997) model relied on the mass transfer theory to predict flavor release from aqueous emulsions. Additionally, the Scatchard plot, or its adaptation as the Klotz plot (Damodaran & Kinsella, 1980, 1981; Suppavorasatit & Cadwallader, 2012), served as a standard method for interpreting binding data. These studies predominantly involve defatted and single protein fractions within a model system. However, understanding whether this interaction persists under dynamic conditions, such as oral processing during food consumption, is highly significant for optimal food design (Barallat-Pérez et al., 2024). In-mouth interactions can occur between proteins and flavors also

between salivary proteins and flavor compounds. As a result of these interactions, aroma release is slowed down, thus affecting the food's aroma perception (Canon & Neyraud, 2016; Mosca & Chen, 2017; Mu & Chen, 2023; Muñoz-González et al., 2022; Ployon et al., 2017). Saliva comprises 98% water and ~ 2% salts, organic compounds, and several proteins. Mucin (M) is the most abundant proteinaceous material (~0.3 wt%) in saliva (Sarkar et al., 2009), together with α -amylase, immunoglobulin, statherin, histatin, proline-rich proteins, and lactoferrin (Canon & Neyraud, 2016). It is characterized by an amphiphilic and heavily glycosylated nature. Within the food-flavor interactions domain, there is a lack of data regarding the *in vitro* interplay between flavored protein-based aqueous model systems (FPBAS), utilizing PI, and mucin.

Therefore, this study aims to investigate (1) the binding parameters (binding sites, n , and binding constants, K) for each PI when combined with each flavor compound and (2) the contribution of mucin to the protein-flavor binding process. To achieve these goals, two plant-based PI (SPI and LPI) and one animal-based PI (whey protein isolate (WPI)) were selected. PI were combined with a homologous series of carbonyl compounds and/or pig gastric mucin. The interactions in all sample combinations were analyzed using static headspace Gas Chromatography-Mass Spectrometry (HS-GC-MS).

5.2. Materials and Methods

5.2.1. Flavor compounds

Ten analytical grade ($\geq 98\%$) flavor compounds were selected based on their spatial configuration, chain length, and wide use in the food industry: 2-hexanone, 2-heptanone, 2-octanone, 2-nonanone, 2-decanone, hexanal, heptanal, octanal, nonanal, and decanal, which were purchased from Sigma-Aldrich (Zwijndrecht, the Netherlands) (Table S5.1).

5.2.2. Protein sources

The investigation used SPI SUPRO[®] XT219D IP from Solae (St. Louis, Missouri, USA), LPI 10600 from ProLupin (Grimmen, Germany), and WPI BiPro[®]

from Davisco International (Le Sueur, Minnesota, USA). **Table S5.2** displays the manufacturer's specifications. Proteins were selected based on their chemical structure, physicochemical properties, and prevalence in plant-based food substitutes. The protein batches were packed and stored in a cool (10–15 °C) and dry environment to minimize result discrepancies.

5.2.3. Other chemicals or materials

Na_2HPO_4 and $\text{NaH}_2\text{PO}_4 \cdot 2\text{H}_2\text{O}$ from Sigma-Aldrich.

5.2.4. Preparation of food flavor stock solutions

Each flavor compound was individually prepared in a sodium phosphate buffer solution (pH 7.0, 50 mM) following an adapted protocol based on Barallat-Pérez et al., 2023. Five initial concentrations were prepared for each flavor: 1, 2.5, 5, 10, and 20 mg/L. To ensure complete dissolution, the flavor stock solutions underwent ultrasonic treatment in a water bath (Elma Schmidbauer GmbH, Singen, Germany) for 1 hour at 30 °C.

5.2.5. Preparation of food protein solutions

An adapted approach from Wang & Arntfield, 2015 was employed to prepare protein solutions. SPI, LPI, and WPI were individually utilized at an initial concentration of 2(w/v)% in sodium phosphate buffer (pH 7.0, 50 mM). The samples underwent vortexing for 10–20 seconds (3200 rpm, using Genie II, Genie™, Sigma-Aldrich, Florida, USA). Then, they were placed in an ultrasonic water bath at 30 °C for 20 minutes to ensure thorough solution blending. Multiple vortexing cycles followed, lasting 10–20 seconds each, to achieve uniform mixture distribution.

5.2.6. Preparation of artificial saliva

Artificial saliva was prepared at room temperature (20–22 °C) and pH 7.0, 50 mM, following an adapted version of Van Ruth et al., 2001, which included: NaHCO_3 , $\text{K}_2\text{HPO}_4 \cdot 3\text{H}_2\text{O}$, NaCl, KCl, $\text{CaCl}_2 \cdot 2\text{H}_2\text{O}$, NaN_3 , and pig gastric mucin, provided by Sigma-Aldrich (Zwijndrecht, the Netherlands). To prevent clumping,

mucin was added very gradually to the solution. Considering the significant variability of mucin levels among individuals (1.19 ± 0.1 - 3.01 ± 1.0 mg/mL) (Acuña et al., 2021; Kejriwal, 2014) due to differences in genetics, environmental factors, age, hydration status, oral health, use of medications, and inter-and intra-individual variability, artificial saliva was prepared at two different concentrations of mucin: 0.1(w/v)% and 0.01(w/v)%.

5.2.7. Binding parameters determination

Binding parameters were computed from the Scatchard plots and/or Klotz plots (Bi et al., 2022; Suppavorasatit & Cadwallader, 2012; Wongprasert et al., 2024) [5.1] to increase understanding of the mechanisms involved.

$$\frac{1}{v} = \frac{1}{n} + \frac{1}{nK[L]} \quad [5.1]$$

where $[L]$ is the free flavor concentration in the aqueous phase (mol/L); v is the number of moles of flavor bound per mole of total protein (mol/mol); K is the binding constant (M^{-1}), and n is the number of independent binding sites. The estimated molecular weight for all PI was set at 100.000 g/mol per prior scientific literature findings (Damodaran & Kinsella, 1981; O'Neill & Kinsella, 1987; Jasinski & Kilara, 1985). Binding parameters (n and K) were calculated from the y -intercepts ($1/n$) and slopes of the plots ($1/Kn$), respectively.

5.2.8. Preparation of the Gas Chromatography-Mass Spectrometry samples (GC-MS)

For the HS-GC-MS analysis, samples were prepared using a modified method from Wang & Arntfield, 2015 and on Barallat-Pérez et al., 2023. Control samples comprised food protein and saliva solutions without added flavor. Vials were sealed and kept in a water bath shaker (SW22, Julabo GmbH, Seelbach, Germany) at 30 °C and 125 rpm for 3 hours before the HS analysis (Wang & Arntfield, 2015). Triplicate samples were prepared for analysis.

5.2.9. Binding measurement and calculation

Protein-flavor-mucin binding was assessed by HS through GC-MS (Agilent- 7890A GC coupled to an Agilent 5975C with triple-axis detector MS, Agilent, Amstelveen, the Netherlands) following a modified method from Wang & Arntfield, 2015 and Barallat-Pérez et al., 2023. Flavor binding to proteins, expressed as a percentage in the absence and presence of protein, was calculated [5.2].

$$Binding (\%) = \left(1 - \frac{HS_1 - HS_2}{HS_3}\right) \times 100 \quad [5.2]$$

where HS_1 denotes the abundance of flavored protein-based aqueous solution in the headspace. HS_2 and HS_3 represent the abundance in the HS when only protein in buffer or flavor in buffer, respectively, is present, without the other component.

Flavor binding to mucin was calculated and expressed in % in the absence and presence of mucin [5.3].

$$Binding (\%) = \left(1 - \frac{HS_1 - HS_2 - HS_4 - HS_5}{HS_3}\right) \times 100 \quad [5.3]$$

where HS_4 (saliva solution + buffer) represents the HS in the absence of flavor, and HS_5 (protein solution + saliva solution) represents the abundance in the HS of the protein-based saliva solution.

5.2.10. Statistical analysis

Binding data were determined in triplicate, with results presented as mean \pm standard deviation. Statistical analysis was performed using RStudio 4.2.1. (Boston, Massachusetts, USA) for a two-way ANOVA on each sample combination. Post-hoc Tukey tests determined significant differences ($p < 0.05$) between samples.

5.3. Results and Discussion

5.3.1. Determination of the binding parameters of protein-flavor aqueous model systems

Figure 5.1 A-F displays the Klotz plots of the binding of carbonyl compounds to WPI, LPI, and SPI in mucin-free solutions. The binding parameters (n and K) were determined by generating double-reciprocal plots from the Klotz equation [5.1].

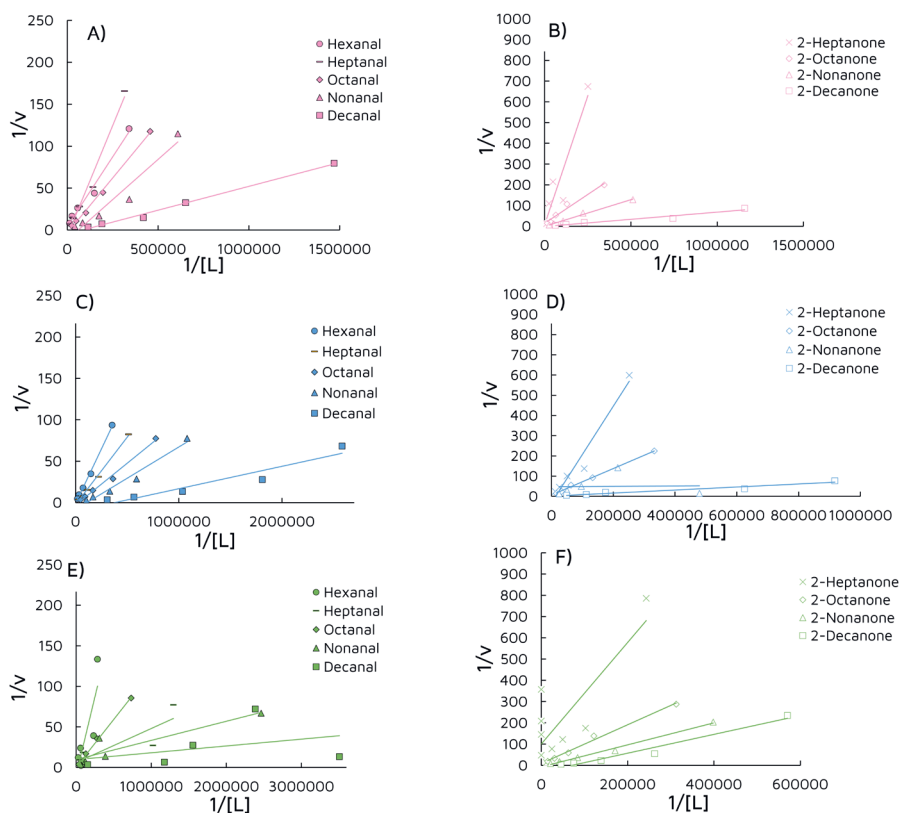


Figure 5.1. Klotz plots for binding of carbonyl compounds to commercial food protein isolates (PI): whey (WPI) (A, B), soy (SPI) (C, D), and lupin (LPI) (E, F) protein isolates. Plots were calculated following equation [5.1]. To optimize data visualization, scales are adjusted differently for the X-axis ($1/[L]$, being L the free ligand concentration in the aqueous phase) and the Y-axis ($1/v$, being v the number of moles of ligand bound per mole of total protein). These adjustments are made based on their respective maximum responses.

Due to mucin's high polydispersity and glycosylation nature, it seems unfeasible to estimate binding parameters for this protein. Mucin peptide chains may vary in size, molecular weight (0.5-20 MDa), and the number of basic units imparting a non-uniform character (Linthorpe & Taylor, 2001; Harding, 1989). Thus, **Figure 5.1 A-F** illustrates the linearity of the plots between PI and carbonyl compounds in mucin-free samples. The double reciprocal plot indicates that the flavors bind to the proteins independently in non-cooperative interactions. In non-cooperative interactions, the binding of one ligand does not influence the binding strength/affinity of a second ligand. As a result, each binding event occurs independently, resulting in a linear relationship (Damodaran & Kinsella, 1981; Gianelli et al., 2003; Houde et al., 2018; Wongprasert et al., 2024).

The binding parameters (n and K) and linear equations for binding carbonyl compounds to PI were derived from equation [5.1], and their values are shown in **Table 5.1**. For most of the protein-flavor combinations (**Table 5.1**), the coefficients of determination (R^2) were greater than 0.94, indicating that the equations explained >94% of the total variation for the plots. The R^2 values of 2-hexanone were excluded due to a low score ($R^2 < 0.1$), indicating a lack of fit between the model and the data. Its high volatility (**Table S5.1**) might limit its binding to proteins, leading to inaccurate parameter quantification.

The number of binding sites (n) differed among the different PI and were influenced by the type of flavor. Experimental values for n varied from $n=0.021$ to $n=7.194$. While some exhibit patterns, such as increased n with longer chain lengths for ketones and SPI, the opposite holds for aldehydes and SPI (**Table 5.1**). Overall, the n values obtained are in line with previous research findings in which the binding between proteins and various flavor compounds was investigated: soy-ketones ($n=4$) (Damodaran & Kinsella, 1981), soy-vanillin ($n=0.48$) (Li et al., 2000), soy-maltol ($n=3.27$) (Suppavorasatit & Cadwallader, 2012), pea-hexanal ($n=4.84$) (Bi et al., 2022), whey-vanillin ($n=0.67$) (Li et al., 2000), soy-citronellol ($n=4.2$) (Guo et al., 2020), pea-methyl anthranilate ($n=0.68$) (Wongprasert et al., 2024) and coconut-vanillin ($n=1.47$) (Temthawee et al., 2020).

Table 5.1. Linear equations and binding parameters (n =binding sites and K =binding constants) obtained from Klotz plots for the binding of carbonyl compounds to commercial food protein isolates (PI) (whey, WPI, soy, SPI, and lupin, LPI).

Protein	Whey Protein Isolate				Soy Protein Isolate				Lupin Protein Isolate			
	n	K (M ⁻¹)	Equation	R ²	n	K (M ⁻¹)	Equation	R ²	n	K (M ⁻¹)	Equation	R ²
2-Heptanone	0.140	2.8·10 ³	y=0.0025x+7.132	0.87	0.032	1.2·10 ⁴	y=0.0024x-31.061	0.96	0.021	1.4·10 ⁴	y=0.0033x-46.313	0.95
2-Octanone	0.073	2.2·10 ⁴	y=0.0006x+13.601	0.96	0.153	9.2·10 ³	y=0.0007x+6.508	0.99	0.114	9.7·10 ³	y=0.0009x+8.7383	0.99
2-Nonanone	4.870	6.8·10 ²	y=0.0003x-0.205	0.99	0.331	1·10 ⁴	y=0.0003x-3.014	0.98	0.145	1.3·10 ⁴	y=0.0005x-6.8868	0.99
2-Decanone	0.674	2.1·10 ⁴	y=0.000007x-1.483	0.95	0.915	1.3·10 ⁴	y=0.00008x+1.092	0.94	0.032	7.7·10 ⁴	y=0.0004x-31.052	0.96
Hexanal	0.240	1.3·10 ⁴	y=0.0003x+4.160	0.98	0.935	3.5·10 ³	y=0.0003x-1.068	0.99	0.098	2.5·10 ⁴	y=0.0004x-10.144	0.71
Heptanal	0.136	1.4·10 ⁴	y=0.0005x-7.342	0.978	0.432	1.1·10 ⁴	y=0.0002x-2.310	0.99	0.166	1.5·10 ⁵	y=0.00005x-6.0163	0.75
Octanal	0.273	1.2·10 ⁴	y=0.0003x-3.657	0.99	0.349	2.8·10 ⁴	y=0.0001x-2.864	0.99	7.194	1.3·10 ³	y=0.0001x+0.139	0.99
Nonanal	0.085	5.8·10 ⁴	y=0.0002x-11.672	0.9403	0.120	1·10 ⁵	y=0.00005x-8.304	0.97	0.101	4.9·10 ⁵	y=0.000002x+9.186	0.82
Decanal	0.210	7.9·10 ⁴	y=0.000006x-4.747	0.993	0.097	3.4·10 ⁵	y=0.00003x-10.230	0.91	0.102	1.2·10 ⁶	y=0.0000008x+9.771	0.14

The reported n values do not necessarily signify the total potential binding sites. Protein processing, such as denaturation (Guo et al., 2015; Semenova et al., 2002; Wang & Arntfield, 2015), may alter, change the distribution, or lose some binding sites. Klotz plots assume that protein binding sites are uniform in number and function (Kühn et al., 2006). But proteins harbor multiple ligand-binding sites that exhibit non-identical subunits differing in structure and spatial arrangement, thus, lacking equivalence (Belleli & Carey, 2018). Therefore, proteins may exhibit both high-affinity and lower-affinity binding sites (Kühn et al., 2006) due to the different amino acid composition of the binding site (Cichero et al., 2018), or structural rearrangement. This could explain the lack of a clear trend regarding the obtained n values (**Table 5.1**).

The binding constant (K) values exhibited variation across different PI and were influenced by the type of flavors. Values varied from $K=6.8 \cdot 10^2 \text{ M}^{-1}$ to $K=1.2 \cdot 10^6 \text{ M}^{-1}$ (**Table 5.1**). Lower K values indicate a weaker affinity between the proteins and flavors, while higher K values suggest stronger binding. Typically, longer flavor chains are associated with higher K , indicating hydrophobic interactions (Wongprasert et al., 2024). In **Table 5.1**, the data shows that aldehydes exhibited higher K values than ketones. An inner location of the keto group (*i.e.*, ketones *vs.* aldehydes) may have led to steric hindrance hindering flavor binding (Barallat-Pérez et al., 2023; Beyeler & Solms, 1974; Damodaran & Kinsella, 1981; Guo et al., 2024; Thissen, 1982).

Although the experimental conditions may differ across different binding studies (Guo et al., 2020; Li et al., 2000; Suppavorasatit & Cadwallader, 2012; Temthawee et al., 2020; Wongprasert et al., 2024), there is still a clear consistency concerning the significant role of flavor's structural properties (functional group and location) in determining n and K values.

5.3.2. Role of mucin in the protein-flavor binding mechanism

To gain a deeper understanding of the intricate dynamics between proteins and flavors when combined with mucin, an artificial saliva solution was utilized, containing mucin as its primary component. HS-GC-MS analyses were

performed, and the binding percentage was calculated [5.2] and [5.3], as illustrated in **Figures 5.2** and **5.3**. **Figure 5.2** illustrates the binding effect of mucin (M) (0.01(w/v)%) on the protein-flavor binding mechanism in protein-aldehyde-based aqueous model systems (PAB) and protein-ketone-based aqueous model systems (PKB), increasing in chain length from C₆ to C₁₀. Controls without mucin (*e.g.*, solely protein and flavor) were included for comparison.

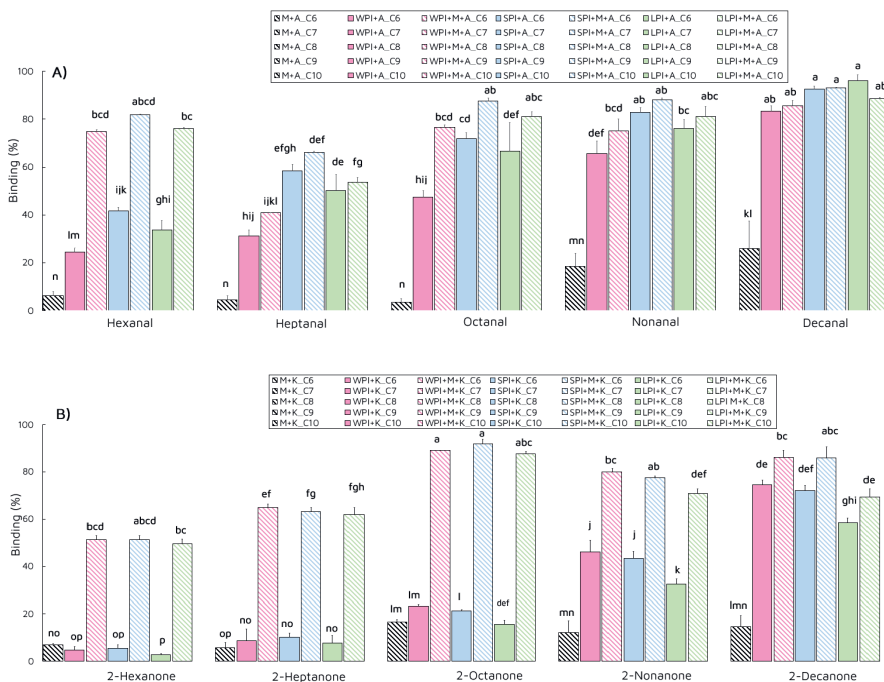


Figure 5.2. Effect of mucin (M) (0.01(w/v)%) on the protein-flavor binding mechanism in **(A)** protein-aldehyde-based aqueous model systems (PAB) and **(B)** protein-ketone-based aqueous model systems (PKB) increasing in chain length from C₆ to C₁₀. The abbreviations “A_” and “K_” indicated the chemical class (aldehydes or ketones), followed by the chain length. Binding (%) was calculated following equations [5.2][5.3]. Results are expressed as the mean \pm standard deviation. Letters denote significant differences ($p < 0.05$). Treatments with the same letter are not significantly different.

Comparing mucin-free solutions, PAB exhibited a higher level of binding (**Figure 5.2 A**) than PKB (**Figure 5.2 B**). The binding (%) ranged from 24.3 ± 2 to 96.0 ± 3 for PAB, whereas for PKB, the binding (%) varied from 4.7 ± 1 to 74.5 ± 2 . No significant differences were found across the studied PI.

It is well known that aldehydes not only bind via reversible and weak hydrophobic interactions flavor compounds but can also participate in irreversible covalent binding through Schiff base formation. In this process, they react with amino groups of the protein to form an imine linkage (Anantharamkrishnan et al., 2020), resulting in stronger bonds.

The addition of mucin (0.01(w/v)%) to either PAB or PKB strongly increased flavor binding (**Figure 5.2**), regardless of the flavor compound or protein used (WPI, SPI, or LPI). The addition of mucin had a more pronounced effect on PKB (**Figure 5.2 B**) than on PAB (**Figure 5.2 A**). Compared to mucin-free solutions, binding (%) was up to fifteen times higher in protein-ketone-mucin-based systems (PKMB) and up to three times higher in protein-aldehyde-mucin-based systems (PAMB). Binding (%) ranged from 49.5%±2 to 86.2%±3 for PKMB and 74.8%±1 to 93.0%±1 for PAMB. As the chain length increases, the hydrophobicity also increases, reducing the impact of mucin addition. Despite ketones potentially hindering binding and their known lower affinity for proteins compared to aldehydes (Shen et al., 2019; Zhang et al., 2023), the higher hydrophilic nature of ketones compared to aldehydes (**Table S5.1**) might be considered a key factor in their greatest effect on PKMB systems. No significant differences were found across the studied protein sources.

As seen in **Figure 5.2**, a greater effect occurred with the most hydrophilic compounds and short-chain flavor compounds (*i.e.*, 2-hexanone, 2-heptanone, hexanal, and heptanal) compared to the most hydrophobic ones and long-chain flavor compounds (*i.e.*, 2-nonanone, 2-decanone, nonanal, and decanal).

Adding mucin to either PAB or PKB resulted in a combined effect that greatly surpassed the individual binding contributions (**Figure 5.2**). Although the exact mechanism is unclear, mucin interacting with proteins is hypothesized to enhance flavor binding by revealing or forming additional hydrophobic pockets, leading to a synergistic binding effect. While research on flavor binding in protein solutions with mucin is limited, synergistic behavior has been observed in other protein-based systems (Ahmad et al., 2022; Feiler et al., 2007; Wang et al., 2023). Ahmad et al., 2022 demonstrated the interaction of mucin with β -Lactoglobulin (BLG),

suggesting structural rearrangements and molecular reorganization that alter its affinity and access to binding sites. Likewise, Wang et al., 2023 confirmed soy isoflavones' synergistic effect on WPI by inducing its unfolding and enhancing their functional properties.

To gain deeper insights into the role of mucin in flavored protein-based aqueous model systems (FPBAS: PAMB and PKMB) and consider the significant variability of mucin levels among individuals (Acuña et al., 2021; Kejriwal, 2014), mucin concentrations were increased to 0.1(w/v)%. **Figure 5.3** shows the effect of mucin (0.1(w/v)%) on PKB, increasing in chain length from C₆ to C₁₀. Since no significant differences were previously reported among the studied WPI, SPI, or LPI (**Figure 5.2**), the comparison was limited to the animal protein (WPI) and one plant protein (SPI) (**Figure 5.3**).

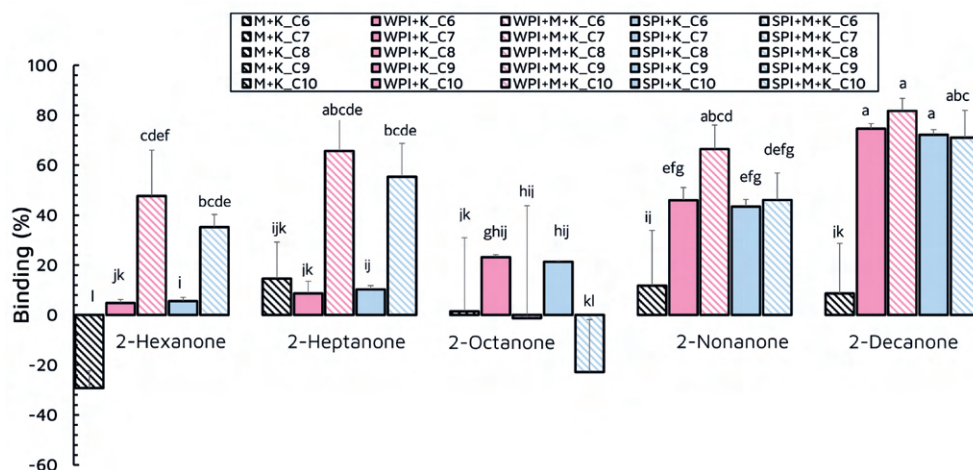


Figure 5.3. Effect of mucin (M) 0.1(w/v)% on the protein-flavor binding mechanism. The abbreviation "K_" indicated the chemical class (ketones), increasing in chain length from C₆ to C₁₀. Binding (%) was calculated following equations [5.2][5.3]. Results are expressed as the mean \pm standard deviation. Letters denote significant differences ($p < 0.05$). Treatments with the same letter are not significantly different.

As seen in **Figure 5.3**, flavor binding is still noticeably higher upon mucin addition (0.1(w/v)%) to PKB, as already seen in **Figure 5.2**. Compared to mucin-free solutions, binding (%) was up to ten times higher in PKMB. The binding (%) ranged from 4.7 ± 1 to 74.5 ± 2 for PKB, whereas for PKMB, the binding (%) varied from -

22.83±21 to 81.72%±5. No significant differences were found across the studied PI.

Non-covalent interactions may prevail in the studied aqueous model system (**Figure 5.3**). Mucin adopts a randomly coiled conformation at the studied pH (pH 7.0). Even though mucins have a negative charge, primarily from sialic acid residues and sulfated sugars, mucins typically exhibit low isoelectric points (pI 2-3.0) (Çelebioğlu et al., 2020). Similarly, the studied PI carry a negative charge (pI 4.3) (Dinu et al., 2019; Yılmaz et al., 2021). While electrostatic interactions are unlikely due to repulsive forces, mucin also contains positively charged patches in the non-glycosylated globular regions composed of histidine, arginine, and lysine residues, which may attract the negatively charged WPI (Ahmad et al., 2020). Therefore, hydrophobic interactions can dominate the interaction mechanism (Cook et al., 2017). When mucin encounters the food proteins (**Figure 5.4**), it may adhere to the protein surface by hydrogen bonding, hydrophobic, electrostatic interactions, and/or covalent bonding (Brown et al., 2021).

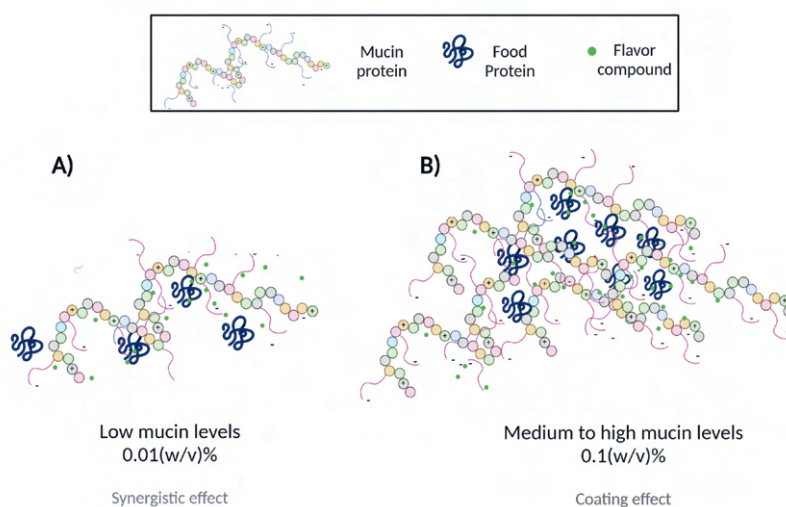


Figure 5.4. Mechanism of interaction in flavored protein-based aqueous systems (FPBAS) in the presence of **(A)** low mucin levels 0.01(w/v)% and **(B)** medium to high mucin levels 0.1(w/v)%. Adapted from Brown et al., 2021. (Biorender software).

Similarly, mucin molecules are known to associate or aggregate with each other (Vingerhoeds et al., 2005), resulting in molecular crowding. Sarkar et al., 2009

observed that artificial saliva (mucin) (0-3 wt%) interacted with lactoferrin and BLG-stabilized emulsions by electrostatic attraction. Hydrophobic interactions between unfolded milk protein and mucin may also occur at low ionic strengths in artificial saliva (Sarkar et al., 2009). Therefore, it is proposed that high levels of mucin may interact and cover the existing food protein binding sites (**Figure 5.4 B**), hiding them from flavor molecules and thus reducing flavor binding (**Figure 5.3**).

In brief, 0.01(w/v)% of mucin appears insufficient to cover the surface of the food protein adequately. Nevertheless, the potential exists for inducing structural alterations that may lead to unfolding the 3D food protein structure, thereby enhancing flavor binding (**Figure 5.4 A**). At higher mucin levels (0.1(w/v)%), mucin may effectively cover the binding sites and lead to the clustering of mucin molecules (**Figure 5.4 B**).

5.4. Conclusions

In summary, binding parameters (binding sites, n , and binding constant, K) were determined from Klotz plots in FPBAS (PAB and PKB). The results suggested a non-cooperative, independent, linear relationship between proteins and flavor compounds. The structural characteristics of the flavors were shown to be significant in determining n and K values, with chain length and position of the functional group being key features of the binding mechanism. In contrast, protein sources showed only a minor impact on flavor binding.

Adding 0.01(w/v)% of mucin to FPBAS significantly increased flavor binding, irrespective of the flavor compound or protein source, potentially suggesting protein unfolding and the exposure of previously hidden hydrophobic pockets. Whereas increasing the mucin concentration to 0.1(w/v)% did not yield a subsequent increase in flavor binding, suggesting the possibility of a coating mechanism occurring on the available food protein binding sites.

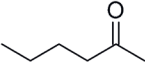
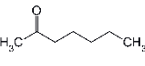
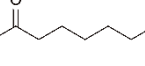
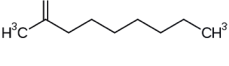
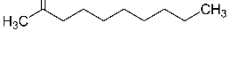
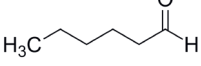
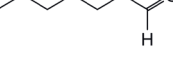
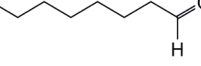
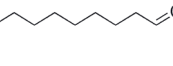
These findings aid in comprehending the essential aspects of flavor binding in the presence and absence of mucin and in the presence of different mucin

concentrations, which are crucial variables when designing and developing novel food products.

The study has some limitations in mimicking what happens during the physiological mastication process. These results were obtained in an aqueous model system at equilibrium, which may not fully replicate all the intricate processes occurring dynamically in the mouth. Therefore, complementary sensory evaluation techniques might need to be explored to provide a more accurate reflection of the actual impact on consumer perception compared to analytical approaches alone.

5.5. Supplementary Material

Table S5.1. Physicochemical and structural features of the selected flavor compounds.

Compound	CAS	Chemical structure ¹	LogP ²	Molecular Weight (g/mol) ³	Vapor pressure ⁴ (mmHg at ~25°C)	Solubility in water ⁵ (mg/L at ~25°C)
2-hexanone (C ₆ H ₁₂ O)	591-78-6		1.4	100.60	0.36	17200.0
2-heptanone (C ₇ H ₁₄ O)	110-43-0		2	114.19	3.00	4280.0
2-octanone (C ₈ H ₁₆ O)	111-13-7		2.4	128.21	1.35	899.0
2-nonanone (C ₉ H ₁₈ O)	821-55-6		3.1	142.24	0.62	370.0
2-decanone (C ₁₀ H ₂₀ O)	693-54-9		3.7	156.26	0.27	76.8
Hexanal (C ₆ H ₁₂ O)	66-25-1		1.8	100.16	11.3	5640.0
Heptanal (C ₇ H ₁₄ O)	111-71-7		2.3	114.19	3.52	1250.0
Octanal (C ₈ H ₁₆ O)	124-13-0		2.7	128.21	1.18	560.0
Nonanal (C ₉ H ₁₈ O)	124-19-6		3.3	142.24	0.37	96.0
Decanal (C ₁₀ H ₂₀ O)	112-31-2		3.7	156.26	0.20	43.52

¹⁻⁵ Properties obtained from PubChem (National Center for Biotechnology Information) (Kim et al., 2023) and the Good Scents Company.

Table S5.2. Manufacturer-specified values of protein and fat content for whey (WPI), soy (SPI), and lupin (LPI) protein isolates. Nutritional information per 100 g of product.

	Total fat (triglycerides) content	Total protein content
WPI	<0.05%	97.6%
SPI	3.1%	91.2%
LPI	3%	91%



Drivers of the in-mouth interaction between lupin protein isolate and selected aroma compounds: a PTR-MS and Dynamic Time Intensity analysis

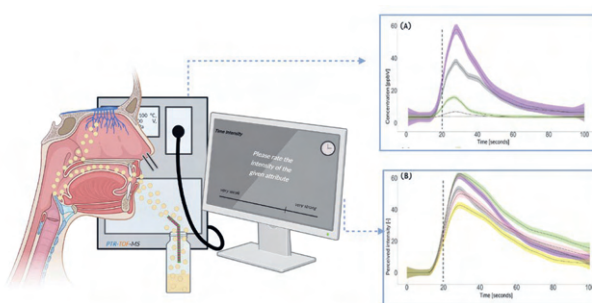
Published as:

Barallat-Pérez, C. B., Pedrotti, P., Oliviero, T., Martins, S., Fogliano, V., Jong, de C.
Drivers of the in-mouth interaction between lupin protein isolate and selected
aroma compounds: a PTR-MS and Dynamic Time Intensity
analysis. *J. Agric. Food Chem.* 2024, 72, 50, 8731-8741. DOI:
10.1021/acs.jafc.3c08819

Abstract

Plant proteins often carry off-notes, necessitating customized aroma addition. *In vitro* studies revealed protein-aroma binding, limiting release during consumption. This study employs *in vivo* nose space Proton Transfer Reaction-Time-Of-Flight-Mass Spectrometry and dynamic sensory evaluation (Time Intensity) to explore in-mouth interactions. In a lupin protein-based aqueous system, a sensory evaluation of a trained "green" attribute was conducted simultaneously with the aroma release of hexanal, nonanal, and 2-nonanone during consumption. Results demonstrated that enlarging aldehyde chains and relocating the keto group reduced maximum perceived intensity (I_{\max_R}) by 71.92% and 72.25%. Protein addition decreased I_{\max_R} by 30.91%, 36.84%, and 72.41%, indicating protein-aroma interactions. Sensory findings revealed a lower perceived intensity upon protein addition. Aroma lingering correlated with aroma compounds' volatility and hydrophobicity, with nonanal exhibiting the longest persistence. *In vitro* mucin addition increased aroma binding four to twelvefold. Combining PTR-ToF-MS and Time Intensity elucidated crucial food behavior, *i.e.*, protein-aroma interactions, pivotal for food design.

Keywords: aroma compounds; release; binding; perception; lupin protein; Proton Transfer Reaction-Mass Spectrometry; Time Intensity; aqueous model systems.



Simultaneous *in vivo* nose space analysis and dynamic sensory evaluation using PTR-ToF-MS and Time Intensity

Graphical design: BioRender and IONICON

TOC Graphic 6. Drivers of the in-mouth interaction between lupin protein isolate and selected aroma compounds: a PTR-MS and Dynamic Time Intensity analysis. (BioRender software).

6.1. Introduction

Plant-based proteins have emerged as a popular substitute for animal proteins in creating innovative plant-based food and beverages. While soybeans (*Glycine max*) and peas (*Pisum sativum* L.) have traditionally taken the spotlight (Ismail et al., 2020), there is growing interest in exploring alternative protein sources. In Western Europe, lupin (*Lupinus angustifolius* L.) protein isolate (LPI) recently gained attention because of its excellent interfacial properties. LPI forms weaker gels than soy protein isolate (SPI) upon heating, making it well-suited for high-protein beverage applications (Berghout, 2015). Unlike soybeans, lupin exhibits a milder bitterness due to its reduced saponin content (Ritter et al., 2022). Despite being considered a potential protein replacement, lupin protein is characterized by cheese-like and sweaty profiles due to 2- and 3-methylbutanoic acids. Detectable but less pronounced cardboard-like, fatty, and green pepper-like off-notes (3-isopropyl-2-methoxypyrazine, *trans*-non-2-enal and *trans, cis*-2,6-nonadienal) may also be present (Bader et al., 2009). These odor qualities can influence the sensory experience and affect its acceptability.

Various technologies are employed in the food industry to enhance (like cultivar selection and control of oxidation and temperature), remove (including soaking, thermal treatments, and enzymatic treatment), and mask (such as the addition of aroma) undesired aroma notes (Roland et al., 2017). Despite the array of available technologies, aroma addition offers an effective and customizable solution to improve the aroma of plant-based foods.

In vitro studies showed that aroma compounds can bind to proteins, forming either weak and reversible bonds via hydrophobic, hydrogen, or electrostatic interactions or irreversible ones like covalent bonds (Anantharamkrishnan et al., 2020; Barallat-Pérez et al., 2023; Bi et al., 2022; Snel et al., 2023). Protein-aroma binding may affect flavor perception by regulating continuous consumption release. Yet, the scenario differs under *in vivo* (dynamic) conditions during oral processing. During food consumption, aroma compounds must diffuse into the aqueous (saliva) phase and then transfer into the air phase of the oral cavity to

enter the nasal cavity. Subsequently, the olfactory receptors perceive the aroma compounds and are ultimately sensed during oral processing (Muñoz-González et al., 2022). This recurring in-mouth event is known as retronasal olfaction (Hannum et al., 2018). Due to the dynamic nature of oral processing and the rapidly changing conditions in the mouth—such as interactions between oral surfaces and foods—aroma compounds rarely reach equilibrium (Mao et al., 2017). Instead, oral processing involves a continuous state of equilibrium, reflecting a dynamic mass transportation phenomenon. The kinetic release of the aroma compounds from food systems is influenced by their molecular structure, thermodynamics, physicochemical characteristics, and the barrier to mass transfer from the food matrix to the air phase (de Roos, 2000; Doyennette et al., 2019; Hannum et al., 2018; Mao et al., 2017; Weterings et al., 2020).

Variables like the composition of the food matrix, conditions of consumption, and individual-specific parameters (*i.e.*, chewing behavior and physiological characteristics) (Doyennette et al., 2019) hold potential significance in modulating sensory perception. In-mouth interactions between salivary proteins and aroma compounds can alter flavored food perception (Doyennette et al., 2019; Muñoz-González et al., 2022). For instance, mucin proteins in saliva alter the distribution equilibria of aroma compounds, slowing their transport to the nasal cavity (Ijichi et al., 2019; Muñoz-González et al., 2022; Ployon et al., 2017).

For decades, flavor research has utilized dynamic techniques such as Atmospheric Pressure Chemical Ionisation-Mass Spectrometry (APCI-MS) and Proton Transfer Reaction Mass Spectrometer (PTR-MS) to monitor volatile release. PTR-MS, coupled with a Time-of-Flight mass spectrometer (PTR-ToF-MS), is particularly suited for measuring *in vivo* aroma release from food products (Pedrotti et al., 2019). When complemented by dynamic sensory analysis like Time Intensity (TI) and the Temporal Dominance of Sensations (TDS), it offers real-time insight into aroma release and perception (Le Calvé et al., 2019; Pionnier et al., 2004). This combination has been employed to investigate the correlation between *in vivo* aroma release and perception in various products, including chewing gum (Pedrotti et al., 2019), ice cream (Chung et al., 2003), mayonnaise (Van Eck et al.,

2021), and chocolate hazelnut spreads (Gonzalez-Estanol et al., 2023). Despite extensive research using GC-MS and PTR-MS in the last decade on aroma compound release and their physicochemical properties (Chen et al., 2023; Esteban-Fernández et al., 2016; Muñoz-González et al., 2019; Muñoz-González et al., 2021; Perez-Jiménez et al., 2020; Pérez-Jiménez et al., 2023), knowledge about plant protein-based systems, particularly with commercial food protein isolates, remains limited.

For this purpose, this study delves into the drivers of the in-mouth interaction between lupin protein isolate and selected aroma compounds (hexanal, nonanal, and 2-nonanone) by coupling dynamic nose space PTR-ToF-MS and TI profiling. LPI was selected for its promising potential in high-protein food products and neutral taste and odor profile. Complementary *in vitro* analyses were performed with pig gastric mucin (M) to investigate the interplay between mucin, protein, and aroma.

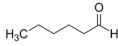
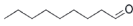
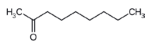
6.2. Materials and Methods

6.2.1. Aroma compounds

Aroma compounds were selected based on their chemical class (aldehydes and ketones), structure (chain length and carbonyl group position), physicochemical properties (volatility, hydrophobicity, water solubility), and common use in beverages. Hexanal, nonanal, and 2-nonanone (Sigma-Aldrich, Zwijndrecht, the Netherlands) with a purity of $\geq 95\%$ were chosen, meeting food-grade standards below their toxicity levels.

Each aroma compound was dissolved in MiliQ water (pH 7.0) at 10 mg/L in 100 mL amber glasses, following a modified version of Wang & Arntfield, 2015. The stock solutions were then placed in a bath at 30 °C for 1 hour to ensure optimal mixing. **Table 6.1** details the selected aroma compounds' molecular structure and physicochemical properties.

Table 6.1. Physicochemical and structural features of the selected aroma compounds.

Compounds	CAS	Chemical structure ¹	Flavor molecular weight (g/mol) ²	Vapor pressure ³ (mmHg)	LogP ⁴	Water solubility (mg/L) ⁵
Hexanal (C ₆ H ₁₂ O)	66-25-1		100.16	11.26	1.8	5640
Nonanal (C ₉ H ₁₈ O)	124-19-6		142.24	0.37	3.3	96
2-nonanone (C ₉ H ₁₈ O)	821-55-6		142.24	0.62	3.1	371

¹⁻⁵ Properties obtained from PubChem (National Center for Biotechnology Information).

6.2.2. Lupin Protein Isolate (LPI)

Lupin Protein Isolate (LPI) 10600 was obtained from ProLupin GmbH (Grimmen, Germany). The manufacturer's specifications indicated that the LPI contained 3 wt% lipid and 91% protein. The protein batches were stored in a cool (10-15 °C), dry area away from light and air to minimize variability in the results. According to the manufacturer's details, LPI was obtained through aqueous extraction and spray drying from seeds of the sweet blue lupine (*Lupinus angustifolius* L.) and had a taste ranging from neutral (pH 7.0) to grassy, accompanied by a grainy and flour-like odor.

The preparation of LPI stock solutions was done according to Barallat-Pérez et al., 2023 and adapted from Wang & Arntfield, 2015. Samples were prepared at 2(w/v)% initial concentration in MiliQ water (pH 7.0). Subsequently, samples were vortexed for 10-20 seconds (3200 rpm, Genie II, Genie™, Sigma-Aldrich, Florida, USA) and kept in a water bath (SW22, Julabo GmbH, Seelbach, Germany) for 20 minutes at 30 °C to provide a proper mixture of the protein solutions. Finally, the solutions were vortexed again (3200 rpm) for another 10-20 seconds to ensure homogeneity.

6.2.3. Other chemicals or materials

Na_2HPO_4 and $\text{NaH}_2\text{PO}_4 \cdot 2\text{H}_2\text{O}$ were analytical grade and purchased from Sigma-Aldrich (St. Louis, Missouri, USA). Artificial saliva was made at 0.01(w/v)%, following the adapted version of Van Ruth et al., 2001. The following ingredients were added per 1000 mL: NaHCO_3 (5.208 g), $\text{K}_2\text{HPO}_4 \cdot 3\text{H}_2\text{O}$ (1.369 g), NaCl (0.877 g), KCl (0.477 g), $\text{CaCl}_2 \cdot 2\text{H}_2\text{O}$ (0.441 g), pig gastric mucin (M) (2.160 g), and NaN_3 (0.5 g), provided by Sigma-Aldrich.

6.2.4. Creation of the flavored lupin protein-based aqueous model systems (FLPBAMS)

Seven aqueous model systems (three containing aroma but no protein, three containing both aroma and protein, and one containing protein but no added aroma) were prepared using MiliQ water (pH 7.0), protein (0 or 1(w/v)% LPI), and hexanal, nonanal, and 2-nonanone, following a modified protocol based on previous work by Barallat-Pérez et al., 2023 and Saint-Eve et al., 2010. The samples were incubated in a water bath shaking at 125 rpm for 3 hours before nose space analysis. Three hours proved adequate timing for achieving equilibrium (Wang & Arntfield, 2015). Supplementary Material, **Table S6.1**, provides an overview of all samples.

A risk assessment was conducted to ensure safety, identify main hazards, and evaluate the likelihood and severity of harm. The risk assessment demonstrated that no exposure risks were involved in participating in the study. *In vitro* and *in vivo* pilot trials were performed to determine optimal sample size (mL) and concentration (mg/L). Food applications typically involve concentrations in parts per billion (ppb) or parts per trillion (ppt) (Heng et al., 2004). Thus, a final aroma concentration of 5 mg/L was selected, consistent with comparable sensory studies (Linthorpe & Taylor, 2000; Muñoz-González et al., 2022; Saint-Eve et al., 2010; Weel, 2004). This concentration is below the recommended maximum usage level according to FEMA GRAS 25th edition (Smith et al., 2011). A 10 mL aqueous model system, meeting food-grade standards, was spiked with aroma

compounds, each added separately. This study was exempt from the obligation to obtain ethical approval from the medical ethical committee overseeing human studies at Wageningen University. It adhered to the principles outlined in the Declaration of Helsinki.

6.2.5. Focus group discussions

Focus group discussions were conducted before the sensory evaluation to gauge consumer preferences for three chosen protein isolates in aqueous solution: SPI, LPI, and pea protein isolate (PPI). The recruitment targeted regular consumers (n=40) of plant-based beverages from Wageningen University. Consumers were asked to select the preferred protein based on the overall taste and odor. LPI emerged as the preferred candidate for the study, with 52.5 % of the panelists choosing it over PPI or SPI (**Figure S6.1**).

6.2.6. Subjects

Ten European female subjects (26±2 years, mean ± SD) were recruited from Wageningen University for this study. The selected criteria included non-smoking status, absence of swallowing disorders, no allergy to lupin, and no use of dental braces. Saliva flow rate (0.145±0.10 g/min, mean ± SD) and mouth volume (75±8.5 g water, mean ± SD) were measured to complement the understanding of *in vivo* aroma release (Doyennette et al., 2019). All participants provided informed, written consent under the European Data Protection Regulation (UE 679/2016) and received financial compensation for their participation.

6.2.7. Sensory training

Participants underwent three training sessions to ensure optimal performance during the study. Additional data in Supplementary Material, **Figure S6.2**, details the initial attributes description during the first training session. Samples were generally described as fruity, synthetic, herbal, lemongrass, sweet,

cucumber, grass, green, bitter, and grain-like (**Figure S6.2**). After reviewing panelist descriptions (**Figure S6.2**) and the odor/taste description found in the literature (Lee, 2009; The Human Metabolome Database), a consensus for all samples was achieved, resulting in selecting the attribute "green". "Green" was defined as "*reminiscent of grass and vegetables, with a slight pungency, accompanied by hints of fruitiness and freshness*" (Lee, 2009). In the first session, they familiarized themselves with the samples and learned the definition of the selected 'green' attribute.

In a second training session, participants learned about the use of EyeQuestion[®] software (version 5, Logic8 BV, Est, The Netherlands) and the sensory methodology.

In the last session, the panelists became acquainted with the nose space pieces on their insertion into the nostrils and the consumption protocol (*i.e.*, swallowing while breathing through the nose space pieces) to instill a sense of fearlessness and comfort in them.

6.2.8. Simultaneous *in vivo* nose space analysis and dynamic sensory evaluation

The protein-aroma binding was assessed concurrently using PTR-ToF-MS and TI. Subjects followed a standardized drinking protocol to reduce variability. *In vivo* nose space experiments were conducted with a high-sensitivity PTR-QiToF-MS (Ionicon Analytik, Innsbruck, Austria) (Sulzer et al., 2014) with a drift tube temperature of 100 °C, voltage of 900 V, and pressure of 460 Pa, resulting in a field density ratio (E/N) of 133 Td. The volatile compounds present in the nose space were introduced into the system through a PEEK capillary line (1/16" OD, 0.01" ID, 0.32) heated to 100 °C with a flow rate of 40 mL/min. The mass resolution ($m/\Delta m$) was at least 4800, and data were collected for the mass range m/z 20-25 (Sulzer et al., 2014).

Figure 6.1 illustrates the simultaneous assessment of aroma release and perception by PTR-ToF-MS and TI. As seen in **Figure 6.1**, the background signal

was measured first for 20 seconds. Each participant inserted two Teflon nose space pieces (6.8 mm diameter, 6.4 cm length) into their nostrils, connected to a heated (100 °C) N.A.S.E. device (Ionicon Analytik, Innsbruck, Austria). They then breathed regularly for 1 minute to establish a breath baseline.

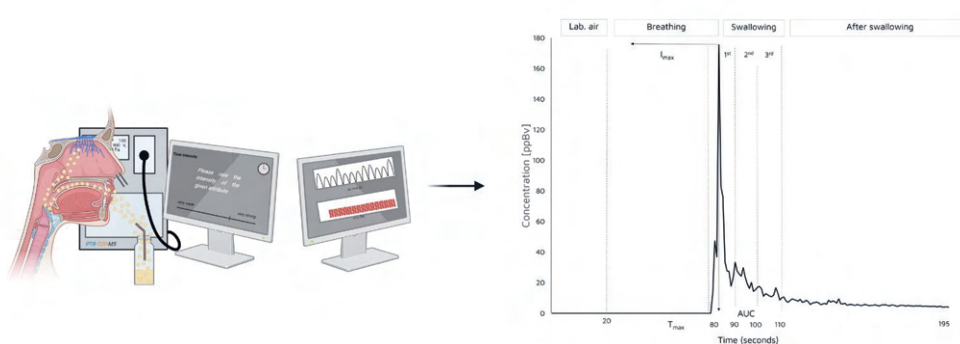


Figure 6.1. Graphical overview of the simultaneous assessment of aroma release and perception (Biorender software; IONICON).

Dynamic sensory evaluation was performed using TI (Cliff & Heymann, 1993) (EyeQuestion® software). Subjects refrained from consuming food or beverages (except water) for 1 hour before the test. Samples were coded with three-digit random numbers and served at 25 ± 5 °C in a 20 mL clear GC-MS glass vial (75.5 mm * 17.5 mm) closed with a screw metallic cap. The samples were randomly assigned to participants during the evaluation sessions to ensure unbiased testing conditions. This means that each participant and session received a random selection of samples with no predictable pattern or order. Samples were offered one by one for consumption and evaluated in triplicate. The panelists rinsed their mouths between samples with water and unsalted crackers. Although rinsing may remove some residual material, this method carries the slight risk of inducing carry-over.

Before starting the TI sensory evaluation, the operator unscrewed the glass vial and introduced the straw. Subsequently, panelists were ready to commence the measurements. The subjects sipped through a straw, held the sample in their mouth for 10 seconds, and then swallowed. After 10 seconds, the subjects

swallowed again. In some cases, a third swallow was needed. Subjects rated the attribute intensity using a 100 mm unstructured line scale with anchors from "very weak" to "very strong" (**Figure 6.1**). Six samples were tested per session to avoid the halo-dumping effect and sensory fatigue and to maintain the subjects' interest (Monteleone & Dinella, 2017).

6.2.9. Preparation of the Gas Chromatography-Mass Spectrometry samples (GC-MS)

A modified method based on Barallat-Pérez et al., 2023 and adapted from Wang & Arntfield, 2015 was employed for Static Headspace GC-MS (HS-GC-MS). Samples consisted of three combinations: LPI + aroma, mucin + aroma, and LPI + aroma + mucin. The concentrations used were 1(w/v)% LPI, 5 mg/L aroma, and 0.01(w/v)% mucin. Reference samples included buffered LPI and mucin solutions without added aroma. Vials were sealed and incubated in a water bath shaker (SW22, Julabo GmbH, Seelbach, Germany) at 30 °C and 125 rpm for 3 hours before headspace analysis. Samples were prepared in triplicate.

6.2.10. Data collection, analysis, and processing

Time Intensity data treatment

The TI data obtained were defined by the parameters: area under the curve (AUC), which represents the total perceived intensity over the entire consumption time; maximum perceived intensity (I_{max}), defined as the highest peak of perceived intensity within a sample; and time to reach the maximum intensity (T_{max}) which corresponds to the time to reach I_{max} . The data were then averaged per panelist (n=10, in triplicate) and further analyzed. Smoothing of TI curves was done via the *geom_smooth* function in the *ggplot2* package of R software version 4.2.1.

PTR-MS data treatment and peak selection

PTR-ToF-MS data was treated with the PTR Viewer software (version 3.4.2.1, Ionicon Analytik, Innsbruck, Austria) for internal mass axis calibration, mass peaks selection and nose space concentrations extraction (parts per billion by volume; ppbV). In this study, $m/z=101.103$ was specifically chosen for hexanal, while for nonanal and 2-nonanone, the $m/z=143.158$ was selected. The primary main fragments of hexanal ($m/z=83.055$) and nonanal/2-nonanone ($m/z=125.142$) were selected based on comprehensive reviews (Acierno et al., 2019; Campbell-Sills et al., 2016; Ghanbari et al., 2019), and prior piloting, *i.e.*, HS analysis of the samples, which revealed the fragmentation pattern of each compound. Accordingly, absolute quantification was derived by summing the values corresponding to the molecule ion fragments.

The results were presented as the mean for a sample size of $n=10$ in triplicate. For each selected mass peak, averaged release curves (concentration in ppbV) were plotted against time (s) for each sample combination. PTR-ToF-MS curves were smoothed via the *geom_smooth* function in the *ggplot2* package of R software version 4.2.1.

Aroma lingering and decay

Calculations were performed to investigate the interaction between aroma molecular structure and their physicochemical properties on lingering and decay rates. Aroma lingering refers to aroma persistence in the mouth after product consumption. Aroma lingering was calculated as the average of $n=10$ individuals tested in triplicate. Each parameter was averaged for all subjects, all replicates, per second, and samples after the third/last swallow until the end of the test. The rate of change (decay rate) for both PTR-ToF-MS and TI data was calculated for each sample combination. Data were fitted to an exponential curve and calculated using the following equation (Sánchez-López et al., 2016) [6.1]:

$$I = at^{-b} \quad [6.1]$$

where I was the intensity at time t . The two parameters obtained from the fitting represented the intensity at the beginning (a) and the decay rate (b) of the aroma compounds (Sánchez-López et al., 2016).

Binding measurement and calculation

Protein-aroma-mucin binding and interaction were assessed by HS through GC-MS (Agilent- 7890A GC coupled to an Agilent 5975C with triple-axis detector MS, Agilent, Amstelveen, the Netherlands) following a modified method from Wang & Arntfield, 2015 and adapted from Barallat-Pérez et al., 2023. Aroma binding to proteins, expressed as a percentage in the absence and presence of protein, was calculated (Wang & Arntfield, 2015) [6.2]:

$$\text{Binding (\%)} = \left(1 - \frac{HS_1 - HS_2}{HS_3}\right) \times 100 \quad [6.2]$$

where HS_1 represents the abundance of the aromatized protein-based aqueous solution in the headspace. HS_2 and HS_3 denote the abundances in the headspace without aroma (HS_2) or protein (HS_3).

Aroma binding to mucin was calculated and expressed in %, in the absence and presence of mucin [6.3]:

$$\text{Binding (\%)} = \left(1 - \frac{HS_1 - HS_2 - HS_4 - HS_5}{HS_3}\right) \times 100 \quad [6.3]$$

where HS_4 (mucin solution + buffer) signifies the headspace abundance without flavor, while HS_5 (protein solution + mucin solution) indicates the headspace abundance of the protein-based mucin solution.

Statistical analysis

For the statistical analysis, GraphPad (Prism 9.3.1471) and RStudio 4.2.1 (Boston, Massachusetts, USA) were utilized to conduct an Analysis of Variance (Two-Way ANOVA) for each sample combination and determine AUC, I_{\max} , and

T_{\max} parameters. Tukey post-hoc tests were then performed to assess significant differences ($p < 0.05$) between each sample combination.

6.3. Results and Discussion

6.3.1. Effect of aroma molecular structure on the *in vivo* aroma release and perception

Chain length

The influence of carbonyl chain length (hexanal, C₆, and nonanal, C₉) on the *in vivo* aroma release and dynamic sensory perception of the "green" attribute in the aqueous model systems is depicted in **Figure 6.2 A-C**. An overview of the *in vivo* aroma release parameters (AUC_R, I_{max_R}, and T_{max_R}) and the dynamic sensory "green" perceived intensity parameters (AUC_S, I_{max_S}, and T_{max_S}) can be found in **Table 6.2**.

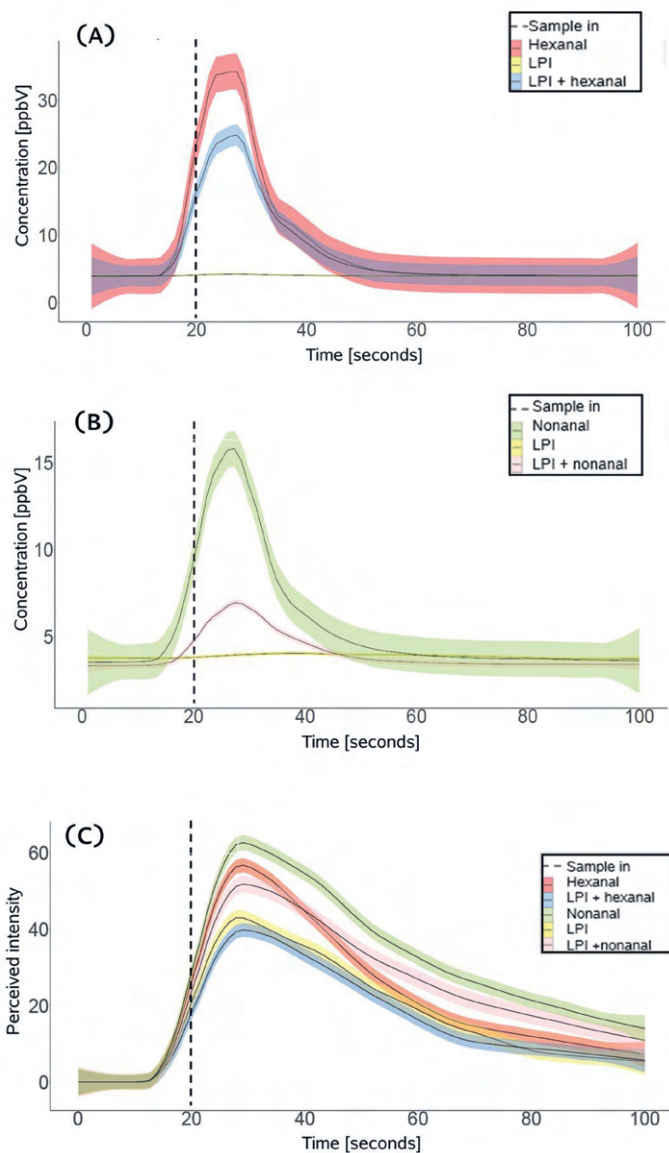


Figure 6.2. Averaged and standard error of (A) *in vivo* hexanal release ($m/z = 83.093 + 101.103$), (B) *in vivo* nonanal release ($m/z = 143.158 + \text{fragments}$), and (C) sensory perceived intensity (hexanal and nonanal) curves during drinking and after swallowing for aqueous model systems containing lupin protein isolate (LPI) only or LPI and hexanal or nonanal ($n=10$ subjects, in triplicate). Scales are adjusted to their maximum responses for better data presentation.

Table 6.2. Summary of parameters (mean \pm SE) describing the *in vivo* hexanal, *in vivo* nonanal, *in vivo* 2-nonanone, and dynamic "green" perceived intensity for flavored lupin protein-based aqueous model systems (FLPBAMS). Letters denote significant differences ($p < 0.05$). Treatments with the same letter are not significantly different.

	LPI	LPI +2-nonanone	LPI + nonanal	LPI + hexanal	2-nonanone	nonanal	hexanal		
	$m/z = 101.103$	$m/z = 143.158$	$m/z = 143.158$	$m/z = 101.103$	$m/z = 143.158$	$m/z = 143.158$	$m/z = 101.103$		
AUC_R	251 \pm 11	d 243 \pm 10	d 1261 \pm 116	a 271 \pm 11	d 581 \pm 41	bc 1515 \pm 116	a 401 \pm 36	cd 727 \pm 69	b
I_{max}_R	6 \pm 2	d 5 \pm 1	d 132 \pm 15	a 16 \pm 2	d 142 \pm 18	bc 209 \pm 28	a 58 \pm 13	cd 207 \pm 32	b
T_{max}_R	12 \pm 2	b 26 \pm 3	a 8 \pm 1	b 7 \pm 1	b 5 \pm 4	b 9 \pm 1	b 10 \pm 2	b 6 \pm 1	b
AUC_S	1800 \pm 268	ab 1800 \pm 268	ab 2155 \pm 295	ab 2127 \pm 287	ab 1555 \pm 211	b 2245 \pm 209	ab 2735 \pm 248	a 2099 \pm 222	ab
I_{max}_S	51 \pm 5	b 51 \pm 5	b 62 \pm 5	ab 60 \pm 5	ab 54 \pm 5	b 70 \pm 4	ab 71 \pm 4	a 67 \pm 4	ab
T_{max}_S	6 \pm 2	a 6 \pm 2	a 7 \pm 2	a 10 \pm 3	a 9 \pm 2	a 6 \pm 1	a 10 \pm 3	a 7 \pm 1	a

The *in vivo* nose space release curves for lupin-free samples and those with nonanal and hexanal (**Figure 6.2 A** and **6.2 B**) exhibited distinct release profiles, despite belonging to the same chemical class. As shown in **Table 6.2**, increasing the chain length significantly decreased AUC_R and I_{max_R} by 44.89% and 71.92%, respectively. No significant differences were observed in T_{max_R} values. The decrease in AUC_R indicates reduced nonanal release over time, while the decline in I_{max_R} may suggest a decrease in the maximum perceived intensity.

Aroma release in food systems is influenced by both thermodynamic (aroma compound volatility) and kinetic factors (mass transfer resistance from liquid to air phase) (de Roos, 2000), characterized by non-equilibrium conditions (Weterings et al., 2020). Oral processing involves continuous equilibrium changes, reflecting dynamic mass transport. Despite hexanal's hydrophilic nature, it is thirty-fold higher volatility compared to nonanal (see **Table 6.1**), suggesting it is the primary driver for aroma release.

Protein inclusion led to a 20.06% decrease in AUC_R for LPI + hexanal and a 32.37% decrease for LPI + nonanal (**Table 6.2**). Similarly, I_{max_R} decreased by 30.91% for LPI + hexanal and 72.41% for LPI + nonanal, indicating weaker aroma detection compared to samples without protein. Protein-aroma interactions may alter aroma release kinetics, resulting in slower release and potentially reducing maximum perceived intensity. The protein's surface contains "*hydrophobic binding sites*" where small ligands, like aroma compounds, may bind. Aldehydes can bind to proteins through reversible or irreversible mechanisms, such as cysteine-aldehyde condensation reactions and Schiff base formation under certain conditions (*e.g.*, pH 6.0-10.0), forming strong amide linkages (Anantharamkrishnan et al., 2020).

Despite clear binding effects observed in the *in vivo* aldehyde release results (**Figure 6.2 A** and **6.2 B**), dynamic sensory evaluation (**Figure 6.2 C**) showed discrepancies. In protein-free samples, increasing chain length slightly increased AUC_S and I_{max_S} by 30.31% and 6.24%, respectively (**Table 6.2**). Upon protein

addition, AUC_S decreased by 25.91% and 22.25%, while I_{\max_S} decreased by 25.92% and 15.23%, respectively (**Table 6.2**).

Unsurprisingly, discrepancies between methodologies are common (Le Quéré & Schoumacker, 2023; Pedrotti et al., 2019; Van Eck et al., 2021), with many analytical techniques lacking the sensitivity of the human nose (Pedrotti et al., 2019). In **Figure 6.2 A** and **Figure 6.2 B**, hexanal and nonanal were not detected in unflavored samples *in vivo*. These two aroma compounds are linked to green and grassy notes (**Figure S6.2**). Faint green notes were found to a certain degree in unflavored samples (**Figure 6.2 C**). Additional insights were gleaned from sensory evaluation (see **Figure S6.3**) to deeper understand lupin off-notes. Light green, grain-like, cereal, butter, fruity, barley, grassy, sour, and lemon-like attributes were commonly selected to describe lupin (**Figure S6.3**). Even though lupin is mildly associated with green notes, its green citation proportion is significantly lower compared to the samples lacking protein (*e.g.*, hexanal, nonanal, and 2-nonanone) and the flavored-protein samples (**Figure S6.3**).

Despite the performance of three training sessions, the variation observed in release and perception (**Figure 6.2 A-B** and **Figure 6.2 C**) may be linked to insufficient training sessions related to the definition of the trained "*green*" attribute. This could have resulted in a dumping effect or hasty responses that do not accurately consider the agreed definition for the selected attribute. However, it is imperative to acknowledge the potential for a carry-over effect. Remaining traces from a previous sample may have persistently appeared in subsequent measurements, affecting the score of the trained "*green*" attribute.

Establishing a direct link between *in vivo* aroma release and perception is challenging due to food matrix effects and inter-individual differences, which often play a significant role (Le Quéré & Schoumacker, 2023; Pedrotti et al., 2019).

Reactivity and position of the carbonyl group on the alkyl chain

The impact of the reactivity and the location of the carbonyl group (keto group) were investigated by comparing the two C₉-length aroma compounds: nonanal and 2-nonanone. **Figures 6.3 A** and **6.3. B** show averaged *in vivo* aldehyde (nonanal) and ketone's (2-nonanone) release and the dynamic sensory "green" perceived intensity curves from aqueous model systems.

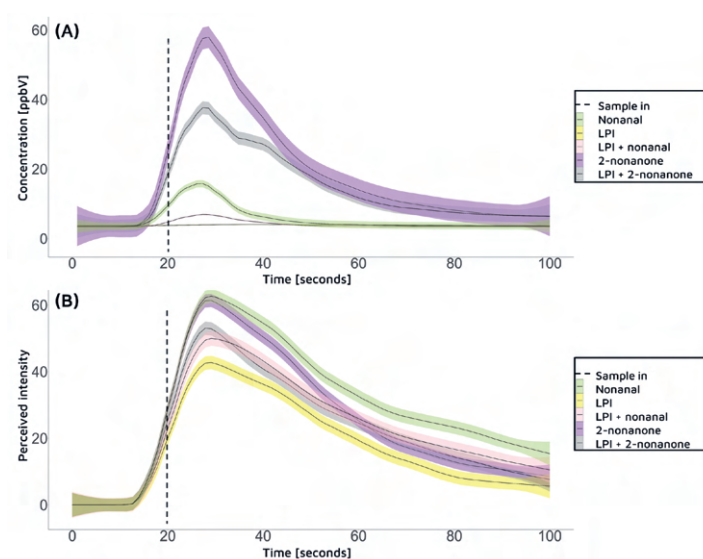


Figure 6.3. Averaged and standard error of (A) *in vivo* nonanal release and *in vivo* 2-nonanone release ($m/z = 143.158 +$ fragments), and (B) sensory perceived intensity (nonanal and 2-nonanone) curves during drinking and after swallowing for aqueous model systems containing lupin protein isolate (LPI) only or LPI and nonanal or 2-nonanone (n=10 subjects, in triplicate).

The *in vivo* aroma release curves for lupin-free samples and those with nonanal and 2-nonanone (**Figure 6.3 A**) displayed distinct profiles despite sharing the same chain length. The lower polarity of the ketone's carbonyl bond and the relocation of the keto group from the middle (2-nonanone) to the edge (nonanal) of the molecule resulted in a significant reduction of AUC_R by 73.52% and I_{max_R} by

72.25%. While no significant differences were observed in T_{max} values, nonanal exhibited a slower release (later T_{max_R} , see **Table 6.2**) compared to 2-nonanone. The decreased AUC_R and I_{max_R} suggested limited or reduced nonanal release over time. Ketones, chemically less reactive than aldehydes (Lee et al., 2018), differ structurally by the position of their carbonyl group within the molecule, influencing their *in vivo* aroma release (**Figure 6.3 A**). Aldehydes form reversible and irreversible bonds, while ketones predominantly bind through weaker hydrophobic interactions (Anantharamkrishnan et al., 2020). Their carbonyl groups are less positively charged due to alkyl group electron donation (Hidalgo & Zamora, 2023), and their proximity may promote steric hindrance, limiting access to the protein binding sites (Esteban-Fernández et al., 2016; Pérez-Jiménez et al., 2023). This spatial configuration results in less precise fitting on the protein's binding sites (Kühn et al., 2008; Zhou & Cadwallader, 2006), indicating an increased *in vivo* release, as observed in **Figure 6.3 A**.

The present findings are consistent with prior *in vitro* investigations involving soy, whey, and myofibrillar proteins with C_5 and C_9 compounds (Damodaran & Kinsella, 1981; Kühn et al., 2008; Shen et al., 2019). These studies emphasized the steric hindrance effect of ketones, indicating an increase in the free energy of association with each relocation of the carbonyl group along the chain (Damodaran & Kinsella, 1981). Furthermore, Shen et al., 2019 observed a marginally higher Stern-Volmer quenching constant for 2-pentanone compared to 3-pentanone, suggesting restricted access of 3-pentanone to hydrophobic binding sites due to the steric hindrance effect of the keto group.

With the introduction of protein to 2-nonanone samples, the AUC_R of LPI + 2-nonanone exhibited a 16.83% decrease. Similarly, the I_{max_R} of LPI + 2-nonanone decreased by 36.84%, indicating potential interactions between protein and aroma. Sensory results showed a moderate disagreement with *in vivo* release results. In protein-free samples, the displacement of the keto group from the middle to the edge of the molecule resulted in a slight increase of both AUC_S and I_{max_S} of 21.8% and 1.87%, respectively (**Table 6.2**). Upon protein addition, LPI + 2-nonanone, AUC_S decreased by 4% and I_{max_S} by 11.05%, respectively. These

results suggested that adding the protein hindered the "green" perceived intensity.

6.3.2. Effect of aroma physicochemical properties on the *in vivo* aroma release and perception

To delve deep into the molecular aspects of the *in vivo* aroma release and sensory perception lingering and decay rates were calculated and are shown in **Table 6.3**.

As seen in **Table 6.3**, a trend was generally observed between the lingering and the aroma's physicochemical properties (*i.e.*, hydrophilicity, water solubility, and volatility) (**Table 6.1**). The aroma with the greatest volatility (*i.e.*, hexanal) was 46.94% less persistent than the most hydrophobic compound (*i.e.*, nonanal) (**Table 6.3**). Therefore, nonanal, characterized by its lowest water solubility and volatility among the compounds (**Table 6.1**), exhibited the most prolonged lingering effect (**Table 6.3**), surpassing also 2-nonanone by 15.93%.

Likewise, in protein-free samples, 2-nonanone exhibited a faster decay rate (*b*) compared to the most water-soluble (*i.e.*, hexanal) and least volatile compound (*i.e.*, nonanal). With the addition of protein, both *a* and *b* [**6.1**] decreased *in vivo* aroma release (PTR-ToF-MS_R) for 2-nonanone and hexanal (**Table 6.3**), possibly suggesting protein-aroma interactions.

Table 6.3. Initial intensity (*a*)(-), decay rate (*b*)(-), and lingering duration for all samples and subjects, *in vivo* aroma release (PTR-ToF-MS_R), and sensory perception (Sensory_S). Data are presented as the average of the three replicates with the standard error. Letters denote significant differences ($p < 0.05$). Treatments with the same letter are not significantly different.

	LPI + 2-nonanone		LPI + nonanal		LPI + hexanal		2-nonanone		nonanal		hexanal	
	<i>a</i>	<i>b</i>	<i>a</i>	<i>b</i>	<i>a</i>	<i>b</i>	<i>a</i>	<i>b</i>	<i>a</i>	<i>b</i>	<i>a</i>	<i>b</i>
PTR-ToF-MS_R	9.509	0.008	3.654	0.002	3.925	0.001	11.138	0.012	3.990	0.002	4.252	0.002
Sensory_S	7.830	0.018	14.238	0.010	8.031	0.016	7.830	0.018	18.985	0.015	11.426	0.016
Lingering	75±9	ab	75±8	ab	71±10	c	74±9	ab	88±6	a	60±10	ab

According to the results (**Table 6.3**), the largest aroma lingering effect (slow decay rate) is related to the aroma's physicochemical properties. In this context, nonanal stands out due to its hydrophobic nature and poor water solubility, as outlined in **Table 6.1**. Consequently, among the compounds investigated (nonanal, hexanal, and 2-nonanone), nonanal exhibited a longer lingering effect.

Moreover, during oral conditions, the interplay between salivary proteins and aroma can also disrupt the distribution equilibrium of aroma compounds (Muñoz-González et al., 2022). Previous studies aimed to determine the drivers of oral aroma persistence by examining different aroma compounds such as esters, alcohols, terpenes, and lactones (Muñoz-González et al., 2020; Perez-Jiménez et al., 2020; Pérez-Jiménez et al., 2021, 2023; Ployon et al., 2017). The compound's hydrophobicity and molecular structure have been considered primary factors. Nevertheless, it should not be overlooked the ability of saliva to metabolize certain aroma compounds, such as diketones and aldehydes, leading to the formation of alcohols (Muñoz-González et al., 2019, 2022; Pérez-Jiménez et al., 2021).

6.3.3. Effect of mucin protein on the *in vitro* aroma release

To better understand variations in the *in vivo* aroma release, it is crucial to consider potential interactions between aromas, proteins, and salivary proteins. The *in vitro* GC-MS data in **Figure 6.4** offer deeper insights into the potential interactions among aroma, proteins, and saliva. Mucin levels in the oral cavity may vary due to significant individual variability influenced by age, oral health, genetics, and other variables (Muñoz-González et al., 2019, 2022). Hence, this analysis utilized minimal mucin (0.01(w/v)%) to investigate whether even small quantities could influence the interaction between commercial LPI and aroma compounds.

As depicted in **Figure 6.4**, the GC-MS binding response (%) increased four to twelve times after adding mucin. **Figure 6.4** indicates that the impact of mucin is particularly pronounced for the most volatile and hydrophilic investigated aroma compound, which is hexanal. In contrast, the effect is less noticeable for the least

volatile and most hydrophobic aroma compound, nonanal. Comparing mucin-free samples (*i.e.*, protein and aroma) to mucin-containing samples (*i.e.*, protein, aroma, and mucin) (**Figure 6.4**), the resulting binding effect does not simply sum up equally and proportionally. Instead, it leads to a higher binding than expected based solely on their individual contributions.

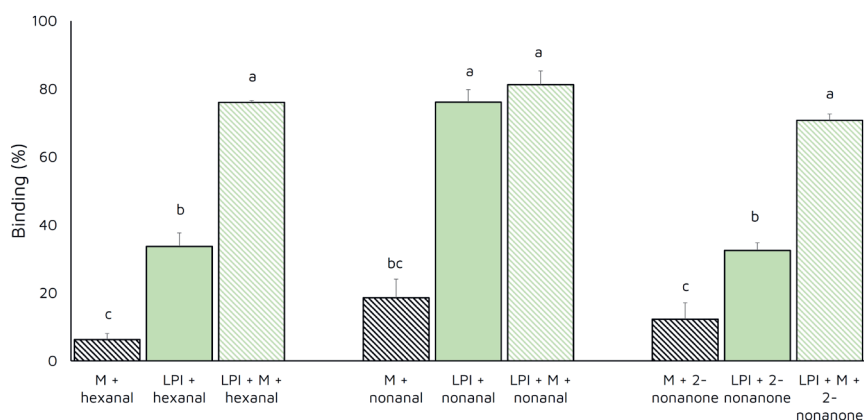


Figure 6.4. Effect of mucin on the protein-flavor binding mechanism. Binding (%) was calculated following equation [6.3][6.4]. Results are expressed as mean \pm standard deviation. Letters denote significant differences ($p < 0.05$). Treatments with the same letter are not significantly different.

Mucins, rich in sialic acid residues (Çelebioğlu et al., 2020), carry a negative charge, facilitating interactions with aldehydes through hydrogen bonding or electrostatic attractions (Muñoz-González et al., 2019). As observed in **Figure 6.4**, mucin exhibits a more pronounced interaction with the most hydrophobic aroma compound, nonanal. Likewise, **Figure 6.4** suggests a synergistic effect of mucin when combined with protein and aroma. Mucins offer a finite number of binding sites (n) (Friel & Taylor, 2001), where small ligands can fit. The combined action of protein, mucin, and aroma may produce a binding with aroma greater than the sum of their individual effects. Although the exact mechanism of this synergistic action remains elusive, we hypothesize that the interaction of mucins with proteins may increase aroma binding by revealing the hidden hydrophobic pockets of the protein, thereby increasing their availability to interact with aroma compounds.

Limited data on aroma binding in protein-mucin mixtures exists, but synergistic behavior has been observed in protein systems (Ahmad et al., 2022; Feiler et al., 2007; Wang et al., 2023). Ahmad et al., 2022 demonstrated cooperative effects between mucin and BLG, modulating the latter's affinity and accessibility to binding sites. Similarly, Wang et al., 2023 noted synergistic effects of soy isoflavones in Whey Protein Isolate by inducing its unfolding.

6.4. Conclusions

The originality of this study lies in its simultaneous assessment of FLPBAMS, achieved by combining high-throughput *in vivo* dynamic tools with sensory profiling using a commercial lupin protein isolate. The study underscores the influence of chain length, location of the keto group, volatility, and hydrophobicity of three aroma compounds on both *in vivo* aroma release and perception. The *in vivo* release findings indicated that longer aldehyde chains and relocation of the keto group significantly reduced I_{\max_R} . Upon protein addition, there was a notable decrease of I_{\max} in both the *in vivo* aroma release and dynamic sensory perception. Due to variations in individual sensory perception and sensitivity differences between analytical techniques and human olfaction, the relationship between *in vivo* aroma release and sensory perception may not always align. The *in vivo* dynamics of aroma release and perception involve complex processes influenced by aroma physicochemical properties. Hydrophobic compounds, less soluble in water, showed prolonged lingering and slower decay rates. Oral processing, marked by saliva-aroma interactions, significantly affects aroma retention, although the precise mechanism remains uncertain.

Concluding protein-aroma binding and release from exclusively three compounds and a simplified model system may not generalize to all aroma compounds or fully replicate real-world food complexity. However, studying model systems and a narrow range of compounds differing in physicochemical properties can offer valuable initial insights into the underlying mechanisms and help to identify trends and patterns in protein-aroma interactions, aiding in food design optimization.

6.5. Supplementary Material

Table S6.1. Overview of all samples in the absence/presence of lupin protein isolate (LPI) and absence/presence of aroma compounds.

Group	Ingredient	Number of samples	Type of sample	Composition
Only aroma compounds (absence of protein)	Hexanal/nonanal/2-nonanone	3	Control 1	5 mg/L
Only protein (absence of aroma compounds)	Lupin Protein Isolate (LPI)	1	Control 2	1(w/v)%
Combination aroma compounds-protein	Hexanal – Lupin Protein Isolate (LPI)	3	Final sample	5 mg/L -1(w/v)%
	Nonanal- Lupin Protein Isolate (LPI)			
	2-nonanone – Lupin Protein Isolate (LPI)			

Figure S6.1. Selection of the preferred protein isolate (Lupin, Pea, and Soy) (n=40) based on the overall taste and odor.

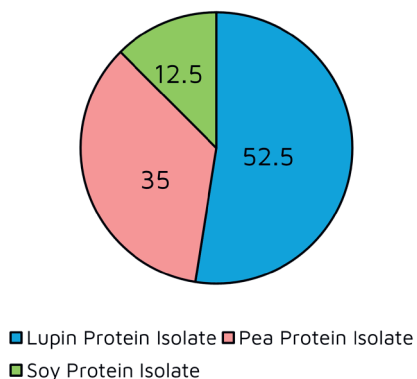


Figure S6.2. Attribute description of **A) Nonanal**, **B) 2-Nonanone**, **C) Hexanal**, and **D) Lupin Protein Isolate (LPI)** over the first training session.

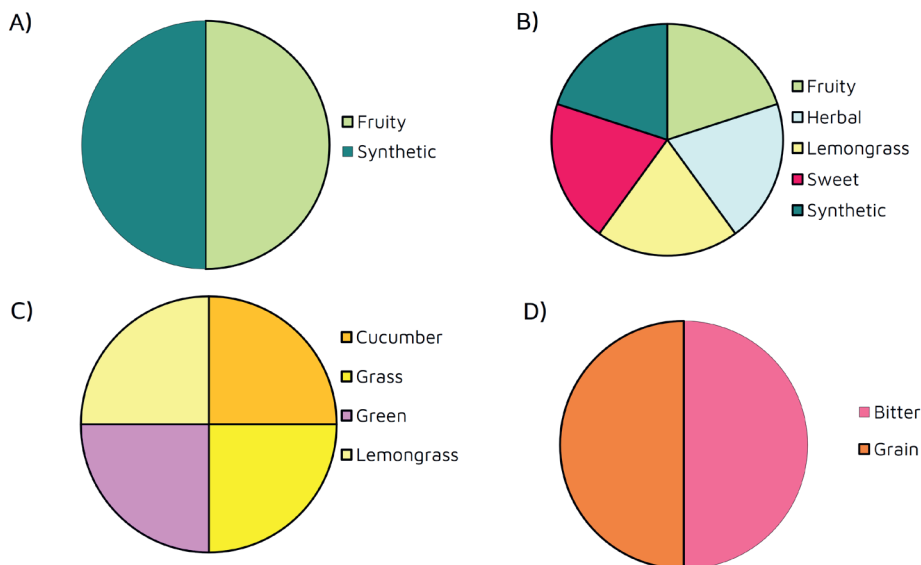
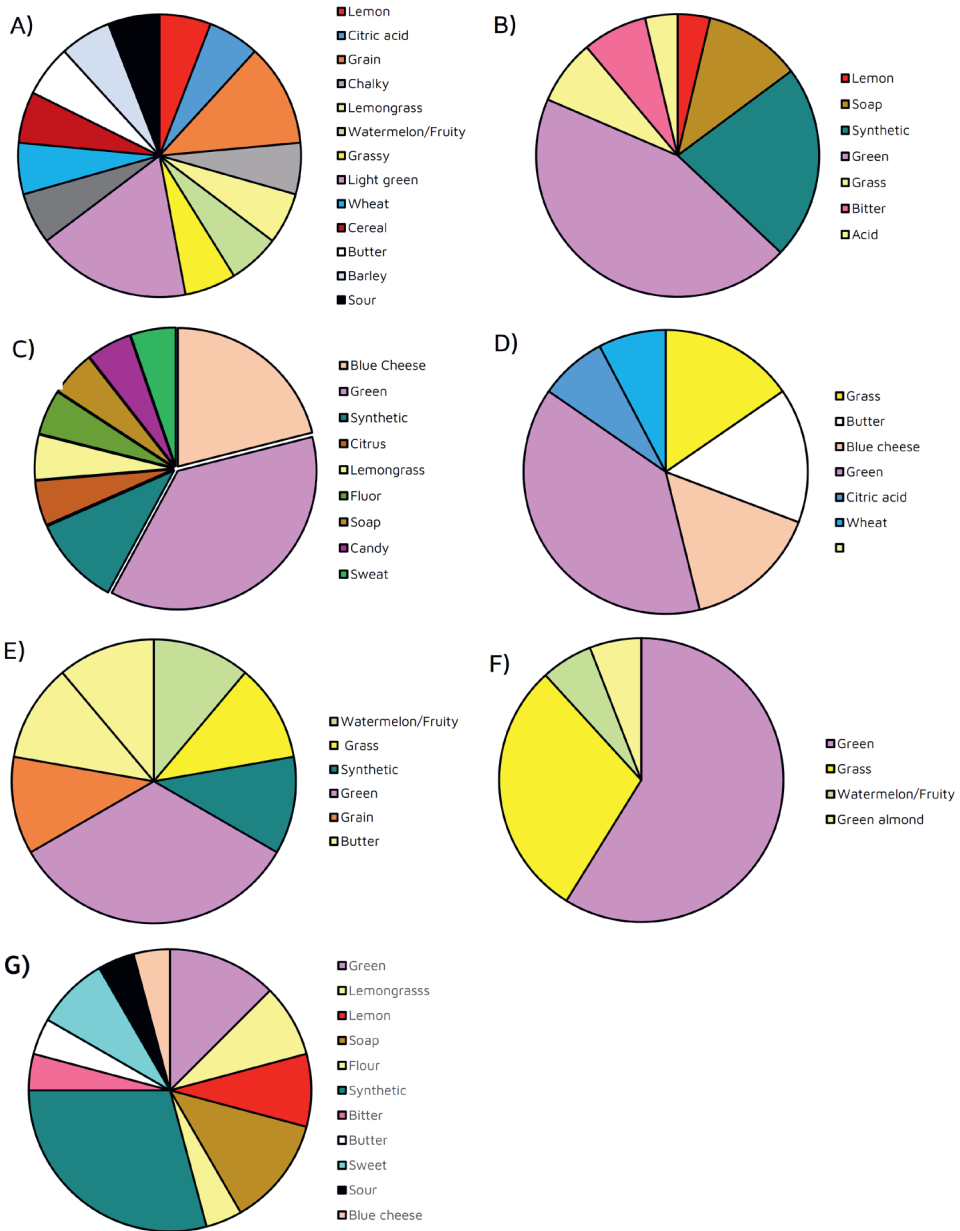


Figure S6.3. Attribute description of **A)** Lupin Protein Isolate (LPI), **B)** Nonanal, **C)** 2-Nonanone, **D)** Hexanal, **E)** LPI + Nonanal, **F)** LPI + 2-Nonanone and **G)** LPI + Hexanal over sensory sessions.



Drivers of the in-mouth interaction between lupin protein isolate and selected aroma compounds: a PTR-MS and Dynamic Time Intensity analysis

Table S6.2. Selected mass peaks obtained by PTR-ToF-MS (Acierno et al., 2019; Campbell-Sills et al., 2016; Ghanbari et al., 2019).

Mass (<i>m/z</i>)	Chemical formula	Tentative Identification
21.022	H ₃ O ₁₈ ⁺	Water molecule
45.035	C ₂ H ₅ O ⁺	Acetaldehyde
47.053	C ₂ H ₆ OH ⁺	Ethanol cluster
49.017	CH ₄ SH ⁺	Methanethiol
55.055	C ₄ H ₇ ⁺	Alkyl fragment (butanal, heptanal)
57.072	C ₄ H ₈ H ⁺	Alcohol fragment
65.061	C ₂ H ₅ OH*H ₃ O ⁺	Ethanol cluster
73.073	C ₄ H ₈ OH ⁺	Isobutanal/2-Butanone (MEK); 2-methylpropanal
83.046	C ₅ H ₆ OH ⁺	Methyl-furan/pyran
83.093	C ₆ H ₁₀ H ⁺	Hexanal fragment
87.084	C ₅ H ₁₀ OH ⁺	2/3-Methylbutanal; C ₅ carbonyls; Pentenol
97.101	C ₇ H ₁₂ H ⁺	C ₇ cycloalkanes
101.061	C ₅ H ₈ O ₂ H ⁺	Aromatic oxidation product; 2,3-Pentadione; Methyl-tetrahydro furanone
101.103	C ₆ H ₁₂ OH ⁺	Hexanal
115.119	C ₇ H ₁₄ OH ⁺	Heptanal; C ₇ carbonyls
125.096	C ₈ H ₁₂ OH ⁺	2-Nonanone/Nonanal fragment
143.158	C ₉ H ₁₈ OH ⁺	2-Nonanone/Nonanal
144.153	C ₉ H ₂₁ NH ⁺	Isotope of 2-nonanone/Nonanal
145.122	C ₈ H ₁₆ O ₂ H ⁺	Ethyl hexanoate/octanoic acid; 2-Pentyl propionate



General Discussion

Behind the Scents! A multidisciplinary approach for unveiling the protein-flavor binding mechanism

Food flavor science is a complex and diverse field that weaves together various disciplines related to the human body, including physiology, neuroscience, sensory science, and the chemical information of flavor molecules, such as biochemistry and physical chemistry (**Figure 7**).

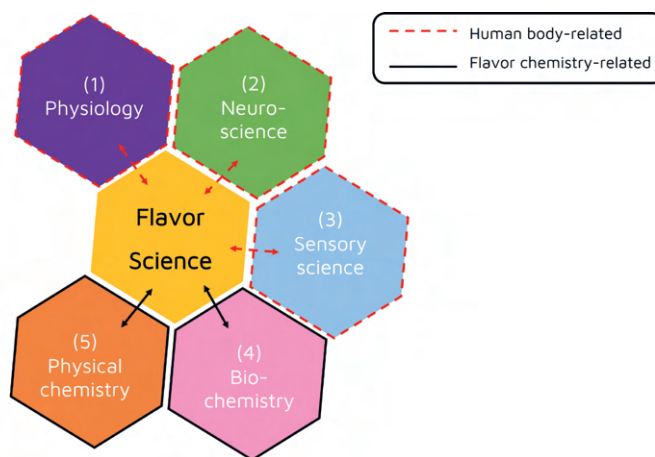


Figure 7. The holistic approach of flavor science and its subclusters.

The integration of the **(1)** anatomy and physiology of the taste system (including food-saliva interactions), **(2)** behavioral responses and cognitive effects, and **(3)** consumer preferences and sensory evaluation provide a comprehensive understanding of how the human body responds to (food) sensory stimuli. On the other side, chemical information such as **(4)** food matrix and architecture (*i.e.*, ingredients interactions, composition, structure, texture, *etc.*) and **(5)** flavor retention, release, and interactions offer details on the underlying mechanisms. Considering the entire framework, it is critical to develop successful, tastier food products that meet and delight the sensory expectations of the consumer. Therefore, to comprehensively understand the matter, it is essential to achieve an in-depth knowledge of each piece of this puzzle separately. This is especially true considering the rising demand for innovative, high-protein plant-based foods with more satisfying flavor profiles, which currently presents both an opportunity

and a challenge. Even though soy (*Glycine max*) and peas (*Pisum sativum* L.) are commonly used in daily cooking, especially in Western Europe, other plant proteins, like lupin (*Lupinus angustifolius* L.), remain underexplored. Generally, plant proteins have off-flavors that cause astringency and bitterness, making them less desirable to consumers. Flavor researchers have tried to mitigate these off-notes through different pathways, where adding desirable flavor compounds is commonly applied. However, these additional flavor compounds interact with food components such as carbohydrates, lipids, and proteins (Temthawee et al., 2020; Yeo et al., 2023), hindering their release during oral processing. Food formulators may compensate by adding extra flavor, potentially leading to product overdosing and an imbalanced flavor profile.

The research described in this Ph.D. thesis aimed to investigate the main drivers of the flavor-binding phenomenon in protein-based food systems using commercial food protein isolates (PI) by following a multidisciplinary approach (*in vitro*, *in silico*, and *in vivo*). The protein-flavor binding phenomenon was methodically reviewed (**Chapter 2**), considering protein and flavor molecule structure and physicochemical properties. *In vitro* static headspace measurements using Gas Chromatography-Mass Spectrometry (GC-MS) (**Chapter 3**) evaluated the binding degree of flavor compounds in the presence of PI and the role of flavor structural and physicochemical properties on the binding phenomenon. *In silico*, a QSAR model was built to corroborate the relevance of flavor structural features to the protein-flavor binding mechanism (**Chapter 4**). To get closer to human conditions, the main salivary protein, mucin, was further explored *in vitro* in **Chapter 5**, aiming to understand its role in the protein-flavor binding mechanism. **Chapter 6** studied, in a lupin protein-based aqueous model system (LPBAS), if the binding mechanism remains under dynamic conditions (*i.e.*, during drinking). For that, *in vivo* high-throughput tools, named Proton Transfer Reaction-Time of Flight-Mass Spectrometry (PTR-ToF-MS) and sensory profiling, Time Intensity (TI), were coupled.

The main results and Interpretations of this Ph.D. thesis are summarized and discussed in **Section 7.1**, followed by methodological considerations (**section 7.2**),

suggestions for future research (**section 7.3**), and principal conclusions (**section 7.4**).

7.1. Discussion of the main findings

The multidisciplinary (*in vitro*, *in silico*, and *in vivo*) approach of this Ph.D. thesis brought initial insights into the molecular interactions between proteins and flavor compounds. **Table 7.1** highlights the main findings of this Ph.D. thesis.

Table 7.1. Summary of the main findings of this Ph.D. thesis.

Chapter	Objectives	Main findings
3	Unraveling the role of flavor structure and physicochemical properties in the binding phenomenon with commercial food protein isolates.	Flavor-binding increases with the flavor's chain length and hydrophobicity. Unsaturation, the location of the keto group, and flavor spatial arrangement are essential in the binding mechanism.
		A slight increase in flavor-binding occurs upon heating due to protein denaturation.
		Protein-flavor binding primarily depends on the flavor compound and is secondary to the protein source.
4	Development of a QSAR model to predict protein-flavor interactions in protein-rich food systems.	From 328 descriptors, just the descriptors associated with flavor hydrophobicity, topology, and geometry determined the protein-flavor binding mechanism. Protein-flavor binding is predictable ($Q^2=0.93$) based on flavor features.
5	Exploring the role of mucin in the protein-flavor binding mechanism.	Protein binding sites (n) ranged from $n=0.021$ to 7.19. Binding constants (K) increased when enlarging the flavor chain length. Mucin interacting with proteins enhanced flavor-binding by exposing hydrophobic pockets at 0.01(w/v)% or surface coverage at 0.1(w/v)%.
6	Determining the main drivers of the in-mouth interaction between lupin protein isolate and selected aroma compounds by coupling PTR-MS and dynamic TI analysis.	Upon protein addition, I_{max} decreased, suggesting protein-flavor interaction and protein masking effect. Longer aldehyde chains and the relocation of the keto group led to a significant reduction in I_{max_R} .

7.1.1. *In vitro* approach: headspace Gas Chromatography-Mass Spectrometry

This Ph.D. thesis demonstrated the binding effect of commercial food protein isolates (PI) in flavored protein-based aqueous model systems (FPBAMS) by GC-MS (**Chapters 3-5**). The analysis showed a significant reduction in the abundance of volatiles in the headspace (HS). For example, **Figure 7.1** illustrates the relative abundance of two different volatiles in the HS. Notably, the binding affinity varies between *Trans-2-6-cis-nonadienal* in the Faba Protein Isolate (FPI) Model System and 1-pentanol in the Pea Protein Isolate (PPI) Model System. Adding FPI to the *Trans-2-6-cis-nonadienal* Model System decreases the abundance of *Trans-2-6-cis-nonadienal* in the HS by 85% (see **Figure 7.1 A**). Instead, adding 1-Pentanol to PPI decreases HS by 2% (**Figure 7.1 B**). This implies that diverse flavor compounds exhibit distinct binding affinities to proteins and *vice versa* (**Figure 7.1 A and B**). Despite the vast array of synthetic flavor compounds, the ones selected in this Ph.D were chosen based on their wide use in the food industry, their diverse physicochemical properties, and structural features (unsaturation, spatial configuration, alkyl chain type, position of the functional group, chain length, and hydrophobicity) offering a more strategic approach.

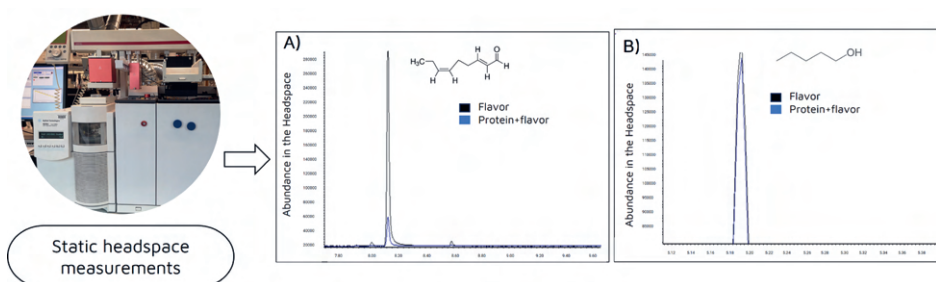


Figure 7.1. A) Binding phenomenon of *Trans-2-6-cis-nonadienal* in Faba Protein Isolate (FPI) Model System; and **B)** 1-pentanol in Pea Protein Isolate (PPI) Model System.

However, whether flavor binding to proteins has an undesirable effect remains questionable. On one hand, during food product development, flavor is preferred

to be retained within the food matrix during storage to preserve its quality—such as reducing flavor loss, maintaining food integrity, and preserving sensory attributes—until consumption. On the other hand, effective flavor release is crucial solely during consumption to ensure the desired sensory experience, improve flavor perception, and meet consumer expectations. The right balance between retention and release is essential for ensuring food sensory acceptability. Despite the intricate nature of the studied commercial food proteins (Soy Protein Isolate (SPI), Lupin Protein Isolate (LPI), Lentil Protein Concentrate (LPC), Whey Protein Isolate (WPI), PPI, and FPI), the *in vitro* findings obtained in **Chapters 3, 4, and 5** indicated that at the applied conditions binding is primarily affected by flavor structure and physicochemical properties such as (1) hydrophobicity (LogP), (2) chain length, (3) spatial configuration, (4) chemical class, (5) the location and number of the functional group, and (6) unsaturation (Barallat-Pérez et al., 2023, 2024). No definitive conclusion has been drawn regarding which parameter among the six listed above holds greater importance in the protein-flavor binding mechanism. However, when comparing flavor compounds with the same carbon length, we showed that flavor's hydrophobicity is essential in determining the binding affinity, confirming findings recently published by other groups (Wongprasert et al., 2024). Hydrophobicity and chain length are often interdependent parameters; long-chain flavor compounds tend to be more hydrophobic than short-chain flavor compounds, thus presenting higher binding capacity.

Beyond hydrophobicity, spatial configuration, chemical class, the location and number of the functional group, and unsaturation confirmed their leading role in protein-flavor binding as well. For instance, Wei et al., 2024 highlighted the relevance of the position of the acetyl group of heterocyclic compounds with thiazoline rings on the binding capacity to myofibrillar proteins: 2-acetyl-2-thiazoline displayed a higher binding affinity compared to 2-acetyl-thiazole. Similarly, Guo et al., 2024 revealed that pyrazine flavor compounds with more alkyl groups demonstrated a higher binding capacity to pea protein than those with fewer groups. Likewise, Li et al., 2024 explored the role of the number and position of methyl groups in furan flavor compounds in their interaction with SPI.

The authors demonstrated that SPI had a more substantial binding capacity for furan flavor compounds with methyl side chains due to their higher molecular flexibility.

In **Chapter 5**, protein binding sites (n) and binding constants (K) were calculated under non-thermal conditions. Results showed that binding sites ranged from $n=0.021$ to 7.19, and K increased when enlarging flavor chain length. In line with other researchers, Guo et al., 2019 found that K increased threefold with each added methylene group in the flavor structure, confirming the significant impact of hydrophobicity and chain length on flavor-binding behavior previously seen in **Chapters 3-6**. Therefore, and aligned with the most recent research in protein-flavor binding (Barallat-Pérez et al., 2023, 2024; Guo et al., 2024; Guo et al., 2019; Li et al., 2024; Snel et al., 2023; Wei et al., 2024), it is confirmed that protein-flavor binding primarily depends on the flavor compound and secondary on the protein source.

During the design of flavored protein-based foods (FPBF), proteins may undergo structural modifications such as unfolding and exposure of protein binding sites (n). This exposure of previously enclosed binding sites allows flavor binding (Sun et al., 2024; Wang & Arntfield, 2015). Therefore, additional experiments (not published) (**Figure 7.2**) were performed using intrinsic fluorescence to understand the flavor binding behavior upon protein heating (**Chapter 3**). These experiments combined LPI and SPI with C₅-length and C₈-length flavor compounds, respectively (**Figure 7.2**). The temperature was set to 95 °C for 30 minutes (pre-heated, PH). Control samples (NH) were not thermally treated. Preliminary results indicated that fluorescence intensity decreased upon heat treatment and flavor addition (**Figure 7.2**), indicating partial or complete unfolding of proteins (Huang et al., 2022; Sun et al., 2024). Moreover, upon flavor addition, fluorescence quenching may also occur, leading to a decrease in protein fluorescence intensity due to numerous molecular interactions, including molecular collision, complex formation, chemical rearrangement, or energy transfer (Zhang et al., 2014).

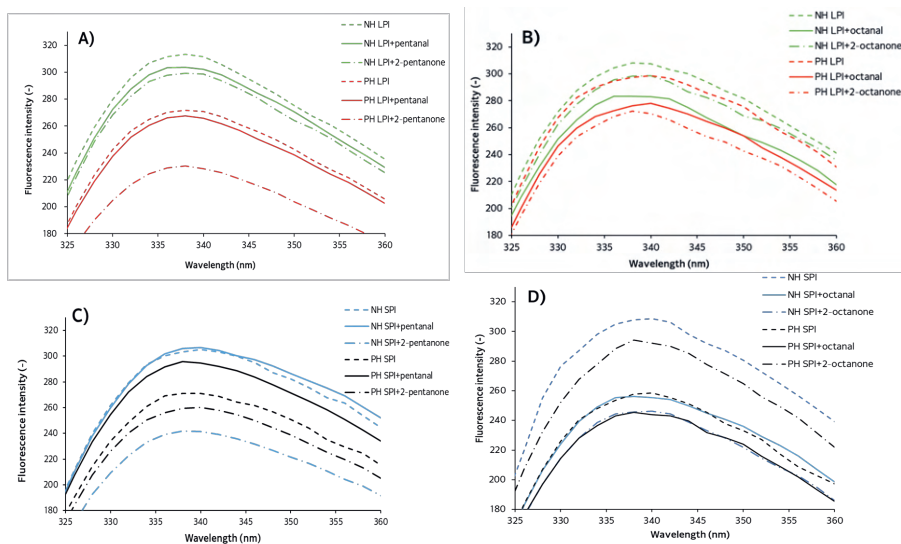


Figure 7.2. Intrinsic fluorescence spectra of pre-heated (PH) and control (NH) samples: **A)** lupin protein isolate (LPI) solutions and C₅-chain length flavor compounds; **B)** LPI solutions and C₆-chain length flavor compounds; **C)** soy protein isolate (SPI) solutions and C₅-chain length flavor compounds; and **D)** SPI solutions and C₆-chain length flavor compounds.

Even though there is no solid correlation, these first results are relevant indications for food developers to consider conformational alterations that FPBF may undergo during processing conditions and initially help to lay the groundwork for optimizing food flavor formulation.

7.1.2. *In silico* approach: computational tools for prediction

Recent advancements in machine learning for predicting food flavor focus on flavor compounds' molecular structure and physicochemical properties, utilizing data from infrared spectroscopy, E-noses, E-tongues, GC-MS, *etc.* Acknowledging the potential of computational tools, significant advancements have been made in accurately predicting aroma profile, intensity, and perception. For instance, predictive models have proved to forecast bitter, sour, and sweet tastes for small molecules based on molecular descriptors (Ji et al., 2022; Ye et al., 2023). Not limited, machine learning has led to the (1) creation of new flavors (*e.g.*, Grilled beef taste by Firmenich or Coca-Cola Y3000, USA), (2) optimization of current food and beverages flavors (*e.g.*, Belgian beer by KU Leuven), (3) flavor

pairing for novel food design (*e.g.*, Flavor iD®), **(4)** unearth new scents (*e.g.*, Osmo AI by Google) and **(5)** generation of new recipes (*e.g.*, Dishgen). These AI-driven methodologies are ready to revolutionize food design, gastronomy, and culinary experiences.

In the domain of flavor interactions, computational tools such as best-fit partial least-squares regression (Tan & Siebert, 2008), QSAR prediction models (Li et al., 2000), molecular docking (Bi et al., 2022; Guo et al., 2024; Wongprasert et al., 2024) and molecular dynamics (Di & Jia, 2023; Sun et al., 2024), helped to understand the molecular interactions underlying the binding mechanism. Therefore, recognizing the capacity of machine learning, a prediction model based on the structure-activity relationship was built in **Chapter 4** to **(1)** predict flavor binding in commercial plant protein-based model systems for diverse flavor compounds and **(2)** reveal the key physicochemical and configurational properties of the flavor compounds, determining the binding mechanism. From 328 descriptors, just descriptors associated with flavor hydrophobicity, topology, and geometry determined the protein-flavor binding mechanism. These results successfully reinforced the *in vitro* results (**Chapters 3** and **5**), where protein-flavor binding primarily depends on the flavor's structural and physicochemical properties, and protein characteristics play a secondary role.

Despite the valuable predicting capacity of the *in silico* prediction model (**Chapter 4**) ($Q^2=0.93$), it cannot fully forecast human variability, food-matrix interactions, and oral processing, including the role of salivary proteins, sensory perception, and cognitive effects. To address this, artificial intelligence (AI) might still be combined with traditional methods, such as sensory profiling.

7.1.3. The role of mucin: an *in vitro* perspective for understanding protein-flavor binding

The physicochemical properties of flavor compounds, saliva composition, and their properties (*e.g.*, enzymatic activity, electrolyte composition, protein content, *etc.*) remain key for unveiling the underlying protein-flavor mechanism. However, due to the complexity of oral processing, the mechanisms governing

the interactions between salivary proteins and food ingredients and their implication on flavor binding and perception still need to be clarified. One of the most studied topics is the relationship between phenolic compounds and salivary proteins. For instance, anthocyanins, tannins, and proanthocyanins form complexes with (proline-rich) saliva proteins, decreasing flavor release (Ployon et al., 2017). Van der Waals forces and hydrogen bonds have been identified as primary binding forces dominating the interaction of (α -amylase) salivary proteins with ferulic acid, epigallocatechin gallate, and epicatechin gallate (Zheng et al., 2020; Jiang et al., 2021). However, the binding mechanism varies based on the types and structures of the compounds (Wu et al., 2022). In the context of saliva-flavor interactions, the role of mucin remains elusive and contradictory across the scientific literature. Some studies indicate that in-mouth saliva reduces aroma release due to hydrophobic interactions and further enzymatic biotransformation and metabolization of flavor compounds, as observed in wine, pectin gels, or bell peppers (Hansson et al., 2003; Muñoz-González et al., 2014; Schwartz et al., 2023; Van Ruth & Buhr, 2003). Others indicated competitive effects between sugar and flavor compounds (Friel & Taylor, 2001), competing for binding to mucin. In contrast Boland, 2004 proposed that flavor release increased from starch gels due to the formation of hydrogen bonds between starch and flavor compounds. Nevertheless, the impact of saliva on flavor release seems to depend on the functional group of the flavor compounds, where ketones and alcohols showed an increase in flavor release when saliva is present. The opposite holds for esters.

To understand how saliva interacts with flavor compounds in the presence of PI, our results in **Chapter 5** demonstrated mucin enhanced flavor-binding in FPBAMS. Due to its nature, mucin may induce structural changes on the protein surface, leading to the unfolding and, thus, exposure of binding sites. At pH 7.0, WPI, SPI, and mucin carry a negative charge (pK 5.2, 4.5, and 2.6, respectively) (Hsein et al., 2015). Despite the negative charge of mucin, it also has positively charged patches in the non-glycosylated globular regions, which, via non-covalent interactions, attract the negatively charged PI. However, when increasing mucin concentrations, it is hypothesized that mucin clusters through disulfide bonds,

specifically through cysteine residues, forming aggregates that cover binding sites (**Chapter 5**) (Çelebioğlu et al., 2020).

An image emerges where the coexistence of food protein, flavor, and mucin affects flavor release. This has implications for the sensorial perception of food. Thus, sensory studies complementary to *in vitro* and *in vivo* techniques are needed to ensure the real-world applicability of the studied food products.

7.1.4. *In vivo* approach: dynamic in-nose space measurements

GC-MS measurements performed in **Chapters 3, 4, and 5** analyzed the flavor compounds in the headspace. Samples were measured under controlled laboratory settings to ensure replicability and consistent results. However, the influence of flavor's physicochemical properties and structure has yet to be sufficiently explored concerning dynamic in-mouth interactions. Whether protein-flavor interactions remain under in-mouth conditions is still unclear but essential for optimal aroma release and sensory experience. Thus, this Ph.D. studied *in vivo* real-time flavor analysis and sensory evaluation simultaneously (PTR-ToF-MS and TI) (**Chapter 6**). Adding protein to flavored aqueous model systems demonstrated a reduction of the maximum perceived intensity (I_{\max}), suggesting an in-mouth protein-flavor binding mechanism (**Figure 7.3**) which validated the observed *in vitro* findings (**Chapters 3-5**). Besides the clear binding effect observed *in vitro* (**Chapters 3-5**), flavor physicochemical properties seemed equally fundamental under in-mouth conditions. Longer aldehyde chains and the keto group relocation significantly reduced I_{\max} (**Chapter 6 and Figure 7.3**) (Barallat-Pérez et al., 2024).

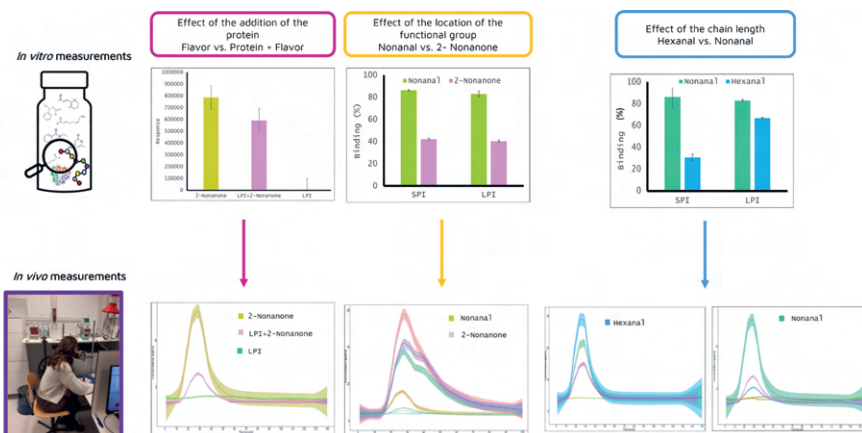


Figure 7.3. Overview of the main findings concerning the effect of flavor addition and flavor structure through *in vitro* static headspace (HS) (**Chapter 3**) and *in vivo* (**Chapter 6**) approaches.

What is next? Should we prioritize dynamic in-nose measurements over static headspace measurements when studying protein-flavor interactions? These two techniques may need to be performed complementary to each other to provide a comprehensive overview of the underlying mechanism, ensure data reliability, and avoid bias as much as possible. Is it possible and scientifically sound to integrate sensory analysis into the process?

7.1.5. Sensory profiling and its role in the flavor domain

Before introducing a new food item to the market, it undergoes sensory evaluation to ensure the food product will be well-received by consumers. However, 80% of food products fail to meet consumer taste expectations (Food Navigator, 2019). Consumer acceptance of new foods is strongly linked to an enjoyable experience, highlighting the relevance of aroma release and perception. Understanding the relationship between aroma compound structure, release, and perception is not straightforward. Sensory perception is a complex and dynamic interplay between oral processing (saliva flow, composition, oral mucosa, jaws, teeth, and tongue movements), food ingredient interactions (including mucin-flavor-protein interactions), and cross-modal interactions. For instance, aroma perception and intensity are reduced when carriers, such as bread and potatoes,

are added to mayonnaise as a consequence of cross-modal (texture and aroma) interactions (Van Eck et al., 2021).

As seen in **Chapter 6**, upon protein addition to flavored lupin protein-based aqueous model system (LPBAS), the attribute was perceived as less intense (lower I_{\max}), revealing a masking protein effect. However, aroma release alone does not fully explain the sensory perception of LPBAS. Flavor physicochemical characteristics (chain length, volatility, and hydrophobicity) and potential carry-over effects should be considered in the design of lupin-based beverages for optimal consumer satisfaction. But can *in vivo* analytical techniques truly explain sensory perception? Combining sensory profiling with dynamic analytical methods is essential for a comprehensive overview of aroma release (Le Quéré & Schoumacker, 2023). On the one hand, analytical techniques identify and monitor volatile release in real-time, whereas sensory techniques capture the dynamic and evolving nature of aroma perception. Recent technological advancements address more than just the growing demand for time-efficient, cost-saving, and sensitive methods to complement sensory science. They are also opening up new possibilities and enhancing our capacity to understand flavor science. For instance, Virtual and augmented reality technologies, such as Virtual TasteTrek[®] Citrus and Virtual Aroma Synthesizer[®], provide immersive experiences using cutting-edge technology. Digital interfaces allow users to explore customizable virtual stores, interact with items, and track eye and hand movements, which offers more genuine insights than traditional surveys. Similarly, electronic sensing devices like SMELLODI measure the chemical behavior of odor molecules, potentially detecting diseases like Parkinson's years before symptoms appear. Additionally, taste sensors like Oissy can 'visualize' food flavors by revealing flavors sensed by the taste buds in the form of quantitative data. These advancements herald a new era in the field, filled with exciting opportunities and potential breakthroughs.

While this Ph.D. thesis has shed light on the interplay between protein and flavor molecules and the crucial role of structure and physicochemical properties in

successful FPD, it also stresses the need for further research and improvement of methodological aspects.

7.2. Methodological considerations

7.2.1. From controlled laboratory settings to ever-lasting dynamic *in vivo* conditions

This Ph.D. thesis used GC-MS, a widely adopted analytical technique, to determine flavor binding. From an instrumental perspective, direct injection of a sample into the GC-MS can lead to several issues that compromise data quality. These include column overloading, carryover caused by syringe contamination, and baseline noise resulting from septum leakage. Likewise, sample preparation can be laborious and time-inefficient. Automated and robotic alternatives may help to reduce sample time preparation and enhance sample throughput. In contrast to static GC-MS measurements, *in vivo* dynamic real-time measurements represent real-life conditions characterized by continuous in-mouth changes and interactions. Factors such as inter- and intra-individual variability (*i.e.*, chewing behavior, saliva composition, rate, gender, cultural background, genetic factors, health status, and cognitive performance) are responsible for the food's sensory perception (Criado et al., 2021; Muñoz-González et al., 2021; Pedrotti et al., 2019; Pérez-Jiménez et al., 2022). In **Chapter 6**, we found great variability in aroma release (**Figures 7.4 A and B**) despite screening participants for smoking status, swallowing disorders, and lupin allergy and ensuring consistent adherence to the swallowing protocol (including timing, frequency, and intervals between samples). **Figures 7.4 A and B** show two main groups of n=10 panelists (P1-P10): the higher-releaser (**Figures 7.4 A and B**: P1, P2, P6, P9, and P10) and lower-releaser groups (**Figures 7.4 A and B**: P3, P4, P5, P7, and P8).

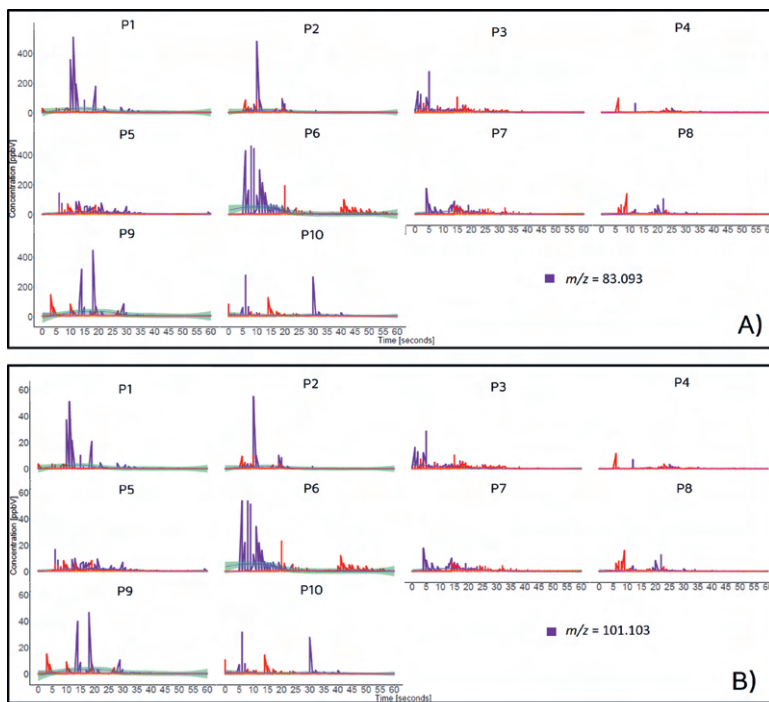


Figure 7.4. Panelists ($n=10$) *in vivo* aroma release for **A)** $m/z = 83.093$ and **B)** $m/z = 101.103$. Time points are not normalized.

The variances in aroma release may account for differences in velum opening and mouth movements (Blee et al., 2011), which leads to differences in oral processing and probably in sensory experience. Understanding the variability in aroma release across panelists helps develop personalized and tailored food products to accommodate the diversity of sensory responses.

Due to this dynamic nature of oral processing and continuous changes in saliva volume, flow, and interaction with the oral mucosa, a carry-over effect or sensory biases can be readily observed during *in vivo* nose space measurements. As shown in **Figures 7.5 A** and **B**, the aroma is persistently released from previous samples in subsequent measurements for some panelists (**Figures 7.5 A**, P3, and **B**, P10). Even though slices of crackers, mineral water, and resting time in between samples were the approaches undertaken for the current study, carry-over was still observed. A deeper understanding of the main factors governing the carry-over effect, potentially related to oral physiology or microbiota, and

alternative strategies to mitigate this effect are needed to gain an understanding of aroma release and perception.

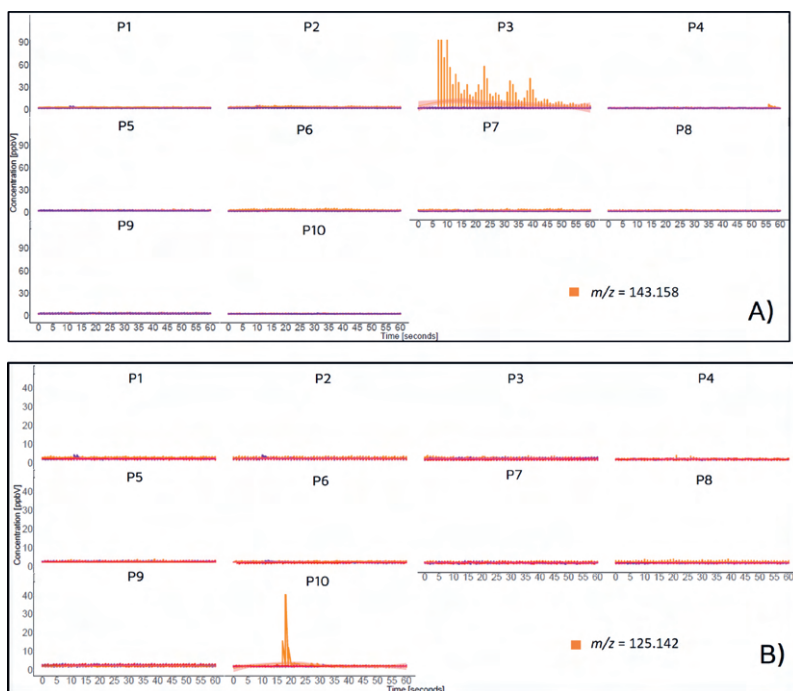


Figure 7.5. The carry-over effect is shown across panelists ($n=10$). Time points are not normalized.

In summary, even though PTR-ToF-MS has successfully demonstrated effective monitoring of volatiles in real-time, established protocol optimization still needs to be improved.

For the study performed in **Chapter 6**, panelists drank through a straw. This aspect demands further discussion, as we hypothesize that the consumption method affects the temporal perception of flavor. It is well-known that when consuming liquids, the mouth closes tightly to prevent leakage into the trachea. As swallowing begins, the velum opens, allowing air to pass through, resulting in flavor molecules coating the pharynx right from the start, even before the first swallow. Sipping (through a straw) involves a sucking mechanism that creates a vacuum so that the greater ambient pressure pushes the beverage through the straw. Using a straw can introduce flavored air into the mouth alongside the

liquid, affecting aroma release dynamics and sensory perception. However, aroma perception is also dynamic; thus, assessing aroma perception through a single intake oversimplifies the complexity of aroma release. We may consider that aroma perception evolves gradually with successive sips (Maheeka et al., 2021; Regan et al., 2019). Therefore, investigating temporal aroma perception with a multiple-sipping approach may help understand the product flavor profile, including changes found during oral processing. Following a multi-sipping approach, we have performed a pilot study to verify the temporal perception of aroma through different consumption methods. Systems were based on LPI spiked with δ -nonalactone. Cups and pouches (**Figure 7.6**) were selected as consumption methods due to their everyday use within the beverage industry (Ghoshal, 2019). Using the check-all-that-apply, trained evaluators ($n=31$) were presented with a pre-selected set of sentences or statements, asking them to choose the provided attributes that best characterize the evaluated sample. Participants were instructed to sip from an 80 mL-filled cup and a pouch (**Figure 7.6**), holding the sample in their mouths for 6 seconds before swallowing. The Chi-Square and Cochran Q tests were utilized to observe significant differences in attribute citation percentage based on the number of sips (Maheeka et al., 2021; Regan et al., 2019).



Figure 7.6. Pouch and cup formats used to study temporal aroma perception in a lupin protein-based aqueous model system (LPBAS).

Figure 7.7 shows attribute citation in LPBAS spiked with δ -nonalactone. Attribute citation significantly decreased after each sip (**Figure 7.7**). Likewise, sipping from

a cup generally led to higher attribute citation (Figure 7.7), except for coconut, where the opposite was observed (Figure 7.7 B).

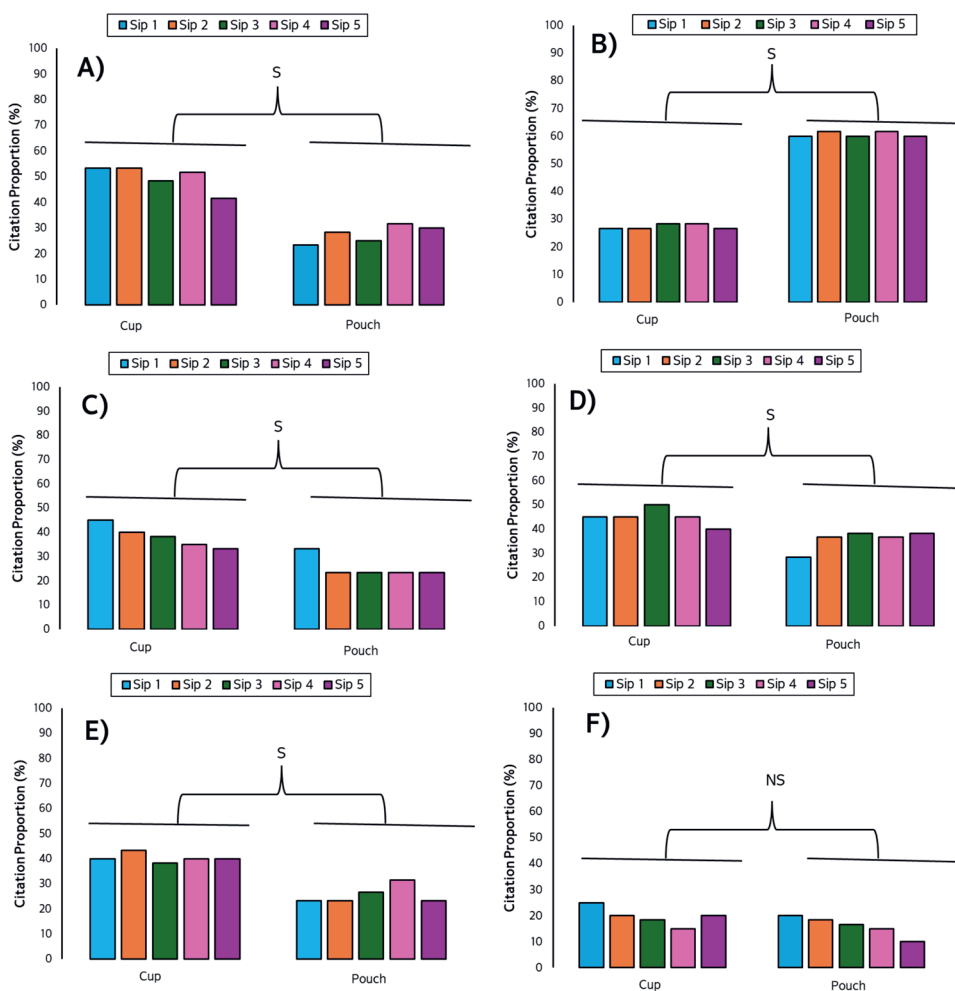


Figure 7.7. Citation proportion (%) of a lupin protein-based aqueous model system (LPBAS) spiked with δ -nonalactone. The letter S indicates significant differences, while the letter NS indicates no significant changes: **A)** Nutty, **B)** Coconut, **C)** Almond, **D)** Beany, **E)** Cereal, and **F)** Sweet attributes.

Unlike drinking from a pouch, drinking from a cup (Figure 7.6) allows immediate contact of the flavored liquid with the surrounding air. This exposure allows the most volatile flavor compounds to be released quickly. Likewise, direct contact of the flavored liquid with the mouth and taste buds will result in faster, increased aroma perception (Maheeka et al., 2021).

Overall, these initial results provided preliminary insights into the temporal dynamics of aroma perception and encouraged the investigation of different consumption methods. Aiming to meet diverse consumer needs and preferences (*i.e.*, portability, convenience, functionality, *etc.*), beverages today come in various packaging. Studies show that different packaging food materials and consumption methods impact flavor perception: Beekman et al., 2021 found that sipping iced coffee through a straw led to a perceived higher flavor intensity compared to drinking from a cup or a cup with a lid; Akiyama et al., 2012 observed that straw color and diameter affected coffee taste; Pramudya et al., 2021 noted that straw material influenced the overall liking of tea. Thus, studying different consumption methods is essential to tailoring flavor experience to cultural and individual differences and preferences to optimize product design (*i.e.*, suitable packaging materials or formats to preserve aroma compounds optimally).

In **Chapter 6**, the TI methodology was used to assess sensory perception. Although it has advantages, participants can only rate one sensory attribute. This way, some information regarding changes in flavor perception over time might be missed. Therefore, complex food systems may prefer Temporal Dominance of Sensations (TDS) or Temporal Check-All-That-Apply (TCATA) analysis.

7.2.2. From aqueous model systems to food applications

One of the major challenges of this Ph.D. is the selection of the protein material used for the study. PI are typically refined ingredients composed of a blend of protein fractions characterized by different structures and spatial arrangements (*e.g.*, β -sheets, α -helix, amino acid residues, *etc.*), residual carbohydrates, and fat. The industrial isolation process may apply harsh conditions such as pH, temperature, and mechanical treatments to achieve high levels of purity and cleanliness. These processing operations might cause structural changes in proteins. As a result, the binding site number, location, and structure might be altered, thus having a different ending result on the flavor-binding affinity. Building on this fact, the results from *in vitro* measurements (**Chapters 3, 4, and 5**) indicate that the protein source plays a secondary role in the protein-flavor binding mechanism. Since no significant differences in flavor-

binding affinity were observed among SPI, PPI, LPI, LPC, FPI, WPI, and bovine serum albumin (BSA) when interacting with the same flavor compound, they could, in principle, be used interchangeably during flavored FPD. However, when selecting proteins for food applications, it is important to consider not only their flavor-binding affinity but also their techno-functional properties, such as solubility, emulsification, gelation, foaming, and heat stability (Karabulut et al., 2024). Composed of ~80% salt-extractable globulins and only a minor fraction of water-soluble albumins (~20%) (Table 2.1), plant proteins are characterized by poor solubility. This solubility issue and its effect on flavor-binding were studied further (Figure 7.8). To achieve this, the soluble proteins were extracted using two-step centrifugation (4700 x g, 20 minutes) in a 50 mM phosphate buffer at pH 7.0.

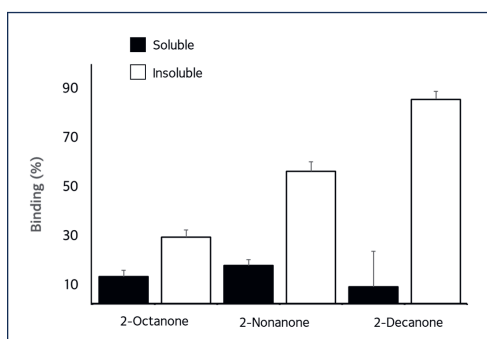


Figure 7.8. Binding (%) of C₈-C₁₀ ketones in the soluble protein fraction (black) and insoluble protein fraction (white) for Pea Protein Isolate (PPI). Fractions were separated by centrifugation.

Figure 7.8 shows the differences in the retention of ketones between PPI's soluble and insoluble fractions. Flavor binding by the insoluble protein fraction was greater than that of the soluble. This effect was most pronounced for 2-decanone. This indicates that lower protein solubility leads to protein-flavor interactions, possibly due to more hydrophobic regions for the flavor to interact (Snel et al., 2023). The general protein compositions of both the soluble and insoluble fractions of pea protein showed similarities, including albumins and globulins (Moll et al., 2023). Based on their flavor-binding capacity, food companies can use these findings to categorize commercial preparations into soluble and insoluble

fractions. The soluble fraction could be used in food applications requiring foaming ability, stability, and capability (*e.g.*, whipped creams, mousses, ice creams, bread, cakes, *etc.*), while the insoluble fraction may be used for applications requiring water or oil-holding capacities (He et al., 2015).

Exploring liquid model systems and a selected range of flavor compounds with diverse physicochemical properties provided valuable preliminary understandings of the underlying protein-flavor interaction (**Chapters 3-6**), facilitating guidelines for food design optimization. When transitioning from aqueous model systems to complex (actual) food products, it is relevant to account for flavor-flavor interactions and competition rather than focusing solely on examining single-flavor compounds, as flavor formulations comprise a mixture of 5-15 different volatile compounds representing 0.01-0.8(w/w)% of the final food composition (Fan et al., 2024). Based on the results obtained in **Chapters 3-6**, we hypothesized that flavor compounds that share (structural) similarities will compete for the same binding sites on proteins. However, aroma release and perception in liquid systems might differ from solid foods (Gonzalez-Estanol et al., 2023; Van Eck et al., 2021). During in-mouth mechanical disruption of solid foods, changes in surface area and particle size (How et al., 2021) impact the flavor transfer from the solid to the vapor phase. Therefore, the relationship between the number of particles, particle size, surface area, and aroma release and perception, especially when novel ingredients come into play, deserves further investigation.

7.3. Future research

With the rapid pace of scientific research and the development of innovative technologies worldwide, flavor science has made significant advancements. However, some promising areas are suggested below to address remaining unanswered questions.

7.3.1. Expanding the horizons: Non-refined ingredients and alternative proteins

Worldwide, unprocessed plant-based foods are commonly found in nature and used in daily cooking. Besides being characterized by a high protein

content, non-refined ingredients include fiber, sugar alcohols, fat (> 1%), phytochemicals, *etc.* Whether non-refined ingredients will behave similarly to the refined ones (“*clean*”) needs further investigation. Starch (Su et al., 2021), sugar (Piccone et al., 2012), salts (Wang & Arntfield, 2015), polysaccharides (Jouquand et al., 2008), polyphenols (Pittari et al., 2022) and sweeteners (Itobe & Kumazawa, 2017) are among the ingredients studied for their interactions with flavor compounds. The complete characterization of the behavior of these interactions remains elusive. Research on complex food systems highlights the difficulty of precisely predicting aroma release based only on individual ingredient studies (Paravisini & Guichard, 2016). This challenge primarily arises from limited knowledge about the structure of various macromolecules and the concurrent effects of other components.

As food technology advances and sustainability becomes a significant concern, food scientists seek further expansion in the variety of available protein sources as alternatives to traditional animal-based proteins. Recently, proteins derived from hemp, quinoa, insects, cultured meat, and fermentation-derived proteins are gaining attention (Caparros et al., 2016; Kurek et al., 2022; Lee et al., 2020; Zahari et al., 2020). However, little is known regarding their influence on the protein-flavor binding mechanism. Will these novel alternative protein sources behave similarly to the studied ones when combined with flavors? Even with the demonstrated minor role of proteins in flavor-binding affinity, exploring alternative proteins may still be beneficial for sustainability, nutritional, techno-functional, and texture/mouthfeel reasons. Unfortunately, food neophobia is widely expanded around the globe, which limits new food uptake. Economic development, cultural background (country-specific, consolidated food culture), gender, age, and education factors tend to explain food neophobia. For instance, French consumers valued spirulina more than German and Dutch consumers. Birch et al., 2019 demonstrated that well-educated and health-conscious consumers are likelier to try new foods. Similarly, due to cross-national differences, Swedish and UK children were more neophobic than Italian and Spanish children and significantly more than Finnish children (Proserpio et al., 2020). These results were ascribed to differences in feeding practices and

different food availability. While not impossible, this protein transition remains challenging.

7.3.2. The new era based on Artificial Intelligence (AI)

As seen in **Chapter 4**, the developed QSAR model showed high predictive ability. This is a hint of what lies ahead. Scientists are still exploring the full potential of AI in our daily lives. Food information may be addressed as a multilayered matrix rather than a one-dimensional matrix to achieve tailored and personalized sensory experiences (**Figure 7.9**). Each layer represents multiple variables necessary for a comprehensive overview of flavor prediction. Beyond feeding the model with just fundamental and molecular-related flavor data and information (**Chapter 4**), food scientists may aim to collect data on alternative occurring food-matrix interactions (*i.e.*, sweeteners/sugars, salt, starch, gelatine, *etc.*) that affect the final flavor profile of food (**Figure 7.9**). As flavor science is multidisciplinary (**Figure 7**), it remains crucial to consider a broader view of data such as how the food is perceived and consumed, current market trends, consumer preferences, culinary traditions worldwide, food background and culture, cooking techniques, *etc.* (**Figure 7.9**) as it may offer new combinations of ingredients, and forecast upcoming flavor trends. Finally, individual-related information adds the finishing touch. By including biological information such as oral physiology (salivary glands, taste buds, saliva rate, and composition), genetics, age, gender, dietary habits, oral and gut microbiota, cognitive effects (memory recall), and an array of many other inter- and intra-personal variables (**Figure 7.9**), new insights might be unveiled to understand the multidimensional complexity of food for a customized sensory experience.

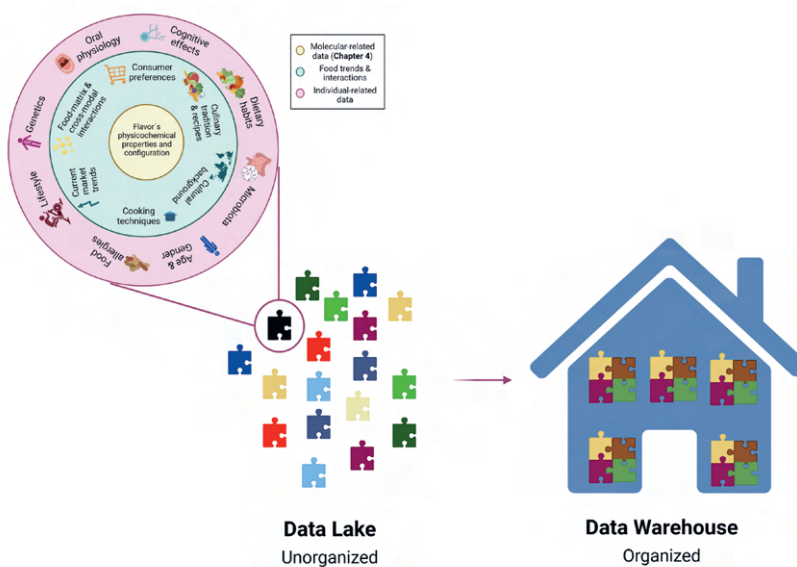


Figure 7.9. Multilayered matrix concerning flavor prediction.

Currently, several flavor repositories, such as VCF, FlavorDB, Flavornet, BitterDB, SuperSweet, and SuperScent, are available online that offer (1) interactive data visualizations (*i.e.*, flavor network), (2) links between chemical features to flavors enabling flavor pairing, and (3) the search for molecules matching a desired flavor (Grover et al., 2022). While the feasibility of these repositories is widely recognized, challenges such as data inaccessibility and lack of data organization persist. Data often remains scattered and unorganized (*i.e.*, data lake) (**Figure 7.9**), hindering their use. With the rapid strides of AI, multinational food and beverage companies, such as McDonald's and KFC, are slowly building up "data warehouses" to achieve organization and to handle their data effectively to be readily available and accessible (**Figure 7.9**). Some examples of the data warehouse applicability within the food sector include the evaluation of how new menu items affect kitchen space, customization of marketing campaigns, understanding consumer preferences, assessing seasonal effects on product sales, devising strategies to address sales fluctuations, designing loyalty programs, and adjusting menu based on consumer preferences and feedback.

Food scientists may encourage the need for compatible data formats with most AI tools, as this may hinder the utilization of AI.

The answer to whether AI is making humankind either more efficient or less competent remains unclear and subjective. We may acknowledge that computational tools should complement rather than entirely replace traditional methodologies since they can not yet capture information concerning human experiences and historical background.

7.4. Conclusions

The growing demand for alternative protein sources facilitates and opens up new ways for innovative food design that aligns with customer preferences. Typically, commercial food protein isolates are characterized by a blend of protein fractions, possible residual fat (<1%), and remaining traces rather than one single and well-characterized protein fraction, which presents both an opportunity and a challenge in FPD. The results of this Ph.D. thesis have shown that flavor compounds interact with PI, concentrates, and fractions. Variations in flavor properties, including physicochemical and configurational attributes, alter the protein-flavor binding mechanism. These differences offer efficient strategies in food design to customize protein-flavor interactions and improve food flavor profiles and, thus, consumer experience. As protein source and residual fat content have a minor impact on the binding mechanism, in principle, they could be used interchangeably when designing flavored protein-based aqueous model systems. The choice of a particular protein over another may depend on the most suitable techno-functional properties required for the final food product application rather than on the flavor-binding affinity. Utilizing cutting-edge, highly sensitive, real-time analytical techniques, such as PTR-ToF-MS, coupled with dynamic sensory profiling, enables us to gain deeper insights into the relationship between flavor compounds, release, and perception, aiding food design. Current advances in flavor science rely on computational strategies to predict flavor-binding affinity. This opens up new paths for research beyond traditional laboratory methods, allowing for the prediction of molecular interactions. However, it is important to recognize that computational tools should

complement traditional methodologies rather than replace them entirely. The findings in this Ph.D. thesis successfully demonstrated comprehension of the essential aspects of flavor-binding and release, which are crucial for flavored food design and development.



References

References

1. Acierno, V., Fasciani, G., Kiani, S., Caligiani, A., & Van Ruth, S. (2019). PTR-QiToF-MS and HSI for the characterization of fermented cocoa beans from different origins. *Food Chem*, 289, 591–602. DOI: 10.1016/j.foodchem.2019.03.095
2. Acuña, M. J., & Juárez, R. P. (2021). Salivary mucin concentration in patients with periodontal disease. *Odontostomatología*, 23(38). DOI:10.22592/ode2021n37e206
3. Adachi, M., Takenaka, Y., Gidamis, A. B., Mikami, B., & Utsumi, S. (2003). Crystal Structure of Soybean Proglycinin A1aB1b Homotrimer. *J. Mol. Biol.*, 305(2), 291–305. DOI: 10.1006/jmbi.2000.4310
4. Adams, R. L., Mottram, D. S., Parker, J. K., & Brown, H. M. (2001). Flavor-Protein Binding: Disulfide Interchange Reactions between Ovalbumin and Volatile Disulfides. *J. Agric. Food Chem*, 49(9), 4333–4336. DOI: 10.1021/jf0100797
5. Ahmad, M., Ritzoulis, C., Pan, W., & Chen, J. (2020). Chemical physics of whey protein isolate in the presence of mucin: From macromolecular interactions to functionality. *International J Biol Macromol*, 143, 573–581. DOI:10.1016/j.ijbiomac.2019.12.069
6. Ahmad, M., Ritzoulis, C., Bushra, R., Meigui, H., Zhang, X., Chen, J., Song, J., Jin, Y., & Xiao, H. (2022). Mapping of β -lactoglobulin – mucin interactions in an in vitro astringency model: Phase compatibility, adsorption mechanism and thermodynamic analysis. *Food Hydrocol*, 129, 107640. DOI: 10.1016/j.foodhyd.2022.107640
7. Akiyama, M., Tatsuzaki, M., Michishita, T., Ichiki, T., Sumi, M., Ikeda, M., Araki, T., & Sagara, Y. (2012). Package Design of Ready-to-Drink Coffee Beverages Based on Food Kansei Model—Effects of Straw and Cognition Terms on Consumer’s Pleasantness. *Food Bioproc Techn*, 5(5), 1924–1938. DOI: 10.1007/s11947-011-0527-5
8. Ammari, A., & Schroen, K. (2018). Flavor Retention and Release from Beverages: A Kinetic and Thermodynamic Perspective. *J Agric Food Chem*, 66(38), 9869–9881. DOI: 10.1021/acs.jafc.8b04459
9. Anantharamkrishnan, V., Hoyer, T., & Reineccius, G. A. (2020). Covalent Adduct Formation Between Flavor Compounds of Various Functional Group Classes and the Model Protein β -Lactoglobulin. *J Agric Food Chem*, 68(23), 6395–6402. DOI: 10.1021/acs.jafc.0c01925
10. Andini, S., Araya-Cloutier, C., Lay, B., Vreeke, G., Hageman, J., & Vincken, J.-P. (2021). QSAR-based physicochemical properties of isothiocyanate antimicrobials against gram-negative and gram-positive bacteria. *LWT*, 144, 111222. DOI: 10.1016/j.lwt.2021.111222
11. Andriot, I., Harrison, M., Fournier, N., & Guichard, E. (2000). Interactions between Methyl Ketones and β -Lactoglobulin: Sensory Analysis, Headspace Analysis, and Mathematical Modeling. *J. Agric. Food Chem*, 48(9), 4246–4251. DOI: 10.1021/jf991261z
12. Andriot, I., Marin, I., Feron, G., Relkin, P., & Guichard, E. (1999). Binding of benzaldehyde by β -lactoglobulin, by static headspace and high performance liquid chromatography in different physico-chemical conditions. *Le Lait*, 79(6), DOI: 10.1051/lait:1999647
13. Añón, M. C., Sorgentini, D. A., & Wagner, J. R. (2001). Relationships between Different Hydration Properties of Commercial and Laboratory Soybean Isolates. *J. Agric. Food Chem*, 49(10), 4852–4858. DOI: 10.1021/jf010384s

14. Aprea, E. (2020). Special Issue "Volatile Compounds and Smell Chemicals (Odor and Aroma) of Food." *Mol*, 25(17), 3811. DOI: 10.3390/molecules25173811
15. Atkins, P. W. Forces between molecules. In: Atkins PW, ed. *Atkins' Molecules*. 2nd ed. Cambridge University Press; 2003:11.
16. Ayed, C., Lubbers, S., Andriot, I., Merabtine, Y., Guichard, E., & Tromelin, A. (2014). Impact of structural features of odorant molecules on their retention/release behaviours in dairy and pectin gels. *Food Res Int*, 62, 846–859. DOI:10.1016/j.foodres.2014.04.050
17. Bader, S., Czerny, M., Eisner, P., & Buettner, A. (2009). Characterisation of odour-active compounds in lupin flour. *J Sci Food*, 89(14), 2421–2427. DOI: 10.1002/jsfa.3739
18. Barallat-Pérez, C., Janssen, H.-G., Martins, S., Fogliano, V., & Oliviero, T. (2023). Unraveling the Role of Flavor Structure and Physicochemical Properties in the Binding Phenomenon with Commercial Food Protein Isolates. *J Agric Food Chem*, 71(50), 20274–20284. DOI: 10.1021/acs.jafc.3c05991
19. Barallat-Pérez, C., Pedrotti, M., Oliviero, T., Martins, S., Fogliano, V., & De Jong, C. (2024). Drivers of the In-Mouth Interaction between Lupin Protein Isolate and Selected Aroma Compounds: A Proton Transfer Reaction–Mass Spectrometry and Dynamic Time Intensity Analysis. *J. Agric. Food Chem*, 72(15), 8731–8741. DOI:10.1021/acs.jafc.3c08819
20. Beauchamp, J., Frasnelli, J., Buettner, A., Scheibe, M., Hansel, A., & Hummel, T. (2010). Characterization of an olfactometer by proton-transfer-reaction mass spectrometry. *Meas Sci Technol*, 21(2), 025801. DOI: 10.1088/0957-0233/21/2/025801
21. Beekman, T. L., Huck, L., Claire, B., & Seo, H.-S. (2021). Consumer acceptability and monetary value perception of iced coffee beverages vary with drinking conditions using different types of straws or lids. *Food Res Int* 140, 109849. DOI: 10.1016/j.foodres.2020.109849
22. Bellelli, A., & Carey, J. (2018). Reversible Ligand Binding: Theory and Experiment. John Wiley & Sons.
23. Berghout, J. A. Functionality-driven fractionation of lupin seeds. Ph.D. Dissertation, Wageningen University and Research, Wageningen, The Netherlands, 2015. <https://edepot.wur.nl/338830>
24. Beyeler, M., & Solms, J. (1974). Interaction of flavor model compounds with soy protein and bovine serum albumin. *LWT Lebensmittel Wissensch Technol*.
25. Bi, S., Pan, X., Zhang, W., Ma, Z., Lao, F., Shen, Q., & Wu, J. (2022). Non-covalent interactions of selected flavors with pea protein: Role of molecular structure of flavor compounds. *Food Chem*, 389, 133044. DOI: 10.1016/j.foodchem.2022.133044
26. Bi, S., Xu, X., Luo, D., Lao, F., Pang, X., Shen, Q., Hu, X., & Wu, J. (2020). Characterization of Key Aroma Compounds in Raw and Roasted Peas (*Pisum sativum* L.) by Application of Instrumental and Sensory Techniques. *J Agric Food Chem*, 68(9), 2718–2727. DOI: 10.1021/acs.jafc.9b07711
27. Biasioli, F., Gasperi, F., Aprea, E., Endrizzi, I., Framondino, V., Marini, F., Mott, D., & Märk, T. D. (2006). Correlation of PTR-MS spectral fingerprints with sensory characterisation of

References

- flavour and odour profile of "Trentingrana" cheese. *Food Qual Prefer*, 17(1–2), 63–75. DOI: 10.1016/j.foodqual.2005.06.004
28. BioRender. <https://www.biorender.com>.
29. Birch, D., Skallerud, K., & Paul, N. (2019). Who eats seaweed? An Australian perspective. *J Int Food & Agribus Mark*, 31(4), 329–351. DOI: 10.1080/08974438.2018.1520182
30. Blankenship, M. L., Grigorova, M., Katz, D. B., & Maier, J. X. (2019). Retronasal Odor Perception Requires Taste Cortex, but Orthonasal Does Not. *Curr Bio*, 29(1), 62–69.e3. DOI: 10.1016/j.cub.2018.11.011
31. Blee, N., Linforth, R., Yang, N., Brown, K., & Taylor, A. (2011). Variation in aroma release between panellists consuming different types of confectionary. *Flavour Fragr J*, 26(3), 186–191. DOI: 10.1002/ffj.2051
32. Bligh, E. G., & Dyer, W. J. (1959). A rapid method of total lipid extraction and purification. *Can. J. Biochem. Physiol*, 37(8), 911–917. DOI: 10.1139/o59-099
33. Boland, A. (2004). Influence of gelatin, starch, pectin and artificial saliva on the release of 11 flavour compounds from model gel systems. *Food Chem*, 86(3), 401–411. DOI: 10.1016/j.foodchem.2003.09.015
34. Bou, R., Navarro-Vozmediano, P., Domínguez, R., López-Gómez, M., Pinent, M., Ribas-Agustí, A., Benedito, J. J., tae, J. M., Terra, X., García-Pérez, J. V., Pateiro, M., Herrera-Cervera, J. A., & Jorba-Martin, R. (2022). Application of emerging technologies to obtain legume protein isolates with improved techno-functional properties and health effects. *Compr. Rev. Food Sci. Food Saf*, 21(3), 2200–2232. DOI: 10.1111/1541-4337.12936
35. Boukid, F., Fanari, F., & Mefleh, M. (2024). Plant-based fermented foods and microbial ingredients in meat analogs. In *Handbook of Plant-Based Meat Analogs* (pp. 169–186). Elsevier. DOI: 10.1016/B978-0-443-21846-0.00015-0
36. Brown, F. N., Mackie, A. R., He, Q., Branch, A., & Sarkar, A. (2021). Protein–saliva interactions: A systematic review. *Food & Funct*, 12(8), 3324–3351. DOI:10.1039/D0FO03180A
37. Buettner, A., & Beauchamp, J. (2010). Chemical input – Sensory output: Diverse modes of physiology–flavour interaction. *Food Qual Prefer*, 21(8), 915–924. DOI: 10.1016/j.foodqual.2010.01.008
38. Buettner, A., & Schieberle, P. (2000). Influence of mastication on the concentrations of aroma volatiles & some aspects of flavour release and flavour perception. *Food Chem*, 71(3):347–354. DOI:10.1016/S0308-8146(00)00199-0
39. Buettner, A., & Welle, F. (2004). Intra-oral detection of potent odorants using a modified stir-bar sorptive extraction system in combination with HRGC–O, known as the buccal odour screening system (BOSS). *Flavour Fragr J*, 19(6), 505–514. DOI: 10.1002/ffj.1473
40. Campbell-Sills, H., Capozzi, V., Romano, A., Cappellin, L., Spano, G., Breniaux, M., Lucas, P., & Biasioli, F. (2016). Advances in wine analysis by PTR-ToF-MS: Optimization of the method and discrimination of wines from different geographical origins and fermented with different malolactic starters. *Int J Mass Spectr*, 397–398, 42–51. DOI:10.1016/j.ijms.2016.02.001

41. Canon, F., & Neyraud, E. (2016). Interactions between saliva and flavour compounds. In E. Guichard, C. Salles, M. Morzel, & A. Le Bon (Eds.), *Flavour* (1st ed., pp. 284–309). Wiley. DOI:10.1002/9781118929384.ch12
42. Caparros Megido, R., Gierts, C., Blecker, C., Brostaux, Y., Haubruge, É., Alabi, T., & Francis, F. (2016). Consumer acceptance of insect-based alternative meat products in Western countries. *Food Qual Prefer*, *52*, 237–243. DOI: 10.1016/j.foodqual.2016.05.004
43. Cayot, N. (2014). *Part B, chapter 7: Food flavors*. In Stephan Drusch and Kirsi Jouppila. (Eds.), *Physical Chemistry for Food Scientists*, Springer, pp.1-33, 2014
44. Çelebioğlu H. Y.; Lee S.; I. S. Chronakis. (2020). Interactions of Salivary Mucins and Saliva with Food Proteins: a Review. *Crit Rev Food Sci Nutr*, *60*, 64–83. DOI: 10408398.2018.1512950
45. Chang, C., Stone, A. K., Green, R., & Nickerson, M. T. (2019). Reduction of off-flavours and the impact on the functionalities of lentil protein isolate by acetone, ethanol, and isopropanol treatments. *Food Chem*, *277*, 84–95. DOI:10.1016/j.foodchem.2018.10.022
46. Charles, M., Romano, A., Yener, S., Barnabà, M., Navarini, L., Märk, T. D., Biasoli, F., & Gasperi, F. (2015). Understanding flavour perception of espresso coffee by the combination of a dynamic sensory method and in-vivo nosespace analysis. *Food Res Int*, *69*, 9–20. DOI: 10.1016/j.foodres.2014.11.036
47. Chen, L., Yan, R., Zhao, Y., Sun, J., Zhang, Y., Li, H., Zhao, D., Wang, B., Ye, X., & Sun, B. (2023). Characterization of the aroma release from retronasal cavity and flavor perception during baijiu consumption by Vocus-PTR-MS, GCxGC-MS, and TCATA analysis. *LWT*, *174*, 114430. DOI: 10.1016/j.lwt.2023.114430
48. Chen, Y., Liu, Y., & Feng, X. (2023). Food Perception: Taste, Smell and Flavour. *Foods*, *12*(19), 3628. DOI: 10.3390/foods12193628
49. Cheng, J., Liu, J.-H., Prasanna, G., & Jing, P. (2017). Spectrofluorimetric and molecular docking studies on the interaction of cyanidin-3-O-glucoside with whey protein, β -lactoglobulin. *Int. J. Biol. Macromol*, *105*, 965–972. DOI: 10.1016/j.ijbiomac.2017.07.119
50. Chobpattana, W., Jeon, I. J., Smith, J. S., & Loughin, T. M. (2002). Mechanisms of Interaction Between Vanillin and Milk Proteins in Model Systems. *J. Food Sci*, *67*(3), 973–977. DOI: 10.1111/j.1365-2621.2002.tb09438.x
51. Chung, S. J., Heymann, H., Grün, I. U. (2003). Temporal release of flavor compounds from low-fat and high-fat ice cream during eating. *J. Food Sci*. *68*(6), 2150–2156. DOI: 10.1111/j.1365-2621.2003.tb07035.x
52. Cichero, E., Fresia, C., Guida, L., Booz, V., Millo, E., Scotti, C., Iamele, L., De Jonge, H., Galante, D., De Flora, A., Sturla, L., Vigliarolo, T., Zocchi, E., & Fossa, P. (2018). Identification of a high affinity binding site for abscisic acid on human lanthionine synthetase component C-like protein 2. *Int J Biochem Cell Biol* *97*, 52–61. DOI:10.1016/j.biocel.2018.02.003
53. Cliff, M., & Heymann, H. (1993). Development and use of time-intensity methodology for sensory evaluation: A review. *Food Res Int*, *26*(5), 375–385. DOI: 10.1016/0963-9969(93)90081-S

References

54. Cook, S. L., Bull, S. P., Methven, L., Parker, J. K., & Khutoryanskiy, V. V. (2017). Mucoadhesion: A food perspective. *Food Hydrocol*, *72*, 281–296. DOI:10.1016/j.foodhyd.2017.05.043
55. Cohen, S.M., Eisenbrand, G., Fukushima, S., Gooderham, N.J., Guengerich F.P., Hecht, S.S., Rietjens, I.M.C.M., and Smith, R.L. (2017). GRAS flavoring substances 28. Flavor & Extract Manufacturers Assoc.
56. Cordelle, S., Redl, A., & Schlich, P. (2022). Sensory acceptability of new plant protein meat substitutes. *Food Qual Prefer*, *98*, 104508. DOI:10.1016/j.foodqual.2021.104508
57. Criado, C., Muñoz-González, C., & Pozo-Bayón, M. Á. (2021). Differences in salivary flow and composition between age groups are correlated to dynamic retronasal aroma perception during wine consumption. *Food Qual Prefer*, *87*, 104046. DOI: 10.1016/j.foodqual.2020.104046
58. Crowe J, Bradshaw T. Molecular interactions: holding it all together. In: Crowe J, Bradshaw T, eds. *Chemistry for the Biosciences: the Essential Concepts*. 3rd ed. Oxford University Press; 2014:88-126.
59. Czubinski, J., Barciszewski, J., Gilski, M., Szpotkowski, K., Debski, J., Lampart-Szczapa, E., Jaskolski, M. (2015). Structure of γ -conglutin: insight into the quaternary structure of 7S basic globulins from legumes. *Acta Crystallogr. D Biol. Crystallogr*, *71*(2), 224-238. DOI: 10.1107/S1399004714025073
60. Damodaran, S., & Kinsella, J. E. (1980). Flavor protein interactions. Binding of carbonyls to bovine serum albumin: Thermodynamic and conformational effects. *J. Agric. Food Chem*, *28*(3), 567–571. DOI:10.1021/jf60229a019
61. Damodaran, S., & Kinsella, J. E. (1981). Interaction of carbonyls with soy protein: Thermodynamic effects. *J. Agric. Food Chem*, *29*(6), 1249–1253. DOI: 10.1021/jf00108a037
62. De Roos, K. B. (2003). Effect of texture and microstructure on flavour retention and release. *Int Dairy J*, *13*(8), 593–605. DOI: 10.1016/S0958-6946(03)00108-0
63. De Roos, K. B. Physiochemical models of flavor release from foods. In *Flavor Release*; Roberts, D. D., and Taylor A. J. Eds.; American Chemical Society, 2000; 763., 126-141.
64. Di, C., & Jia, W. (2023). Capture modes evaluation of four flavor constituents in β -lactoglobulin by high-resolution mass spectrometry and molecular dynamics simulation approaches. *Food Hydrocol*, *145*, 109157. DOI: 10.1016/j.foodhyd.2023.109157
65. Dinu, V., Borah, P. K., Muleya, M., Scott, D. J., Lithgo, R., Patterm, J., Harding, S. E., Yakubov, G. E., & Fisk, I. D. (2022). Flavour compounds affect protein structure: The effect of methyl anthranilate on bovine serum albumin conformation. *Food Chem*, *388*, 133013. DOI: 10.1016/j.foodchem.2022.133013
66. Dinu, V., Gillis, R. B., MacCalman, T., Lim, M., Adams, G. G., Harding, S. E., & Fisk, I. D. (2019). Submaxillary Mucin: Its Effect on Aroma Release from Acidic Drinks and New Insight into the Effect of Aroma Compounds on its Macromolecular Integrity. *Food Biophys*, *14*(3), 278–286. DOI:10.1007/s11483-019-09574-2

67. Doyennette, M., Aguayo-Mendoza, M. G., Williamson, A.-M., Martins, S. I. F. S., & Stieger, M. (2019). Capturing the impact of oral processing behaviour on consumption time and dynamic sensory perception of ice creams differing in hardness. *Food Qual Pref*, *78*, 103721. DOI: 10.1016/j.foodqual.2019.103721
68. Dumont J. P & Land D. G. (1986). Binding diacetyl by pea proteins. *J Agric Food Chem*, *34*(6):1041-1045. DOI:10.1021/jf00072a028
69. Einig R. G. Interaction of Meat Aroma Volatiles with Soy Proteins (1983). PhD diss. University Missouri-Columbia.
70. Ellman, G. L. Tissue sulfhydryl groups. *Arch. Biochem. Biophys.* **1959**, *82*(1), 70–77. DOI: 10.1016/0003-9861(59)90090-6
71. Esteban-Fernández, A., Rocha-Alcubilla, N., Muñoz-González, C., Moreno-Arribas, M. V., & Pozo-Bayón, M. Á. (2016). Intra-oral adsorption and release of aroma compounds following in-mouth wine exposure. *Food Chem* *205*, 280–288. DOI: 10.1016/j.foodchem.2016.03.030
72. Fan, Z., Jeffries, K. A., Sun, X., Olmedo, G., Zhao, W., Mattia, M. R., Stover, E., Manthey, J. A., Baldwin, E. A., Lee, S., Gmitter, F. G., Plotto, A., & Bai, J. (2024). Chemical and genetic basis of orange flavor. *Sci Adv*, *10*(9), eadk2051. DOI: 10.1126/sciadv.adk2051
73. Fatima, N., Emambux, M. N., Olaimat, A. N., Stratakos, A. C., Nawaz, A., Wahyono, A., Gul, K., Park, J., & Shahbaz, H. M. (2023). Recent advances in microalgae, insects, and cultured meat as sustainable alternative protein sources. *Food and Humanity*, *1*, 731–741. DOI: 10.1016/j.foohum.2023.07.009
74. Feiler, A. A., Sahlholm, A., Sandberg, T., & Caldwell, K. D. (2007). Adsorption and viscoelastic properties of fractionated mucin (BSM) and bovine serum albumin (BSA) studied with quartz crystal microbalance (QCM-D). *J Colloid Interface Sci*, *315*(2), 475–481. DOI: 10.1016/j.jcis.2007.07.029
75. Food Navigator. <https://www.foodnavigator.com>
76. Friel, E. N., & Taylor, A. J. (2001). Effect of Salivary Components on Volatile Partitioning from Solutions. *J Agric Food Chem*, *49*(8), 3898–3905. DOI: 10.1021/jf010371e
77. Ghanbari, J., Khajoei-Nejad, G., Erasmus, S. W., & Van Ruth, S. M. (2019). Identification and characterisation of volatile fingerprints of saffron stigmas and petals using PTR-TOF-MS: Influence of nutritional treatments and corm provenance. *Ind Crops Prod*, *141*, 111803. DOI: 10.1016/j.indcrop.2019.111803
78. Ghoshal, G. (2019). Recent Development in Beverage Packaging Material and its Adaptation Strategy. In *Trends in Beverage Packaging* (pp. 21–50). Elsevier. DOI: 10.1016/B978-0-12-816683-3.00002-5
79. Gianelli, M. P., Flores, M., & Toldrà, F. (2003). Interactions of Soluble Peptides and Proteins from Skeletal Muscle on the Release of Volatile Compounds. *J Agric Food Chem*, *51*(23), 6828–6834. DOI: 10.1021/jf0303666
80. Gkionakis, G. A., David Anthony Taylor, K., Ahmad, J., & Heliopoulos, G. (2007). The binding of the flavour of lactones by soya protein, amino acids and casein. *International J Food Sci Techn*, *42*(2), 165–174. DOI: 10.1111/j.1365-2621.2006.01184.x

References

81. Gonzalez-Estanol, K., Khomenko, I., Ciceri, D., Biasioli, F., & Stieger, M. (2023). In vivo aroma release and perception of composite foods using nose space PTR–ToF–MS analysis with Temporal–Check–All–That–Apply. *Food Res Int*, 167, 112726. DOI:10.1016/j.foodres.2023.112726
82. Gremler, H. A. (1974). Interaction of flavor compounds with soy protein. *J Am Oil Chem Soc*, 51(1Part1). DOI: 10.1007/BF02542100
83. Grover, N., Goel, M., Batra, D., Garg, N., Tuwani, R., Sethupathy, A., & Bagler, G. (2022). *FlavorDB2: An Updated Database of Flavor Molecules* (arXiv:2205.05451). arXiv. <http://arxiv.org/abs/2205.05451>
84. Gueguen, J. (1983). Legume seed protein extraction, processing, and end product characteristics. *Plant Foods Hum Nutr*, 32(3–4), 267–303. DOI:10.1007/BF01091191
85. Guichard, E. (2006). Flavour retention and release from protein solutions. *Biotechnol. Adv*, 24(2), 226–229. DOI: 10.1016/j.biotechadv.2005.11.003
86. Gulzar, M. Dry heating of whey proteins under controlled physicochemical conditions: Structures, interactions, and functionalities. Ph.D. Dissertation, Université de Bretagne Occidentale, Brest, France, 2011. <https://hal.inrae.fr/tel-02807314>
87. Guo, J., He, Z., Wu, S., Zeng, M., & Chen, J. (2019). Binding of aroma compounds with soy protein isolate in aqueous model: Effect of preheat treatment of soy protein isolate. *Food Chem*, 290, 16–23. DOI: 10.1016/j.foodchem.2019.03.126
88. Guo, J., He, Z., Wu, S., Zeng, M., & Chen, J. (2020). Effects of concentration of flavor compounds on interaction between soy protein isolate and flavor compounds. *Food Hydrocol*, 100, 105388. DOI:10.1016/j.foodhyd.2019.105388
89. Guo, Y., Gong, Q., Sun, F., Cheng, T., Fan, Z., Huang, Z., Liu, J., Guo, Z., & Wang, Z. (2024). Interaction mechanism of pea proteins with selected pyrazine flavors: Differences in alkyl numbers and flavor concentration. *Food Hydrocol*, 147, 109314. DOI:10.1016/j.foodhyd.2023.109314
90. Guo, F., Xiong, Y. L., Qin, F., Jian, H., Huang, X., & Chen, J. (2015). Surface Properties of Heat-Induced Soluble Soy Protein Aggregates of Different Molecular Masses. *J Food Sci*, 80(2). DOI:10.1111/1750-3841.12761
91. Hageman, J. A., Engel, B., de Vos, R. C. H., Mumm, R., Hall, R. D., Jwanro, H., Crouzillat, D., Spadone, J. C., & van Eeuwijk, F. A. (2017). Robust and Confident Predictor Selection in Metabolomics. In S. Datta & B. J. A. Mertens (Eds.), *Statistical Analysis of Proteomics, Metabolomics, and Lipidomics Data Using Mass Spectrometry* (pp. 239–257). Springer International Publishing. DOI: 10.1007/978-3-319-45809-0_13
92. Hannum, M., Stegman, M. A., Fryer, J. A., & Simons, C. T. (2018). Different Olfactory Percepts Evoked by Orthonasal and Retronasal Odorant Delivery. *Chem Sens*, 43(7), 515–521. DOI: 10.1093/chemse/bjy043
93. Hansen, A. P.; Booker, D. C. (1996). Flavor interaction with casein and whey protein. In *Flavor-Food Interactions*; McGorin, R. J, Leland, J. V., Eds.; ACS Symposium Series, Vol. 633; American Chemical Society, pp 75–89. DOI: 10.1021/bk-1996-0633.ch007

94. Harding, S. E. (1989). The macrostructure of mucus glycoproteins in solution. *Adv Carbohydr Chem Biochem*, 47, 345–381.
95. Hansson, A., Giannouli, P., & Van Ruth, S. (2003). The Influence of Gel Strength on Aroma Release from Pectin Gels in a Model Mouth and in Vivo, Monitored with Proton-Transfer-Reaction Mass Spectrometry. *J Agric Food Chem*, 51(16), 4732–4740. DOI: 10.1021/jf030050y
96. Harrison, M., Hills, B. P., Bakker, J., & Clothier, T. (1997). Mathematical Models of Flavor Release from Liquid Emulsions. *J Food Sci* 62(4), 653–664. DOI:10.1111/j.1365-2621.1997.tb15429.x
97. Harwatt, H., Sabaté, J., Eshel, G., Soret, S., & Ripple, W. (2017). Substituting beans for beef as a contribution toward US climate change targets. *Clim Change*, 143(1–2), 261–270. DOI: 10.1007/s10584-017-1969-1
98. Hayes, M. (2023). Challenges regarding protein provision for the growing global population: improving the environmental impact of traditional protein supply chains and maximising use of coproducts and alternative, new resources. *Global Chall*, 7(5). DOI: 10.1002/gch2.202300059
99. He, Z., Li, W., Guo, F., Li, W., Zeng, M., & Chen, J. (2015). Foaming Characteristics of Commercial Soy Protein Isolate as Influenced by Heat-Induced Aggregation. *International J Food Prop*, 18(8), 1817–1828. DOI: 10.1080/10942912.2014.946046
100. Heenan, S., Soukoulis, C., Silcock, P., Fabris, A., Aprea, E., Cappellin, L., Märk, T. D., Gasperi, F., & Biasioli, F. (2012). PTR-TOF-MS monitoring of *in vitro* and *in vivo* flavour release in cereal bars with varying sugar composition. *Food Chem*, 131(2), 477–484. DOI: 10.1016/j.foodchem.2011.09.010
101. Hendrix, T. M.; Griko, Y.; Privalov, P. (1996). Energetics of structural domains in α -lactalbumin. *Protein Sci*. 5(5), 923–931. DOI: 10.1002/pro.5560050514
102. Heng, L., Van Koningsveld, G. A., Gruppen, H., Van Boekel, M. A. J. S., Vincken, J.-P., Roozen, J. P., & Voragen, A. G. J. (2004). Protein–flavour interactions in relation to development of novel protein foods. *Trends Food Sci Technol*, 15(3–4), 217–224. DOI: 10.1016/j.tifs.2003.09.018
103. Hernandez-Munoz, P., Kanavouras, A., Villalobos, R., & Chiralt, A. (2004). Characterization of Biodegradable Films Obtained from Cysteine-Mediated Polymerized Gliadins. *J. Agric. Food Chem*, 52(26), 7897–7904. DOI:10.1021/jf0491613
104. Hidalgo, F. J., & Zamora, R. (2023). Ketone-phenol reactions and the promotion of aromatizations by food phenolics. *Food Chem*, 404, 134554. DOI: 10.1016/j.foodchem.2022.134554
105. Houde, M., Khodaei, N., & Karboune, S. (2018). Assessment of interaction of vanillin with barley, pea and whey proteins: Binding properties and sensory characteristics. *LWT*, 91, 133–142. DOI: 10.1016/j.lwt.2018.01.022
106. How, M. S., Jones, J. R., Morgenstern, M. P., Gray-Stuart, E., Bronlund, J. E., Saint-Eve, A., Trelea, I. C., & Souchon, I. (2021). Modelling the role of oral processing on in vivo aroma

References

- release of white rice: Conceptual model and experimental validation. *LWT*, *141*, 110918. DOI: 10.1016/j.lwt.2021.110918
107. Hsein, H., Garrait, G., Beyssac, E., & Hoffart, V. (2015). Whey protein mucoadhesive properties for oral drug delivery: Mucin–whey protein interaction and mucoadhesive bond strength. *Col Surf B: Biointer*, *136*, 799–808. DOI: 10.1016/j.colsurfb.2015.10.016
108. Hsiao, Y.-H., Yu, C.-J., Li, W.-T., & Hsieh, J.-F. (2015). Coagulation of β -conglycinin, glycinin and isoflavones induced by calcium chloride in soymilk. *Sci. Rep*, *5*(1), 13018. DOI: 10.1038/srep13018
109. Huang, X., Sun, L., Liu, L., Wang, G., Luo, P., Tang, D., & Huang, Q. (2022). Study on the mechanism of mulberry polyphenols inhibiting oxidation of beef myofibrillar protein. *Food Chem*, *372*, 131241. DOI: 10.1016/j.foodchem.2021.131241
110. Ijichi, C., Wakabayashi, H., Sugiyama, S., Ihara, Y., Nogi, Y., Nagashima, A., Ihara, S., Niimura, Y., Shimizu, Y., Kondo, K., & Touhara, K. (2019). Metabolism of Odorant Molecules in Human Nasal/Oral Cavity Affects the Odorant Perception. *Chem Sens*, *44*(7), 465–481. DOI: 10.1093/chemse/bjz041
111. IONICON <https://www.ionicon.com>
112. Ismail, B. P., Senaratne-Lenagala, L., Stube, A., & Brackenridge, A. (2020). Protein demand: Review of plant and animal proteins used in alternative protein product development and production. *Anim Front* *10*(4), 53–63. DOI: 10.1093/af/vfaa040
113. Itobe, T., & Kumazawa, K. (2017). Taste-aroma Interactions in Lemon-flavored Model Beverages: Influence of Sweeteners on Aroma Perception and In Vivo Aroma Release. *Food Sci Tech Res*, *23*(1), 51–56. DOI: 10.3136/fstr.23.51
114. Jasinski, E., & Kilara, A. (1985). Flavor binding by whey proteins.
115. Ji, H., Pu, D., Yan, W., Zhang, Q., Zuo, M., & Zhang, Y. (2023). Recent advances and application of machine learning in food flavor prediction and regulation. *Trends in Food Sci Techn*, *138*, 738–751. DOI: 10.1016/j.tifs.2023.07.012
116. Jiang, S., Altaf Hussain, M., Cheng, J., Jiang, Z., Geng, H., Sun, Y., Sun, C., & Hou, J. (2018). Effect of heat treatment on physicochemical and emulsifying properties of polymerized whey protein concentrate and polymerized whey protein isolate. *LWT*, *98*, 134–140. DOI:10.1016/j.lwt.2018.08.028
117. Jouquand, C., Aguni, Y., Malhiac, C., & Grisel, M. (2008). Influence of chemical composition of polysaccharides on aroma retention. *Food Hydrocol*, *22*(6), 1097–1104. DOI: 10.1016/j.foodhyd.2007.06.001
118. Jouenne, E., & Crouzet, J. Determination of apparent binding constants for aroma compounds with β -lactoglobulin by dynamic coupled column liquid chromatography (2000). *J Agric Food Chem*, *48*(11):5396-5400. DOI::10.1021/jf000 423k
119. Kano K. (1993). Selectivities in cyclodextrins chemistry. In: Dugas H, Schmidtchen FP, eds. Biorganic Chemistry Frontier. Vol 3. Springer, 1–23.

120. Karabulut, G., Goksen, G., & Mousavi Khaneghah, A. (2024). Plant-based protein modification strategies towards challenges. *J Agric Food Res*, 15, 101017. DOI: 10.1016/j.jafr.2024.101017
121. Kejrival, S. (2014). Estimation of Levels of Salivary Mucin, Amylase and Total Protein in Gingivitis and Chronic Periodontitis Patients. *J Clin Diag Res*. DOI:10.7860/JCDR/2014/8239.5042
122. Kew, B., Holmes, M., Stieger, M., & Sarkar, A. (2021). Oral tribology, adsorption and rheology of alternative food proteins. *Food Hydrocol*, 116, 106636. DOI: 10.1016/j.foodhyd.2021.106636
123. Kim, W., Wang, Y., & Selomulya, C. (2020). Dairy and plant proteins as natural food emulsifiers. *Trends Food Sci Technol*, 105, 261–272. DOI: 10.1016/j.tifs.2020.09.012
124. Kim, S., Chen, J., Cheng, T., Gindulyte, A., He, J., He, S., Li, Q., Shoemaker, B. A., Thiessen, P. A., Yu, B., Zaslavsky, L., Zhang, J., & Bolton, E. E. (2023). PubChem 2023 update. *Nucleic Acids Res*, 51(D1), D1373–D1380. DOI:10.1093/nar/gkac956
125. Kühn, J., Considine, T., & Singh, H. (2006). Interactions of Milk Proteins and Volatile Flavor Compounds: Implications in the Development of Protein Foods. *J. Food Sci*, 71(5). DOI: 10.1111/j.1750-3841.2006.00051.x
126. Kühn, J., Considine, T., & Singh, H. (2008). Binding of Flavor Compounds and Whey Protein Isolate as Affected by Heat and High Pressure Treatments. *J. Agric. Food Chem*, 56(21), 10218–10224. DOI: 10.1021/jf801810b
127. Kurek, M. A., Onopiuk, A., Pogorzelska-Nowicka, E., Szpicer, A., Zalewska, M., & Póttorak, A. (2022). Novel Protein Sources for Applications in Meat-Alternative Products—Insight and Challenges. *Foods*, 11(7), 957. DOI: 10.3390/foods11070957
128. Kurpiewska, K., Biela, A., Loch, J. I., Świątek, S., Jachimska, B., & Lewiński, K. (2018). Investigation of high pressure effect on the structure and adsorption of β -lactoglobulin. *Colloids Surf B: Biointerfaces*, 161, 387–393. DOI:10.1016/j.colsurfb.2017.10.069
129. Kurska, M. B., Jankowski, A., & Rudnicki, W. R. (2010). Boruta—a system for feature selection. *Fundamenta Informaticae*, 101(4), 271–285. DOI: 10.3233/FI-2010-288
130. Kyriakopoulou, K., Dekkers, B., & Van Der Goot, A. J. (2019). Plant-Based Meat Analogues. In *Sustainable Meat Production and Processing* (pp. 103–126). Elsevier. DOI:10.1016/B978-0-12-814874-7.00006-7
131. Lam, A. C. Y., Can Karaca, A., Tyler, R. T., & Nickerson, M. T. (2018). Pea protein isolates: Structure, extraction, and functionality. *Food Reviews Int* 34(2), 126–147. DOI: 10.1080/87559129.2016.1242135
132. Landy, P., Druaux, C., & Voilley, A. (1995). Retention of aroma compounds by proteins in aqueous solution. *Food Chem*, 54(4), 387–392. DOI: 10.1016/0308-8146(95)00069-U
133. Le Calvé, B., Saint-Léger, C., Gaudreau, N., & Cayeux, I. (2019). Capturing key sensory moments during biscuit consumption: Using TDS to evaluate several concurrent sensory modalities. *J Sens Stud*, 34(6), e12529. DOI:10.1111/joss.12529

References

134. Le Quéré, J.-L., & Schoumacker, R. (2023). Dynamic Instrumental and Sensory Methods Used to Link Aroma Release and Aroma Perception: A Review. *Mol* 28(17), 6308. DOI: 10.3390/molecules28176308
135. Lee, J. Green tea: Flavour characteristics of a wide range of teas including brewing, processing, and storage variations and consumer acceptance of teas in three countries. Ph.D. Dissertation, Kansas State University, Kansas, USA, 2009.
136. Lee, S., Bae, H. Y., & List, B. (2018). Can a Ketone Be More Reactive than an Aldehyde? Catalytic Asymmetric Synthesis of Substituted Tetrahydrofurans. *Angew Chem Int Ed* 57(37), 12162–12166. DOI: 10.1002/anie.201806312
137. Lee, H. W., Lu, Y., Zhang, Y., Fu, C., & Huang, D. (2021). Physicochemical and functional properties of red lentil protein isolates from three origins at different pH. *Food Chem*, 358, 129749. DOI: 10.1016/j.foodchem.2021.129749
138. Lee, H. J., Yong, H. I., Kim, M., Choi, Y.-S., & Jo, C. (2020). Status of meat alternatives and their potential role in the future meat market—A review. *Asian-Austr J Anim Sci*, 33(10), 1533–1543. DOI: 10.5713/ajas.20.0419
139. Li, Y., Xu, J., Sun, F., Guo, Y., Wang, D., Cheng, T., Xu, M., Wang, Z., & Guo, Z. (2024). Spectroscopy combined with spatiotemporal multiscale strategy to study the adsorption mechanism of soybean protein isolate with meat flavor compounds (furan): Differences in position and quantity of the methyl. *Food Chem*, 451, 139415. DOI: 10.1016/j.foodchem.2024.139415
140. Li, Z., Grün, I. U., & Fernando, L. N. (2000). Interaction of Vanillin with Soy and Dairy Proteins in Aqueous Model Systems: A Thermodynamic Study. *J. Food Sci*, 65(6), 997–1001. DOI: 10.1111/j.1365-2621.2000.tb09406.x
141. Li-Chan, E.; Nakai, S.; Wood, D. F. (1984). Hydrophobicity and solubility of meat proteins and their relationship to emulsifying properties. *J. Food Sci*, 49(2), 345–350. DOI: 10.1111/j.1365-2621.1984.tb12418.x
142. Linforth, R., & Taylor, A. J. (2000). Persistence of Volatile Compounds in the Breath after Their Consumption in Aqueous Solutions. *J Agri Food Chem*, 48(11), 5419–5423. DOI: 10.1021/jf000488n
143. Lingiardi, N., Galante, M., De Sanctis, M., & Spelzini, D. (2022). Are quinoa proteins a promising alternative to be applied in plant-based emulsion gel formulation? *Food Chem*, 394, 133485. DOI: 10.1016/j.foodchem.2022.133485
144. Lippolis, A., Roland, W. S. U., Bocova, O., Pouvreau, L., & Trindade, L. M. (2023). The challenge of breeding for reduced off-flavor in faba bean ingredients. *Front. Plant Sci*, 14, 1286803. DOI: 10.3389/fpls.2023.1286803
145. Lopez T. L., van Belzen, L., Michalet, M., Janinet, O., & Dalmas, S (2018). The impact of plant proteins on vanilla flavour perception. DOI:10.3217/978-3-85125-593-5-15
146. Ma, K. K., Grossmann, L., Nolden, A. A., McClements, D. J., & Kinchla, A. J. (2022). Functional and physical properties of commercial pulse proteins compared to soy derived protein. *Future Foods*, 6, 100155. DOI: 10.1016/j.fufo.2022.100155

147. Maheeka, W. N. R. P., Godfrey, A. J. R., Ellis, A., & Hort, J. (2021). Comparing temporal sensory product profile data obtained from expert and consumer panels and evaluating the value of a multiple sip TCATA approach. *Food Qual Prefer*, *89*, 104141. DOI: 10.1016/j.foodqual.2020.104141
148. Manski, J. M., Van Der Goot, A. J., & Boom, R. M. (2007). Advances in structure formation of anisotropic protein-rich foods through novel processing concepts. *Trends Food Sci. Technol*, *18*(11), 546–557. DOI:10.1016/j.tifs.2007.05.002
149. Mao, L., Roos, Y. H., Biliaderis, C. G., & Miao, S. (2017). Food emulsions as delivery systems for flavor compounds: A review. *Crit Rev Food Sci Nutr*, *57*(15), 3173–3187. DOI: 10.1080/10408398.2015.1098586
150. Maruyama, N.; Adachi, M.; Takahashi, K.; Yagasaki, K.; Kohno, M.; Takenaka, Y.; Okuda, E.; Nakagawa, S.; Mikami, B.; Utsumi S. (2001). Crystal structures of recombinant and native soybean β -conglycinin β homotrimers. *Eur. J. Biochem*, *268*(12), 3595–3604. DOI: 10.1046/j.1432-1327.2001.02268.x
151. Messian, J.-L., Chihi, M. L., Sok, N., & Saurel, R. (2015). Effect of globular pea proteins fractionation on their heat-induced aggregation and acid cold-set gelation. *Food Hydrocol*, *46*, 233–243. DOI: 10.1016/j.foodhyd.2014.11.025
152. Mills, O. E.; Solms, J. (1984). Interaction of selected flavor compounds with whey proteins. *Lebensm.-Wiss. Technol*, *17*, 331–335
153. Moll, P., Salminen, H., Seitz, O., Schmitt, C., & Weiss, J. (2023). Characterization of soluble and insoluble fractions obtained from a commercial pea protein isolate. *J Disp Sci Tech*, *44*(13), 2417–2428. DOI: 10.1080/01932691.2022.2093214
154. Monahan, F. J., German, J. B., & Kinsella, J. E. (1995). Effect of pH and temperature on protein unfolding and thiol/disulfide interchange reactions during heat-induced gelation of whey proteins. *J. Agric. Food Chem*, *43*(1), 46–52. DOI: 10.1021/jf00049a010
155. Monteleone, E.; Dinnella, C. General considerations. In *Time-Dependent Measures of Perception in Sensory Evaluation*; Hort, J., Kemp, S.E., Hollowood, T., Eds.; Wiley-Blackwell: Chichester, UK, 2017; pp. 159–181.
156. Mosca, A. C., & Chen, J. (2017). Food-saliva interactions: Mechanisms and implications. *Trends Food Sci Tech*, *66*, 125–134. DOI:10.1016/j.tifs.2017.06.005
157. Mu, R., & Chen, J. (2023). Oral bio-interfaces: Properties and functional roles of salivary multilayer in food oral processing. *Trends Food Sci Tech*, *132*, 121–131. DOI:10.1016/j.tifs.2023.01.003
158. Müller, C., & Hofmann, T. (2007). Quantitative Studies on the Formation of Phenol/2-Furfurylthiol Conjugates in Coffee Beverages toward the Understanding of the Molecular Mechanisms of Coffee Aroma Staling. *J. Agric. Food Chem*, *55*(10), 4095–4102. DOI:10.1021/jf070095p
159. Muñoz-González, C., Feron, G., Guichard, E., Rodríguez-Bencomo, J. J., Martín-Álvarez, P. J., Moreno-Arribas, M. V., & Pozo-Bayón, M. Á. (2014). Understanding the Role of Saliva in

References

- Aroma Release from Wine by Using Static and Dynamic Headspace Conditions. *J Agric Food Chem*, 62(33), 8274–8288. DOI: 10.1021/jf503503b
160. Muñoz-González, C., Canon, F., Feron, G., Guichard, E., & Pozo-Bayón, M. (2019). Assessment Wine Aroma Persistence by Using an in Vivo PTR-ToF-MS Approach and Its Relationship with Salivary Parameters. *Mol*, 24(7), 1277. DOI: 10.3390/molecules24071277
161. Muñoz-González, C.; Pérez-Jiménez, M., Pozo-Bayón, M. Á. (2020) Oral persistence of esters is affected by wine matrix composition. *Food Res Int.* 135, 109286. DOI: 10.1016/j.foodres.2020.109286
162. Muñoz-González, C.; Pozo-Bayón, M. Á.; Canon, F. (2021). Understanding the Molecular Basis of Aroma Persistence Using Real-Time Mass Spectrometry. *Dynamic Flavor: Capturing Aroma Using Real-Time Mass Spectrometry*, 67–75. Eds. Jonathan D. Beauchamp, vol 1402.
163. Muñoz-González, C., Brule, M., Martin, C., Feron, G., & Canon, F. (2022). Molecular mechanisms of aroma persistence: From noncovalent interactions between aroma compounds and the oral mucosa to metabolism of aroma compounds by saliva and oral cells. *Food Chem*, 373, 131467. DOI:10.1016/j.foodchem.2021.131467
164. Ng, P. K. W., Hoehn, E., & Bushuk, W. (1989). Binding of Vanillin by Fababean Proteins. *J. Food Sci*, 54(1), 105–107. DOI: 10.1111/j.1365-2621.1989.tb08578.x
165. O’Kane, F. E. (2004). Molecular characterization and heat-induced gelation of pea vicilin and legumin. PhD diss. Wageningen University & Research.
166. O’Neill, T. E., & Kinsella, J. E. (1987). Binding of alkanone flavors to .beta.-lactoglobulin: Effects of conformational and chemical modification. *J Agric Food Chem*, 35(5), 770–774. DOI: 10.1021/jf00077a030
167. O’Keefe S. F. (1988). Binding of Volatile Flavor Compounds to Purified Soy Proteins in an Aqueous Model System. PhD diss. Iowa State University.
168. Overbosch, P., Afterof, W. G. M., & Haring, P. G. M. (1991). Flavor release in the mouth. *Food Rev Int*, 7(2), 137–184. DOI:10.1080/87559129109540906
169. Pagès-Hélary, S., Andriot, I., Guichard, E., & Canon, F. (2014). Retention effect of human saliva on aroma release and respective contribution of salivary mucin and α -amylase. *Food Res Int*, 64, 424–431. DOI:10.1016/j.foodres.2014.07.013
170. Paravisini, L., & Guichard, E. (2016). Interactions between aroma compounds and food matrix. In E. Guichard, C. Salles, M. Morzel, & A. Le Bon (Eds.), *Flavour* (1st ed., pp. 208–234). Wiley. DOI: 10.1002/9781118929384.ch9
171. Pedrotti, M., Spaccasassi, A., Biasioli, F., & Fogliano, V. (2019). Ethnicity, gender and physiological parameters: Their effect on in vivo flavour release and perception during chewing gum consumption. *Food Res Int* 116, 57–70. DOI: 10.1016/j.foodres.2018.12.019
172. Pelletier, E., Sostmann, K., Guichard, E. Measurement of interactions between β -lactoglobulin and flavor compounds (esters, acids and pyrazines) by affinity and exclusion size chromatography (1998). *J Agric Food Chem*. 46(4):1506-1509. DOI: 10.1021/jf970 725v

173. Pérez, C. B; Oliviero, T.; Fogliano, V., Janssen, H. G.; Martins, S. I. Flavour them up! Exploring the challenges of flavored plant-based foods. *Flavour Fragr. J.* **2023**, *38*(3), 125-134. DOI: 10.1002/ffj.3734
174. Perez-Jiménez, M., Esteban-Fernández, A., Muñoz-González, C., & Pozo-Bayón, M. A. (2020). Interactions among Odorants, Phenolic Compounds, and Oral Components and Their Effects on Wine Aroma Volatility. *Mol*, *25*(7), 1701. DOI: 10.3390/molecules25071701
175. Pérez-Jiménez, M., Muñoz-González, C., & Pozo-Bayón, M. A. (2021). Oral Release Behavior of Wine Aroma Compounds by Using In-Mouth Headspace Sorptive Extraction (HSSE) Method. *Foods*, *10*(2), 415. DOI: 10.3390/foods10020415
176. Pérez-Jiménez, M., Sherman, E., Ángeles Pozo-Bayón, M., Muñoz-González, C., & Pinu, F. R. (2023). Application of untargeted volatile profiling to investigate the fate of aroma compounds during wine oral processing. *Food Chem*, *403*, 134307. DOI: 10.1016/j.foodchem.2022.134307
177. Piccone, P., Lonzarich, V., Navarini, L., Fusella, G., & Pittia, P. (2012). Effect of sugars on liquid-vapour partition of volatile compounds in ready-to-drink coffee beverages. *J Mass Spectr* *47*(9), 1120–1131. DOI: 10.1002/jms.3073
178. Piombino, P., Moio, L., & Genovese, A. (2019). Orthonasal vs. retronasal: Studying how volatiles' hydrophobicity and matrix composition modulate the release of wine odorants in simulated conditions. *Food Res Int*, *116*, 548–558. DOI: 10.1016/j.foodres.2018.08.072
179. Pionnier, E., Nicklaus, S., Chabanet, C., Mioche, L., Taylor, A. J., Le Quéré, J. L., & Salles, C. (2004). Flavor perception of a model cheese: Relationships with oral and physico-chemical parameters. *Food Qual Prefer*, *15*(7–8), 843–852. DOI: 10.1016/j.foodqual.2004.04.011
180. Pittari, E., Piombino, P., Andriot, I., Cheyrier, V., Cordelle, S., Feron, G., Gourrat, K., Le Quéré, J.-L., Meudec, E., Moio, L., Neiers, F., Schlich, P., & Canon, F. (2022). Effects of oenological tannins on aroma release and perception of oxidized and non-oxidized red wine: A dynamic real-time in-vivo study coupling sensory evaluation and analytical chemistry. *Food Chem*, *372*, 131229. DOI: 10.1016/j.foodchem.2021.131229
181. Ployon, S., Morzel, M., & Canon, F. (2017). The role of saliva in aroma release and perception. *Food Chem* *226*, 212–220. DOI:10.1016/j.foodchem.2017.01.055
182. Plug, H., Haring P. G. M. The role of ingredient-flavor interactions in the development of fat-free foods. (1993). *Trends Food Sci Technol*, *4*(5):150-152. DOI: 10.1016/0924-2244(93)90035 -9
183. Pramudya, R. C., Singh, A., & Seo, H.-S. (2021). A sip of joy: Straw materials can influence emotional responses to, and sensory attributes of cold tea. *Food Qual Prefer*, *88*, 104090. DOI: 10.1016/j.foodqual.2020.104090
184. Proserpio, C., Almlí, V. L., Sandvik, P., Sandell, M., Methven, L., Wallner, M., Jilani, H., Zeinstra, G. G., Alfaro, B., & Laureati, M. (2020). Cross-national differences in child food neophobia: A comparison of five European countries. *Food Qual Prefer*, *81*, 103861. DOI: 10.1016/j.foodqual.2019.103861

References

185. Regan, E., O'Neill, G. J., Hutchings, S. C., & O'Riordan, D. (2019). Exploring how age influences sensory perception, thirst and hunger during the consumption of oral nutritional supplements using the check-all-that-apply methodology. *Food Qual Prefer*, *78*, 103736. DOI: 10.1016/j.foodqual.2019.103736
186. PubChem. National Library of Medicine. National Center for Biotechnology Information. Home Page. <https://pubchem.ncbi.nlm.nih.gov>
187. RCSB Protein Database. Home Page. <https://www.rcsb.org>
188. REGULATION (EC) No 1334/2008 OF THE EUROPEAN PARLIAMENT AND OF THE COUNCIL of 16 December 2008 on flavourings and certain food ingredients with flavouring properties for use in and on foods and amending Council Regulation (EEC) No 1601/91, Regulations (EC) No 2232/96 and (EC) No 110/2008 and Directive 2000/13/EC. <https://eur-lex.europa.eu>.
189. Reineccius, G. (2010). Instrumental Methods of Analysis. In *Proceedings of The Society for Analytical Chemistry* (Vol. 4, pp. 229–265). DOI: 10.1002/9781444317770.ch9
190. Reineccius, G. A. (2022). Flavor interactions with proteins. *Curr Opin Food Sci*, *47*, 100884. DOI: 10.1016/j.cofs.2022.100884
191. Reineccius, G. Flavor release from foods. In *Taylor and Francis*, 2nd ed.; Flavor Chemistry and Technology; CRC Press, 2006; pp 154. DOI: 10.1201/9780203485347
192. Reipurth, M. F. S., Hørby, L., Gregersen, C. G., Bonke, A., & Perez Cueto, F. J. A. (2019). Barriers and facilitators towards adopting a more plant-based diet in a sample of Danish consumers. *Food Qual Prefer*, *73*, 288–292. DOI: 10.1016/j.foodqual.2018.10.012
193. Repoux, M., Labouré, H., Courcoux, P., Andriot, I., Sémon, É., Yven, C., Feron, G., & Guichard, E. (2012). Combined effect of cheese characteristics and food oral processing on *in vivo* aroma release. *Flavour Fragr. J*, *27*(6), 414–423. DOI:10.1002/ffj.3110
194. Ritter, S. W., Gastl, M. I., & Becker, T. M. (2022). The modification of volatile and nonvolatile compounds in lupines and faba beans by substrate modulation and lactic acid fermentation to facilitate their use for legume-based beverages—A review. *Compr Rev Food Sci Food Saf*, *21*(5), 4018–4055. DOI: 10.1111/1541-4337.13002
195. Roberts, D. D., Pollien, P., Antille, N., Lindinger, C., & Yeretizian, C. (2003). Comparison of Nosespace, Headspace, and Sensory Intensity Ratings for the Evaluation of Flavor Absorption by Fat. *J. Agric. Food Chem*, *51*(12), 3636–3642. DOI: 10.1021/jf026230+
196. Robinson, K. A., St-Jacques, A. D., Bakestani, I. D., Beavington, B. A. G., & Loewen, M. C. (2022). Pea and lentil 7S globulin crystal structures with comparative immunoglobulin epitope mapping. *Food Chemistry: Molecular Sciences*, *5*, 100146. DOI: 10.1016/j.fochms.2022.100146
197. Roland, W. S. U., Pouvreau, L., Curran, J., Van De Velde, F., & De Kok, P. M. T. (2017). Flavor Aspects of Pulse Ingredients. *Cereal Chem*, *94*(1), 58–65. DOI: 10.1094/CCHEM-06-16-0161-F

198. Rossi, A., Marti-Renom, M. A., & Sali, A. (2006). Localization of binding sites in protein structures by optimization of a composite scoring function. *Protein Sci*, 15(10), 2366–2380. DOI: 10.1110/ps.06224750
199. Sadeghi, R., Colle, M., & Smith, B. (2023). Protein composition of pulses and their protein isolates from different sources and in different isolation pH values using a reverse phase high performance liquid chromatography method. *Food Chem* 409, 135278. DOI: 10.1016/j.foodchem.2022.135278
200. Saffarionpour, S. (2024). Off-Flavors in Pulses and Grain Legumes and Processing Approaches for Controlling Flavor-Plant Protein Interaction: Application Prospects in Plant-Based Alternative Foods. *Food Bioproc Tech* 17(5), 1141–1182. DOI: 10.1007/s11947-023-03148-4
201. Saint-Eve, A., Déléris, I., Feron, G., Ibarra, D., Guichard, E., & Souchon, I. (2010). How trigeminal, taste and aroma perceptions are affected in mint-flavored carbonated beverages. *Food Qual Prefer*, 21(8), 1026–1033. DOI: 10.1016/j.foodqual.2010.05.021
202. Sánchez-López, J. A., Ziere, A., Martins, S. I. F. S., Zimmermann, R., & Yeretian, C. (2016). Persistence of aroma volatiles in the oral and nasal cavities: Real-time monitoring of decay rate in air exhaled through the nose and mouth. *J Breath Res*, 10(3), 036005. DOI: 10.1088/1752-7155/10/3/036005
203. Sandberg, A.-S. (2011). Developing functional ingredients: A case study of pea protein. In *Functional Foods* (pp. 358–382). Elsevier. DOI: 10.1533/9780857092557.3.358
204. Sarkar, A., Goh, K. K. T., & Singh, H. (2009). Colloidal stability and interactions of milk-protein-stabilized emulsions in an artificial saliva. *Food Hydrocol*, 23(5), 1270–1278. DOI: 10.1016/j.foodhyd.2008.09.008
205. Scatchard, G. (1949). The attractions of proteins for small molecules and ions. *Ann N Y Acad Sci*, 51(4), 660–672. DOI: 10.1111/j.1749-6632.1949.tb27297.x
206. Schieberle, P.; Grosch, W. (1992) Changes in the concentrations of potent crust odorants during storage of white bread. *Flavour Fragr. J*, 7, 213–218. DOI: 10.1002/ffj.2730070408
207. Schreuders, F. K. G., Dekkers, B. L., Bodnár, I., Erni, P., Boom, R. M., & Van Der Goot, A. J. (2019). Comparing structuring potential of pea and soy protein with gluten for meat analogue preparation. *J. Food Eng*, 261, 32–39. DOI: 10.1016/j.jfoodeng.2019.04.022
208. Schwartz, M., Neiers, F., Feron, G., & Canon, F. (2023). In-mouth metabolism of flavor compounds. In *Flavor* (pp. 87–101). Elsevier. DOI: 10.1016/B978-0-323-89903-1.00003-7
209. Semenova, M. G., Antipova, A. S., Belyakova, L. E., Polikarpov, Y. N., Wasserman, L. A., Misharina, T. A., Terenina, M. B., & Golovnya, R. V. (2002). Binding of aroma compounds with legumin. III. Thermodynamics of competitive binding of aroma compounds with 11S globulin depending on the structure of aroma compounds. *Food Hydrocol*, 16(6), 573–584. DOI: 10.1016/S0268-005X(02)00019-X
210. Seuvre, A. M., & Voilley, A. Physico-chemical interactions in the flavor-release process. In: Buettner A, ed. *Handbook of Odor*. Springer; 2017:273–302

References

211. Sha, L., & Xiong, Y. L. (2022). Comparative structural and emulsifying properties of ultrasound-treated pea (*Pisum sativum* L.) protein isolate and the legumin and vicillin fractions. *Food Res Inter*, *156*, 111179. DOI: 10.1016/j.foodres.2022.111179
212. Shen, H., Huang, M., Zhao, M., & Sun, W. (2019). Interactions of selected ketone flavours with porcine myofibrillar proteins: The role of molecular structure of flavour compounds. *Food Chem*, *298*, 125060. DOI: 10.1016/j.foodchem.2019.125060
213. Shrestha, S., Hag, L. V. T., Haritos, V. S., & Dhital, S. (2021). Lupin proteins: Structure, isolation and application. *Trends Food Sci Techn*, *116*, 928–939. DOI: 10.1016/j.tifs.2021.08.035
214. Singh, N. (2017). Pulses: An overview. *J Food Sci Tech*, *54*(4), 853–857. DOI: 10.1007/s13197-017-2537-4
215. Smith, R. L.; Waddell, W. J.; Cohen, S. M.; Fukushima, S.; Gooderham, N. J.; Hecht, S. S.; Marnett, L. J.; Porthogese, P. S.; Rietjens, I.; Adams, T. B.; Gavin, C. L.; McGowen, M. M.; Taylor, T. V. GRAS flavoring substances 25. *Food Techn*. 2011, *65*(7), 44–75.
216. Snel, S. J. E., Pascu, M., Bodnár, I., Avison, S., Van Der Goot, A. J., & Beyrer, M. (2023). Flavor-protein interactions for four plant protein isolates and whey protein isolate with aldehydes. *LWT*, *185*, 115177. DOI: 10.1016/j.lwt.2023.115177
217. Snel, S. J. E., Pascu, M., Bodnár, I., Avison, S., Van Der Goot, A. J., & Beyrer, M. (2023). Flavor-protein interactions for four plant proteins with ketones and esters. *Heliyon*, *9*(6), e16503. DOI: 10.1016/j.heliyon.2023.e16503
218. Sotriffer, C., Klebe, G. (2002). Identification and mapping of small-molecule binding sites in proteins: computational tools for structure-based drug design. *Il Farmaco*, *57*(3):243–51. DOI: 10.1016/s0014-827x(02)01211-9
219. Steinbeck, C., Han, Y., Kuhn, S., Horlacher, O., Luttmann, E., & Willighagen, E. (2003). The Chemistry Development Kit (CDK): An Open-Source Java Library for Chemo- and Bioinformatics. *J. Chem. Inf. Comput*, *43*(2), 493–500. DOI: 10.1021/ci025584y
220. Su, K., Brunet, M., Festrings, D., Ayed, C., Foster, T., & Fisk, I. (2021). Flavour distribution and release from gelatine-starch matrices. *Food Hydrocol*, *112*, 106273. DOI: 10.1016/j.foodhyd.2020.10627
221. Sulzer, P., Hartungen, E., Hanel, G., Feil, S., Winkler, K., Mutschlechner, P., Haidacher, S., Schottkowsky, R., Gunsch, D., Seehauser, H., Striednig, M., Jürschik, S., Breiev, K., Lanza, M., Herbig, J., Märk, L., Märk, T. D., & Jordan, A. (2014). A Proton Transfer Reaction-Quadrupole interface Time-Of-Flight Mass Spectrometer (PTR-QiTOF): High speed due to extreme sensitivity. *Int J Mass Spectr*, *368*, 1–5. DOI: 10.1016/j.ijms.2014.05.004
222. Sun, X., Yu, Y., Saleh, A. S. M., Akhtar, K. H., Li, W., Zhang, D., & Wang, Z. (2024). Conformational changes induced by selected flavor compounds from spices regulate the binding ability of myofibrillar proteins to aldehyde compounds. *Food Chem*, *451*, 139455. DOI: 10.1016/j.foodchem.2024.139455

223. Suppavorasatit, I., & Cadwallader, K. R. (2010). Flavor-Soy Protein Interactions. In K. R. Cadwallader & S. K. C. Chang (Eds.), ACS Symposium Series (Vol. 1059, pp. 339–359). *Am Chem Soc*. DOI: 10.1021/bk-2010-1059.ch021
224. Suppavorasatit, I., & Cadwallader, K. R. (2012). Effect of Enzymatic Deamidation of Soy Protein by Protein–Glutaminase on the Flavor-Binding Properties of the Protein under Aqueous Conditions. *J. Agric. Food Chem*, 60(32), 7817–7823. DOI:10.1021/jf301719k
225. Sushko, I., Novotarskyi, S., Körner, R., Pandey, A. K., Rupp, M., Teetz, W., Brandmaier, S., Abdelaziz, A., Prokopenko, V. V., Tanchuk, V. Y., Todeschini, R., Varnek, A., Marcou, G., Ertl, P., Potemkin, V., Grishina, M., Gasteiger, J., Schwab, C., Baskin, I. I., ... Tetko, I. V. (2011). Online chemical modeling environment (OCHEM): Web platform for data storage, model development and publishing of chemical information. *J. Comput. Aided Mol. Des*, 25(6), 533–554. DOI: 10.1007/s10822-011-9440-2
226. Tachibana, K., Fukazawa, A., Nishide, R., & Ohkawa, T. (2021). Estimation of important binding sites in compounds that interact with proteins. *Comput Biol Chem Journal*, 93, 107511. DOI: 10.1016/j.compbiolchem.2021.107511
227. Tan, Y., & Siebert, K. J. (2008). Modeling Bovine Serum Albumin Binding of Flavor Compounds (Alcohols, Aldehydes, Esters, and Ketones) as a Function of Molecular Properties. *J Food Sci*, 73(1). DOI: 10.1111/j.1750-3841.2007.00591.x
228. Temthawee, W., Panya, A., Cadwallader, K. R., & Suppavorasatit, I. (2020). Flavor binding property of coconut protein affected by protein-glutaminase: Vanillin-coconut protein model. *LWT*, 130, 109676. DOI:10.1016/j.lwt.2020.109676
229. The Good Scents Company Information System. <https://www.thegoodscentscompany.com>
230. The Human Metabolome Database. <https://hmdb.ca>
231. Thissen, J.A. (1982). Interaction of off-flavor compounds with soy protein isolate in aqueous systems: Effects of chain length functional group and temperature. M.S. Thesis. Iowa State University Library, Ames.
232. Tiong, A. Y. J., Crawford, S., Jones, N. C., McKinley, G. H., Batchelor, W., & Van T Hag, L. (2024). Pea and soy protein isolate fractal gels: The role of protein composition, structure and solubility on their gelation behaviour. *Food Struct*, 40, 100374. DOI: 10.1016/j.foostr.2024.100374
233. Toppur, B., & Jaims, K. J. (2021a). Determining the best set of molecular descriptors for a Toxicity classification problem. *RAIRO - Oper. Res*, 55(5), 2769–2783. DOI: 10.1051/ro/2021134
234. Tromelin, A., & Guichard, E. (2004). 2D- and 3D-QSAR Models of Interaction between Flavor Compounds and beta-Lactoglobulin Using Catalyst and Cerius2. *QSAR Comb Sci*, 23(4), 214–233. DOI: 10.1002/qsar.200430859
235. Tulbek, M. C., Lam, R. S. H., Wang, Y. (C.), Asavajaru, P., & Lam, A. (2017). Pea. In *Sustainable Protein Sources* (pp. 145–164). Elsevier. DOI: 10.1016/B978-0-12-802778-3.00009-3

References

236. Tyapkova, O., Siefarth, C., Schweiggert-Weisz, U., Beauchamp, J., Buettner, A., Bader-Mittermaier, S. (2016). Flavor release from sugar-containing and sugar-free confectionary egg albumen foams *LWT-Food Sci Technol*, 69, 538-545. DOI:10.1016/j.lwt.2016.01.075
237. UniProtKB/Swiss-Prot Protein Database. <https://www.uniprot.org/uniprot> otkb
238. Utz, F., Spaccasassi, A., Kreissl, J., Stark, T. D., Tanger, C., Kulozik, U., Hofmann, T., & Dawid, C. (2022). Sensomics-Assisted Aroma Decoding of Pea Protein Isolates (*Pisum sativum* L.). *Foods*, 11(3), 412. DOI: 10.3390/foods11030412
239. Vainio, M. J., & Johnson, M. S. (2007). Generating Conformer Ensembles Using a Multiobjective Genetic Algorithm. *J. Chem. Inf. Model*, 47(6), 2462-2474. DOI: 10.1021/ci6005646
240. Van Eck, A., Pedrotti, M., Brouwer, R., Supamong, A., Fogliano, V., Scholten, E., Biasioli, F., & Stieger, M. (2021). *In Vivo* Aroma Release and Dynamic Sensory Perception of Composite Foods. *J. Agric. Food Chem*, 69(35), 10260-10271. DOI: 10.1021/acs.jafc.1c02649
241. Van Ruth, S. M., Grossmann, I., Geary, M., & Delahunty, C. M. (2001). Interactions between Artificial Saliva and 20 Aroma Compounds in Water and Oil Model Systems. *J. Agric. Food Chem*, 49(5), 2409-2413. DOI: 10.1021/jf001510f
242. Verfaillie, D., Janssen, F., Van Royen, G., & Wouters, A. G. B. (2023). A systematic study of the impact of the isoelectric precipitation process on the physical properties and protein composition of soy protein isolates. *Food Res Int*, 163, 112177. DOI: 10.1016/j.foodres.2022.112177
243. Vingerhoeds, M. H., Blijdenstein, T. B. J., Zoet, F. D., & Van Aken, G. A. (2005). Emulsion flocculation induced by saliva and mucin. *Food Hydrocol*, 19(5), 915-922. DOI:10.1016/j.foodhyd.2004.12.005
244. Viry, O., Boom, R., Avison, S., Pascu, M., & Bodnár, I. (2018). A predictive model for flavor partitioning and protein-flavor interactions in fat-free dairy protein solutions. *Food Res Int*, 109, 52-58. DOI:10.1016/j.foodres.2018.04.013
245. Wang, B., Zhang, Q., Zhang, N., Bak, K. H., Soladoye, O. P., Aluko, R. E., Fu, Y., & Zhang, Y. (2021). Insights into formation, detection and removal of the beany flavor in soybean protein. *Trends Food Sci Technol*, 112, 336-347. DOI: 10.1016/j.tifs.2021.04.018
246. Wang, K., & Arntfield, S. D. (2014). Binding of carbonyl flavours to canola, pea and wheat proteins using GC/MS approach. *Food Chem*, 157, 364-372. DOI: 10.1016/j.foodchem.2014.02.042
247. Wang, K., & Arntfield, S. D. (2015). Binding of selected volatile flavour mixture to salt-extracted canola and pea proteins and effect of heat treatment on flavour binding. *Food Hydrocol*, 43, 410-417. DOI: 10.1016/j.foodhyd.2014.06.011
248. Wang, K., & Arntfield, S. D. (2017). Effect of protein-flavour binding on flavour delivery and protein functional properties: A special emphasis on plant-based proteins. *Flavour Fragr J*, 32(2), 92-101. DOI: 10.1002/ffj.3365
249. Wang, N., Ma, Z., Ma, L., Zhang, Y., Zhang, K., Ban, Q., & Wang, X. (2023). Synergistic modification of structural and functional characteristics of whey protein isolate by soybean

- isoflavones non-covalent binding and succinylation treatment: A focus on emulsion stability. *Food Hydrocol*, *144*, 108994. DOI: 10.1016/j.foodhyd.2023.108994
250. Wang, Y., Tuccillo, F., Niklander, K., Livi, G., Siitonen, A., Pöri, P., Edelmann, M., Sawadogo-Lingani, H., Maina, N. H., Jouppila, K., Lampi, A.-M., Sandell, M., Piironen, V., Honkapää, K., Sözer, N., Coda, R., Knaapila, A., & Katina, K. (2024). Masking off-flavors of faba bean protein concentrate and extrudate: The role of in situ and in vitro produced dextran. *Food Hydrocol*, *150*, 109692. DOI: 10.1016/j.foodhyd.2023.109692
251. Wang, Q., & Ismail, B. (2012). Effect of Maillard-induced glycosylation on the nutritional quality, solubility, thermal stability and molecular configuration of whey protein. *Int Dairy J*, *25*(2), 112–122. DOI: 10.1016/j.idairyj.2012.02.009
252. Weel, K. G. Release and perception of aroma compounds during consumption. Ph.D. Dissertation, Wageningen University and Research, Wageningen, The Netherlands, 2004. <https://edepot.wur.nl/121557>
253. Weerawatanakorn, M., Wu, J.-C., Pan, M.-H., & Ho, C.-T. (2015). Reactivity and stability of selected flavor compounds. *J Food Drug Anal*, *23*(2), 176–190. DOI: 10.1016/j.jfda.2015.02.001
254. Wei, M., Liu, X., Xie, P., Han, A., Lei, Y., Yang, X., Liu, Y., Zhang, S., & Sun, B. (2024). Investigating the interactions between selected heterocyclic flavor compounds and beef myofibrillar proteins using SPME-GC-MS, spectroscopic, and molecular docking approaches. *J Mol Liq* *403*, 124878. DOI: 10.1016/j.molliq.2024.124878
255. Weterings, M., Bodnár, I., Boom, R. M., & Beyrer, M. (2020). A classification scheme for interfacial mass transfer and the kinetics of aroma release. *Trends Food Sci Technol*, *105*, 433–448. DOI: 10.1016/j.tifs.2019.04.012
256. Williams, J. E., Duncan, S. E., Williams, R. C., Mallikarjunan, K., Eigel, W. N., & O'Keefe, S. F. (2006). Flavor Fade in Peanuts During Short-term Storage. *J Food Sci*, *71*(3), S265–S269. DOI: 10.1111/j.1365-2621.2006.tb15652.x
257. Wishart, D. S., Guo, A., Oler, E., Wang, F., Anjum, A., Peters, H., Dizon, R., Sayeeda, Z., Tian, S., Lee, B. L., Berjanskii, M., Mah, R., Yamamoto, M., Jovel, J., Torres-Calzada, C., Hiebert-Giesbrecht, M., Lui, V. W., Varshavi, D., Varshavi, D., ... Gautam, V. (2022). HMDB 5.0: The Human Metabolome Database for 2022. *Nucleic Acids Res*, *50*(D1), D622–D631. DOI: 10.1093/nar/gkab1062
258. Wongprasert, T., Mathatheeran, P., Chen, X., Vilaivan, T., Suriya, U., Rungrotmongkol, T., & Supparasatit, I. (2024). Molecular interactions by thermodynamic and computational molecular docking simulations of selected strawberry esters and pea protein isolate in an aqueous model system. *LWT*, *198*, 115964. DOI:10.1016/j.lwt.2024.115964
259. Wu, G., Mao, R., Zhang, Y., Zhu, L., Karrar, E., Zhang, H., Jin, Q., & Wang, X. (2022). Study on the interaction mechanism of virgin olive oil polyphenols with mucin and α -amylase. *Food Bioscience*, *47*, 101673. DOI: 10.1016/j.fbio.2022.101673
260. Xiang, L., Jiang, B., Xiong, Y. L., Zhou, L., Zhong, F., Zhang, R., Bin Tahir, A., & Xiao, Z. (2023). Beany flavor in pea protein: Recent advances in formation mechanism, analytical

References

- techniques and microbial fermentation mitigation strategies. *Food Biosci*, *56*, 103166. DOI: 10.1016/j.fbio.2023.103166
261. Yang, J., De Wit, A., Diedericks, C. F., Venema, P., Van Der Linden, E., & Sagis, L. M. C. (2022). Foaming and emulsifying properties of extensively and mildly extracted Bambara groundnut proteins: A comparison of legumin, vicilin and albumin protein. *Food Hydrocol* *123*, 107190. DOI: 10.1016/j.foodhyd.2021.107190
262. Yang, N., Yang, Q., Chen, J., & Fisk, I. (2021). Impact of capsaicin on aroma release and perception from flavoured solutions. *LWT*, *138*, 110613. DOI: 10.1016/j.lwt.2020.110613
263. Ye, J., Li, A., Zheng, H., Yang, B., & Lu, Y. (2023). Machine Learning Advances in Predicting Peptide/Protein-Protein Interactions Based on Sequence Information for Lead Peptides Discovery. *Adv Biol*, *7*(6), 2200232. DOI: 10.1002/adbi.202200232
264. Yeo, H., Linforth, R., MacNaughtan, W., Williams, H., Hewson, L., & Fisk, I. D. (2023). Effect of sweeteners and carbonation on aroma partitioning and release in beverage systems. *Food Res Int* *164*, 112373. DOI: 10.1016/j.foodres.2022.112373
265. Yilmaz, H., Lee, S., & Chronakis, I. S. (2021). Interactions of β -Lactoglobulin with Bovine Submaxillary Mucin vs. Porcine Gastric Mucin: The Role of Hydrophobic and Hydrophilic Residues as Studied by Fluorescence Spectroscopy. *Mol*, *26*(22), 6799. DOI:10.3390/molecules26226799
266. Yoshizawa T, Shimizu T, Taichi M, et al. Crystal structure of basic 7S globulin from soybean. RCSB, PDB 183584, 3AUP; 2011. DOI: 10.2210/pdb3A UP/pdb
267. Zhang, B., Peng, J., Pan, L., & Tu, K. (2023). A novel insight into the binding behavior between soy protein and homologous ketones: Perspective from steric effect. *J. Mol. Liq*, *369*, 120895. DOI: 10.1016/j.molliq.2022.120895
268. Zahari, I., Ferawati, F., Helstad, A., Ahlström, C., Östbring, K., Rayner, M., & Purhagen, J. K. (2020). Development of High-Moisture Meat Analogues with Hemp and Soy Protein Using Extrusion Cooking. *Foods*, *9*(6), 772. DOI: 10.3390/foods9060772
269. Zhang, H., Yu, D., Sun, J., Guo, H., Ding, Q., Liu, R., & Ren, F. (2014). Interaction of milk whey protein with common phenolic acids. *J Mol Str*, *1058*, 228–233. DOI: 10.1016/j.molstruc.2013.11.009
270. Zhao, J., Cao, Y., & Zhang, L. (2020). Exploring the computational methods for protein-ligand binding site prediction. *Comput Struct Biotechnol J*, *18*, 417–426. DOI: 10.1016/j.csbj.2020.02.008
271. Zheng, Y., Tian, J., Yang, W., Chen, S., Liu, D., Fang, H., Zhang, H., & Ye, X. (2020). Inhibition mechanism of ferulic acid against α -amylase and α -glucosidase. *Food Chem*, *317*, 126346. DOI: 10.1016/j.foodchem.2020.126346
272. Zhou, Q., & Cadwallader, K. R. (2006). Effect of Flavor Compound Chemical Structure and Environmental Relative Humidity on the Binding of Volatile Flavor Compounds to Dehydrated Soy Protein Isolates. *J. Agric. Food Chem*, *54*(5), 1838–1843. DOI: 10.1021/jf052269d



Summary

Background and objective:

Over the last few years, plant protein-based foods have encroached on meat and dairy products as consumers switch to a more plant-based diet. Notably, pulses are gaining popularity when used in innovative food products, *e.g.*, vegan and vegetarian products, as they are an excellent source of protein. However, off-flavors reduce the consumer acceptability of such products. To tackle this issue, flavor compounds are added. However, these flavors bind (reversibly or irreversibly) to the protein, affecting their release. To address this, it is crucial to understand the interaction between plant proteins and flavor compounds. The research described in this thesis aims to investigate the effects of the structural and physicochemical properties of flavors and the protein source on the protein-flavor binding mechanism and the sensory perception of flavored plant-based aqueous model systems.

Methods:

Aqueous model systems were prepared by combining one flavor compound (*i.e.*, hydrophobic or hydrophilic) with one protein isolate (*i.e.*, plant or animal protein). Protein-flavor binding was examined using GC-MS. Commercial protein isolate (PI) characteristics, including fat content, hydrophobicity, particle size, ζ -potential, and polydispersity, were determined using spectrofluorimetric and NMR technology. Sensory perception was assessed using dynamic sensory profiling (Time Intensity), and *in vivo* aroma release was determined using Proton Transfer Reaction Mass Spectrometry (PTR-MS). The subjects who participated in the studies were young, European, allergy-free female adults. Saliva flow and oral cavity capacity were measured by the spitting method.

Results:

This Ph.D. thesis demonstrated the binding effect of protein isolates (PI) to flavor compounds using HS-GC-MS (**Chapters 3-5**), indicated by a clear reduction of the headspace (HS). Protein-flavor binding primarily depends on the flavor compound and is secondary to the protein source (**Chapter 3**). Changing protein sources had a minor effect on the protein-flavor binding mechanism,

whereas substantial differences in flavor binding were observed due to the flavor's physicochemical and structural properties. Flavor binding increased with the flavor's chain length and hydrophobicity. The change in the flavor's spatial configuration from spherical to linear-shaped and the displacement of the carbonyl group from the inner part of the molecule toward the edge led to a significant binding increase from 13.73-18.19% to 52.76-54.60% (**Chapter 3**). Steric hindrance and molecular rigidity seem to be the responsible underlying mechanisms. Beyond hydrophobicity, topological, electronic, and geometrical descriptors complementarily contribute to the observed protein-flavor binding (**Chapter 4**). Only 28 of the initial 328 descriptors consistently outperformed randomized data, indicating a relationship with protein-flavor binding linked to flavor structure and physicochemical properties. The Random Forest model constructed showed a strong correlation between predicted and experimental values ($Q^2=0.93$) for flavor compounds outside the training set and a high predictive ability for the validation of flavor compounds ($Q^2=0.88$) (**Chapter 4**). Results suggested a linear relationship between food proteins and flavors, where binding affinity (K) increased with the flavor chain length, and binding sites (n) ranged from $n=0.021$ to 7.194 (**Chapter 5**). When adding mucin (0.01(w/v)%) to flavored protein-based aqueous model systems, flavor binding increased up to fifteen times in protein-ketone-mucin-based systems and up to three times in protein-aldehyde-mucin-based systems. As the chain length increases, the hydrophobicity also increases, reducing the impact of mucin addition. Further increases in mucin concentration (0.1(w/v)%) increased flavor binding up to ten times (**Chapter 5**). In brief, 0.01(w/v)% of mucin appears insufficient to cover the surface of the food protein adequately. Nevertheless, there is potential for inducing structural alterations that may lead to unfolding the 3D food protein structure, thereby enhancing flavor binding. At higher mucin levels, mucin may effectively cover the binding sites, leading to the clustering of mucin molecules. Under in-mouth conditions, protein-flavor binding still remains, as shown by a decrease of the maximum perceived intensity (I_{\max}) by 30.91%, 72.41%, and 36.84% after the inclusion of the protein in hexanal, nonanal, and 2-nonanone aqueous model systems. Increasing the chain length and relocating the keto group

from the middle to the edge of the molecule led to a significant decrease in I_{max} by 71.92% and 72.25%, respectively (**Chapter 6**). Upon adding lupin protein to flavored aqueous model systems, sensory perception decreased by 11.05%. These results suggested that adding the protein hindered the perceived intensity given by the flavor compound.

Conclusions:

Protein-flavor binding primarily depends on the flavor's physicochemical properties and structural features. Changes in the flavor compound rather than the protein source can mainly control protein-flavor binding affinity. If binding is undesired, we suggest choosing spherical-shaped, short-chain length, hydrophilic, and saturated flavor compounds with the functional group located in the middle of the structure. Food sensory perception is complex, and interactions between protein, flavor compounds, and salivary proteins (mucin) in the mouth imply a significant change in sensory perception. These results can be particularly interesting when designing environmentally friendly foods and adjusting flavor mixtures for optimal recipes.



Resumen

Contexto y objetivo:

En los últimos años, los alimentos a base de proteínas vegetales están ganando terreno frente a la carne y los productos lácteos, a medida que los consumidores adoptan una dieta más basada en plantas. En particular, las legumbres están cobrando fuerza cuando se utilizan en productos alimenticios innovadores, como productos veganos y vegetarianos, ya que son una excelente fuente de proteínas. Sin embargo, los aromas desagradables, presentes o producidos posteriormente, reducen la aceptabilidad de esos productos por los consumidores. Para hacer frente a este problema, los científicos añaden compuestos saborizantes. Sin embargo, los compuestos saborizantes se unen (reversible o irreversiblemente) a la proteína, afectando su liberación. Para abordar esta cuestión, es crucial comprender la interacción entre proteínas vegetales y compuestos saborizantes. La investigación descrita en esta tesis tiene como objetivo investigar los efectos de las propiedades estructurales y fisicoquímicas de los compuestos saborizantes y la fuente de proteínas en el mecanismo de interacción de proteína-compuestos saborizantes y la percepción sensorial de sistemas basados en proteínas de origen vegetal y compuestos saborizantes.

Métodos:

Se prepararon sistemas acuosos modelo mediante la combinación de un compuesto saborizante (hidrofóbico o hidrofílico) junto con un aislado de proteína (de origen animal o vegetal). Se examinó la interacción de proteínas y compuestos saborizantes utilizando espectrometría de masas (GC-MS). Las características de las proteínas aisladas comerciales (PI), incluyendo el contenido de grasa, la hidrofobicidad, el tamaño de las partículas, el potencial ζ y la poli-dispersidad, fueron determinadas por la tecnología espectrofluorimétrica y la tecnología NMR, respectivamente. Se evaluó la percepción sensorial utilizando el perfil sensorial dinámico (intensidad del tiempo) y se determinó la liberación en vivo de aroma utilizando la espectrometría de masa de la reacción de transferencia de protones (PTR-MS). Los sujetos que participaron en los estudios fueron mujeres jóvenes de

origen europeo sin alergias. Se midió el flujo de saliva y la capacidad de la cavidad oral mediante el método de propulsión de la saliva.

Resultados:

Esta tesis de doctorado demostró el efecto de interacción de proteínas aisladas de origen vegetal y animal en sistemas acuosos modelo a través de una reducción clara del espacio de cabeza (**Capítulos 3-5**). La interacción de la proteína a los compuestos saborizantes depende principalmente del tipo de compuesto saborizante y es secundaria a la fuente de proteína (**Capítulo 3**). El cambio de fuentes de proteínas tuvo un efecto menor en el mecanismo de interacción proteína-compuestos saborizante, mientras que se observaron diferencias sustanciales en la interacción de compuestos saborizantes dependiendo de sus propiedades fisicoquímicas y estructurales. La interacción de los compuestos saborizantes aumentó con la longitud de la cadena y la hidrofobicidad. El cambio de la configuración espacial del compuesto saborizante de esférica a lineal, el desplazamiento del grupo carbonilo desde la parte interna de la molécula hacia el borde y la insaturación molecular condujeron a un aumento significativo de la interacción de 13.73-18.19 a 52.76-54.60% (**Capítulo 3**). La obstrucción estérica y la rigidez molecular parecen ser los mecanismos subyacentes responsables. Más allá de la hidrofobicidad, los descriptores topológicos, electrónicos y geométricos contribuyen complementariamente a la interacción de proteínas y compuestos saborizantes (**Capítulo 4**). Solo 28 de los 328 descriptores iniciales superaron consistentemente los datos aleatorios, lo que indica una relación con la interacción de proteínas y compuestos saborizantes vinculada a la estructura del compuesto saborizante y las propiedades fisicoquímicas. El modelo construido mostró una fuerte correlación entre los valores predichos y experimentales ($Q^2=0.93$) para los compuestos saborizantes fuera del conjunto de entrenamiento y una alta capacidad predictiva para la validación de los compuestos saborizantes ($Q^2=0.88$) (**Capítulo 4**). Los resultados sugirieron una relación lineal entre las proteínas alimentarias y los compuestos saborizantes, donde la afinidad de interacción (K) aumentó con la longitud de la cadena del compuesto saborizante, y los sitios de interacción de proteínas (n)

variaron de $n = 0.021$ a 7.194 (**Capítulo 5**). Cuando se añadió la proteína de la saliva (mucina $0.01(w/v)\%$) a los sistemas acuosos modelo a base de proteína y compuestos saborizantes, la interacción de los compuestos saborizantes aumentó hasta quince veces en los sistemas basados en proteína-cetona-mucina y hasta tres veces en los sistemas acuosos modelo en proteínas-aldehído-mucina. A medida que aumenta la longitud de la cadena, también aumenta la hidrofobicidad, reduciendo el impacto de la adición de mucina. Un aumento adicional de la concentración de mucina $0.1(w/v)\%$ aumentó la interacción de los compuestos saborizantes hasta diez veces (**Capítulo 5**). En resumen, $0.01(w/v)\%$ de mucina parece insuficiente para cubrir adecuadamente la superficie de la proteína. Sin embargo, existe el potencial para inducir alteraciones estructurales que pueden conducir al despliegue de la estructura 3D de la proteína alimentaria, favoreciendo así la interacción de los compuestos saborizantes. A niveles más altos de mucina, esta puede cubrir eficazmente los sitios de interacción, lo que conduce al agrupamiento de estas moléculas. Durante el procesamiento de alientos y bajo condiciones orales, la interacción de proteínas con compuestos saborizantes sigue existiendo, como lo demuestra una disminución de la intensidad máxima en 30.91% , 72.41% , y 36.84% tras la inclusión de la proteína. El aumento de la longitud de la cadena y el desplazamiento del grupo carbonilo del centro al extremo de la molécula llevaron a una reducción significativa de 71.92 y 72.25% , respectivamente (**Capítulo 6**). La percepción sensorial de los sistemas acuosos modelo basados disminuyó en un 11.05% tras la adición de la proteína del algarrobo. Estos resultados sugieren que la adición de la proteína ha impedido la intensidad percibida del compuesto saborizante.

Conclusiones:

La interacción entre proteínas y compuestos saborizantes depende principalmente de las propiedades fisicoquímicas y de las características estructurales de los compuestos saborizantes. Los cambios en el tipo de compuesto saborizante, en lugar de la fuente de proteína, pueden controlar principalmente la afinidad de interacción entre proteínas y compuestos saborizantes. Si la interacción es indeseable, sugerimos elegir compuestos de

forma esférica, de longitud de cadena corta, hidrofílicos y saturados, con el grupo funcional ubicado en el centro de la estructura. La percepción sensorial de los alimentos es compleja, y las interacciones entre las proteínas, los compuestos saborizantes y las proteínas salivales (mucina) en la boca implican un cambio significativo en la percepción sensorial. Estos resultados pueden ser particularmente interesantes al diseñar alimentos respetuosos con el medio ambiente y ajustar las mezclas de compuestos saborizantes para una receta óptima.



Appendices

Acknowledgments

List of publications

Overview of completed training
activities

About the author

Failure is often a stepping stone towards success.

Thomas Edison.

Four years condensed into 241 pages... What a journey it has been! It is incredible to think how it all began 8 years ago. Back then, I decided to seek an international experience, step out of my comfort zone, and journey to Wageningen for what I thought would be a brief stay. Yet, here I am, 8 years later, with a PhD in hand! This achievement is not mine alone; it is the dedication and commitment of those around me that have made a difference. I am deeply grateful for the unwavering encouragement and guidance I have received throughout this journey. Your assistance has helped me reach this milestone and shaped who I am today.

I have no words to express my gratitude and endless admiration for the core people involved in this Ph.D project. First, to my dear and daily supervisor, **Teresa Oliviero**. This would not have been possible without you. Thanks for always believing in me, even when I doubted about myself. Thanks for embracing my vulnerability and being always there for me in every single "crisis" I had. I am forever thankful. **Sara I.F.S. Martins**, you taught me to voice myself out and take that leap. You are a clear example of a strong woman who can achieve the feat she committed to. Thanks for encouraging me to be the best version of myself. To my dear promotor, **Vincenzo Fogliano**, grazie mille! Thanks for your seemingly endless energy, persistent availability, approachability, and the helicopter view offered at all times.

Aside from the core team, I would like to express my sincere gratitude to the scientific advisors who played a crucial role in this Ph.D. project. **Catrienus de Jong**, your guidance, expertise in flavor, and ability to make science enjoyable have been invaluable. **Michele Pedrotti**, your support, Ph.D. tips, and (giant!) patience with the PTR-ToF-MS data handling is priceless. **Hans-Gerd Janssen**, your exceptional knowledge has been a great help during this journey. Thank you for the unique opportunity to work and conduct my experiments at Unilever, a turning point in my Ph.D.

Nothing could have been the same without all the FQDders: **Corine, Kimberley,** and **Lisa**; thank you for the countless help, guidance, and support throughout my Ph.D.! **Shiksha**, thank you for making FQD a home just right after I landed in NL. **Pieter**, thank you for being my buddy and introducing me to FQD. **Marianna**, thank you for being the best hotel roommate I could imagine during the PhD trip to Spain; I admire your constant passion for life. All the FQDers: **Annelies, Arianne, Arnau, Bei, Ebru, Edoardo, Erik, Fabiola, Fleur, Jelle, Jiaying, Julie, Kasper, Keching, Laura, Luc, Luigi, Marialena, Marjanne, Momo, Qing², Ruth, Swantje, Tomer, Xiagnan, Yajing, Yifan², Zekun, Zongyao**. Thanks for making me feel like I am always at home in FQD. Each of you has a beautiful soul! **Lise, Tijana,** and **Sara**, it was a real pleasure to bond together during the Mexico trip and share meals, evenings, and fun. **Josep**, thank you for the brilliant idea of the Spanish mafia group, where we shared food, (many) coffees, and a great karaoke night! **Rutger** and **Andrea**, thank you for agreeing and joining me in the adventure of the “PTR-MS ecosystem,” where we shared tips, dramas, and wisdom.

Thanks to my office mates for your daily encouragement and smiles: **Juliana, Eda, Lucas, Melania, Thisun, Seren,** and **Siwei**. Thanks for all the fun, talks, city trips, shared BBQs, parties, and dinners we enjoyed. Thanks for making every single day worth it. Thanks for the joy and happiness you, all seven, brought into my life. **Thisun**, I am especially grateful for your steadfast encouragement and your constant concern about my mental well-being. Thank you for always being there for me and for accepting to be my paranymph. I am endlessly thankful for our friendship. **Seren**, my Mexican buddy, friend, and paranymph, you shine with your unique and captivating personality. Your support has been immeasurable. I truly value every moment we have shared.

Although, not PhD FQDer, but also FQDer, **Elisa**, not only mi sport and clay partner but my yellow person. Amiga, llena de pasión, energía y admiración por la vida. Eres un diamante en bruto. No tengo palabras para expresar que feliz soy de haberte encontrado, conocido y contar contigo en mi vida!. And last but not least, mi querida y gran amiga **Diana**, lo conseguimos, lo hicimos! y gran parte esto es gracias a ti. Por jamás juzgarme, por darme tu apoyo incondicional y ser mi



psicóloga a tiempo parcial. Por animarme cada día a superarme y a no tirar la toalla.

Thanks to all my supervised students (**Elianne, Benjamin, Shengying, Amber, Pol, Sarp, Timothy, and Ishaan**). I hope you all learned a bit from me and the passionate domain of flavors. I want to especially thank **Emma**, whom we learned together about saliva but became friends after all. Thanks for being such a source of energy at all times.

Outside FQD, but still *Wageningers*: **Gerard** gracias por haberme entendido siempre, por tu empatía y comprensión incluso cuando ni yo misma me encontraba, por animarme a amar la ciencia hasta en su versión más amarga. Gracias por haberte unido al reto de la media maratón...Lo conseguimos! y por el maravilloso viaje en carretera desde Madrid a Wageningen. **María**, por ser luz y terremoto en la versión más plena y verdadera, por ver el vaso siempre medio lleno y por darme esa mano amiga siempre que lo he necesitado. **Anne** gracias por ser fuente de inspiración, y por siempre darme tu enfoque pragmático de la vida. **Raagvendra**, what can I tell you housemate? thanks accepting being my housemate by 2022. I really appreciate all the life moments and tons of funny anecdotes we have lived together. EMFS girls, **Christel, Elise, and Aadi** thank you for continuously walking by my side after EMFS. Thanks for making this PhD journey more lightful.

Nevertheless, this adventure is also possible thanks to all Unilever people, especially the analytical group: **Oscar, Herreld, Ed, Krishna, and Wilma**. Thanks, **Boudewijn**, for the excellent collaboration, the long discussions, and the enriching brainstorming sessions. Gracias, **Luis y Braulio** por cada rato que pasamos bebiendo café y riendo sobre la vida y sus caprichos. **Karina**, sino te lo dije, te admiro mucho! Gracias por no solo compartir flavor knowledge pero también por la valentía que te caracteriza. Of course, I would like to thank **Kees** especially. Thank you for including me in the running group with **Remko, Alice, Julien, Mus et al**. Thanks for all the joyful moments we have had during sports.

Por supuesto, como mi corazón ha estado dividido en todo momento entre España y Holanda, gracias a mis tres ángeles de la guardia: **Lau, Celia e Isa!** Gracias chicas por confiar en mí sin importar como, dónde y cuando, por darme esa energía para continuar y por vuestro amor cada día. Gracias **Laura** por diseñar la portada de esta tesis, y plasmar juntas la amistad y el conocimiento en una obra de arte. Gracias **Manu** por haber aparecido en la última etapa de mi doctorado y haberme dado esa paz y amor para terminar. Por seguir sumando juntos.

Y por último a las personas más importantes de mi vida: **Mama, papa, Javito y Pablete...** Gracias por vuestro apoyo y amor incondicional. Sin vosotros nada de esto hubiera sido posible. Gracias por guiarme y apoyarme en cada decisión tomada. Gracias por ser mi referencia a seguir. Os quiero familia. Y esto también va dedicado a mis **yayos**, porque sé lo orgullosos que estarían. Siempre de una estrella a otra estrella.

I am thrilled and pleased to have spent this wonderful journey with all of you!

And for all the readers...I hope you will enrich your life with flavorful moments!

Wageningen, 21st of October, 2024

Porque me di la oportunidad de intentarlo, porque lo hice, porque dejé todo atrás para perseguirlo...y lo logré!





List of Publications

1. Pérez, C. B.; Oliviero, T.; Fogliano, V.; Janssen, H. G.; Martins, S. I. F. S. Flavor them up! Exploring the challenges of flavored plant-based foods. *Flavor Fragr. J.* **2023**, *38*(3), 125-134. DOI: 10.1002/ffj.3734
2. Barallat-Pérez, C. B.; Janssen, H. G.; Martins, S.; Fogliano, V.; Oliviero, T. Unraveling the role of flavor structure and physicochemical properties in the binding phenomena with commercial food protein isolates. *J Agric Food Chem.* **2023**, *71*, 50, 20274-20284. DOI: 10.1021/acs.jafc.3c05991
3. Barallat-Pérez, C.; Pedrotti, M.; Oliviero, T.; Martins, S.; Fogliano, V.; de Jong, C. Drivers of the In-Mouth Interaction between Lupin Protein Isolate and Selected Aroma Compounds: A Proton Transfer Reaction-Mass Spectrometry and Dynamic Time Intensity Analysis. *J Agric Food Chem.* **2024**. DOI: 10.1021/acs.jafc.3c08819



Overview of completed training activities

Discipline-specific activities

Sensory Perception and Food Preference, VLAG, WUR (NL).	2021
Conference: 16 th edition Weurman Flavour Research Symposium, INRAE, Online (FR).	2021
Plant-based foods research conference, Bridge2Foods, Online (NL).	2021
Conference: Challenges in Food Flavors Volatilomics, Poznan (PL).	2022
Conference: Workshop in Food flavors and Plant proteins, Montreux (CH).	2022
Meeting series: Unilever Flavor Learning Initiative, Wageningen (NL).	2022
Meeting series: Unilever Strictly Science, Wageningen (NL).	2022
Conference: 13 th Wartburg Symposium, Eisenach (DE).	2023
Chemometrics, Multivariate Analysis, VLAG, WUR (NL).	2023
Conference: 17 th edition Weurman Flavour Research Symposium, WUR (NL).	2024
Conference: 3 rd conference on Science and Technology for Meat and Dairy Analogues, WUR (NL).	2024

General courses

Research Data Management Course, VLAG, WUR (NL).	2021
Webinar: How to present online? VLAG, WUR (NL).	2021
The Essentials of Scientific Writing & Presenting, VLAG, WUR (NL).	2021
An Introduction to LaTeX, VLAG, WUR (NL).	2021

Introduction to R, VLAG, WUR (NL).	2021
Stress Identification and Management, VLAG, WUR (NL).	2022
Basic Statistics, VLAG, WUR (NL).	2023
Applied statistics, VLAG, WUR (NL).	2023

Assisting in teaching and supervision activities

Thesis supervision of 3 BSc and 6 MSc students, VLAG, WUR (NL).	2020-2024
FQD - Food Flavour Design 37806 Practical, WUR (NL).	2020-2024

Other activities

Preparation of Research Proposal, WUR (NL).	2020
PhD Study Trip Organization	2021-2022
FQD Lunch with Champions, WUR (NL).	2020-2024
FQD Student Colloquia, WUR (NL).	2020-2024
PhD Study Trip to Spain	2022
PhD Study Trip to Mexico	2024

Awards

2020 GIRACT's European Ph.D. in Flavor Research Award for Ph.D. project research proposal.



About the author

About the author

Cristina Barallat Pérez was born in Madrid (Spain) on the 21st of September 1994. In 2012, she started her undergraduate professional degree with a Food Science and Technology Bachelor at the Complutense University of Madrid and finished by 2016. Her bachelor's thesis was conducted at the CSIC-ICTAN, where she focused on developing healthier meat food products by replacing saturated lipids with vegetable oils.



In a bid to move abroad, she moved to Wageningen (The Netherlands), where she conducted an ERASMUS+ internship at the Microbial Ecology Group at the Laboratory of Microbiology (2016-2017).

She then joined the European Master in Food Studies at Wageningen University & Research, combining her passion for food science and traveling, and thus studied at four leading universities across Europe in Food Technology (University College of Cork, AgroParistech, and Lund University) alongside Wageningen University & Research (2017-2019). During her MSc thesis and internship, she moved to Geneva (Switzerland) and worked for nine months at DSM-Firmenich, focusing on flavor release and retention of meat alternatives. This experience made her enthusiastic about flavor science, encouraging her to move to Zürich (Switzerland). She kept learning about flavor at Givaudan, where she worked with citrus beverages and their flavor profile (2019-2020).

In August 2020, she moved back to Wageningen University & Research to start her Ph.D. at the Department of Food Quality and Design in collaboration with Unilever. Her project aimed to unveil the key factors underlying the protein-flavor binding mechanism and its final impact on aroma release and perception in plant-based systems. The main aim is to guide food manufacturers in flavor creation and efficiently design novel plant-based food products with consumer-desired flavor profiles while minimizing flavor dosing.

Email – cbarallat@gmail.com

Linkedin - www.linkedin.com/in/cristinabarallatperez

Colophon

This thesis was printed by ProefschriftMaken (proefschriftmaken.nl)

Edition: 65 copies

Cover design by Laura Lanseros

Cristina Barallat Pérez, 2024

